

Applications (04 Apr. 2015)

William J. Hinze

Dept. of Earth, Atmospheric, & Planetary Sciences,
Purdue University,
West Lafayette, IN 47906

Ralph R.B. von Frese

School of Earth Sciences,
The Ohio State University,
Columbus, OH 43210

Aff H. Saad

Saad GeoConsulting,
1627 South Hearthside Drive,
Richmond, TX 77406

Contents

0.1	Overview of the Applications of Gravity and Magnetic Methods to Subsurface Exploration	<i>page 1</i>
1	Environmental and Engineering Investigations	3
1.1	<i>Overview</i>	3
1.2	Introduction	4
1.3	Geological Mapping and Site Characterization	5
1.4	Landfill Investigations	19
1.5	Buried Bedrock Topography Mapping	27
1.6	Subsurface Property Studies	38
1.7	Subsurface Void Mapping	44
1.8	Buried Ferro-Metallic Material Identification	50
1.9	Archaeological Exploration and Evaluation	59
1.10	Time-lapse Studies	65
2	Mineral Resource Exploration	72
2.1	<i>Overview</i>	72
2.2	Introduction	72
2.3	Geological Mapping	77
2.4	Indirect Exploration for Mineral Deposits	87
2.4.1	Diamondiferous Intrusives	88
2.4.2	Uranium Mineralization in the Athabasca Basin, Canada	93
2.4.3	Olympic Dam Granite-Breccia Mineral Deposit, Australia	95
2.4.4	Porphyry Copper Deposits	100
2.4.5	Mafic/Ultramafic Mineral Deposits	106
2.5	Direct Exploration for Mineral Deposits	113
2.5.1	MacDonald Mines Property, Quebec, Canada	114

2.5.2	Barite Deposits	115
2.5.3	Faro Lead/Zinc Deposit, Yukon Territory, Canada	117
2.5.4	Bathurst Mining District, New Brunswick, Canada	117
2.5.5	Volcanogenic Massive Sulfide Deposits	118
2.5.6	Rare Earth Elements	120
2.5.7	Iron Ores	124
2.6	Summary	129
3	Energy Resource Exploration	132
3.1	<i>Overview</i>	132
3.2	Introduction	133
3.3	Hydrocarbon Exploration and Exploitation	134
3.3.1	Basin Studies	136
3.3.2	Structural Elements	136
3.3.3	Limited Seismic Quality Regions	138
3.3.4	Basement Configuration	142
3.3.5	Integrated Interpretation with Seismic Reflection Profiling	147
3.3.6	Hydrocarbon Field Studies	150
3.3.7	1) Structural Features	150
3.3.8	a) Anticlines	150
3.3.9	b) Faults	152
3.3.10	c) Salt Features	155
3.3.11	2) Stratigraphic Features	158
3.3.12	a) Reefs	161
3.3.13	b) Direct Detection of Hydrocarbons	162
3.3.14	c) Stratigraphic Lithologic Variations	167
3.3.15	Exploitation	172
3.4	Coal Exploration and Exploitation	177
3.5	Geothermal Exploration and Exploitation	181
4	Applications to Lithospheric Studies	187
4.1	<i>Overview</i>	187
4.2	Introduction	188
4.3	Impact Craters and Basins	190
4.3.1	Gravity Anomaly Signatures	192
4.3.2	Magnetic Anomaly Signatures	198
4.3.3	Summary	206
4.4	Continent-Ocean Boundaries	207
4.4.1	Gravity Anomalies	208
4.4.2	Magnetic Anomalies	210

4.4.3	Passive Margin Examples	212
4.4.4	a) North American Atlantic Margin	212
4.4.5	b) Africa and South America Atlantic Margins	215
4.4.6	Active Margin Examples	222
4.5	Continental Rifts	227
4.5.1	Gravity Attributes	232
4.5.2	Magnetic Attributes	238
4.5.3	Examples of Modern Continental Rifts	239
4.5.4	a) European Cenozoic Rift System	239
4.5.5	b) East African Rift System	241
4.5.6	c) Rio Grande Rift	246
4.5.7	d) Baikal Rift System	250
4.5.8	Examples of Paleorifts	253
4.5.9	a) Oslo Rift	253
4.5.10	b) Midcontinent Rift System	256
	<i>References</i>	263

0.1 Overview of the Applications of Gravity and Magnetic Methods to Subsurface Exploration

The following four chapters supplement the text "Gravity and Magnetic Exploration: Principles, Practices, and Applications" by William J. Hinze, Ralph R. B. von Frese, and Afif H. Saad which was published by Cambridge University Press in 2013. These chapters provide an overview of the applications of gravity and magnetic methods to subsurface exploration. They are not comprehensive in coverage or description of individual examples of uses, but rather illustrate the range of applications of these geophysical methods as available in the scientific and technical literature. Applications cited range from very local to worldwide scales and from historical to present-day uses. The purpose of these overviews is to provide the user with examples that will lead to a better understanding of the methods and to foster development of new applications. They supplement Chapter 14 of the text which introduces the reader to the applications of the methods.

These chapters were originally intended to be included in the book, but space limitations prevented this without significantly increasing its cost. Placing these chapters on the book's website is advantageous because this permits the use of color figures as appropriate and the relative ease in updating the applications as new uses are reported for the gravity and magnetic methods in subsurface exploration. The individual descriptions of the applications are not discussed in detail and in many cases just referenced, thus interested readers are directed to the original citations for specifics on the applications and the methodologies used to acquire, process, and interpret the data.

The breadth of application of the methods is impressive. As a result the applications have been subdivided into four chapters according to their uses. The *first* chapter deals with the application to environmental and engineering studies as well as a few examples of the application of gravity and magnetic methods to archaeological investigations. For the most part the scale of these studies is in the meter to 10s of meters range with depth of investigations focused on the upper 30 m of the Earth, but some investigations, especially those directed to site characterization involving critical structures and features, are at a regional scale measured in 100s of kilometers and involve crustal depths.

The *second* chapter is directed toward the use of gravity and magnetic methods to mineral exploration. As in the first chapter, the scales vary greatly and the applications include a broad range of minerals both metallic and non-metallic.

The *third* chapter involves energy resources including oil and gas, as well as coal and geothermal resources. Geophysics, including gravity and magnetic methods, has had a dominant role in the discovery of the vast petroleum reservoirs of the Earth. It is these studies that have provided a major stimulus for developing the instrumentation and methodologies that are used today in gravity and magnetic investigations.

The *fourth* chapter reports on investigations of the lithosphere with gravity and magnetic methods. The applications discussed in this chapter involve primarily crustal scale studies mapping the geology and processes of the crust and the uppermost mantle. These investigations have been greatly facilitated in the past half century by gravity and magnetic investigations using aircraft and satellites.

Environmental and Engineering Investigations

1.1 Overview

Gravity and magnetic methods are useful in a wide range of applications for environmental, engineering, archaeological, and other near-surface investigations. Of particular importance is the use of the methods in site characterization, which involves determining the geology and physical attributes (rock-mass properties) of the near-surface Earth materials at the location of current or proposed critical or environmentally-important structures. The gravity method has been successful in locating bedrock valleys that often are the site of prolific groundwater aquifers and in mapping geologic basins that contain groundwater supplies. An additional principal use of the gravity method has been in identifying underground voids, both natural and man-made that are of importance because of the threat they pose to man or because of their archaeological importance. Gravity measurements are also potentially useful in monitoring on-going processes that change the subsurface mass such as by the movement of water into or out of a formation or by the change in the surface elevation and mass caused by tectonic, volcanic, or environmental processes. The magnetic method because of its ease and efficiency of operation and analysis and its application to the study of buried ferro-metallic objects is widely used in a variety of environmentally related studies. It has also found broad use in archaeological investigations due to the presence of ferrous materials and the disturbance of magnetic soils and rocks by man. The limited size and low intensity of many gravity and magnetic source anomalies require high density and precision surveying. This is a major limitation to the use of the gravity method, but far less of a problem in the magnetic method as a result of the greater efficiency that is readily attained in observing and analyzing results. Accordingly, the magnetic method is preferred to the gravity method in near-surface studies as long as the

anomaly source is not mass controlled. Over the past decade improvements in instrumentation have fostered the expanded use of tensor measurements of gravity and magnetic fields that are being used to enhance interpretation of anomalies. Furthermore the availability of high-precision gravity measurements from earth-orbiting satellites are increasingly being used to evaluate temporal variations in mass associated with continental and regional changes in hydrologic regimes and glacial ice deposits.

1.2 Introduction

Gravity and magnetic methods of geophysical exploration have an important role in engineering, environmental, and archeological investigations and general geological mapping. Recent technological improvements in observing, processing, and analyzing data from these studies have made these methods more efficient and more sensitive, and thus applicable to an increasing range of problems. The methods are especially useful in mapping the location of steep contacts between formations of different germane properties. Accordingly, they commonly are used in the reconnaissance stage of investigation to localize features such as faults and lithologic contacts for intensive studies with higher resolution methods that require more expensive, time-consuming field surveying procedures or by direct geological exploration. The magnetic method which is especially efficient in both the observation and processing of data is particularly useful in this regard.

Engineering and environmental studies as well as archaeological investigations generally are limited to shallow depths, and thus these investigations are referred to as near-surface (Butler, 2005). The definition of the depth limit of near-surface studies is imprecise, but the vast majority of these studies are limited to the first 30 meters of the Earth as a result of the objective of the study and the resolving power of the methods considering the size of the objects under investigation. However, as described by Butler (2005) there are important problems where the depth range of the study is greater than 300 meters, as for example in site investigations of the structural and lithologic integrity of the regional geology surrounding critical structures such as dams, bridges, and nuclear power plants. Investigations to localize appropriate subsurface geological features that provide ground water assessments for industrial, agricultural, domestic, and municipal uses are generally limited to the first 300 meters at most, and thus are another major use of geophysics in the near-surface.

Both gravity and magnetic methods are frequently used in conjunction with other geophysical methods or direct geological studies for seldom do

they provide the complete answer to a subsurface problem. The ambiguity in the interpretation of gravity and magnetic data prevent this. None-the-less, there are notable exceptions to this generality in which the methods have special capabilities; for example, in locating ferro-metallic materials with the magnetic method and mapping near-surface subsurface voids with the gravity method. The relatively small size of sources generally involved in these studies and limitations in the precision of the methods favor studies which involve intense physical property differences. Accordingly, the gravity method is commonly restricted to sources of high density contrast such as subsurface voids and the magnetic method to the study of objects of strong magnetization contrasts such as those associated with ferro-metallic objects.

The following sampling of applications of the gravity and magnetic methods to near-surface investigations illustrate the scale and amplitude of anomalies associated with specific near-surface features and the types of information that can be extracted from these data. They have been selected to serve as guidelines for assessing the application of the methods and as a catalyst to defining new uses. It is particularly important to observe the dense network of high-precision measurements required in many of the near-surface case history applications.

1.3 Geological Mapping and Site Characterization

Geological maps are a fundamental source of information for site characterization for both engineering and environmental purposes. However, due to limited rock outcrops and drill holes, geological maps often are insufficiently precise to meet the objectives of these studies. Gravity and magnetic mapping can be used to supplement direct sources of information in the preparation of geological maps. These methods are particularly useful where anomalies can be extrapolated from direct geological information, either drillhole information or outcrops, into unmapped regions. The magnetic method is especially useful where crystalline rocks containing magnetic minerals are involved because of its high resolution and the ease and rapidity of making magnetic observations and related data reduction.

Mapping with gravity and magnetics can be done at a range of scales for mapping related to siting purposes depending on the specific objectives and the study region. In local studies of a specific site, measured in 10s to 100s of meters, mapping is commonly focused on rock-mass characterization to determine strength and hydrologic properties indirectly from the interpreted distribution of the germane physical properties, either the density or magnetic properties of the rocks. In the study of somewhat larger regions,

measured in kilometers to 10s of kilometers, the studies may be directed to actual geological mapping of the lithologic units and their structure as well as determining the bedrock configuration. On even more regional scales the studies are directed, for example, to the presence of neo- or paleotectonic features which may be tectonically active, and thus have seismogenic potential (e.g., Hinze and Hildenbrand (1988)).

The pattern of anomaly maps, particularly magnetic maps, indicates the structure of geological units and their structural fabric which are important in site characterization. The curvilinear pattern of anomalies shows the folding of magnetic units and disruptions of these patterns give evidence of location of faults and igneous intrusive contacts. An example is shown in Figure 1.1 which is a shaded relief magnetic anomaly map of central Ontario, Canada. The illumination angle of 75° emphasizes the curvilinear pattern associated with generally northerly-striking dikes that cut across the dominant easterly-trend of the basement crystalline rocks of the region. In this case the strain associated with the deformed continental crust has been ascertained from reconstruction of the dike swarm anomalies to their original distribution suggested by paleomagnetic studies of the dikes (Bird et al., 1999). This strain information is useful in characterizing the geological history of the region. Additionally, the shaded-relief map shows the dike anomalies disrupted along an anomaly trend striking south-southwest from the northeastern corner of the map that is caused by upthrust high-grade, magnetic gneisses associated with the Kapuskasing structural zone. The faults of this zone and their related vertical and horizontal displacements are an important element of the tectonic history of the region.

Igneous intrusives are ideal targets for study by gravity and magnetic methods because of their large volume, steep contacts, and physical property contrasts with the country rock which they intrude. Anomalies reaching amplitudes of up to a few tens of milligals (mGal) in gravity and 100s of nanoteslas (nT) in magnetics have been mapped over felsic as well as mafic intrusives with generally negative and positive amplitudes, respectively, although notable exceptions to this generality occur in magnetic mapping. The possible cause-and-effect relationship between mafic intrusives and earthquakes suggested by the association of intrusives and earthquake epicenters in seismically active regions have made mapping of these features an important part of site characterization for critical engineering structures [e.g., Kane (1977)]. The relationship between earthquakes and mafic plutons has been explained in a variety of ways. A simple explanation is that rigidity variations in the crust associated with the plutons passively modify the prevailing stress field causing concentrations of stress, and thus the localization

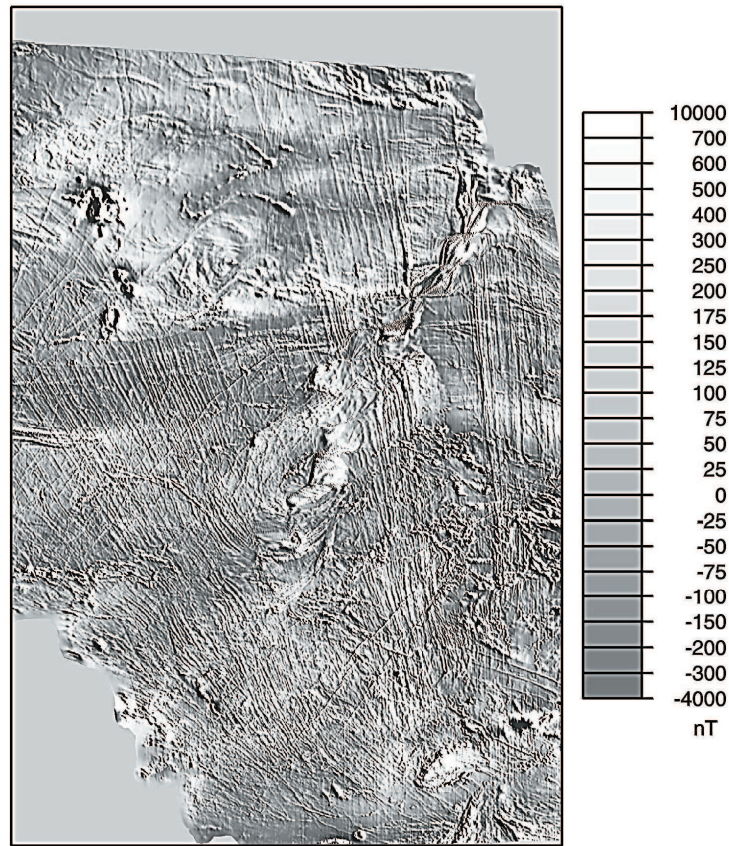


Figure 1.1 Shaded-relief magnetic anomaly map of central Ontario, Canada using a data grid interval of 500 m and an illumination angle of 75° to emphasize N-S trending anomalies. The curvilinear trend of the dike swarm anomalies and their disruption along a SSW-trend are important in deciphering the tectonic history of the region. Adapted from Bird et al. (1999) with the permission of ASEG and CSIRO Publishing. Available at <http://www.publish.csiro.au/nid/224/paper/EG999101.htm>

of earthquakes [e.g., Hinze et al. (1988)]. Ravat et al. (1987) have modeled the +40 mGal gravity anomaly (Figure 1.2) associated with the Bloomfield mafic pluton which is interpreted as being buried by approximately 2 km of sedimentary rocks. This is one of several intrusives which have been identified by gravity and magnetic mapping along the margins of the seismically active New Madrid rift complex in the central U.S. The fault margins of the rift complex are readily mapped by the magnetic anomalies as illustrated

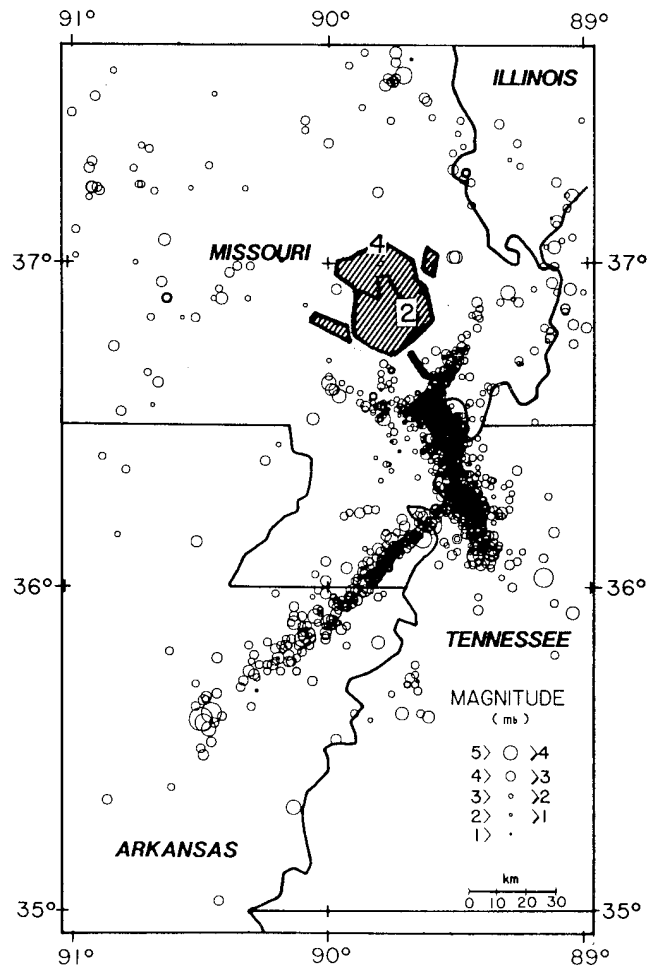


Figure 1.2 Residual Bouguer gravity anomaly map of the Bloomfield pluton in southeastern Missouri showing the location of historical earthquake epicenters. Contour interval 5 mGals. Adapted from Ravat et al. (1987).

in Figure 1.3 of the second vertical derivative of the reduced-to-pole total intensity anomalies (Hildenbrand et al., 1977).

Gravity measurements have also been used to map the configuration of granitic plutons and salt diapirs that are being considered for the location of storage excavations [e.g., Petersen and Saxov (1982); Aitken et al. (1983)]. Both features commonly produce negative gravity anomalies of the order of 10 mGal as a result of the lower density of the intrusive granite compared to the intruded crystalline rock complex and of the salt in relationship to

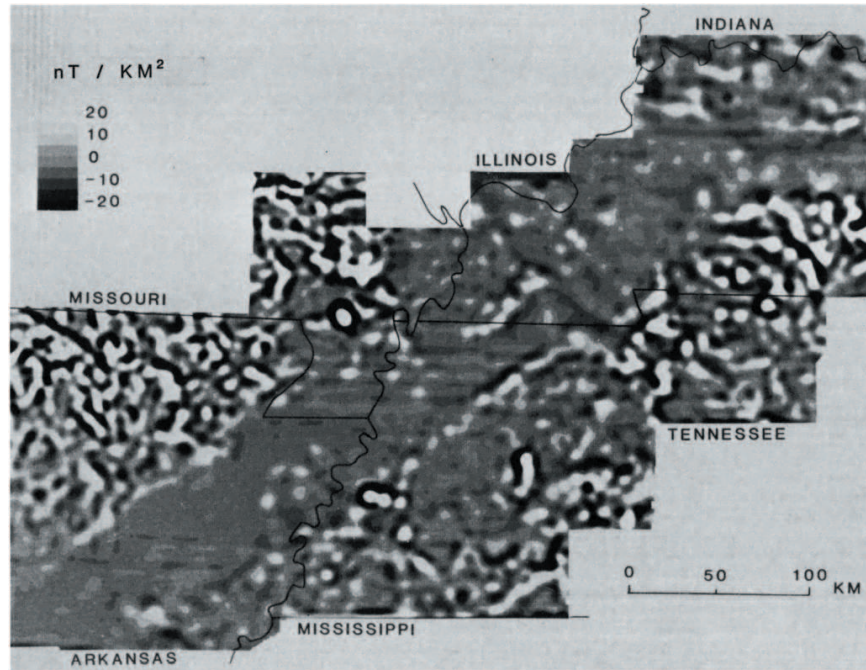


Figure 1.3 Second vertical derivative map of the reduced-to-pole total magnetic intensity anomaly map that has been used to map the margins of the New Madrid rift complex by the change in the character of anomalies. Within the rift complex the anomalies are subdued due to the greater depth to the sources. Adapted from Hildenbrand and Ravat (1997).

the adjacent sedimentary rocks. Figure 1.4 shows the almost circular negative gravity anomaly of about 12 mGal associated with the Totstrup salt structure of Denmark and Figure 1.5 is the residual gravity anomaly map as a result of high-pass filtering with a cut-off of wavelengths greater than 16 km. The latter map which clearly isolates the structure attempts to remove deeper and more regional geological effects from the gravity pattern.

Faults which are of special importance in not only earthquake hazard investigations, but also in engineering and groundwater studies, often can be mapped due to the juxtaposition of rocks of contrasting magnetic or density properties brought about by displacements along the fault [e.g., Astier and Paterson (1989); Zeil et al. (1991)]. This is illustrated in Figure 1.6 by the identification of the tectonically significant Commerce geophysical lineament in the shaded-relief map of the reduced-to-pole total magnetic intensity anomaly associated with the Reelfoot rift at the northern end of the New Madrid rift complex in southern Illinois. Another example of the use of

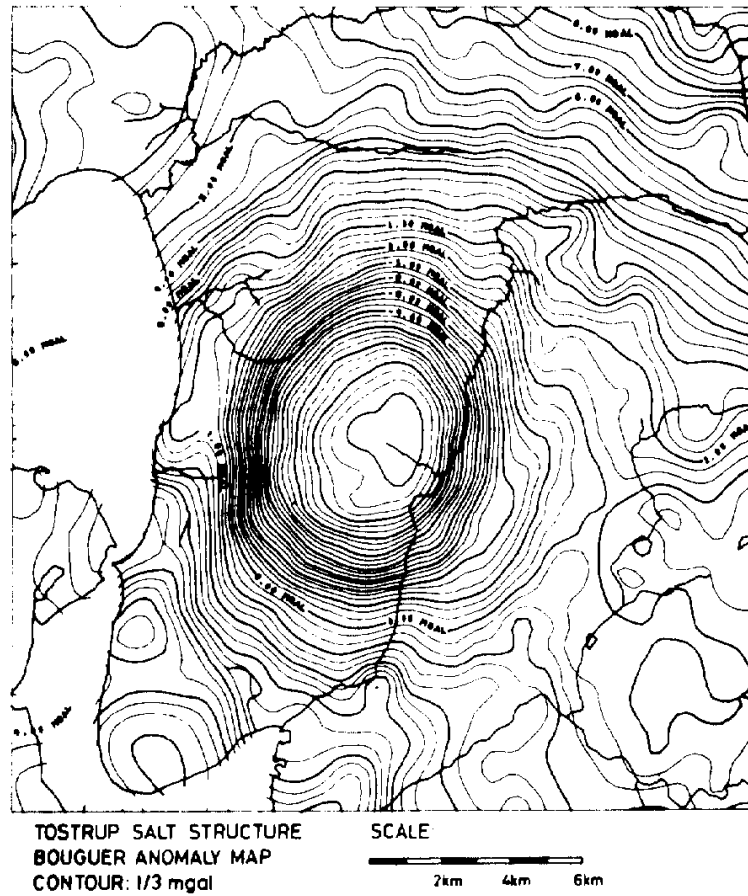


Figure 1.4 Bouguer gravity anomaly map of the Tostrup salt structure. The contour interval is one-third of a milligal. Adapted from Petersen and Saxov (1982).

the magnetic method in this regard is illustrated in Figure 1.7. Figure 1.7(a) shows a high-angle contact magnetic anomaly inferred to represent a faulted contact between quartz monzonite and schist near Dover, New Hampshire, while Figure 1.7(b) gives the location of drill holes used to investigate the source of the anomaly, and Figure 1.7(c) shows the trend of water-producing fractures in the boreholes that approximately parallel the strike of the fault zone.

Faults also may be directly reflected by linear positive magnetic anomalies due to magnetite originating in fault zones by low-grade metamorphism [e.g., Frohlich (1989); Singh and Rao (1990)] or by linear magnetic minima

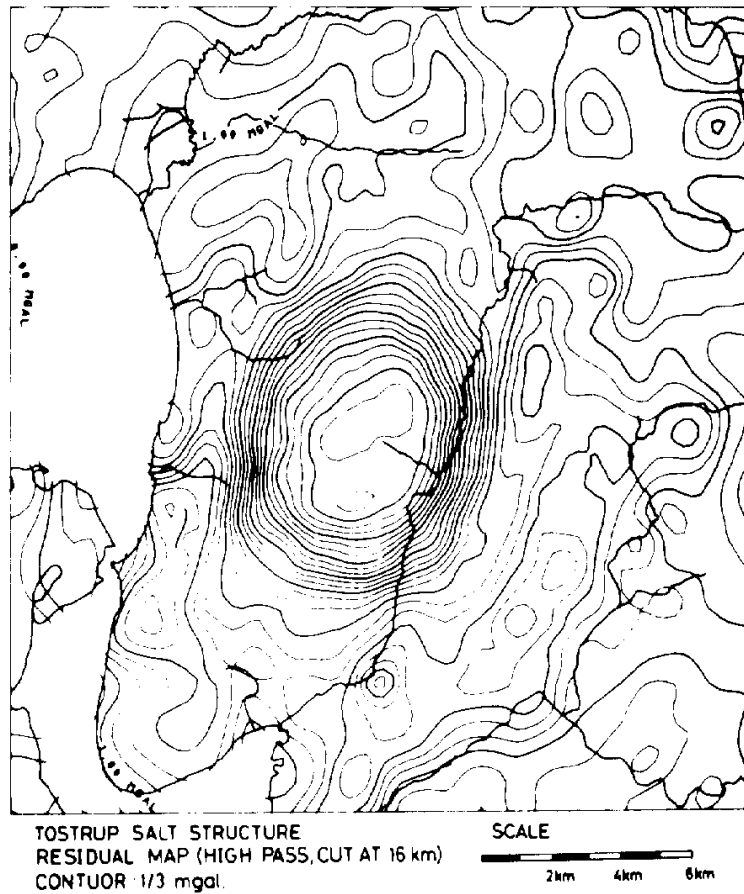


Figure 1.5 High-pass filtered Bouguer gravity anomaly map of the Tostrup salt structure shown in Figure 1.4. Anomaly wavelengths greater than 16 km have been suppressed in this map. The contour interval is one-third milligal. Adapted from Petersen and Saxov (1982).

due to a decrease in magnetic properties of a fault zone by alteration of magnetite to non-magnetic minerals from solutions moving through a permeable fracture zone. Henkel and Guzman (1977) illustrate a linear cross-striking magnetic anomaly minimum in Scandinavia which is believed to be related to destruction of magnetite in a fracture zone in crystalline rocks (Figure 1.8). ten Brink et al. (2007) have mapped a largely minimum magnetic anomaly associated with the Dead Sea transform (Arava) fault (Figure 1.9) and the shift of magnetic anomalies along the fault shows the 105–110 km left-lateral displacement between the Arabian plate to the west as illustrated in Figure

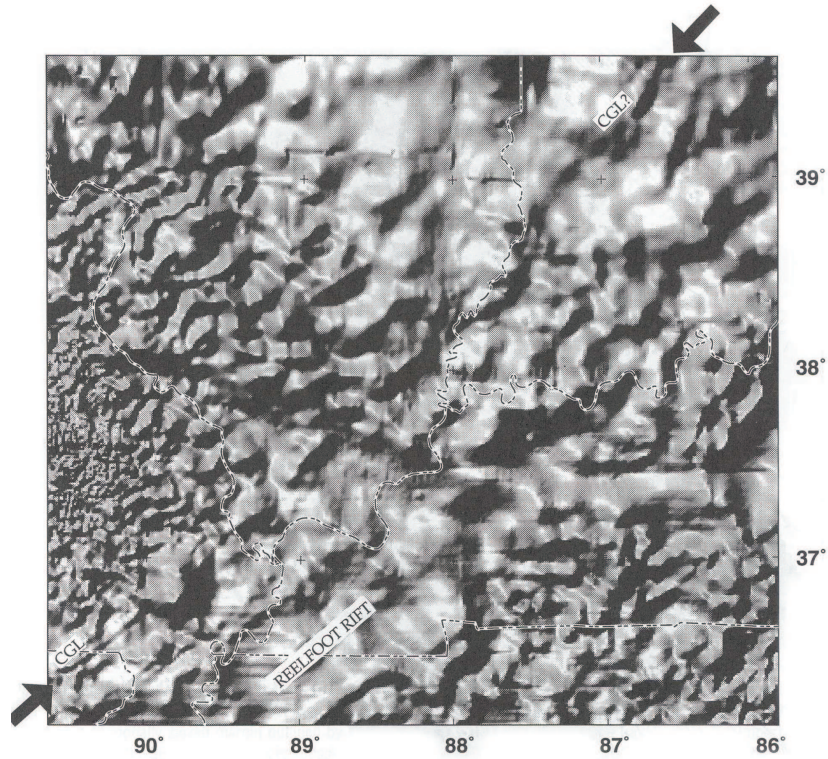


Figure 1.6 Shaded-relief map of the reduced-to-pole total magnetic intensity anomaly field of the Reelfoot Rift at the head of the Mississippi Embayment, USA. The arrows highlight the tectonically significant Commerce geophysical lineament (CGL). Adapted from Hildenbrand and Ravat (1997)

1.10. Magnetic anomalies also can be used to map dikes that may interrupt the flow of groundwater. The interrupted flow may modify the occurrence and quality of groundwater [e.g., Street and Engel (1990); Humphreys et al. (1990)], and thus constitute an important environmental concern.

Gravity anomaly mapping is an important tool for site characterization of potential nuclear waste repositories [e.g., Petersen and Saxov (1982); Wynn and Roseboom (1987); Lodha et al. (1990); Norton et al. (1997)]. Although useful in defining the geologic framework of these sites, the gravity method is especially useful in mapping faults that need to be evaluated as potential seismic hazards. At the proposed Nevada high-level waste repository site at Yucca Mountain, gravity anomalies have proved helpful in locating the optimum position of seismic reflection surveys and in interpreting those surveys (Brocher et al., 1998). Figure 1.11 shows the geological model based on

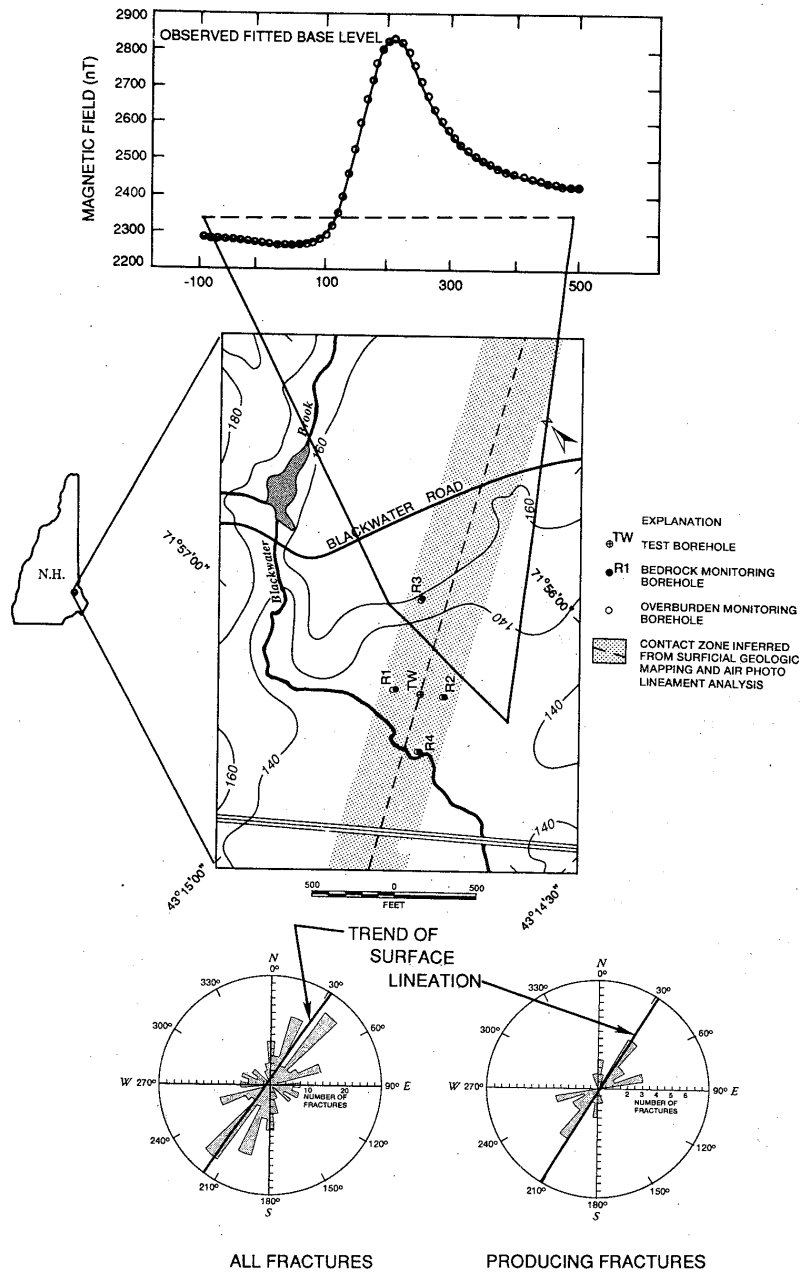


Figure 1.7 Relationship of a magnetic anomaly to a fault contact between quartz monzonite and schist near Dover, New Hampshire. (a) Observed magnetic anomaly along a transect perpendicular to the trend of the anomaly. (b) Location of magnetic profile, fault trend, and drill holes. (c) Orientation of all and water producing fractures encountered by the drill hole as determined from an acoustic televiewer log of the hole. Adapted from Paillet (1993).

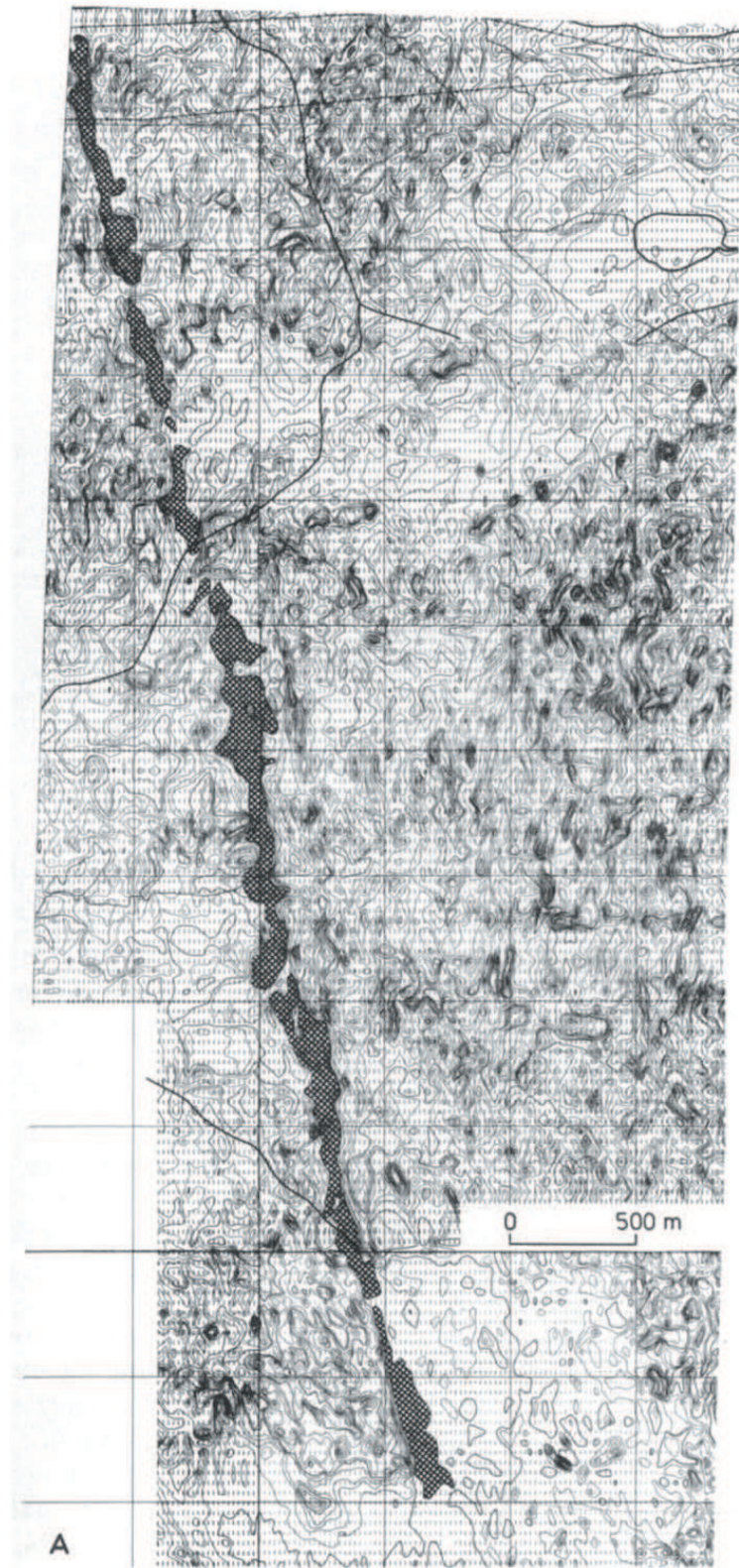


Figure 1.8 Linear magnetic minimum [patterned] shown on an aeromagnetic map over the crystalline bedrock in Scandinavia. The minimum is related to a fault zone where the magnetite has been altered to non-magnetic form. Adapted from Henkel and Guzman (1977).

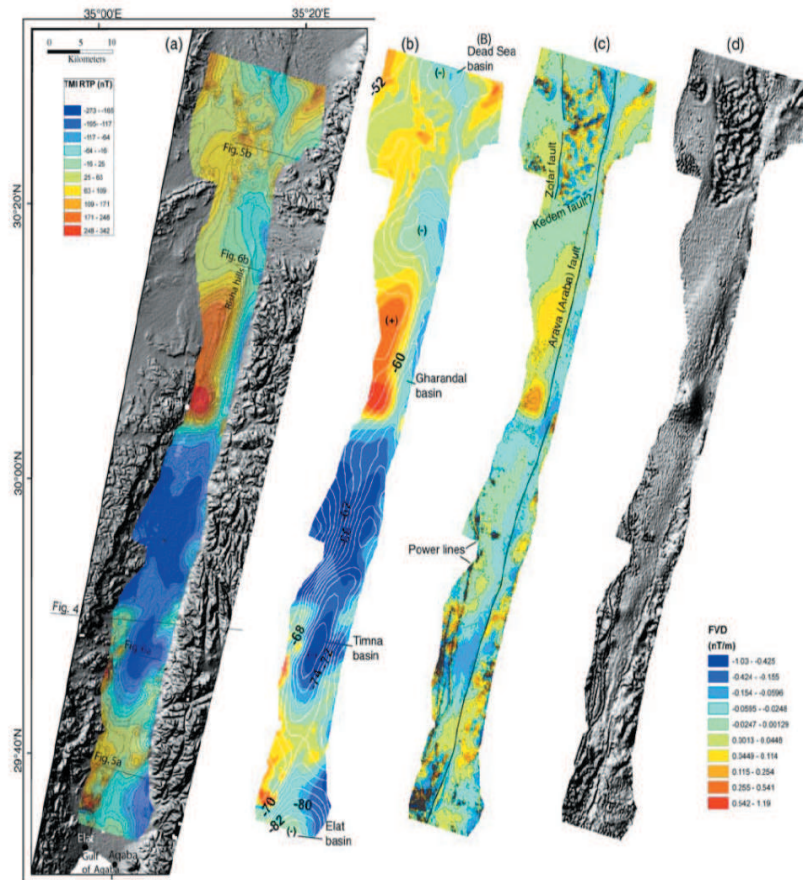


Figure 1.9 (a) Reduced-to-pole total magnetic intensity anomaly map superposed on shaded relief of the topography. The contour interval is 20 nT. (b) Bouguer gravity anomaly contours (contour interval is 2 mGal) superposed on the reduced-to-pole total magnetic intensity anomaly. (c) First vertical derivative of the reduced-to-pole total magnetic intensity anomaly map. Solid lines are interpreted fault traces from the magnetic anomaly data. Note the negative related to the Arava fault. (d) Shaded-relief of the map in (c) illuminated from the west to highlight the fault trace. The linear high-amplitude magnetic anomalies in the southwestern part of the survey area are due to high-voltage power lines. Adapted from ten Brink et al. (2007).

seismic reflection surveying, gravity and magnetic anomaly data, and both surface and subsurface geological information whose gravity expression duplicates the isostatic anomaly profile. The gravity data have been used to map the alluvial basins and the major structures of the region and are par-

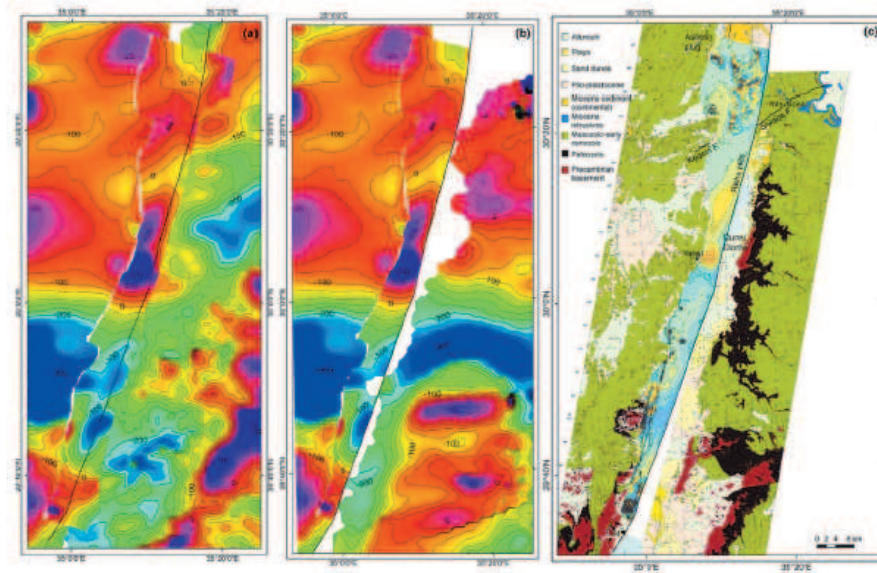


Figure 1.10 (a) Regional total magnetic intensity anomaly map of the Dead Sea valley region upward continued to 900 m. The contour interval is 20 nT. The solid line is the trace of the Arava fault as shown in Figure 1.9. (b) The same map as shown in (a) with the eastern side of the map shifted southward by 111 km along the Arava fault to produce a continuous north-south gradient in the regional magnetic field at 30°N. (c) First vertical derivative of the reduced-to-pole total magnetic intensity anomaly map superposed on a simplified geologic map of the region. The area east of the Arava fault is shifted southward by 107 km. Adapted from ten Brink et al. (2007).

ticularly useful in locating and determining the nature of the major faults and verifying the general structure of the region interpreted from the seismic reflection data. This is important along the profile shown in Figure 1.11, but also is significant because the structures along this profile can be extended along the strike of the gravity anomalies into portions of the region where seismic reflection data are unavailable. The gravity method also has proven useful at the Yucca Mountain site in mapping minor faults with vertical displacements of 200 m or less by anomalies of up to 2 mGal [e.g., Ponce and Oliver (1998); Ponce (1996)].

Gravity anomaly mapping also may map the actual fault zone provided the zone is wide, relatively shallow, and has a contrasting density with the country rock. The latter often occurs because of the increase in porosity

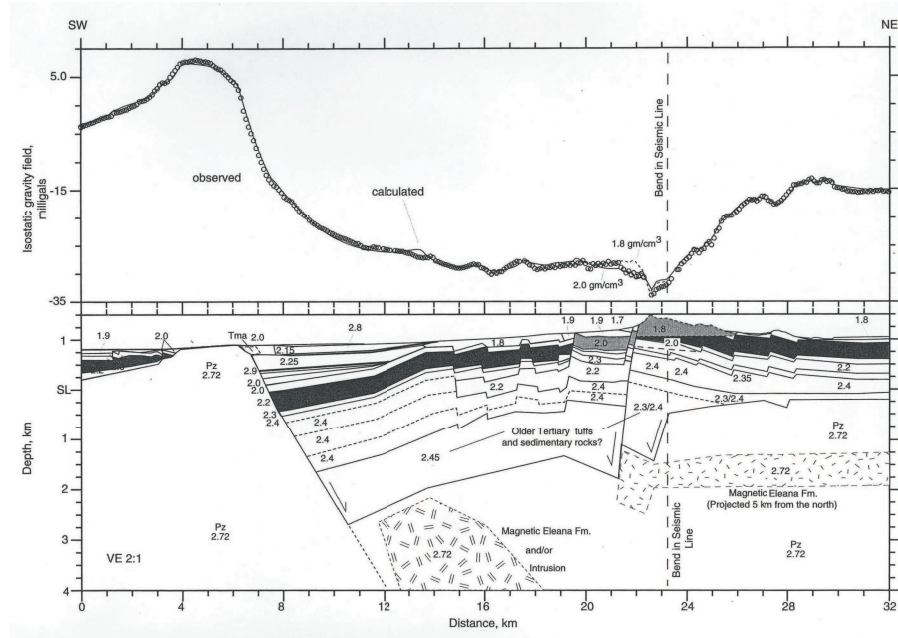


Figure 1.11 Observed isostatic [solid line] and calculated [open circles] gravity anomalies across a model of the Yucca Mountain, Nevada region as determined from seismic reflection, gravity anomaly, magnetic anomaly, and surface and subsurface geological information. Densities are given in g/cm^3 . The strata in the basins above the Paleozoic sedimentary and crystalline rocks (Pz) are Tertiary or recent tuffs or alluvial sediments. [Adapted from Brocher et al. (1998)]

of the fault zone associated with brecciation of the rock during faulting. Stewart and Wood (1990) show the observed and modeled gravity anomalies across a faulted carbonate bedrock terrain (Figure 1.12). The lower density fracture zone is reflected in the negative gravity anomaly. Figure 1.13 shows a vertical gradient profile across a faulted series of rock units (Fajkiewicz, 1976). Particularly striking is the modeled tectonic breccia associated with an intense negative vertical gradient gravity anomaly.

The magnetic method also has a role in geological mapping of the potential nuclear waste repository site at Yucca Mountain, Nevada. Linear magnetic anomalies have isolated basin-bounding faults as well intrabasin faults. The latter are a result of faulting that juxtaposes volcanic units of varying magnetic polarization, while the former are caused by the contrasts in the properties of basement and volcanic units of the ranges with the sediments of the basins as illustrated in Figure 1.14. Magnetic mapping has also

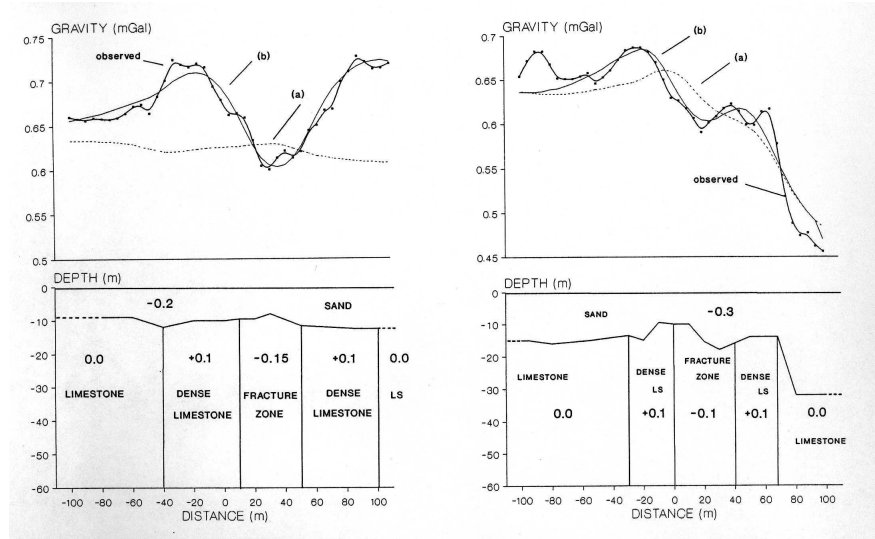


Figure 1.12 Observed and modeled gravity anomaly profile across a limestone bedrock terrain. Profile [a] shows the modeled anomaly assuming uniform bedrock and profile [b] is based on lateral variations within the bedrock including the low density zone associated with the fracture zone in the limestone. Adapted from Stewart and Wood (1990).

been important in estimating the potential hazard from volcanism at the Yucca Mountain site. Predicting this hazard is dependent on the volcanic activity in the region during the past several million years. Volcanic centers are mapped on the surface in the nearby vicinity to the proposed site, but other volcanoes have been buried by sediments derived from erosion of the surrounding ranges. These buried basaltic centers are intensely magnetic in comparison to the surrounding clastic sediments and generally more magnetic than the felsic volcanic ash deposits that make up the bedrock in Yucca Mountain; thus, the buried basaltic rocks are readily mapped by the magnetic method [e.g., Langenheim et al. (1993); Blakely et al. (2000); O'Leary et al. (2002); Perry et al. (2005)]. Figure 1.14 shows the buried reversely magnetized volcano (B) in the Amargosa desert (southwest corner) marked by an intense reversed magnetic anomaly. Smaller, more deeply buried volcanoes to the west are indicated by the anomalies identified by the symbols F, G, and H. Figure 1.15 presents a more detailed, higher resolution view of these anomalies as a result of a surface magnetic survey of the region. The greater resolution obtained by the surface measurements is useful in increasing the precision of the location and the nature of these buried volcanic rocks.

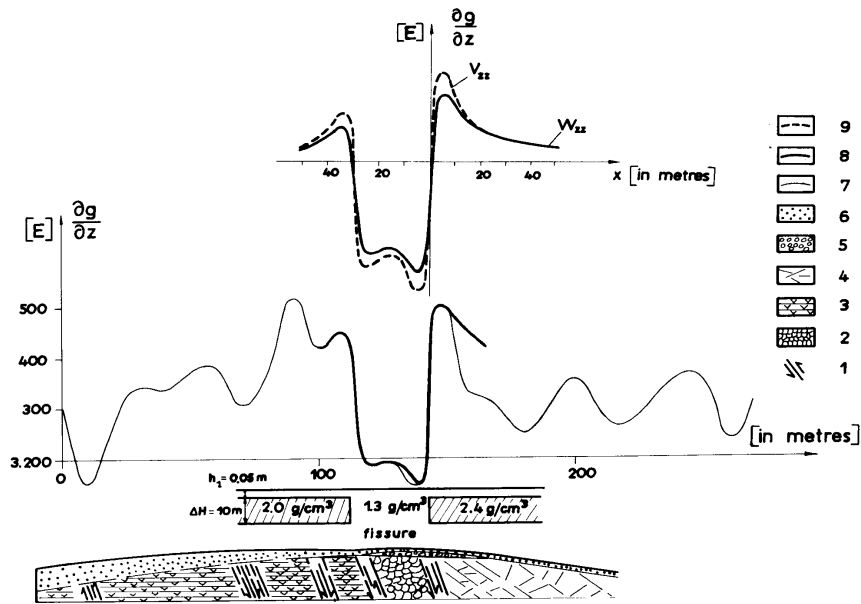


Figure 1.13 Observed and modeled vertical gravity gradients in Eötvös units (E) across a series of geologic units as portrayed in the lower panel where the geologic media are [1] faults, [2] tectonic breccia, [3] porphyry tuff, [4] limestone, [5] calcareous gravel, and [6] sand. The heavy line is the calculated vertical gravity gradient from the simplified physical model of the fissure zone that is shown immediately below the profile. Adapted from Fajkiewicz (1976).

1.4 Landfill Investigations

The non-invasive characterization of the volume and contents of abandoned sanitary landfills that are poorly described by historical records poses an environmental problem that can be studied by gravity and magnetic methods [e.g., Roberts et al. (1990a,b); Fenning and Williams (1997)]. Figure 1.16 shows the residual gravity anomaly reaching an amplitude of 0.2 mGal associated with the Thomas Farm multicomponent abandoned landfill in the glaciated midcontinent of the U.S. (Roberts et al., 1990a). The landfill was located in a ravine cut into glacial sediments and filled over a period of 30 years generally with domestic trash, concrete construction debris, and vegetative cuttings. Although records of the contents were not maintained, the results of the magnetic survey in Figure 1.17 testify to the occurrence of considerable ferrous objects. Gravity stations were located at intervals of 5 to 10 m along traverse lines as shown in Figure 1.16. The root mean

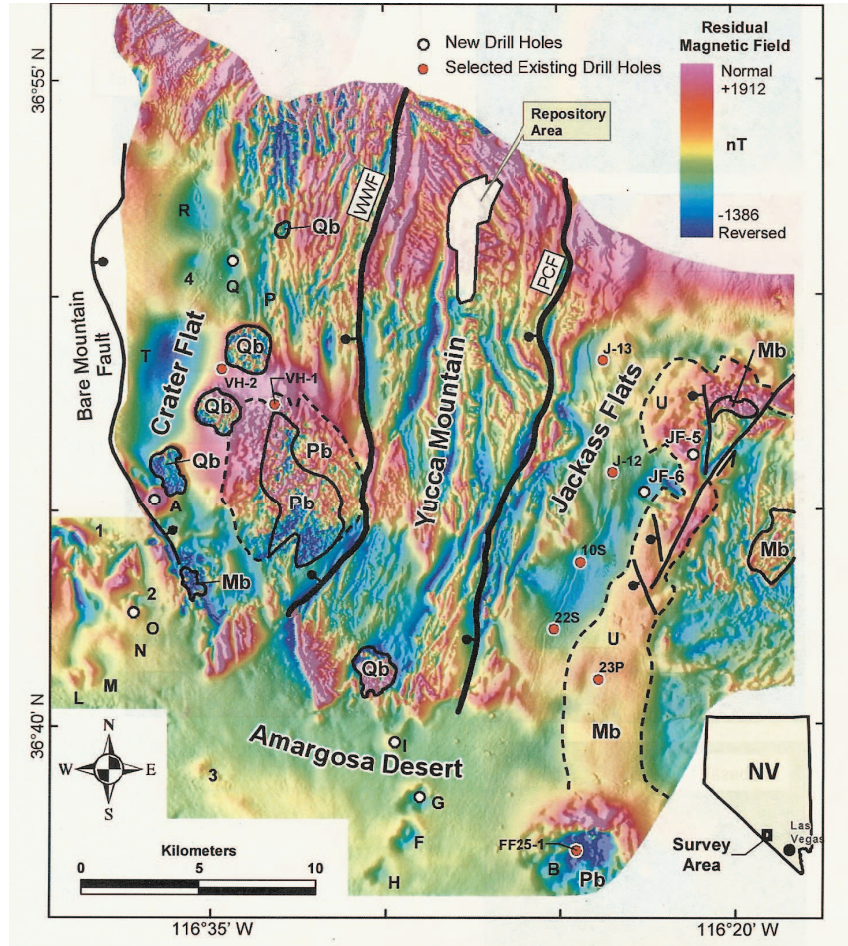


Figure 1.14 High-resolution aeromagnetic anomaly map and locations of holes (solid white circles) drilled to determine if the magnetic anomalies are derived from basalts. Solid red circles indicate selected pre-existing drill holes that provide key constraints on the location of buried basalt near Yucca Mountain. Qb = Quaternary basalt, Pb = Pliocene basalt, Mb = Miocene basalt. Adapted from Perry et al. (2005).

square error of the complete Bouguer gravity anomaly is of the order of $\pm(0.015 - 0.020)$ mGal. The residual gravity map was obtained by removing a third-degree polynomial surface fitted to the anomaly values exterior to the landfill anomaly from the observed anomaly.

The residual gravity anomaly map compares well with the isopach map of the landfill derived from topographic maps prepared prior to initiation of the landfill and after it was closed (Figure 1.18). The maximum thickness of

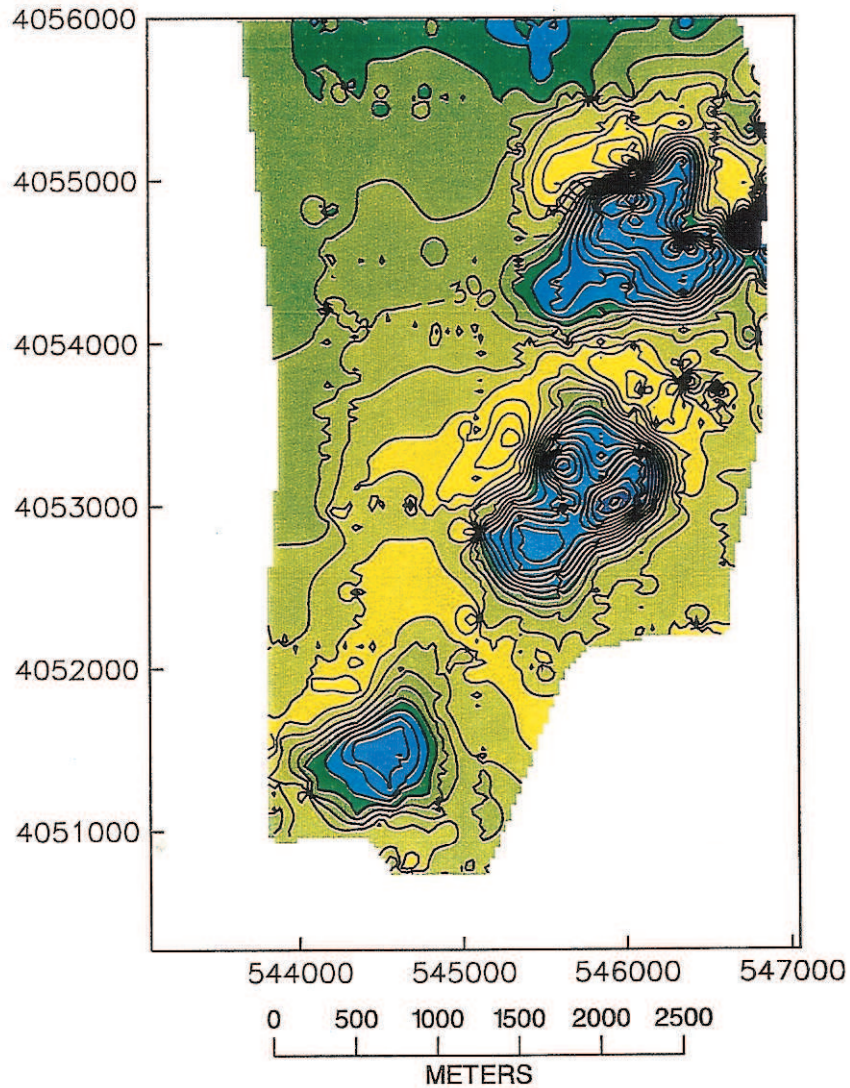


Figure 1.15 Surface (~ 1 m) total magnetic intensity anomalies of anomalies (north to south) G, F, and H identified in Figure 1.14. These anomalies locate the position of buried reversely magnetized Pliocene basalt volcanoes occurring along a north-northeasterly trend in Amargosa Valley. The contour interval is 10 nT and the numbers on the margin of the map are UTM coordinates. Note the useful detail provided by the surface measurements and the decreasing gradient and amplitude of the anomalies from south to north as a result of the increasing depth to the basalt due to the thickening of the non-magnetic alluvial sediments in the Valley. Adapted from Magsino et al. (1998).

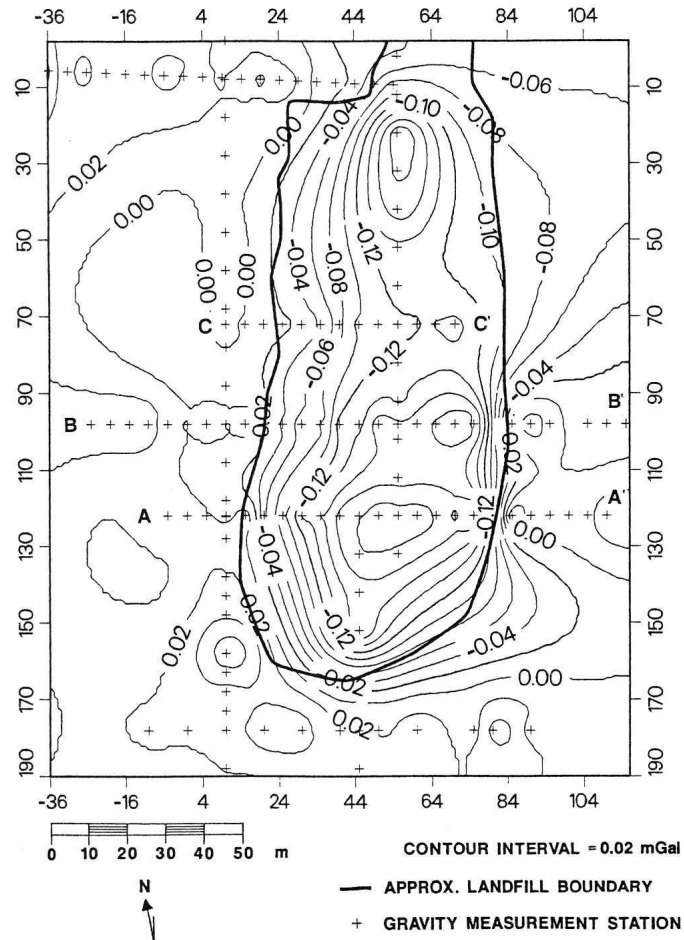


Figure 1.16 Residual gravity anomaly contour map of the Thomas Farm landfill, West Lafayette, IN determined by subtracting the best fitting third order polynomial surface exterior to the landfill from the complete Bouguer gravity anomaly. Adapted from Roberts et al. (1990a).

the landfill is of the order of 13 m. Forward modeling of the residual anomaly profiles using finite length two-dimensional modeling techniques suggests a mean density contrast of 530 kg/m^3 between the landfill and the enclosing glacial till.

Inversion of the gravity anomaly profiles using the known landfill cross-section as a constraint permitted calculation of the density contrast that gave the best-fitting calculated anomaly (Figure 1.19). In turn, these den-

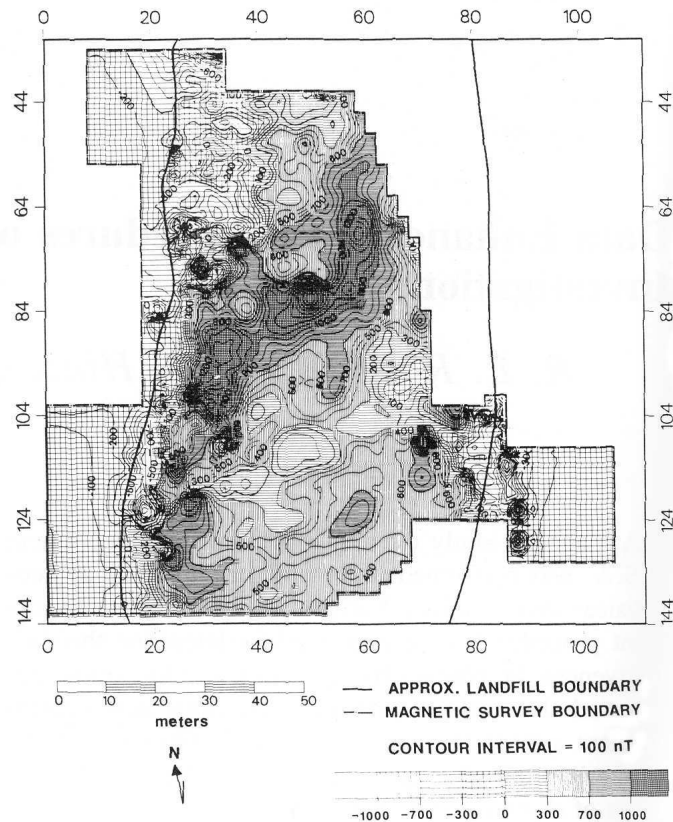


Figure 1.17 Total field magnetic intensity map observed at 1 m height over the Thomas Farm landfill site, West Lafayette, IN. Adapted from Roberts et al. (1990b).

sity contrasts were used to discriminate portions of the landfill containing primarily domestic-type trash in the northern portion from the lower density construction refuse, brush cuttings, and tree limbs of the southern portion. The interpreted density values together with appropriate assumptions indicate an overall porosity of roughly 45%. The use of the gravity method at the Thomas Farm landfill site shows that the gravity method can be useful in defining the limits of abandoned landfills and their contents. The gravity method is particularly useful in studies of landfills when combined with the results of investigations by other geophysical methods as it was at the Thomas Farm site. Magnetic, GPR, electromagnetic, resistivity, and seismic refraction and reflection methods were combined with the gravity method to arrive at a successful characterization of this landfill [e.g., Leap et al.

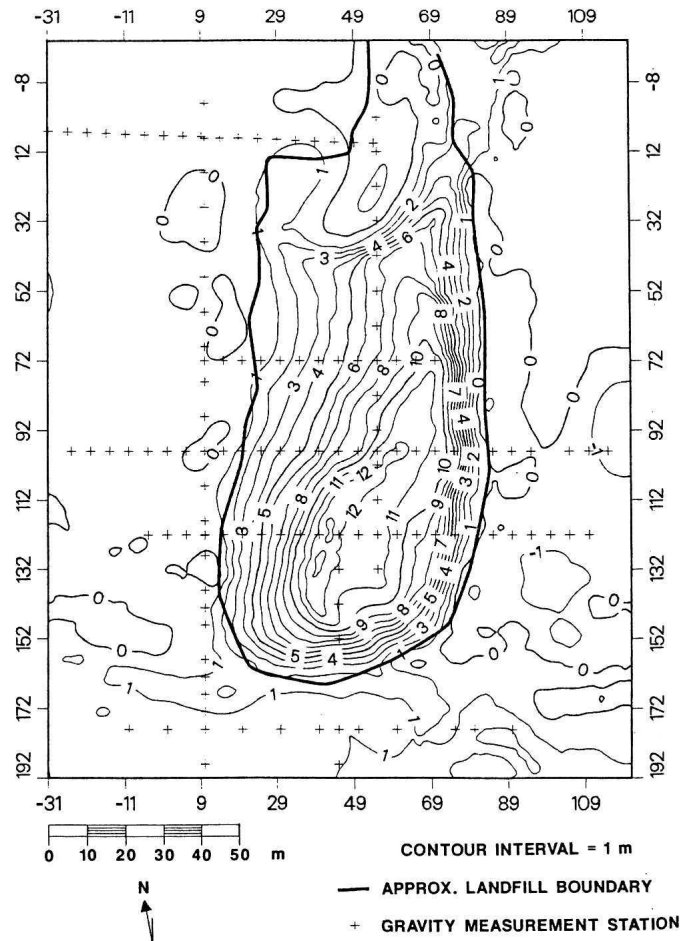


Figure 1.18 Isopach map of the Thomas Farm landfill, West Lafayette, IN determined by subtracting the pre-landfill topography from the topography of the site following closure of the landfill. The contour interval is 1 m. Adapted from Roberts et al. (1990a).

(1991)]. A similarly successful use of the gravity method in a multicomponent geophysical survey was reported for the Woburn landfill site in England (Fenning and Williams, 1997).

The total field magnetic intensity observed at a height of 1 m above the surface of the Thomas Farm landfill delineates the distribution of the fill material by virtue of the intense anomalies related to the ferrous metals in the landfill. Identification of specific metallic sources associated with the most

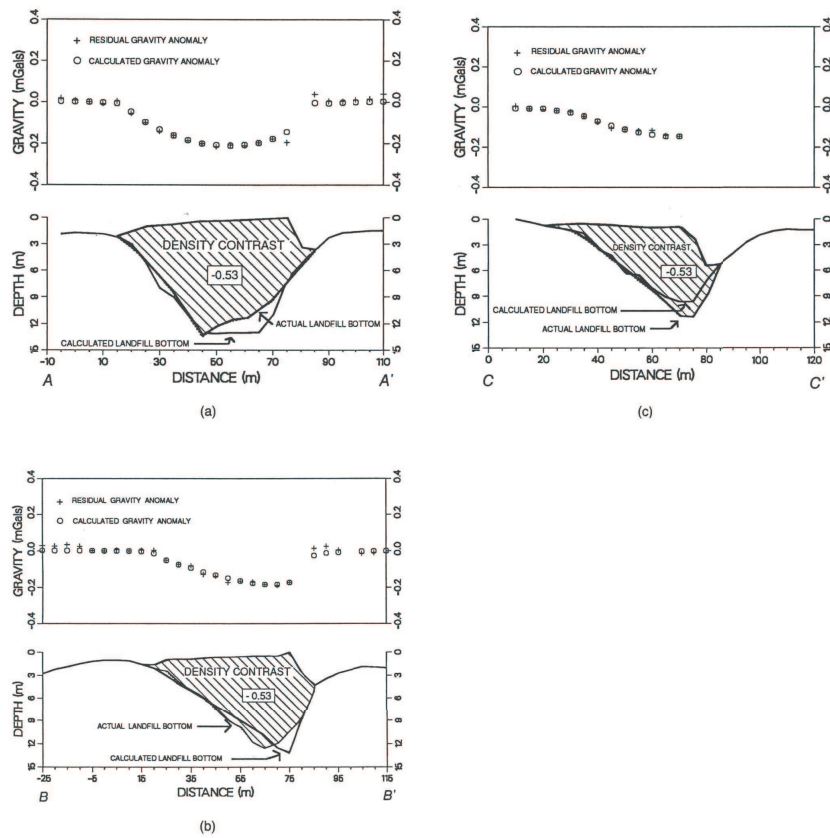


Figure 1.19 Results of the inversion of the gravity anomalies observed over the Thomas Farm landfill, West Lafayette, IN by constraining the source of the anomaly to the actual landfill configuration. The locations of the profiles are shown in Figure 1.16. The density contrasts shown on the profiles are in g/cm^3 and are indicative of the material included in the landfill at the position of the profile. Adapted from Roberts et al. (1990a).

intense magnetic maxima has been corroborated with ground-penetrating radar. The comparatively less intense and broader gradient magnetic anomalies in the southern portion of the landfill are believed to be associated with a change in landfill composition late in its history from domestic trash in the northern part to vegetative cuttings and construction debris to the south. Roberts et al. (1990b) using data from the 1-meter square magnetic observation network showed that enhancement of the data using wavenumber domain processing can be useful in interpreting the landfill magnetic anomalies. For example, upward continuation of the data as illustrated in the anomaly profiles of Figure 1.20 show the profoundly increasing atten-

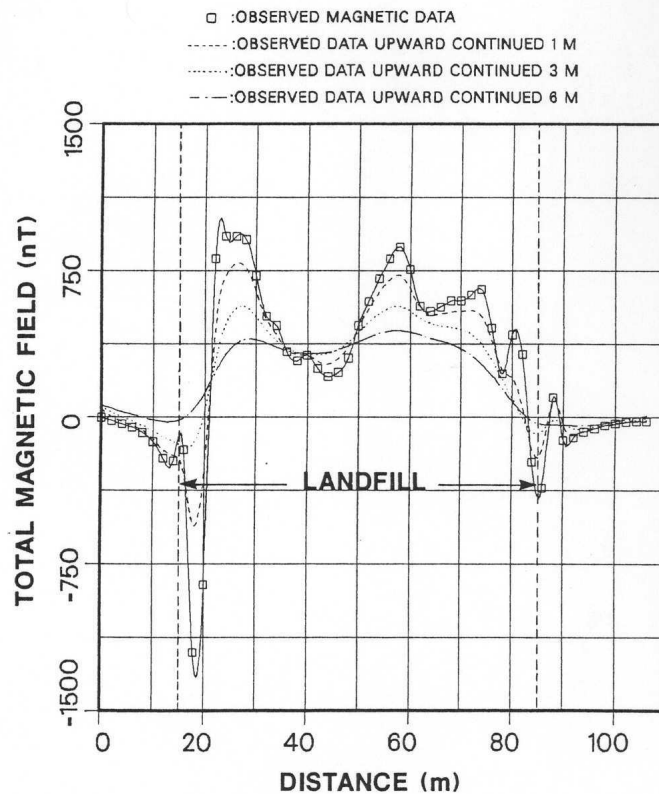


Figure 1.20 Observed total field magnetic intensity and upward continued total field to heights of 1, 3, and 6 m along a profile perpendicular to the axis of the Thomas Farm landfill site. Note the attenuation of the high-wavenumber anomalies associated with near-surface sources with increasing height. Adapted from Roberts et al. (1990b).

uation of the shallow-sourced anomalies with increasing height. The 6-m upward continued magnetic anomaly data in this figure provide an excellent integrated view of the landfill's content where distortions by the anomalies of the shallow sources are minimized.

The computed vertical gradient magnetic data that focus on the shallow-sourced anomalies are also in very good agreement with the observed vertical gradient anomalies except where the gradients are a maximum (Figure 1.21). Thus, the dual-level observation of the magnetic field for determination of the vertical gradient can be eliminated except where temporal magnetic variations are the principal reason for vertical gradient measurements.

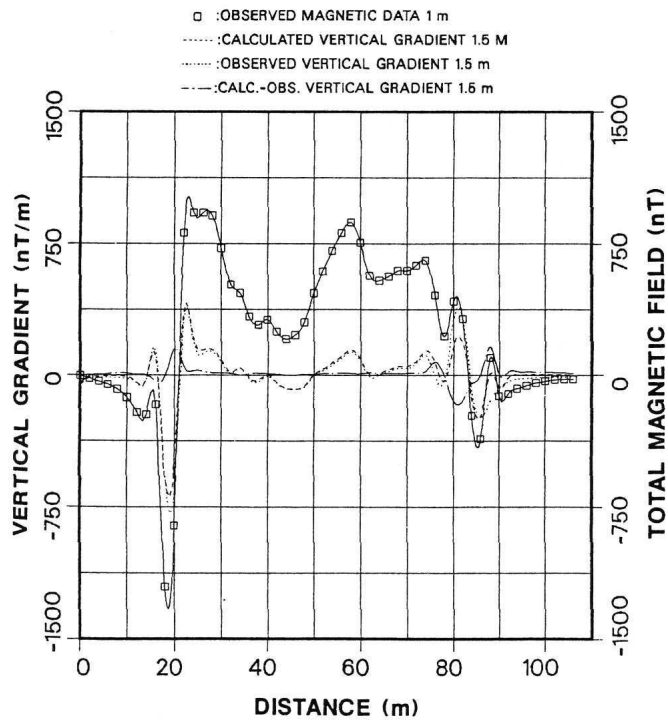


Figure 1.21 Observed total field magnetic intensity, observed and calculated vertical gradient of the total field, and the difference between the observed and calculated vertical gradient field along the same profile shown in Figure 1.20. Note the close correspondence of the observed and calculated vertical gradients except in regions of high vertical gradients. Adapted from Roberts et al. (1990b).

1.5 Buried Bedrock Topography Mapping

Knowledge of the depth and configuration of the bedrock surface lying beneath unconsolidated surface deposits is of considerable value in planning construction projects such as highways, dams, bridges, and buildings and in ground water investigations to find aquifers and groundwater flow paths. Where the density of the bedrock, either sedimentary or crystalline rocks, is relatively consistent, the gravity method has proven to be especially useful and efficient in mapping the bedrock surface if ancillary geological or geophysical data on the depth to this surface are available. Further, where these ancillary data are available it is possible to use inversion techniques on the gravity data to determine the density of the overlying sediments which may be helpful in constraining the hydrologic properties of the sediments.

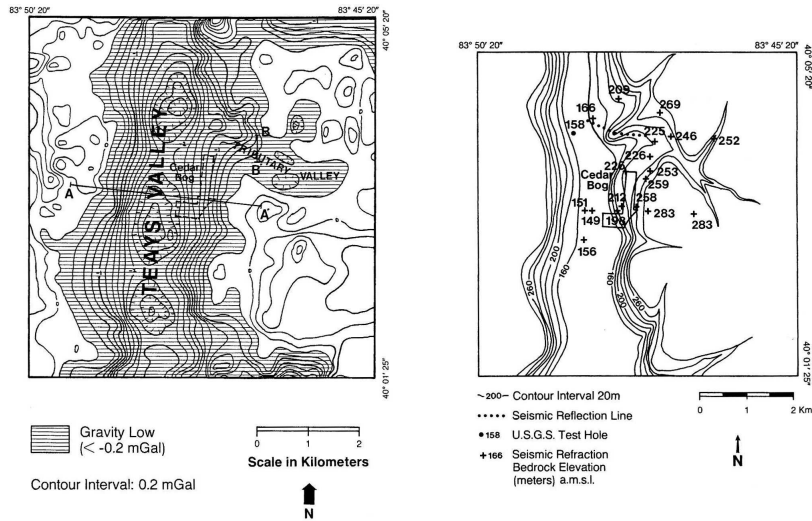


Figure 1.22 Residual Bouguer gravity anomaly over the buried Teays bedrock valley in Ohio [left] and bedrock contour map of the valley [right] showing drill hole and seismic refraction control used in constructing the bedrock contour map. Adapted from Wolfe and Richard (1990).

The gravity method is particularly applicable to this problem because of the marked density contrast that generally occurs between the bedrock and the overlying sediments. The magnetic method is also useful in mapping the depth to bedrock of isolated magnetic property contrasts that occur within crystalline bedrock.

The correlation of negative gravity anomalies with buried bedrock valleys due to the increased thickness of the lower density sediments in the valley is well illustrated in 1.22. These maps show the Bouguer gravity anomaly map over the buried Teays bedrock valley in Ohio which has been mapped independently with drill data and seismic refraction profiling (Wolfe and Richard, 1990). The anomaly map was obtained by subtracting a third degree polynomial surface that was fit to the gravity data. The bedrock along the axis of the gravity anomaly which reaches values in excess of -2 mGal is limey shale [density = 2650 kg/m^3] and limestone [2700 kg/m^3] is the bedrock on the flanks where the tributaries to the main bedrock valley enter. The gravity stations are estimated to have a relative error of ± 0.03 mGal. Forward modeling of the gravity anomaly data along profile AA of Figure 1.22 shows that low density glacial outwash [1950 kg/m^3] occurs in a late stage valley in the center of the bedrock valley which is primarily filled with glacial silt [2100 kg/m^3] and in its higher levels by glacial till

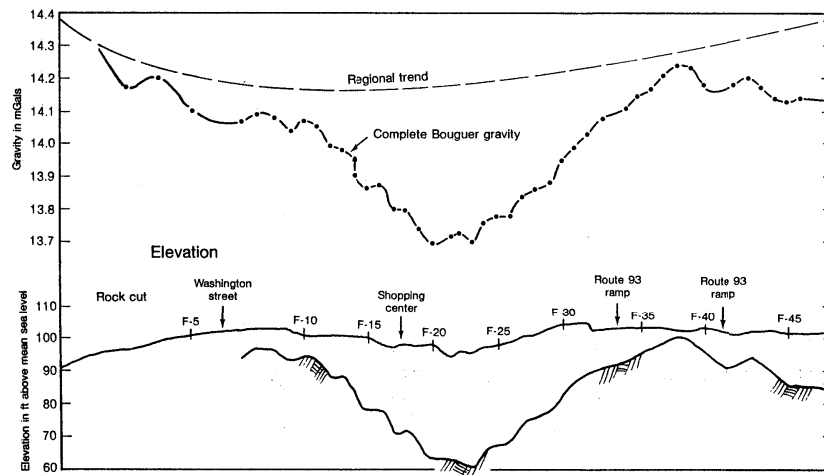


Figure 1.23 Bouguer gravity anomaly profile and the configuration of the buried bedrock topography in Massachusetts. Adapted from Kick (1985).

[2310 kg/m^3]. The correlation of negative gravity anomalies also is well illustrated in Figure 1.23 which shows the regional gravity anomaly trend and the complete Bouguer gravity anomaly over a bedrock topography valley in Massachusetts (Kick, 1985). Hall and Hajnal (1962) in a study of buried valleys in Saskatchewan show that the density contrasts within the glacial drift overlying the bedrock can be as large as those between the bedrock and drift. As a result the gravity method can map potential aquifers in intradrift sediments, but they also may cause erroneous estimates of the depth to the bedrock if they are not factored into the interpretation.

Eaton and Watkins (1970) show the effect of varying water table elevation in a buried bedrock valley cut into a homogeneous granite on the resulting gravity anomaly (Figure 1.24). Assuming a sediment grain density of 2670 kg/m^3 and a porosity of the sediments of 0.33, the gravity anomalies on the left of the figure are based on 0% specific retention in the non-saturated sediments, while those on the right are calculated assuming the specific retention of these sediments is 20% - i.e., the sediments overlying the water table retain 20% water saturation against the force of gravity. Obviously, the height of the water table and the water content of the overlying sediments contribute to gravity anomaly variations which complicate the determination of the depth to bedrock from gravity anomalies.

One of the principal problems in mapping buried bedrock topography is the isolation of the gravity anomaly derived from the density contrast

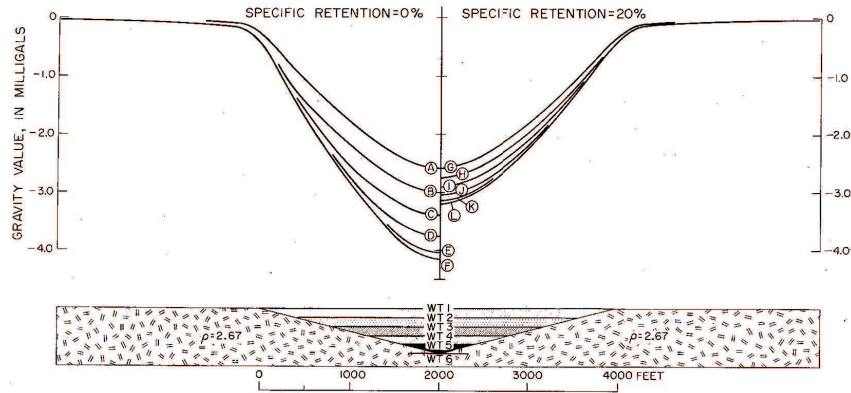


Figure 1.24 Cross-section of an idealized bedrock valley cut into granitic rocks and associated computed gravity anomalies. Bedrock density is 2670 kg/m^3 , valley sediment grain density is also 2670 kg/m^3 , and the porosity of the sediments in the valley is 0.33. Gravity anomalies correspond to water table levels [WT 1 corresponds to Curve A, etc.]. The gravity anomalies on the left assume a specific retention of the unsaturated zone of 0.0 and those on the right a specific retention of 0.2. Adapted from Eaton and Watkins (1970).

at the bedrock-sediment interface. Many techniques have been developed to solve this problem. The principal approach has been low-cut filtering of the anomaly data to eliminate regional anomalies derived from below the bedrock surface. Similarly intrasediment variations may be minimized by high-cut filtering of the data. However, the gravity-geologic method (Ibrahim and Hinze, 1972; Adams and Hinze, 1990) has proven successful in minimizing the anomaly isolation problem where the near-surface bedrock has a consistent density and where sufficient control on the bedrock surface is available from drilling or other geophysical measurements to constrain the isolation of the residual anomalies.

Adams and Hinze (1990) applied the method to mapping the bedrock topography of Tippecanoe County, IN shown in Figure 1.25. The bedrock surface was determined by comparing the simple Bouguer gravity anomaly map (Figure 1.26) with the regional gravity anomaly map (Figure 1.27) based on bedrock control points randomly distributed across the region. A total of 28 bedrock depth control points spread over the area were not used in preparing Figure 1.27, but rather served to check the precision of the bedrock elevation determinations. The results can be evaluated from Figure 1.28 where the calculated bedrock elevations are plotted against elevations from seismic refraction and drillhole data. The maximum error is 25 ft (≈ 8

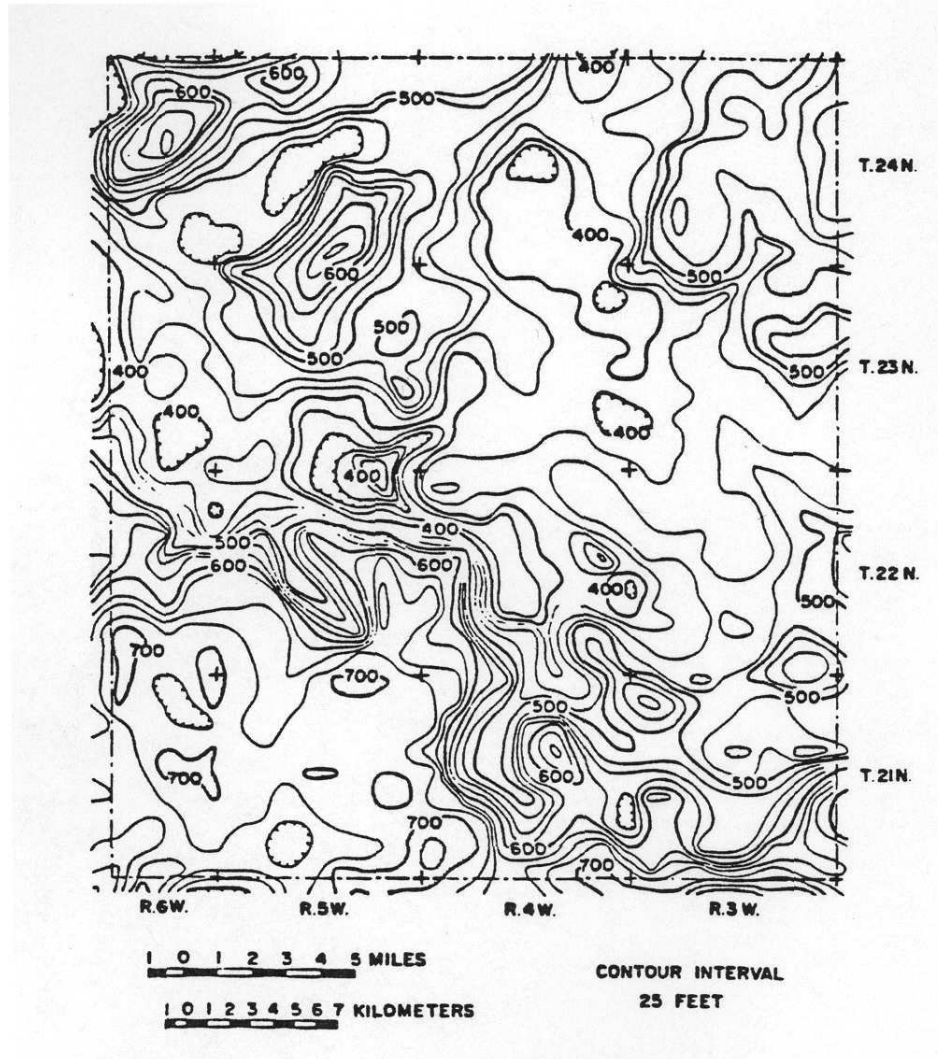


Figure 1.25 Bedrock topography contour map of Tippecanoe County, IN based on the gravity-geologic method. The contour interval is 25 ft. Adapted from Adams and Hinze (1990).

m). The least squares line (solid) compares favorably with the zero-error line (dashed). The error is probably due to interpolation of gravity anomalies at the site of the drill hole and variations in the assumed constant density contrast.

Mapping of the bedrock surface beneath glaciers, both continental and mountain types, is analogous to mapping the base of surface sediments. The

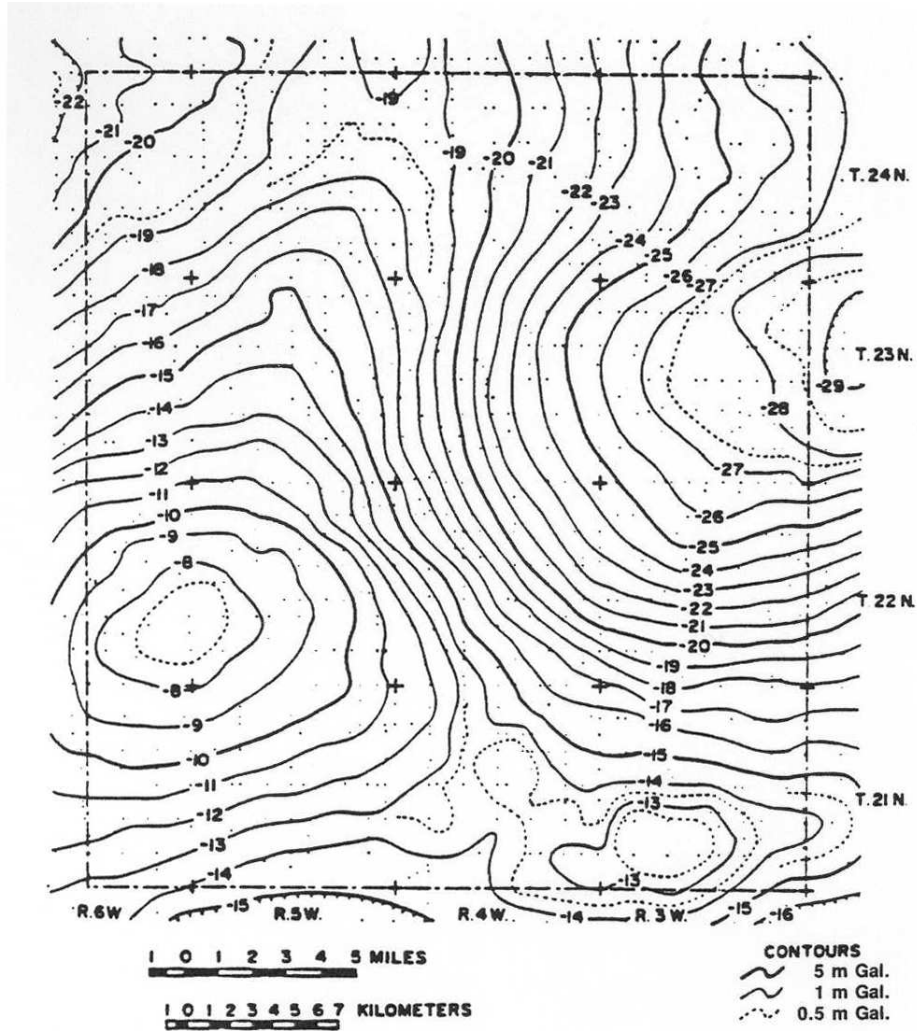


Figure 1.26 Simple Bouguer gravity anomaly map of Tippecanoe County, IN. Dots are locations of gravity stations. The primary contour interval is 1 mGal. Adapted from Adams and Hinze (1990).

low density of ice makes this application particularly attractive because of the resulting large density differentials. The problems of mapping sub-glacial topography are similar to those of mapping buried bedrock topography. As a result various schemes are used to isolate the anomaly associated with the topography and to tie the interpretation to results of geophysical methods of higher resolving power and direct measurements from drilling. As such

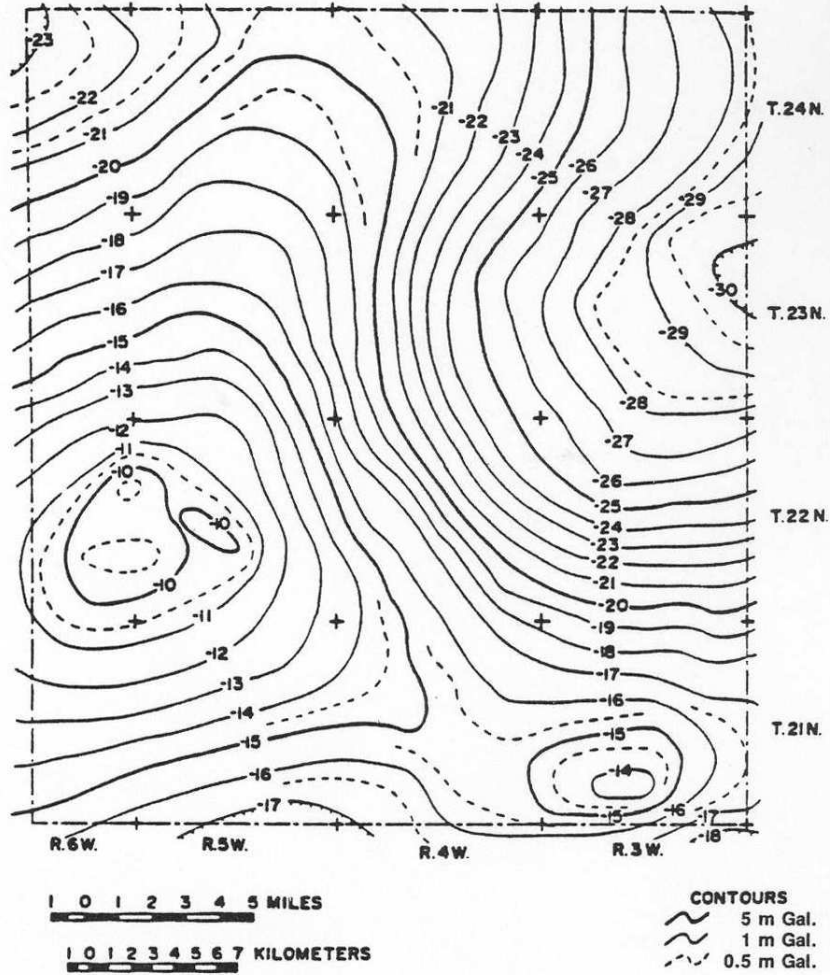


Figure 1.27 Regional gravity anomaly map based on the gravity-geologic method in which the effects of bedrock topography variations have been stripped from the simple Bouguer gravity anomaly map (Figure 1.26). Adapted from Adams and Hinze (1990).

the gravity method is used to provide detail between more definitive measurements [e.g., Levato et al. (1999)]. Measurements of the volume of ice in glaciers are of interest in developing local or regional hydrologic budgets.

Gravity methods have proven useful for not only mapping the bedrock surfaces that are a result of erosion, but also in mapping alluvial basins that

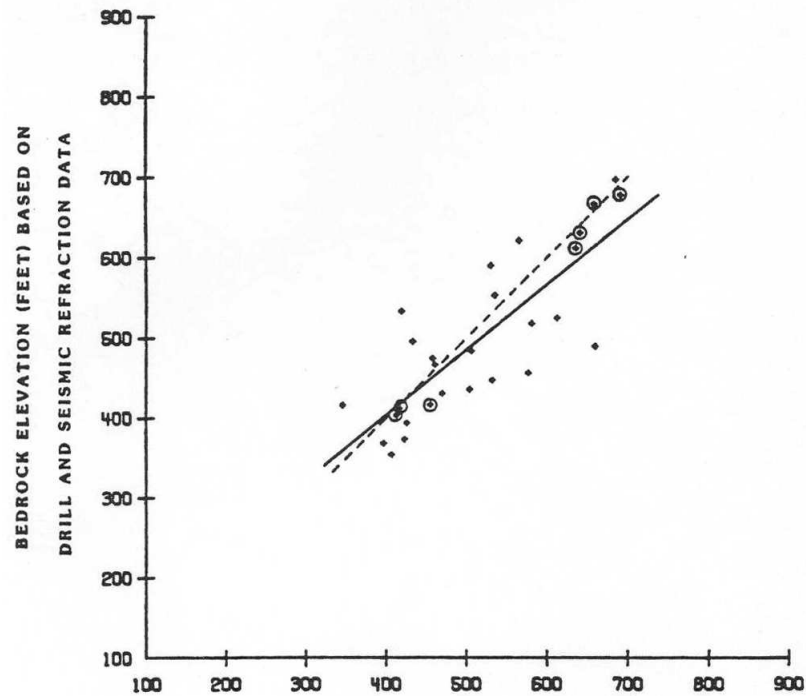


Figure 1.28 Comparison of gravity-geologic determined bedrock elevations and bedrock elevations obtained from drill-hole and seismic refraction data. Circled points are drill-hole data, solid line is least-squares linear fit to all the data and dashed line is zero error line. Adapted from Adams and Hinze (1990).

have been structurally developed by faulting and have subsequently been filled with low-density alluvial sediments from the surrounding highlands. A useful illustration of the gravity method's use in this regard was presented by Abbot and Louie (2000). Figure 1.29 shows an observed gravity anomaly profile across the Reno-Truckee Meadows alluvial basin together with the calculated gravity derived from the model profile in the figure. Abbot and Louie (2000) point out that mapping these alluvial valleys may be important to earthquake hazard analysis because the basins can trap earthquake surface waves and amplify the magnitude and lengthen the duration of seismic shaking at the surface. Mapping alluvial basins also is important because they are an important source of water. This is particularly true in the semi-arid regions of the southwestern U.S.

An interesting example of determining the depth of a basin in this region by non-linear inversion is presented by Richardson and MacInnes (1989). The

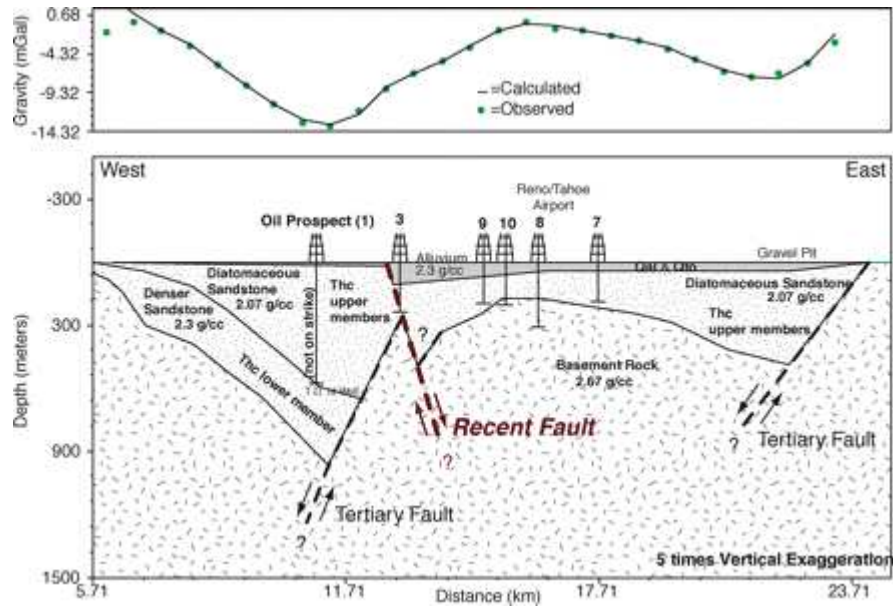


Figure 1.29 Cross-section of the Reno-Truckee Meadows alluvial basin together with observed and computed gravity anomaly profiles. Vertical exaggeration is 5. Adapted from Abbot and Louie (2000).

basis of their analysis is the residual gravity anomaly map of the Avra Valley, Arizona which was isolated from the observed gravity with a smooth polynomial fit to the observed gravity of the region (Figure 1.30). The anomaly related to the valley fill exceeds -25 mGal and is due to a density contrast between the alluvium [2200 to 2400 kg/m^3] and the bedrock [2640 kg/m^3] that is of the order of -240 kg/m^3 . Richardson and MacInnes (1989) performed a three-dimensional polyhedral model inversion of the anomaly data which resulted in the bedrock contour map of the valley in Figure 1.31. The depth reaches in excess of 3 km in the northern portion of the valley mapped in the gravity data. Gauss' law can be used to calculate the volume of the ground water in these alluvial basins from integration of the gravity anomaly. Theoretically this volume can be determined uniquely from the volume of the anomalous mass, but in practice it is limited by the configuration of the source, the accuracy of the residual-regional separation, and the assumptions made regarding the density, storage coefficient, and porosity of the basin-fill material (West and Sumner, 1972). The advantage of this method for determining the volume of water available in a basin or valley is that no definitive information must be known regarding its configuration.

The magnetic method has a high sensitivity to the depths of the anomaly

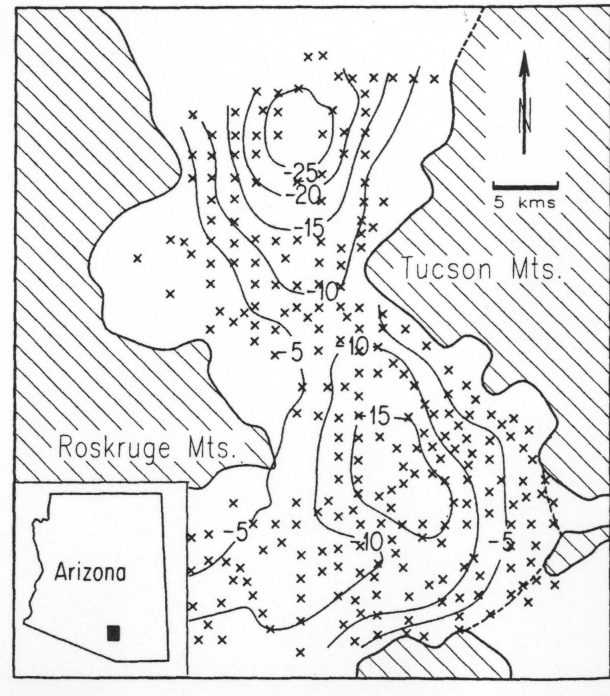


Figure 1.30 Residual Bouguer gravity anomaly map of the Avra valley, AZ. Station locations within the valley are indicated by crosses. Contour interval is 5 mGal. Adapted from Richardson and MacInnes (1989).

sources. Accordingly, it is possible to map the depth to the bedrock surface in crystalline-rock terranes at the location of specific, highly magnetic sources by the inversion of their anomalies. For example, Dentith et al. (1992) mapped the base of the weathered surface material overlying greenstone and granitoid rocks at depths measured in tens of meters in southwestern Australia using magnetic anomalies. However, anomalies simply derived from the contrast between the crystalline bedrock and the overlying unconsolidated materials are seldom used in this manner because of the difficulty in separating the anomalies due to the varying bedrock surface interface from minor variations in the magnetic properties of the bedrock.

Another example of the use of gravity and magnetic anomaly data to obtain information useful in groundwater assessment and management has been presented by Elawadi et al. (2012) for an extensive region in southwestern Saudi Arabia adjacent to the Red Sea rift. This is a difficult area to evaluate because of the presence of surface basaltic lava flows and intrusives. Accordingly, the investigators have done extensive processing of

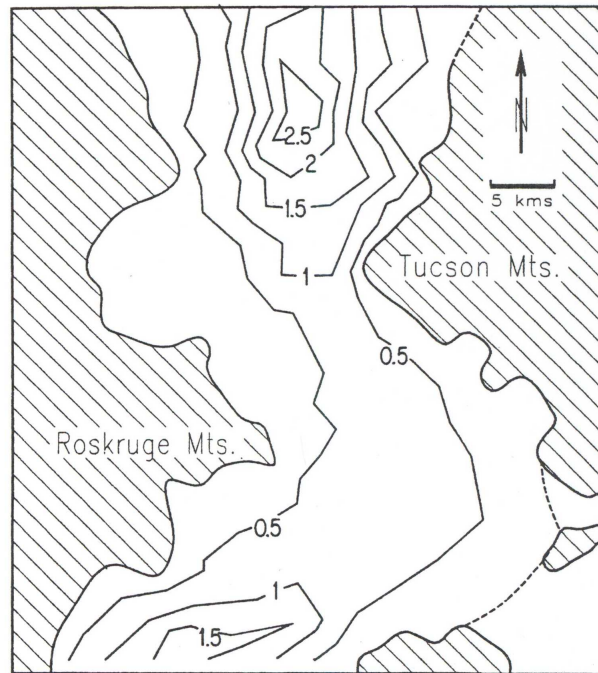


Figure 1.31 Contour map of the depth to bedrock in the Avra valley, AZ based on non-linear inversion. Contour interval is 0.5 km. Adapted from Richardson and MacInnes (1989).

both data sets to enhance the interpretation including wavenumber filtering, reduction-to-pole, horizontal and vertical differentiations, Euler deconvolution, analytic signal, and local wavenumber (source parameter imaging) depth determinations. Figure 1.32 shows the complex magnetic pattern of the region in this reduced-to-pole total magnetic intensity map, Figure 1.33 gives a structural interpretation of the region superposed on the first vertical derivative of the Bouguer gravity anomaly map. Figure 1.34 is the enhanced residual reduced-to-pole total magnetic intensity anomaly map that portrays the surface basaltic flows and intrusives using a combination of horizontal derivatives, second vertical derivatives, and analytic signal processing. Finally, Figure 1.35 maps the depth to basement in the region utilizing the local wavenumber method. The extensive processing of these data has resulted in interpretations that would otherwise not be possible.

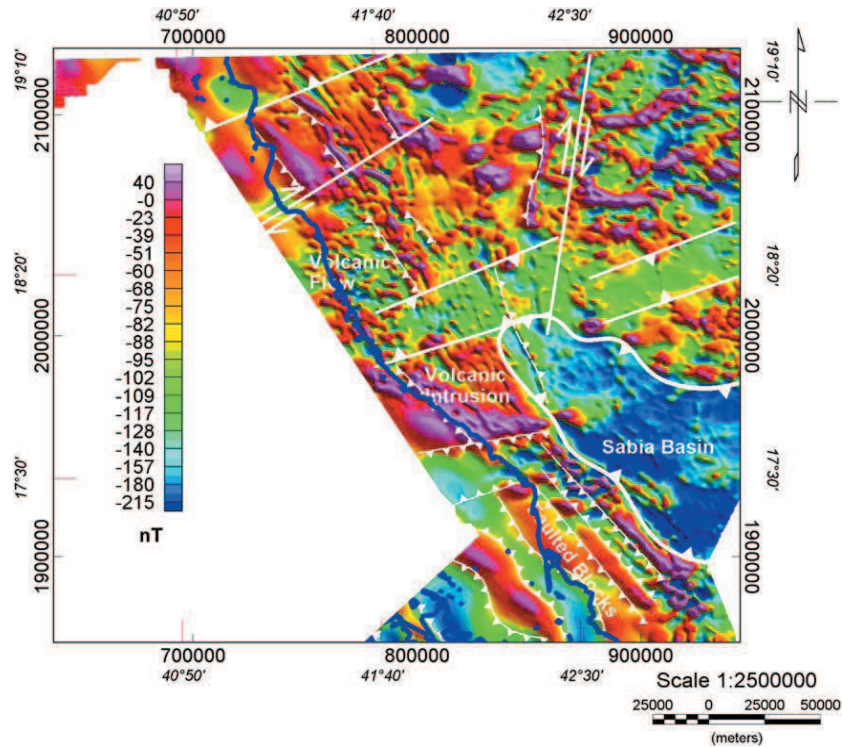


Figure 1.32 Reduced-to-pole total magnetic intensity anomaly map of southwestern Saudi Arabia with major interpreted geological features. The thick blue line is the edge of the Red Sea. The eastern portion of the map area is primarily made up of Proterozoic meta-sedimentary and volcanic rocks, while the region along the Red Sea consists of Tertiary and Quaternary basalts and related intrusions as well as sedimentary basins. The margin of the Red Sea is dominated by northwest trending horsts and grabens associated with the development of the Red Sea rift. Adapted from Elawadi et al. (2012). Available at doi:10.1088/1742 – 2132/9/327

1.6 Subsurface Property Studies

The properties of subsurface units can be determined indirectly from inversion of gravity and magnetic anomaly to the respective densities and magnetic polarizations of the anomaly sources. The usefulness of this process is largely dependent on the sensitivity and reliability of the conversion of these geophysical properties to other physical, engineering, and hydrologic properties of interest. Unfortunately, geophysical properties are not very definitive predictors of other properties at least to the degree of precision required in most engineering and environmental applications. One exception is the estimation of porosity from density when the mineral density of the anomalous

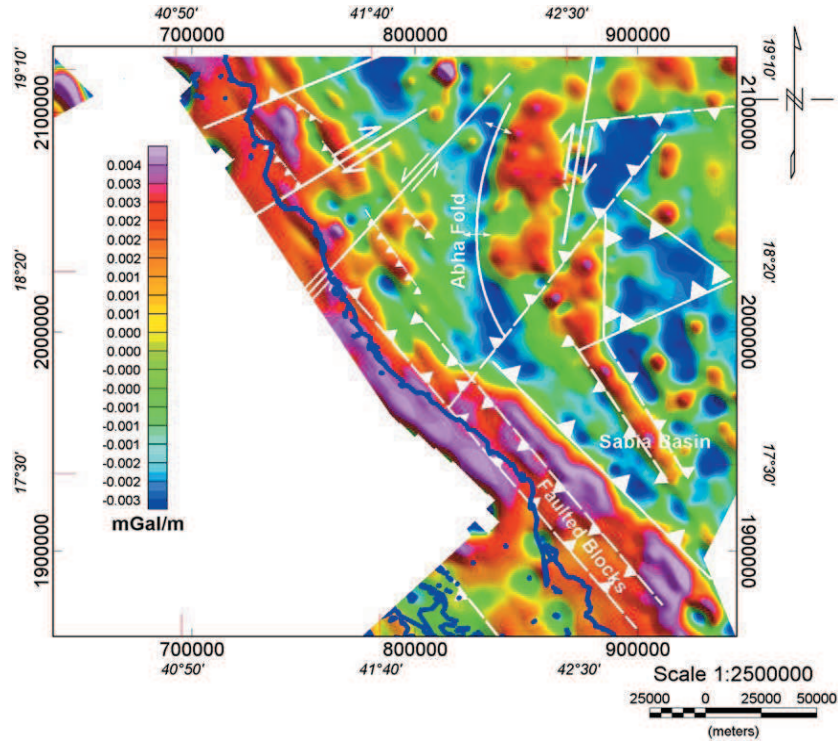


Figure 1.33 First vertical derivative of the Bouguer gravity anomaly map of southwestern Saudi Arabia with major interpreted geological features. Adapted from Elawadi et al. (2012). Available at doi:10.1088/1742 – 2132/9/327

source can be reliably estimated. Another exception is the use of magnetic polarization to identify anthropogenic ferrous materials that are associated with intense magnetizations. As a result gravity and magnetic methods are used to determine subsurface properties only under special conditions.

One of those special conditions is the detection of subsurface semi-permanent ice in arctic regions. Rampton and Walcott (1974), for example, used the gravity method to detect the presence of ice and estimate the thickness of excess ice in regions of ice-covered topography in the Canadian arctic. The usefulness of the method is based on the difference in the density of ice ($\approx 900 \text{ kg/m}^3$) and frozen saturated sediments which generally range in density from 1900 to 2100 kg/m^3 . The result is a negative density differential of about 1100 kg/m^3 . Figure 1.36 shows the cross-section of Involved Hill as determined from comparing gravity modeling with the profile from

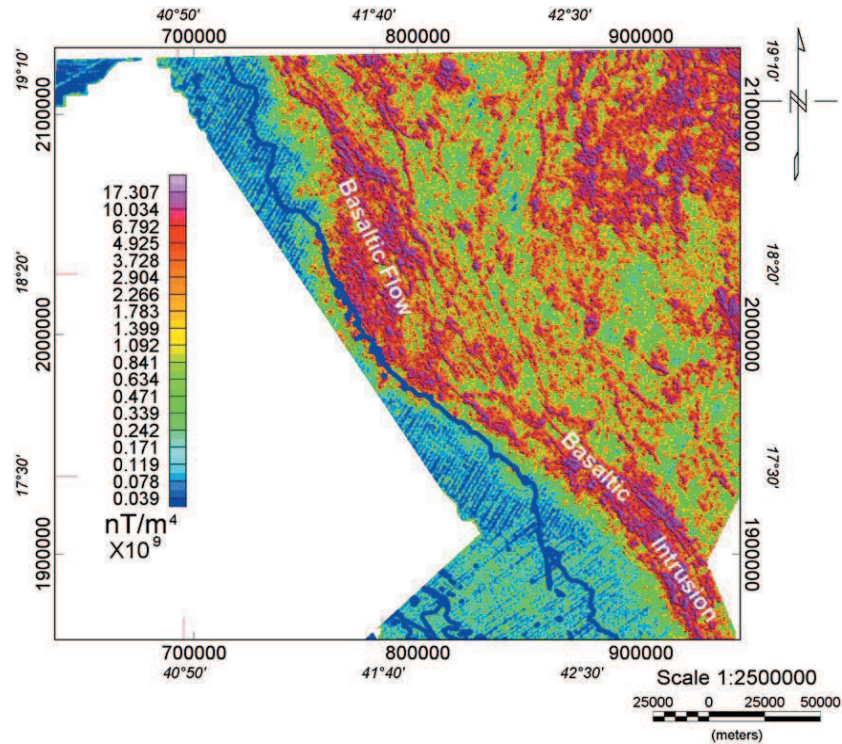


Figure 1.34 Enhanced reduced-to-pole total magnetic intensity anomaly map of southwestern Saudi Arabia derived from horizontal derivative, second vertical derivative, and analytic signal processing. Adapted from Elawadi et al. (2012). Available at doi:10.1088/1742 – 2132/9/327

drilling. The close correlation of these cross-sections validates the use of the gravity method in this application.

This case history and the marked density differential between ice and frozen saturated sediments suggests other applications in localizing and studying the presence or gaps in the occurrence of ice in the subsurface of permafrost regions. Microgravity surveys, for example, can map man-made subsurface changes, such as melting of permafrost beneath surface structures and the emplacement of concrete in subsurface voids.

Another interesting example of the application of the gravity method to determining subsurface properties is for determining the density of stockpiles of strategic ores maintained by the U.S. Defense National Stockpile Center (Sjostrom and Berry, 1996; Butler et al., 1997). The method of Nettleton (1939) or one of the subsequently developed analytical methods can help evaluate the *in situ* density of the stockpiles, and thus the tonnage

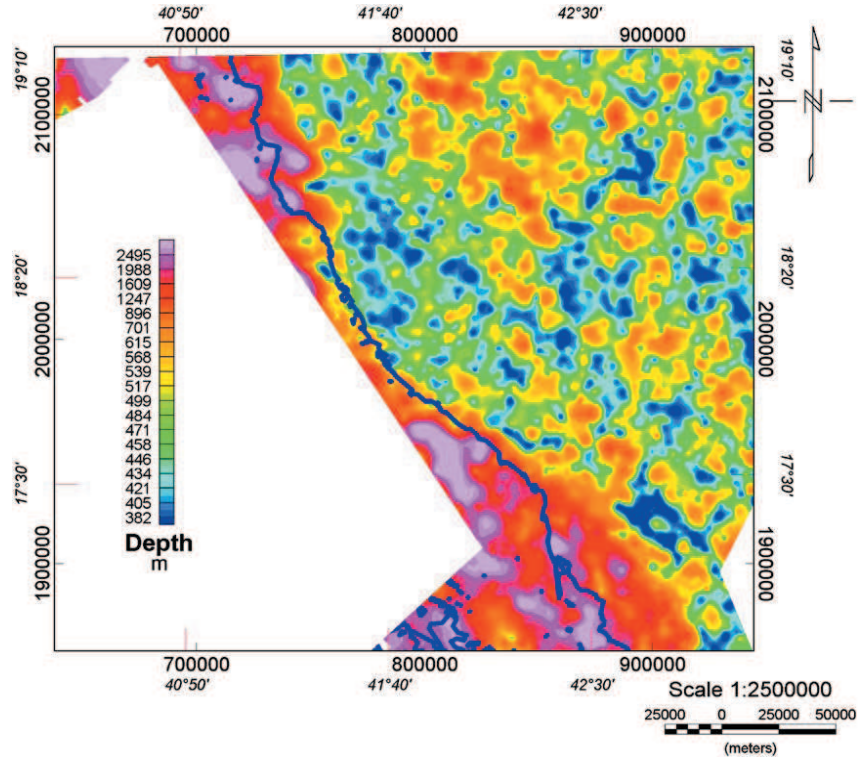


Figure 1.35 Local wavenumber (source parameter imaging) depth determination of southwestern Saudi Arabia. Adapted from Elawadi et al. (2012). Available at doi:10.1088/1742 – 2132/9/327

of ore present in the stockpile. This density is determined by minimizing the correlation between the topographic elevation and the computed gravity anomaly by varying the density of the mass included in the topographic relief. Figure 1.37 illustrates the topography of a profile over a stockpile of high-carbon ferrochrome that was gravimetrically surveyed and a plot of values used in a method of determining densities from these measurements developed by Parasnis (1979). In this case the least squares line through the measurements has a slope, and thus a density of 3025 kg/m^3 . Conventional methods of determining density are subject to error due to heterogeneity in the densities of the ore samples and difficulties in estimating the pore space of the stockpile. Although this method commonly is performed on gravity profiles, the method of determining *in situ* density can be obtained from areal measurements as well [e.g., Grant and Elsharty (1962)]. In a similar manner it is possible to determine the densities of topographic features for a number of other applications related to *in situ* densities, for example, the

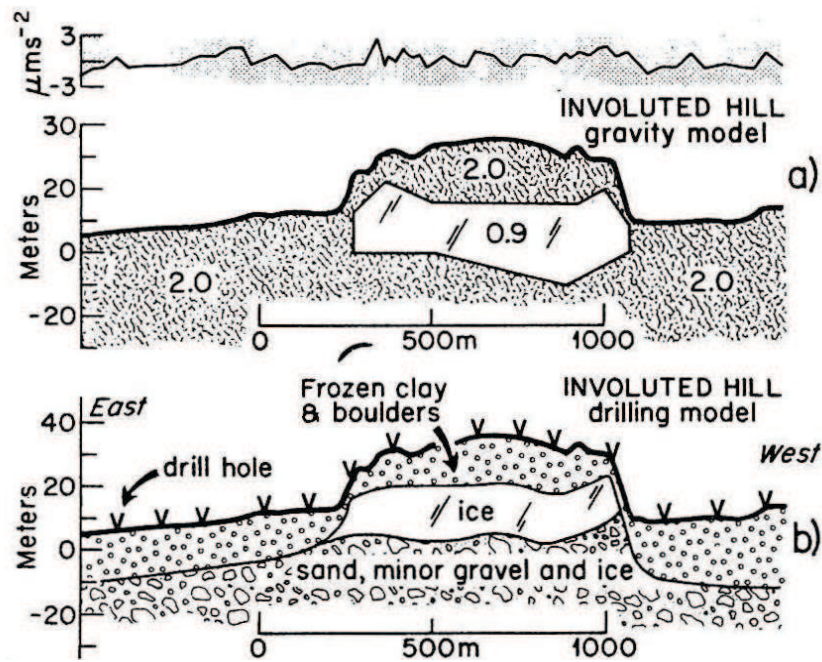


Figure 1.36 (a) Involuteds Hills cross-section showing the location of the ice lens derived from gravity modeling and (b) drill holes. The upper profile shows the residual between the observed and modeled gravity. $1\mu\text{ m/s}^2 = 0.1\text{ mGal}$. Adapted from Rampton and Walcott (1974).

degree of water saturation of a hill. Another example is the determination of the density of bioreactor landfills because of its importance in the biodegradation of anaerobic landfills. Harris et al. (2013) have illustrated the use of gravity for this purpose with the mapping of both spatial and temporal variations in the density of a bioreactor landfill in Quebec using Gauss's theorem to determine the density of the landfill from successive gravity surveys as the landfill was constructed.

Magnetics can be used to characterize surface concentrations of magnetite in clastic sediments. Magnetite is preferentially deposited with other heavy minerals and lithologic fragments in high-energy fluvial and lacustrine environments and is present to varying degrees in sediments reflecting their provenance. For example, kames and eskers in de-glaciated terranes are relatively rich in magnetite in the northern midcontinent of North America (Onesti and Hinze, 1970) resulting in significant local magnetic anomalies. Chandler (1985) has shown that eskers can be mapped with aeromagnetic surveys, providing important information on the hydrogeology of an area,

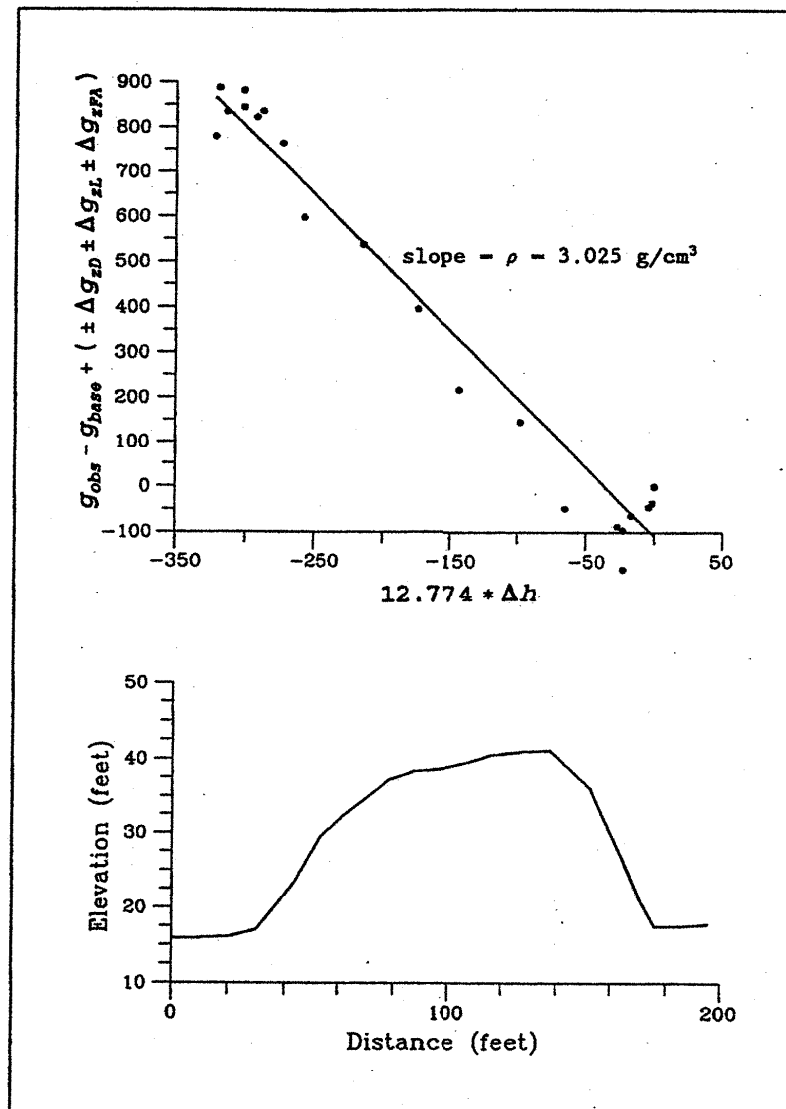


Figure 1.37 Illustration of the application of Parasnis' method for computing the density of the high-carbon ferrochrome stockpile whose profile is shown in the lower panel. The slope of the least squares line in the upper panel indicates a density of 3.025 g/cm^3 . Adapted from Sjostrom and Berry (1996).

and Gay (2004) has given several examples of magnetic anomalies derived from glacial till detected in aerial surveys. Stream channels also have been

mapped in the alluvial terrain of the southwestern U.S. with the magnetic method (Mahrer et al., 1984).

1.7 Subsurface Void Mapping

Natural cavities in the subsurface, such as caves and ice crevasses, and man-made subterranean openings, including mine workings, tunnels, and tombs commonly are the target of near-surface geophysical studies (Daniels, 1988). The gravity method is particularly amenable to these studies because of the large density contrast between the void and the surrounding Earth material. This is particularly true when the void is air filled so that the density of the void is negligible, but even where the openings are filled with water the density differential remains one of the highest within the Earth. The use of magnetic methods in this application is limited to specialized subsurface conditions.

Numerous examples occur that show gravity anomalies associated with natural caves and solution areas. Figure 1.38 shows the residual gravity anomaly of roughly 0.35 mGal associated with a known cavity in limestone (Butler, 1984). Figure 1.39 is the complete Bouguer gravity anomaly map prepared from a microgravity survey within the limits of Grand Rapids, Michigan after the collapse of the surface material into a cavity within the gypsum which underlies portions of the city (Oray and Sanderson, 1967). The gravity anomaly which reaches a maximum magnitude of 0.25 mGal extends southeasterly from the surface collapse zone. The successful mapping of this hazard was useful in assessing the potential danger that the cave posed to the city.

A similar result was obtained with a gravity survey in the Al-Dahr residential area of Kuwait (Al-Rifaiy, 1990). Analysis of the gravity data identified anomalies of the order of -0.20 to -0.80 mGal associated with solution cavities in a bedrock limestone formation at a depth of roughly 35 m and the related collapsed and filled zones within the clastic sediment layer overlying the bedrock. Drilling on gravity minima indicated that the gravity anomalies delimit areas of moderate to high risk related to migration of surface material into the limestone cavities and vertical migration of collapse features to the surface. Figure 1.40 indicates the position of a rubble-filled solution cavity in a limestone formation where the gravity anomaly is caused not only by the solution cavity, but also by the fractured collapse zone above the cavity (Yuhr et al., 1993). It is significant to note that observed gravity anomalies over subsurface openings are frequently greater than the corresponding calculated anomalies because of jointing, stress relief, and solutioning in-

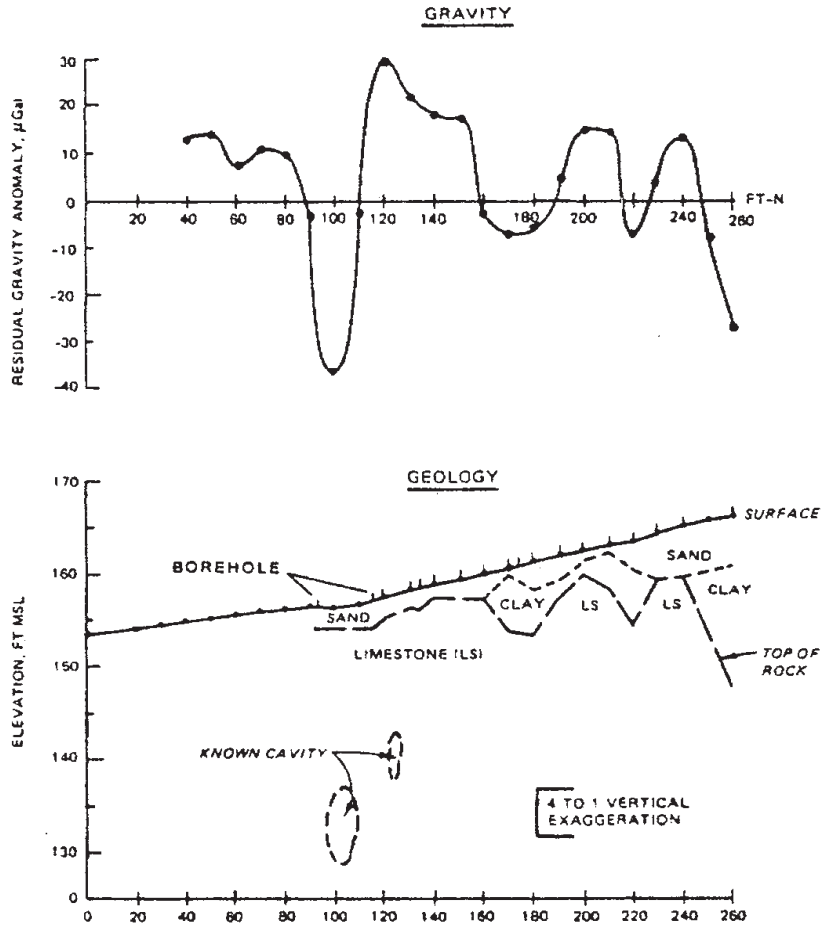


Figure 1.38 Residual gravity anomaly plotted over near-surface cross-section of the Earth. Note the negative gravity anomaly with an amplitude of 0.35 mGal over the known cavity in limestone. Adapted from Butler (1984).

duced by the void in the surrounding rocks. Areas of potential solutioning, and thus potential foundation problems have been mapped in Figure 1.41 in the vicinity of a dam by the associated negative gravity anomalies (Yule et al., 1998). Several of the negative gravity anomalies reach magnitudes in excess of -0.20 mGal. Beres et al. (2001) have shown the useful integration of ground penetrating radar results with microgravity surveying in the mapping and characterization of caves in the Jura Mountains. Hammond and Murphy (2003) report the mapping of solution cavities in South Africa



Figure 1.39 Complete Bouguer gravity anomaly map over a near-surface solution cavity in Grand Rapids, MI. Contour interval is 0.05 mGal. The colored area at the northwest end of the gravity anomaly minimum marks the limits of a surface collapse zone. Adapted from Oray and Sanderson (1967).

using the gravity tensor measurements mapped by the FTG Bell Geospace airborne gravity gradiometer.

Abandoned underground workings may be a hazard for construction and to population centers because of the possibility of collapse of the overlying rocks and surface material into the opening. As a result of their density contrast with the adjacent rocks these features are commonly the target of gravity surveys. Neumann (1967) shows the residual gravity anomaly, which reaches an amplitude of -0.30 mGal in the left map of Figure 1.42, that is associated with an underground quarry. The right map shows the position of the quarry workings. An underground coal mine in southern Wales is clearly indicated in the gravity anomaly profile shown in Figure 1.43 from Bishop et al. (1997). The residual negative anomaly related to the mine working in the upper seam of Figure 1.43 has an amplitude of the order of -0.25 mGal. Rene (2000) conducted a gravity survey over the abandoned, water-filled Gheens Mill Cementville Mine in southeastern Indiana. This mine, which occurs at a depth of approximately 8 m and has an estimated height of 4.3 m, produces a gravity anomaly of -1.43 mGal. Figure 1.44 shows a map of the mine and its modeled gravity anomaly assuming a density contrast of -1650 kg/m³. The two profiles across the mine in Figure 1.44 compare the observed and modeled gravity anomalies.

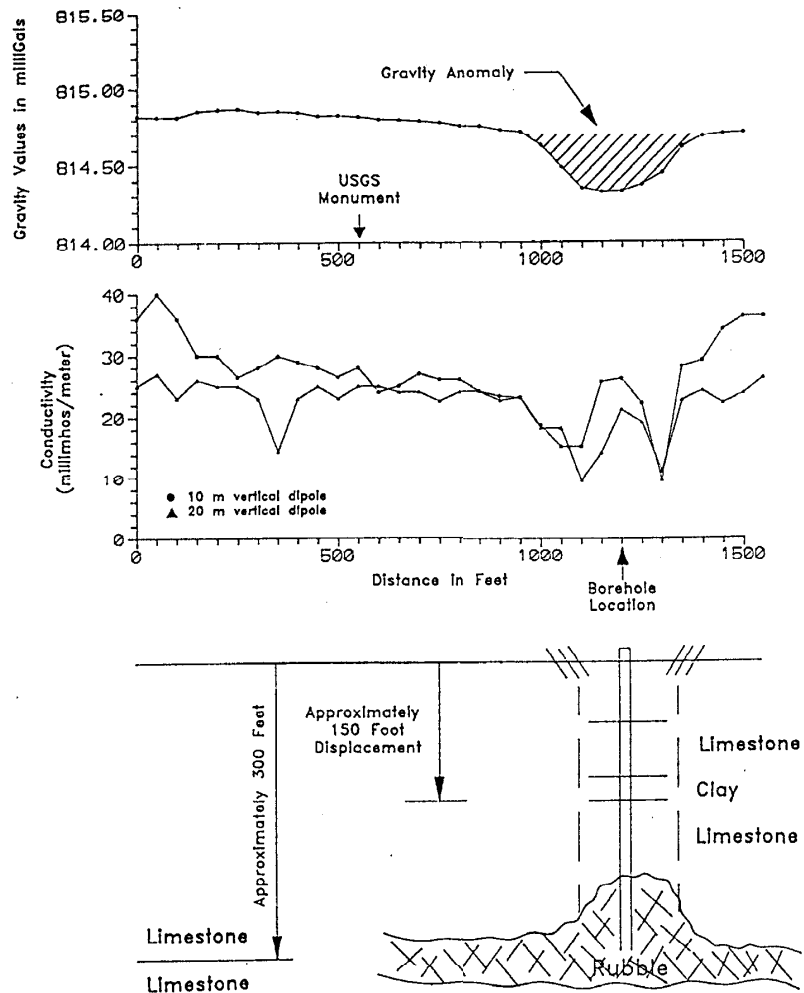


Figure 1.40 Electromagnetic and gravity anomaly profile showing a gravity minimum associated with a rubble-filled solution cavity in limestone. Adapted from Yuhr et al. (1993).

Gravity methods also may be used in detecting hidden subsurface chambers and tunnels, but the anomalies are of low amplitude because of the typically small volume of the voids. As a result extreme care must be exercised in conducting and reducing the data of surveys for these subterranean features. Cuss and Styles (1999) show the usefulness of the gravity method in mapping poorly mapped tunnels in municipalities. Won et al. (2004) show

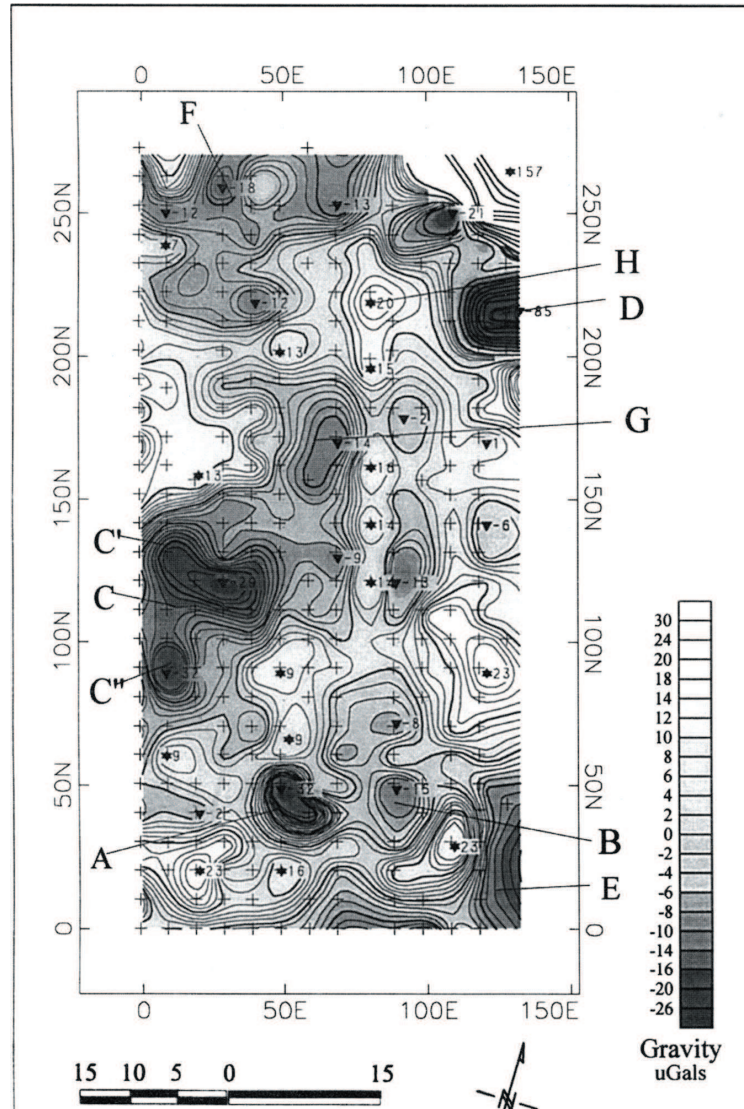


Figure 1.41 Residual gravity anomaly map showing the location of negative anomalies that may be related to solution zones in the carbonate bedrock in the vicinity of the Wilson Dam, AL. Contour interval is 0.10 mGal. Adapted from Yule et al. (1998).

the detection of a palace wine cellar by the gravity method during weapons inspections in Baghdad, Iraq and Blizkovsky (1979) presents a case history of the detection of burial tombs in the floor of a church. The anomalies detected over the tombs, which are of the order of magnitude of 0.10 mGal

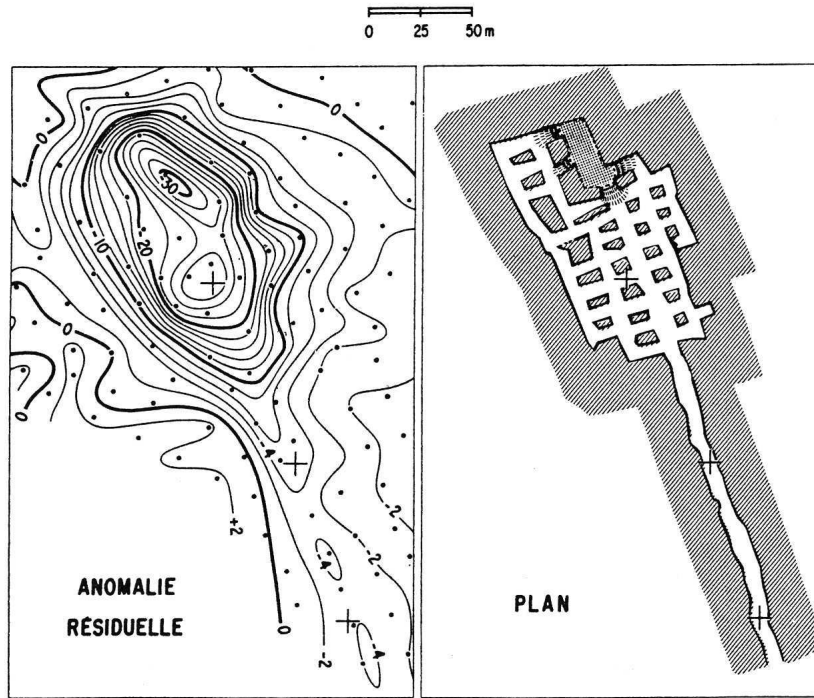


Figure 1.42 Residual gravity anomaly (left) associated with an underground quarry (right). Contour interval of the gravity map is 0.02 mGals. Adapted from Neumann (1967).

only, present a coherent picture after corrections are made for the walls of the church and its crypts. In general, the use of the gravity method in archaeological studies has been limited by the time and effort to reduce data for elevation and terrain effects (Wynn, 1986). However, the advent of GPS technology has seriously reduced the impact of this limitation.

The magnetic method also has been useful in characterizing near-surface lithologies and structures in specialized situations. For example, lava tubes where magma has drained from the interior of flows leaving long, narrow voids supported by the surrounding crystallized lava have been mapped by the magnetic method (Arzate et al., 1990) and man-made openings in an iron formation have also been detected (Cohen et al., 1992). More recently Rybakov et al. (2005) have reported on the successful use of micromagnetics to map underground openings in low-magnetization sediments in the Dead Sea rift region. They have mapped total magnetic anomalies of only a few nanoteslas in amplitude associated with verified subsurface voids. The mag-

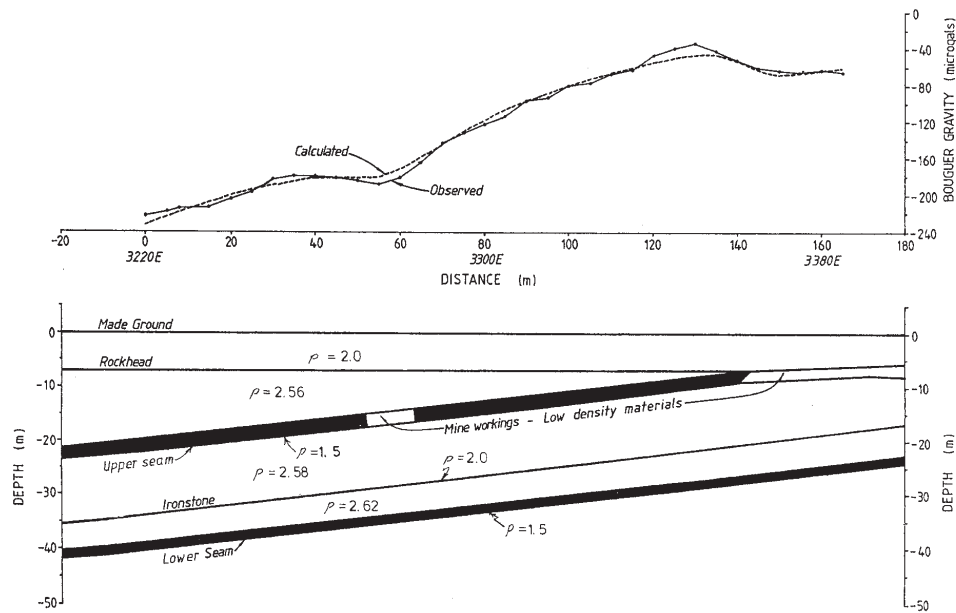


Figure 1.43 Observed and compute gravity anomaly over an underground coal mine in southern Wales. Densities (ρ) are in g/cm^3 . Adapted from Bishop et al. (1997).

netic method may not be as precise in mapping underground voids as the gravity method, but where magnetization contrasts do occur it is an attractive alternative because of the relative ease of making and reducing magnetic measurements to a usable form.

1.8 Buried Ferro-Metallic Material Identification

There is an increasing demand to locate buried metal drums and tanks which contain hazardous materials, to detect borehole casings of abandoned wells which may pose an environmental hazard, and to find other hidden iron and steel objects. Ferro-metallic objects are intensely magnetic (Figure 1.45) if they are not altered to non-magnetic oxides, and therefore are readily detectable by magnetic mapping of sufficient resolution. This is one of the principal uses of the magnetic method in near-surface studies and site characterization. With sufficient surveying detail it is possible to not only locate and determine the size of the sources, but also estimate their approximate depth from anomaly characteristics.

It has been commonplace to place hazardous wastes in steel drums and

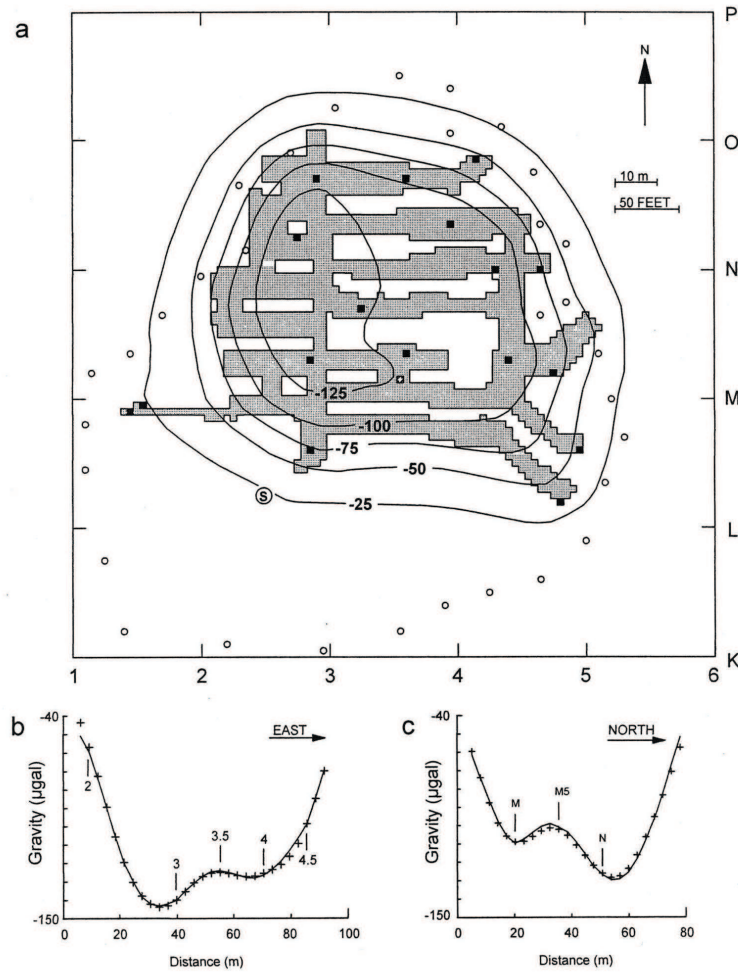


Figure 1.44 (a) Map of the Gheens Mill Cementville Mine, IN showing the inverse model of the mine workings (stippled), contours of the modeled gravity anomaly field at 0.25-mGal intervals, drill holes that penetrated the mine workings (closed circles), drill holes that did not penetrate the mine (open circles), and backfilled slope shaft (S). (b) and (c) modeled gravity (plus signs) and residual Bouguer gravity anomaly profiles along west-to-east and south-to-north profiles, respectively. Adapted from Rene (2000).

bury them to minimize their impact on humans and the environment. Unfortunately, with time these drums undergo corrosion permitting the waste to leak out and interact with infiltrating ground water. As a result there has been a global effort to identify the location of the buried waste-containing

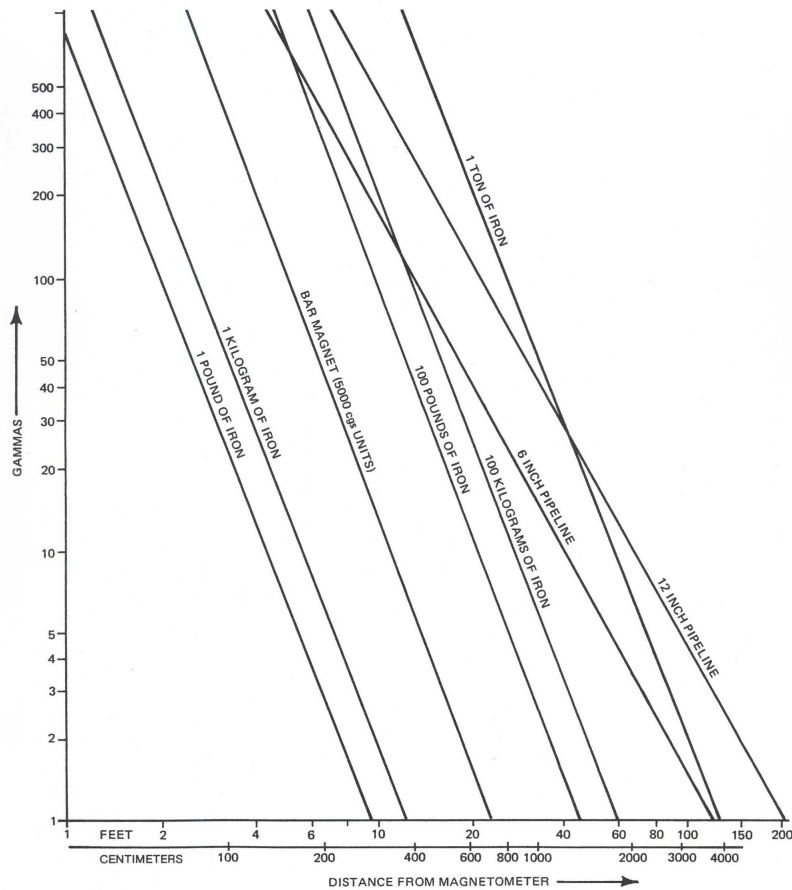


Figure 1.45 Chart for estimating anomalies from typical objects [assuming a dipole magnetic moment of 5×10^5 CGSu/ton] as a function of distance between source and sensor. The estimates valid only to within an order of magnitude. Adapted from Breiner (1973).

drums and retrieve them for remediation. Magnetic methods are used widely for this mapping purpose [e.g., Tyagi et al. (1983)]. The success of the method is dependent on the ability to discern the drum anomalies from the background magnetic variations. A critical factor in this is a sufficiently detailed survey that will have multiple stations located within an anomaly level that is above local noise levels. This will depend on the depth of the drums because of the decrease in the amplitude and broadening of the anomaly with increasing depth of burial (Figure 1.46), the less profound effects of drum orientation (Figure 1.47), and the background magnetic noise level.

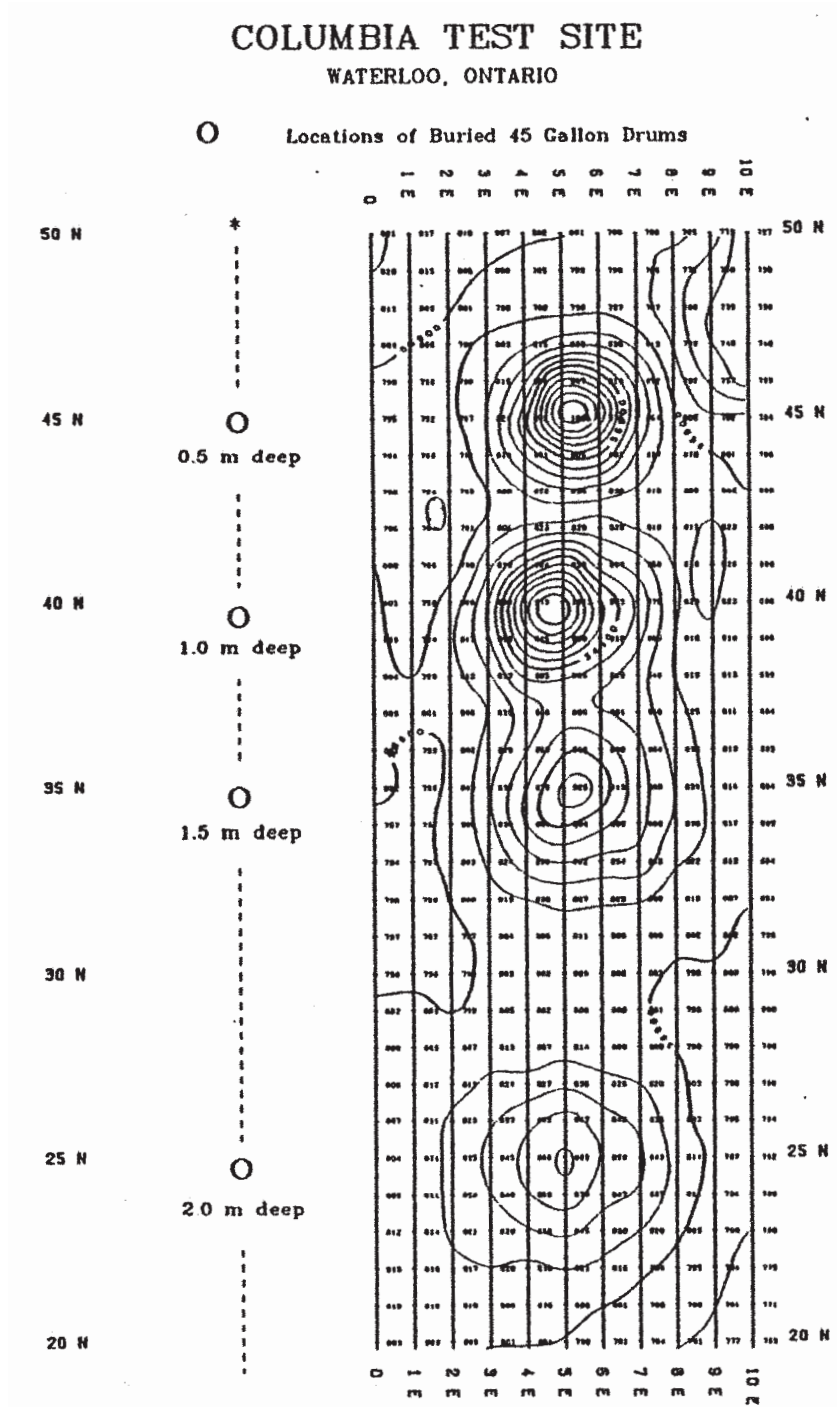


Figure 1.46 Total magnetic intensity anomaly map over four 45 gallon steel drums buried at 0.5, 1.0, 1.5, and 2.0 m as indicated. The contour interval is 20 nT. Adapted from Seigel (1993).

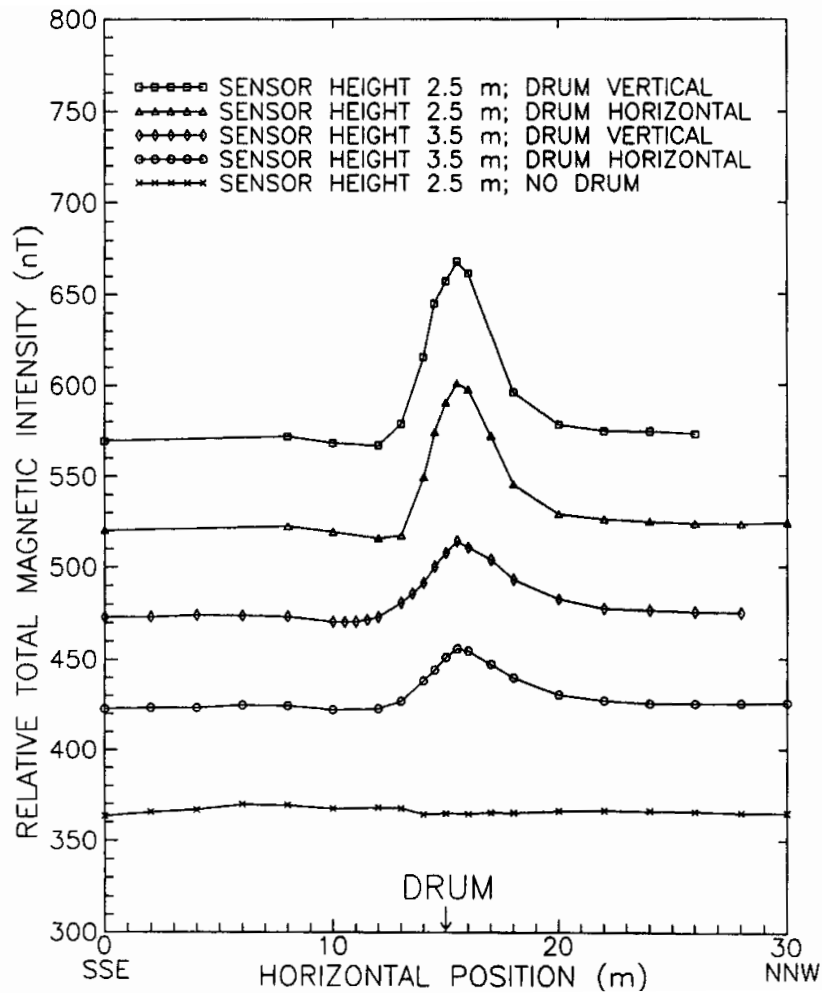


Figure 1.47 Total magnetic intensity anomaly profiles across a site without and with a 44 gallon drum oriented both horizontally and vertically at heights of 2.5 and 3.5 m. Anomaly profiles are separated for clarity of presentation. Adapted from Emerson et al. (1990) with the permission of ASEG and CSIRO Publishing. Available at <http://www.publish.csiro.au/nid/224/paper/EG992065.htm>

Except in very high noise level regions a maximum separation between stations is of the order of 2 m and single buried drums can be mapped at depths of up to several meters.

Clusters of drums concentrated in a burial location will make the target easier to detect and map because of the increase in the anomaly areal size and amplitude. Figure 1.48 shows an example of locating a small dump of

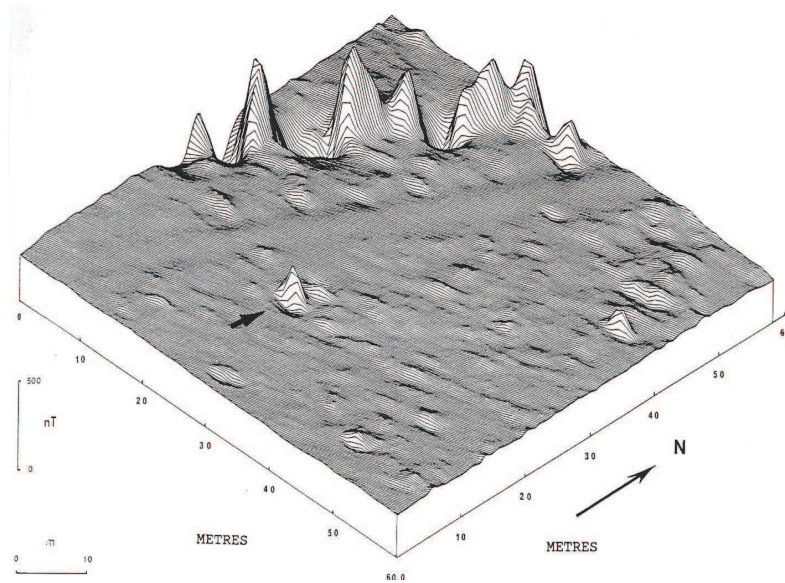


Figure 1.48 Isometric diagram of the magnetic anomaly field over an area in Australia believed to include the site of a small dump of ferro-metallic canisters that contain highly toxic waste. The anomaly at the tip of the arrow is believed to be the anomaly associated with the canisters. Also identified in this image is an intense linear anomaly due to a buried sewer pipe and a subtle, smooth, linear anomaly parallel to the pipe resulting from removal of the magnetic surface material during road construction. Adapted from Stanley and Cattach (1990) with the permission of ASEG and CSIRO Publishing. Available at <http://www.publish.csiro.au/nid/224/paper/EG990001.htm>

metal canisters containing toxic wastes from Australia (Stanley and Cattach, 1990). The isometric diagram of the total magnetic field intensity indicates the position of the dump at the tip of the arrow. This illustration also shows a linear intense magnetic anomaly pattern transecting the northwest portion of the figure locating the position of a buried metal sewer pipe. The smooth pattern of the magnetic background that parallels the sewer pipe anomaly reflects the removal of the magnetic topsoil from the surface in constructing a roadway. Buried steel storage tanks also are suitable targets for the magnetic method. Figure 1.49 shows the intense observed total field and vertical gradient magnetic anomalies over underground storage tanks (Schilinger, 1990). The increased resolution of the location of the tanks is readily seen in the vertical gradient anomalies.

The magnetization of steel drums and tanks is complex reflecting the amount and type of steel used in the drum, its mechanical, thermal, and

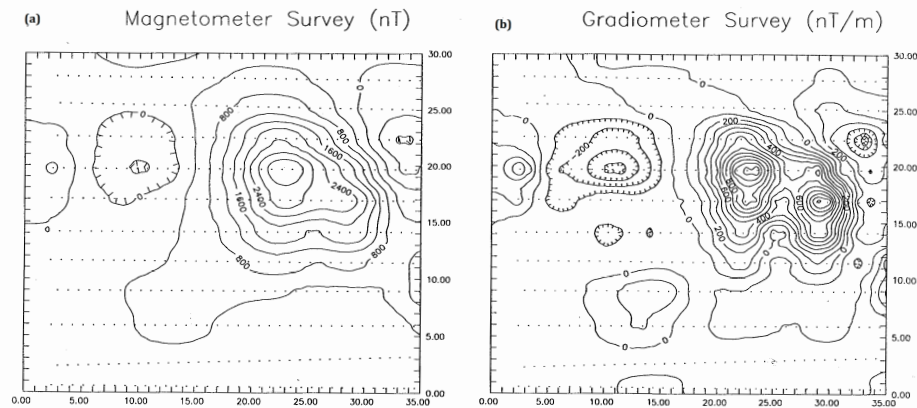


Figure 1.49 (a) Total magnetic intensity anomaly map with contour interval of 400 nT, and (b) vertical gradient of the total field with contour interval of 100 nT/m. The anomaly in the right center is believed to be over a steel tank. The two separate vertical gradient anomalies may mark the ends of the tank. Adapted from Schilinger (1990).

corrosion history, and shape demagnetization. Both induced and remanent magnetization potentially are significant in determining the magnetization, but Emerson et al. (1990) and Ravat (1996) found that the induced component is much larger than the remanent component in unrusted drums. The magnetic moment of steel typically ranges from 100 to 1000 A/m² per ton with one ton causing an anomaly of roughly 100 nT at 8 meters, diminishing to 1 nT at 40 meters (Emerson et al., 1990). Steel rusts when exposed to oxidation producing a much lower magnetization iron oxide. As a result it is anticipated that the magnetization of underground steel objects will decrease as they rust (Emerson et al., 1990), although the relationship between rusting and magnetization is complex.

The metal casing in abandoned wells makes them an attractive target for the magnetic method. As illustrated in Figure 1.50, high-density surface magnetic observations readily map the location of abandoned wells by virtue of the intense magnetic anomalies associated with their casing (Martinek, 1988). To increase the efficiency of mapping abandoned boreholes in oil and gas fields Frischknecht et al. (1983) showed that anomalies from cased wells can be observed in aeromagnetic investigations up to altitudes of the order of 75 m (Figure 1.51). The limiting altitude of successful aeromagnetic surveying is dependent on the size and depth extent of the casing and the background magnetic noise levels.

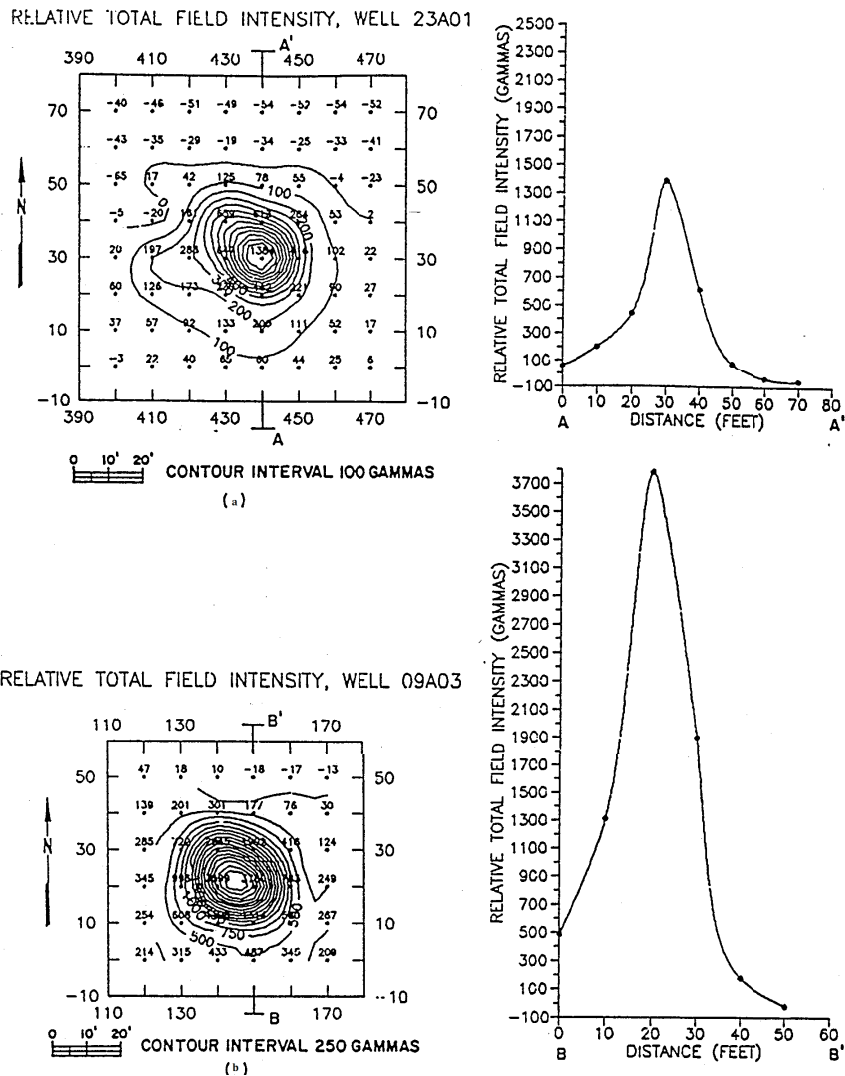


Figure 1.50 Examples of surface total magnetic intensity anomaly maps and profiles across two vertical steel well casings. Note the difference in the contour interval of the two maps. (a) Galvanized steel casing 1/8 inch thick and 24 inches in diameter extending to a reported depth of 63 feet. (b) Steel casing 1/8 inch thick and 4.5 inches in diameter extending to a reported depth of 500 feet. Adapted from Martinek (1988).

Unexploded ordnance, which causes problems in reclaiming land formerly used as military firing and bombing ranges, are also located by the magnetic method [e.g., Butler (2001), butler-et-al-12, doll-et-al-12]Temp]. The limited

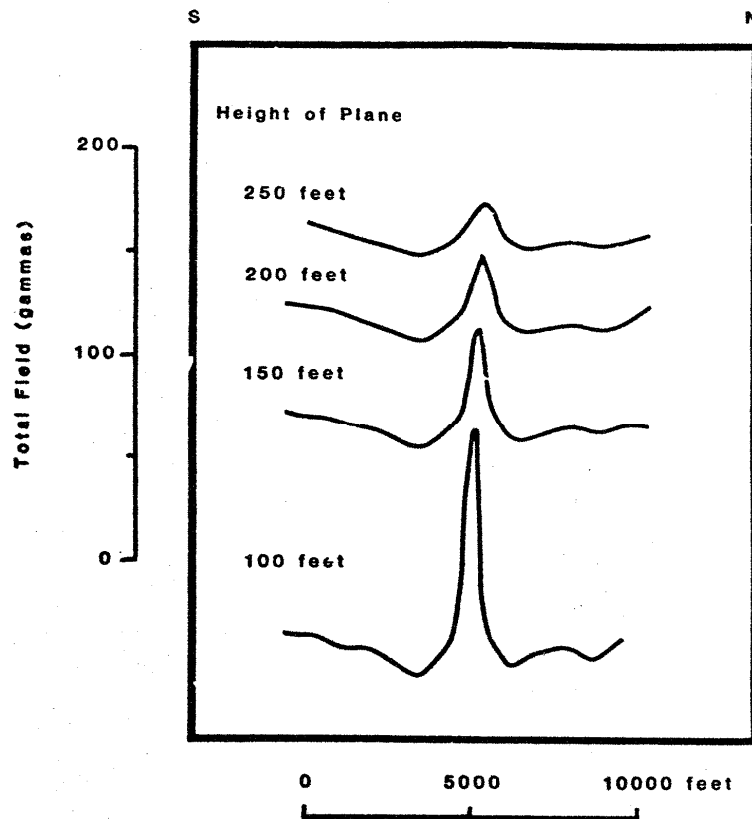


Figure 1.51 Stacked total magnetic intensity anomaly profiles [north-south] observed over a cased well in the Piney Creek, Colorado area at heights of 100, 150, 200, and 250 feet [30, 45, 60, and 75 meters] above the ground surface. Adapted from Frischknecht and Raab (1984).

size and amount of ferrous materials of many ordnance pieces makes them a challenging target particularly in magnetically noisy environments because the anomaly amplitudes decrease rapidly with increasing source/sensor separation. Figure 1.52 illustrates the approximate maximum total field magnetic anomalies associated with a variety of different ordnance pieces as a function of source depth. Detection of these targets is difficult where buried at much more than a few meters of depth even in relatively magnetically quiet environments. Specialized survey techniques are employed to expedite the surveying of extensive regions for ordnance. For example, magnetic sensors in booms that are flown on helicopters at only a few meters above the

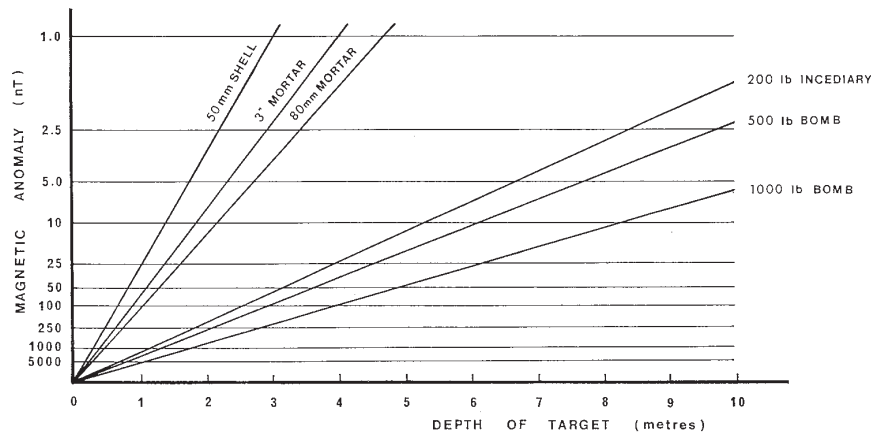


Figure 1.52 Examples of approximate maximum magnetic anomaly of a variety of explosive ordnance pieces as a function of depth below the magnetic sensor. To be detected the ordnance must be at depth below the sensor that does not result in anomaly amplitudes that are less than a threshold value (usually several nT) above the background magnetic anomalies that are of approximately the same size as the ordnance anomalies. Adapted from Stanley and Cattach (1990). Available at <http://www.publish.csiro.au/nid/224/paper/EG990001.htm>

surface are used to maximize the intensity of the target anomalies while efficiently surveying large areas. Characterization of the range of signatures of specific pieces of buried ordnance is an important step in discriminating anomalies of live ammunition from those due to inert ferrous objects.

1.9 Archaeological Exploration and Evaluation

The non-invasive nature of the gravity and magnetic methods makes them well suited for studying the culturally sensitive, fragile subsurface environments of archeological sites. To date, the gravity method has enjoyed relatively limited direct application in archaeology. However, it has been very effective in locating ancient mining and other underground workings in urban settings where seismic and electrical methods are difficult to apply due to the excessive noise levels. In Europe, for example, modern buildings and development are threatened for cities founded on ancient unmapped mine workings that are now lost beneath many layers of urban growth. Gravity detection of these subsurface menaces is possible because they commonly involve voids that define strong negative density contrasts at relatively shallow depths. Vertical gradient gravity anomalies have a higher resolution

than normal anomalies, and thus have found important uses in archaeological studies. Examples include using vertical gradient gravity anomalies to map out the subsurface channels of streams in downtown Boston that were lost when the early inhabitants paved them over (Griffiths and King, 1981), and the buried 14th century Ming Dynasty mausoleums of Mao Ling and Ding Ling in Beijing, China (Hao and Wang, 2000).

The magnetic method has a much more central role in locating and studying historical and pre-historical archeological sites because of its relative efficiency and effectiveness, and the wide variety of magnetic sources related to human inhabitation. As previously discussed (Chapter 10.6) intense magnetic anomalies are not only associated with buried ferro-metallic objects, but near-surface sources result from human disturbance of soils that are vertically stratified with respect to their magnetic properties as a result of chemical changes, and with fired iron-rich clays. The latter are associated with intense and stable thermal remanent magnetization acquired when iron-rich materials are subjected to temperatures in excess of roughly 600°C. As a result, industrial sites, hearths, kilns, ditches, pits, burial sites, foundations, roadways, and underground chambers among others are likely to produce mappable magnetic anomalies. However, limitations in the information provided by and application of the magnetic method often lead to the use of the method in conjunction with other geophysical methods [e.g., Wynn (1990)]. Magnetic methods may be complicated by unwanted signals from anthropogenic ferro-metallic objects and localized highly magnetic earth materials and commonly require a meter or less separation between stations and observation height above the surface. Current technology makes it possible to detect sub-nanotesla anomalies in regions of low background magnetic anomaly levels and to make these measurements rapidly at sites located and mapped by GPS surveying with location and geophysical data sent to a central processor and storage facility by telemetry [e.g., Hill et al. (2004)]. Furthermore, the use of vertically-paired sensors separated at distances of 0.5 to 1 meter to measure the vertical gradient of the total magnetic intensity field eliminate the diurnal effects and improve the horizontal resolution of sources.

The rest of this section gives a few examples illustrating archaeological uses of the method. One of the more dramatic of magnetic signatures used in archaeology is those associated with fired clay. Figure 1.53 shows the roughly 40 nT anomaly associated with a 1800 BCE Australian aboriginal fire-hearth. The magnetic method is not only useful in locating potential archeological sites such as hearths to salvage from construction activities and to optimize locating further surface or subsurface studies, but also in

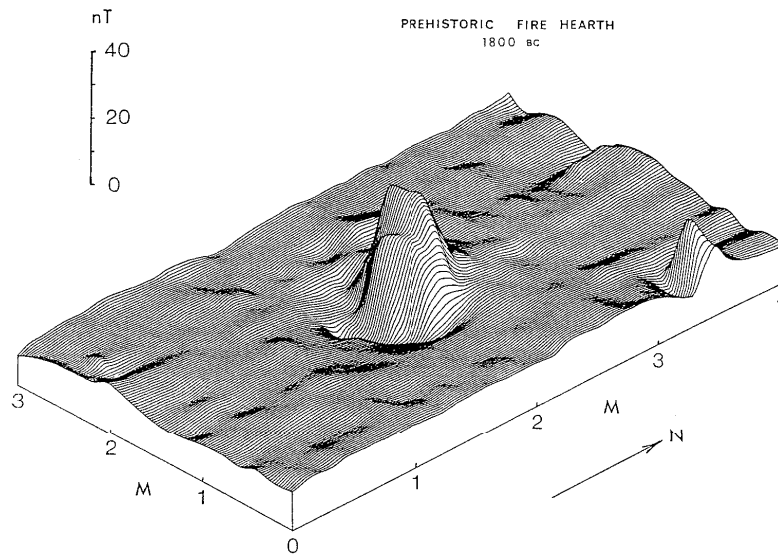


Figure 1.53 An isometric representation of the measured total magnetic field over an Australian aboriginal fire-hearth at Bunda Lake in western New South Wales. Adapted from Stanley and Cattach (1990). Available at <http://www.publish.csiro.au/nid/224/paper/EG990001.htm>

investigating the source of the anomalies. The nature of the sources can be evaluated taking into account the spatial configuration of the anomaly and the relative amplitude of the positive and negative anomaly components. Thus, the source of anomalies can be evaluated with non-invasive procedures. Figure 1.54 is the total intensity magnetic anomaly map of the Fort Ouiatenon site located along the Wabash River near West Lafayette, Indiana. This fort was the site of the first European settlement in Indiana, being established by the French in 1717, and continued in existence for nearly a century. After test excavations discovered the original site, a detailed magnetic survey was conducted to isolate favorable areas for further archaeological study. Figure 1.54 gives the magnetic survey results that revealed numerous anomalies of varying character concentrated mostly in the central and western portions of the site. von Frese and Noble (1984) interpreted the magnetic anomalies for the locations of cabin hearths, stockade trenches, graves and refuse pits, wells, and numerous iron artifacts (e.g., gun parts, household utensils, slag iron from the blacksmith's forge, etc.) as shown in Figure 1.55.

The Fort Ouiatenon magnetic survey (Figure 1.54) was obtained by care-

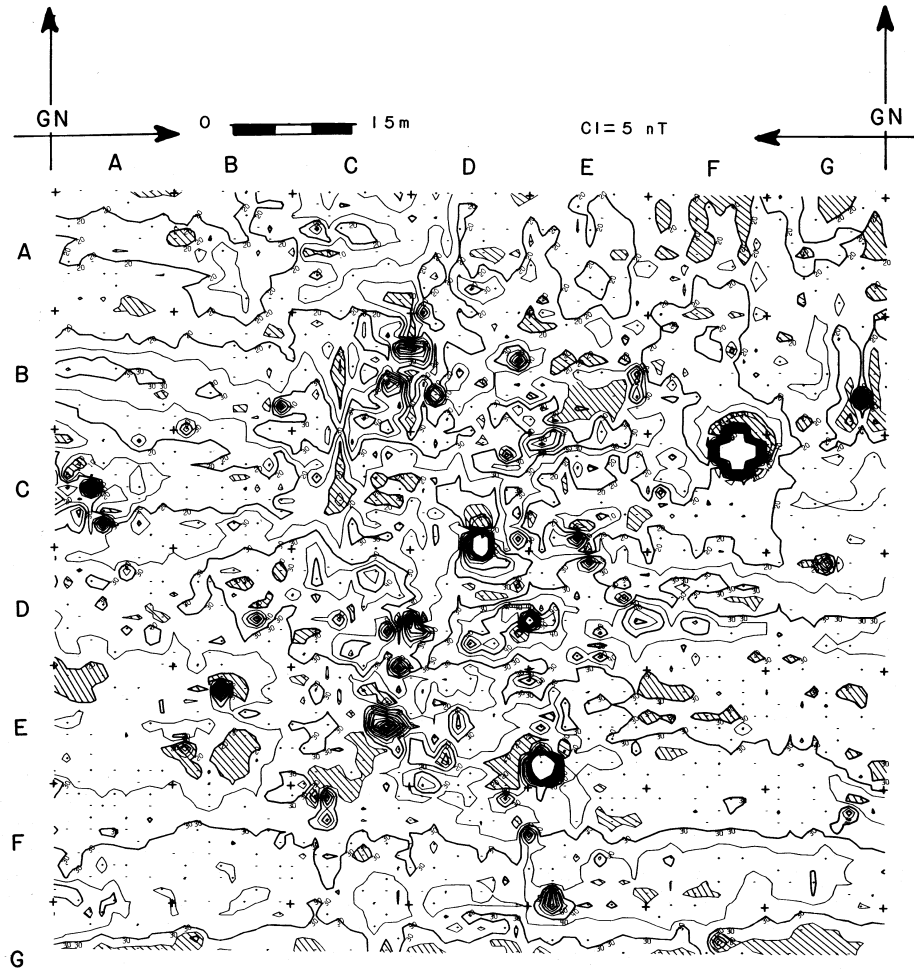


Figure 1.54 Total magnetic intensity anomalies of the Fort Ouiatenon site, West Lafayette, IN. The contour interval is 5 nT and magnetic anomaly minima are shaded. Geomagnetic north (GN) is 0.5° east of geographic north and the inclination of the Earth's magnetic field is approximately 72° . Station interval is 1.5 m and observations were made 0.5 m above the surface. Adapted from von Frese and Noble (1984).

fully establishing a 65×71 grid of stations at the interval of 1.5 m across the site. A single proton precession magnetometer measured each station at 0.5 m above ground level and also monitored the base stations at roughly 20–30 minute intervals. Today, the same field survey and anomaly processing can be completed in a matter of a few hours using an array of 6–12 magnetometers drawn behind an all-terrain vehicle [ATV] equipped with an

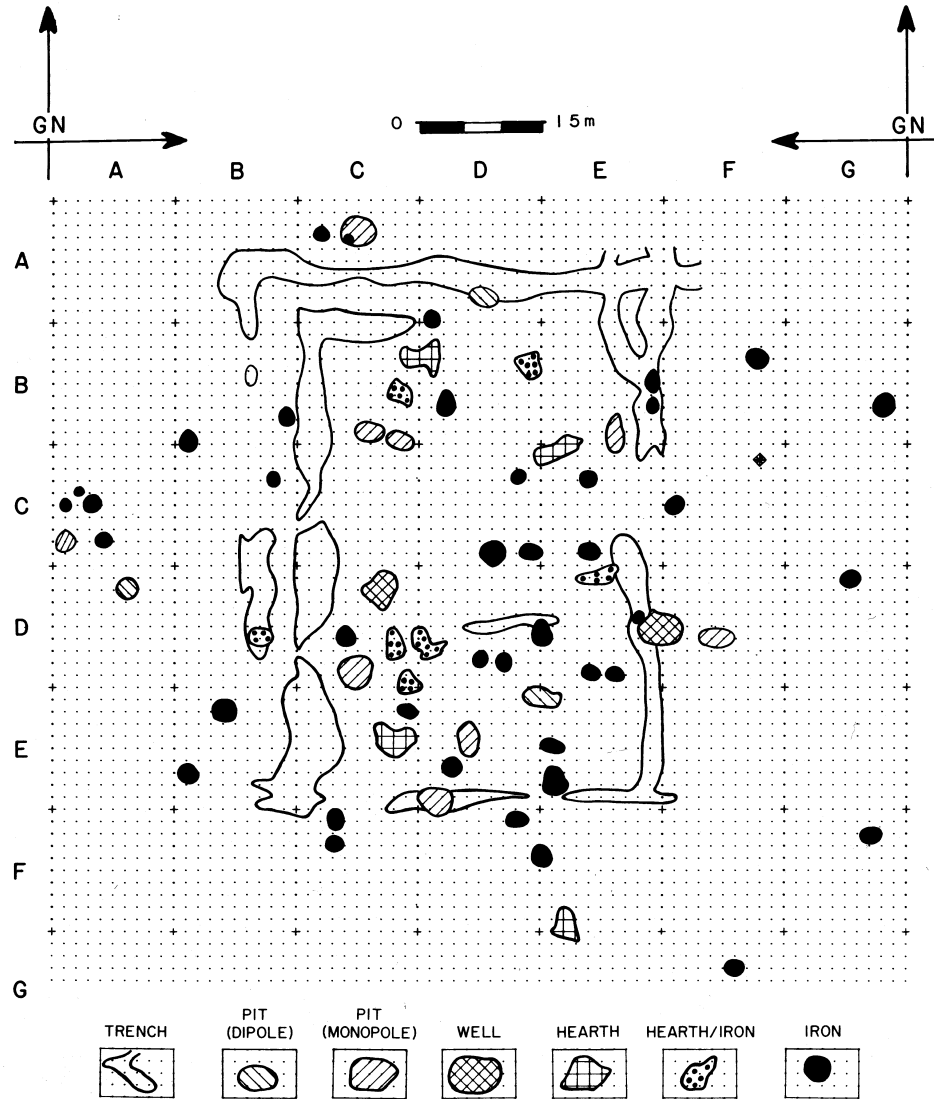


Figure 1.55 Distribution of magnetic artifacts of the Fort Ouiatenon site, West Lafayette, IN interpreted from the magnetic map in Figure 1.54. Adapted from von Frese and Noble (1984).

on-board GPS receiver and laptop computer to process the measurements for the anomaly map in real-time. Having the anomaly map in real-time greatly optimizes the geophysicist's efforts in the field where it is now possible to adjust the survey to better map archaeologically interesting anomalies as they are encountered. The use of magnetometer arrays within meters of

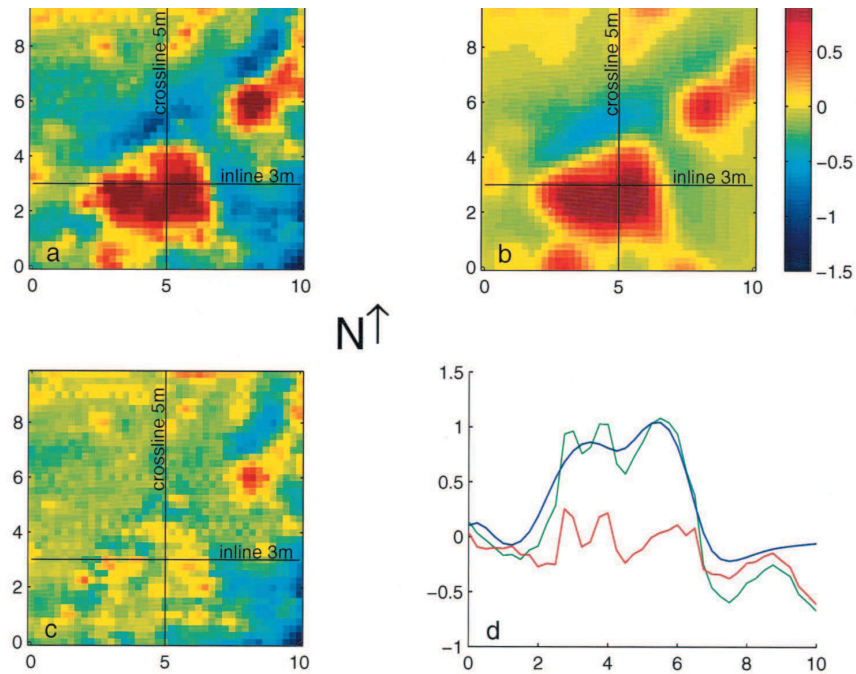


Figure 1.56 (a) Observed vertical magnetic gradiometer map in nT/m across a medieval pit house in northern Switzerland. (b) Computed vertical magnetic gradient map from the inversion model derived from the observed data and constraining magnetic susceptibility information. (c) Residual vertical gradient magnetic field differences between maps (a) and (b). (d) Comparisons of the 'inline 3m' transects from map (a) [green] and map (b) [blue] and their differences [red]. Adapted from Herwanger et al. (2000).

the sea bed and lake and river bottoms also has wide marine archeological application [e.g., Bascom (1976); Blackman (1973)].

Another interesting example of magnetics in archeological exploration is the use of magnetic gradiometer data to not only identify medieval infilled pit houses in northern Switzerland (Herwanger et al., 2000), but to provide quantitative information regarding the three-dimensional configuration of these houses. The soil that infilled the pit houses after their abandonment has a greater magnetic susceptibility than the sand and gravel deposits in which they were dug. As a result there is a positive magnetic anomaly associated with the infilled houses. To avoid the effect of magnetic fields derived from a local electrical railroad line, a dense vertical-magnetic gradiometer survey was conducted of the study area. Figure 1.56 shows a magnetic gradi-

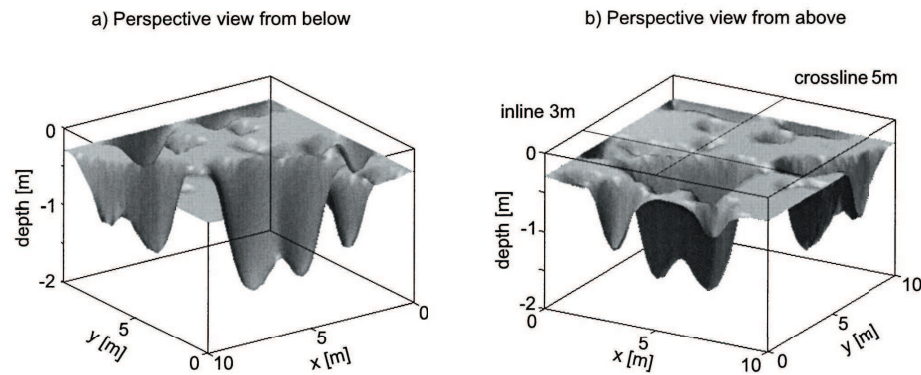


Figure 1.57 Perspective view of results of the inversion of vertical magnetic gradiometer data for the configuration of the infilled medieval pit houses in northern Switzerland. Adapted from Herwanger et al. (2000).

ent profile across one of the anomalies observed in the survey. The intensity of the anomaly is only of the order of 1 nT/m and the anomaly is only a few meters wide. The configuration of the pit house was interpreted by generalized inversion of the areal gradiometer data using a large number of equally sized vertical rectangular blocks [e.g., Li and Oldenburg (1996)] constrained with a magnetic susceptibility contrast [$\approx 4 \times 10^{-4}$ SIu] determined from measurements on samples of topsoil and underlying sand and gravel deposits. Figure 1.56 gives a comparison of the vertical magnetic gradient computed from the inversion model and the observed gradient. The result of the two-dimensional inversion is shown in the perspective diagram of Figure 1.57. The depth of the pit-house was verified by subsequent drilling of the site.

1.10 Time-lapse Studies

Temporal gravity variation investigations, often referred to as time-lapse or 4-D gravity studies, are receiving increasing interest because of their potential applications to a variety of geoscience and engineering problems. These variations cover a broad spectrum of time periods and are derived from multiple sources (Torge, 1989; Biegert et al., 2008) at both regional and local scales. Regional sources are derived from astronomic and planetary dynamics as well as large tectonic changes within the Earth. Most sources of interest to near-surface studies are more local, ranging in scale from meters to several kilometers. Local subsurface sources of interest to these studies are natu-

ral changes in fluid and gas content, movement of magma, and man-made effects.

For most applications the magnitude of the variations are so small that the measurements must be of high precision and the rate of observations must be commensurate with the period of the gravity perturbations. Commonly oversampling is necessary because of the need to separate out noise in the measurements. Sources of error in temporal variations of gravity were described previously in Chapter 6, but detailed consideration of those of particular interest to time-lapse gravity studies are presented in the journal articles of the 4-D gravity monitoring special section of *Geophysics* introduced by Biegert et al. (2008), e.g. (Ferguson et al., 2008; Zumberge et al., 2008). Of particular concern to measurements made for monitoring local temporal variations are long-term drift in the gravity sensors and tidal components and changes in calibration and external effects such as atmospheric pressure variations and microseismic effects. Soil moisture effects also may be important depending on the climatic conditions and the hydrologic properties of the soil. The precision of reduced gravity measurements are reported to be of the order of 5 μGal or less.

A major source of temporal variations is changes in the height of the gravity observation site. Assuming a density of the surface soil of 1800 kg/m^3 , a 0.10 mGal gravity change is associated with approximately a 7.5 cm variation in elevation. Regional changes in surface height may be related to tectonic changes and isostatic responses to mass variations. On a local level, variations in surface elevation may be associated with changes in water levels in lakes, rivers, and reservoirs. For example, Ervin and McGinnis (1986) observed a 0.45 mGal change in gravity related to variation in the stage of the nearby Mississippi River and resulting elevation changes. Another local source of elevation variations are withdrawals of fluids, either oil or water, and gas from the subsurface. Subsidence associated with extraction of fluids may have rates of decimeters per year and total effects may measure several meters.

A potential application of the gravity method is to monitor the time variations in water levels within the adjacent subsurface. Evidence for this is found in several repeat gravity surveys. For example, Lambert and Beaumont (1977) showed measurable changes in gravity related to seasonal variations in ground water levels in New Brunswick (Figure 1.58) and Hunt and Tosha (1994) described the gravity effect associated with fluid depletion from shoreline zones around a lake in New Zealand that had experienced water level changes between gravity surveys. Repeat gravity surveys have proven useful in mapping not only subsurface water level changes, but re-

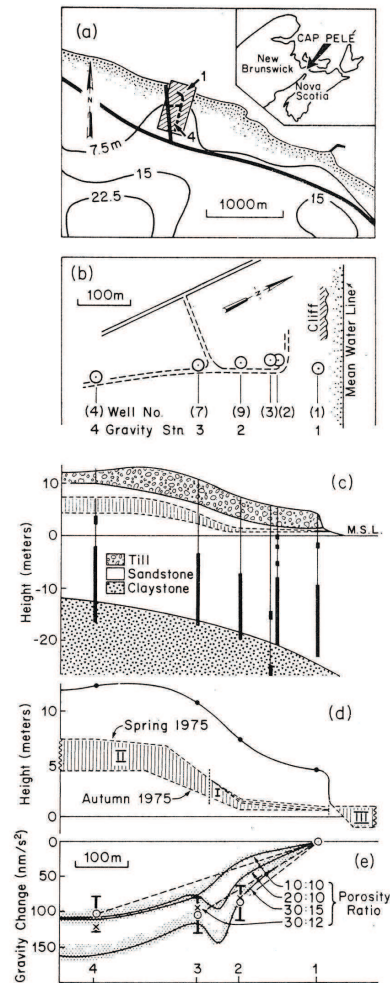


Figure 1.58 Observed relative gravity changes (e) at Cap Pele, New Brunswick, Canada (a) and associated with seasonal [Spring, 1975 to Autumn, 1975] (b) ground water level variations and (c) fluctuating tidal water mass. Panel (e) also shows modeled gravity changes for different porosity ratios between region I and II. The vertical bars on the gravity observations [open circles] of (e) are the 90% confidence limits. The best agreement between observed and modeled gravity assumes the porosity ratio of 30 : 12. Adapted from Lambert and Beaumont (1977).

lating these to the hydrologic properties of the subsurface [e.g., Pool and Eychaner (1995); Chapman et al. (2008); Pool (2008); Jacob et al. (2009)] and also have been used to monitor changes in both space and time of mass in geothermal systems during exploitation [e.g., Allis and Hunt (1986)]. In-

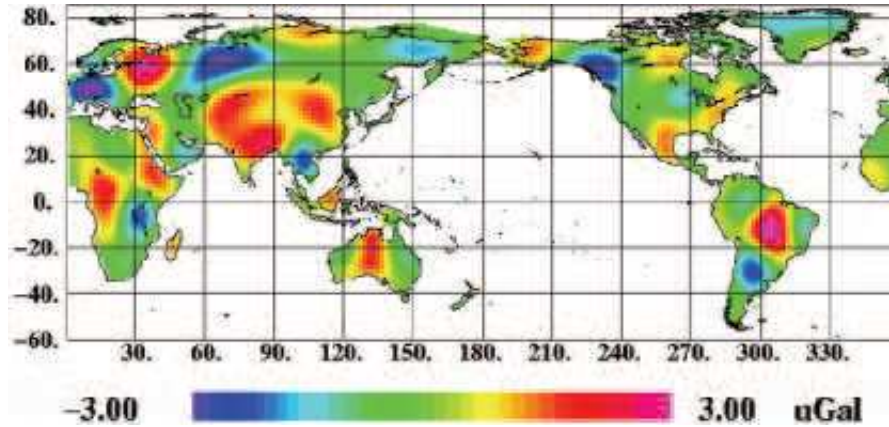


Figure 1.59 Global terrestrial gravity changes in μGal at the Earth's surface between 2002 and 2003 from the GRACE satellite mission. Adapted from Anderson and Hinderer (2005).

terest has developed in studying the gravity effect of extraction of natural gas from gas fields and the insertion of water into the Earth to aid in the secondary recovery of hydrocarbons as a means of studying the nature of subsurface reservoirs and the varying position of gas/water interfaces. Studies by Hare et al. (1999) showed that these are feasible objectives of temporal gravity measurements.

The twin satellites from the joint US-German GRACE mission that was launched in March, 2002 (Tapley et al., 2004; Wahr et al., 2004) have also observed global inter-annual gravity changes related to terrestrial water changes (Anderson and Hinderer, 2005). More recently the higher resolution results from the complementary GOCE satellite launched in 2009 have provided more detailed results. The results from GRACE are capable of measuring the inter-annual changes in ground water with an accuracy of $0.4 \mu\text{Gal}$ corresponding to 9 mm water thickness on spatial scales greater than 1300 km. Figure 1.59 from Anderson and Hinderer (2005) gives the terrestrial gravity field changes between 2002 and 2003 at the Earth's surface where the Bouguer plate correction implies $1 \mu\text{Gal}$ change for 2.4 cm change in water thickness. The prominent $3 \mu\text{Gal}$ decrease in central Europe reflects the loss of ground waters from the 2002 flooding that occurred with the record breaking heat-wave in 2003. Similarly, the $2 \mu\text{Gal}$ decrease in western Canada reflects water loss from the drought in 2003. Extensive 2003 flooding in India most likely produced the $2.5 \mu\text{Gal}$ increase over eastern India. The almost $1.5 \mu\text{Gal}$ gravity increase over central Australia reflects the terrestrial water change that occurred in going from the 4th driest year on

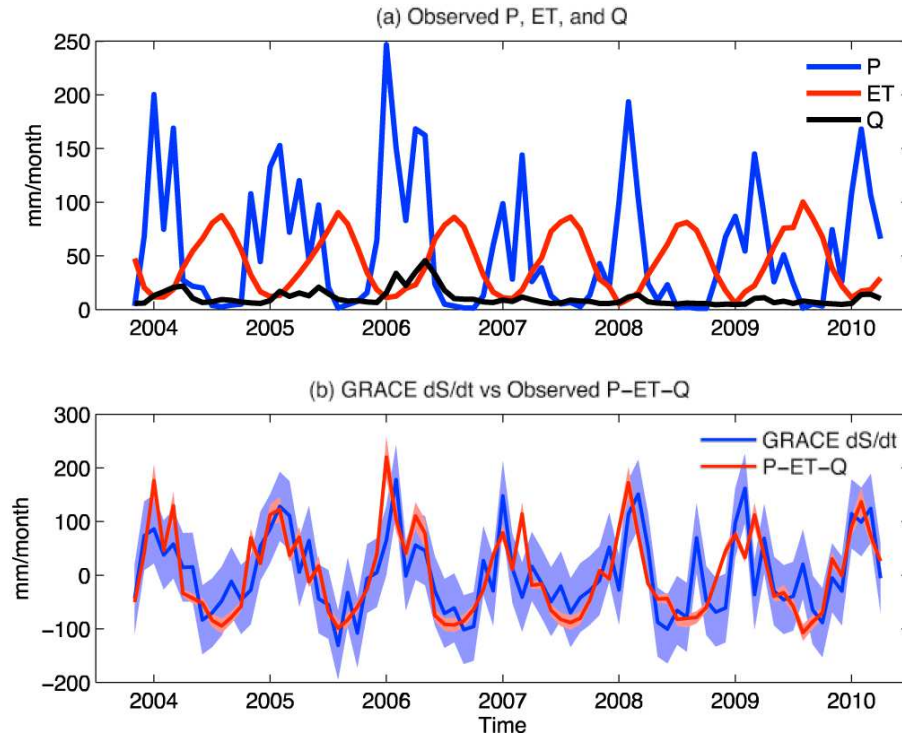


Figure 1.60 (a) Measured precipitation (P), evapotranspiration (ET), and streamflow (Q) (mm/month) from October 2003 to March 2010. The precipitation minus the evapotranspiration and streamflow is the water storage in the Sacramento and San Joaquin basins. (b) Comparison between measured total water storage change and that from GRACE observations. Blue shading shows the GRACE errors and the red shading gives the uncertainty in the measured values. Adapted from Famiglietti et al. (2011).

record in 2002 to a normal year in 2003. Famiglietti et al. (2011) investigated GRACE-mapped temporal gravity variations to show water storage in California's Sacramento and San Joaquin river basins had declined by 31.0 ± 2.7 mm/yr from October, 2002 to March, 2010 [Figure 1.60]. Associated studies indicate that roughly two-thirds of this loss is due to ground water depletion in the Central Valley of California. Temporal gravity variations from the GRACE and GOCE mission observations continue to provide regional hydrologic mass balance data as well as information on ocean circulation and the changes in the ice mass balance of Greenland and Antarctic [e.g., Schrama et al. (2007); Chen et al. (2010); King et al. (2012); Rummel et al. (2011)]. An illustration of the change in the global water thickness from

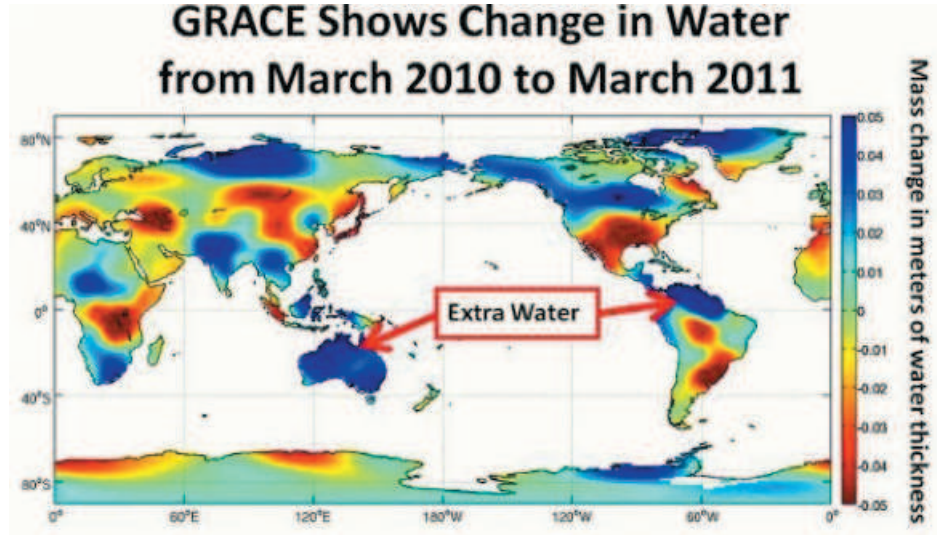


Figure 1.61 Mass changes in meters of global water thickness between March 2010 and March 2011 obtained from gravity observations made by the GRACE satellite mission. The red areas indicate a deficiency in water and the blue regions are where there was an excess of water. Courtesy of NASA/JPL-Caltech.

March 2010 to March 2011 as derived from gravity observations made with the GRACE satellite mission is shown in Figure 1.61.

Temporal gravity changes also have been investigated to determine their potential in identifying precursors to subsurface events which may lead to natural disasters. The method has proven to be potentially useful in monitoring the activity of volcanoes that may lead to eruptions which could be hazardous (Battaglia et al., 2008). Volcanic eruptions are preceded or accompanied in most instances by subsurface changes that may be monitored at the surface (e.g., Kazama et al. (2015)). Examples are surface deformation due to injection or withdrawal of magma, water, or gases, enhanced seismic activity, and changes in the composition of discharging gases. Temporal gravity variations on and adjacent to volcanoes are affected in a very direct manner by the surface elevation due to inflation or deflation of the surface. However, observed gravity variations cannot be explained by elevation changes alone. For example, Sanderson et al. (1983) interpreted gravity changes of several tens of microgals on Mount Etna associated with the 1981 eruption as due to magma intrusion at depth and Rymer and Brown (1987) found that cyclic changes in density of the order of 30 kg/m^3 in the magma pipe of the Poás volcano in Costa Rica may reflect the development of local

gas pockets. The gravity changes are of the order of $100 \mu\text{Gal}$ with periods of 10 to 45 days. Also, Crider et al. (2008) have interpreted a gravity increase on the Mount Baker volcano as a result of densification of a magma body due to deformation and degassing and perhaps shallow pyrite precipitation. These examples show that gravity can be used to monitor the movement of magma and gases within volcanic complexes which could lead to improved prediction of eruptive events (Rymer and Brown, 1987). Continuous gravity observations at a network of stations on and adjacent to active volcanoes offer the promise of determining the nature of magma movement within a volcano that may lead to periods of activity or quiescence. This requires independent measurement of the change in elevation of the observation sites and careful consideration of anomalous instrumentation response and changes due to non-volcanic sources. Hayes et al. (2006) have found by simulation that changes in density at depth and the resultant gravity anomaly temporal variations can be used as a proxy for the strain accumulation in fault networks. They have applied their simulations to moderate to large earthquake events which have occurred in California showing that observable gravity signals associated with them should be capable of being monitored.

Attempts have been made to associate temporal magnetic field variations with potential large earthquakes as the possible result of magnetostrictive effects in the Earth, but acceptable evidence has been limited to date. However, Currenti et al. (2007) have observed close temporal correlation between changes in the magnetic field and earthquakes during the 2002 – 2003 eruption of Mount Etna which they ascribed to a piezomagnetic mechanism. Satellite magnetic observations also may offer the possibility of monitoring global variations in ocean currents because moving sea water induces electric field currents with secondary magnetic fields (Maus and Kuvshinov, 2004). These signals are only a few nanoteslas in amplitude at the Earth's surface, but sufficiently large in scale that regionally averaged satellite observations may resolve them. For example, Tyler et al. (2003) showed that the M2 tidal signal can be mapped from night-side CHAMP magnetic observations in general agreement with the induced field predictions of an ocean flow model determined from satellite radar altimetry (Erofeeva and Egbert, 2002).

Mineral Resource Exploration

2.1 Overview

Gravity and magnetic methods have a rich history in the exploration for mineral deposits at a wide variety of scales. Although these methods, particularly the magnetic method, have a role in the direct exploration for mineral deposits, the primary use of the methods is in regional geological mapping of favorable terranes for the occurrence of deposits and in more detailed studies for the identification of structures and rock types that host particular types of deposits. The magnetic method is particularly useful in this regard because of the relative ease and low cost of the data acquisition and its high resolution. However, the magnetic method is limited to mapping formations and detecting deposits that have magnetization contrasts associated with the generally trace minerals, magnetite and pyrrhotite. Furthermore, the magnetic method is highly sensitive to source depth which decreases the amplitude of anomalies, and thus their detectability with increasing source depth. Gravity mapping is also employed to identify appropriate terranes, structures, and rock types for specific types of ore deposits and is applicable to problems related to the evaluation and exploitation of potential ore deposits. For more than a half century aeromagnetic mapping has greatly facilitated mineral exploration and in the past decade technological developments have made it possible to conduct airborne gravity studies at a precision and resolution useful in mineral exploration using not only measurements of the field intensity, but their gradients and tensors.

2.2 Introduction

The rising population of the Earth and its desire to improve the quality of life leads to an increasing need for mineral resources. This insatiable demand

has been and continues to be fueled by the growing desire to increase living standards especially in developing nations. The challenge of meeting this need must be met at least in part by new ore deposit discoveries lying largely near the Earth's surface to supplement current mineral reserves. These new deposits are likely to show little if any direct surface evidence of their existence, and thus will need to be discovered by a combination of traditional geological methods and geophysical techniques that remotely sense the deposits in the subsurface.

Mineral resources in the broadest sense include all commodities that can be economically extracted from the Earth. However, for the purposes of describing the application of gravity and magnetic methods to mineral exploration, coverage will be confined to ores, both metallic and non-metallic, which can be extracted for a profit, but exclude such valuable Earth commodities as ground water, sand and gravel, oil and gas, and coal. The exploration for these resources is described in other chapters of this website.

Over most of history, mineral and metal deposits were found by "prospectors" searching for surface evidence of mineralization in nearby rocks and stream deposits. In more recent times, ore deposits have been found through geological mapping backed up by geochemical exploration, increasingly aided by geophysical exploration. The success of geophysical methods in mineral exploration has been variable. Direct detection has proven useful on a consistent basis with regard to only a few ores, such as iron in the form of magnetite, radioactive uranium ores, and some metallic mineralized zones. In contrast, geophysics, especially magnetic and gravity methods, at a range of scales provide significant information for developing conceptual models where ore minerals are concentrated and finding appropriate regions and sites that match these models. As such geophysical methods, including gravity and magnetic exploration, find their primary application in indirect mineral exploration as a supplement to geological and geochemical investigations.

The breadth of mineral resource exploration by gravity and magnetic methods is large, ranging from the search for ores of aluminum to zinc. Ores have a wide diversity of physical properties, and they can occur in a variety of geologic settings that include essentially all types of rocks, sediments, soils, and alluvium. As a result a broad range of geophysical methods are used in exploration for ores [e.g., Dentith et al. (1994); Dentith and Mudge (2014)].

Traditionally electric and electromagnetic methods have had an especially prominent role in ore exploration because many ores are metallic (electronic) conductors, and thus have high conductivities and interfacial polarization

in contrast with surrounding rock formations. As a result many metallic mineralized zones are readily detected by electrical methods of exploration. Somewhat more experimental or specialized geophysical methods have been useful to exploration programs. Seismic methods have had a secondary role in mineral exploration, but recent improvements in the processing and interpretation of reflection imaging has shown their significant use in ore body investigations of layered rocks including metamorphic and igneous as well as sedimentary rocks. Radiometric methods have also had an important use in the search for naturally radioactive minerals and associated ores.

All geophysical methods are applicable to drillhole logging as well as surface studies. Their use in logging is particularly useful after a potential ore body is identified because of the need for definitive information on ore location and extent and grade for evaluating ore bodies and mine planning during the exploitation phase of resource development. Logging is readily used in exploitation because drill holes investigating ore deposits are relatively shallow, usually measured in tens or hundreds of meters.

Despite the lack of intense magnetization in ores except for magnetite-rich iron ores, the magnetic method has been and continues to be a primary technique of searching out new ore deposits. This is the case because either the presence or lack of magnetite, the principal magnetic mineral in rocks, has proven useful in identifying geologic environments that are favorable for a variety of ores. The magnetic method and electromagnetic methods lend themselves to relatively rapid and inexpensive observation from airborne platforms which have greatly stimulated their use over broad areas of the continents at a variety of scales.

Also, many ores have significantly higher density (commonly of the order of twice) than common rock forming minerals, therefore even when disseminated in ores, as long as volumes are large and the bodies compact, the resulting densities are sufficiently great that the gravity method may be useful in mineral resource exploration. Furthermore, gravity studies have had a major use, as has the magnetic method, in mapping regional and local geology for developing conceptual exploration models. Airborne mapping of gravity, especially gradients of gravity, are taking on an increasing role in mineral exploration because of their higher resolution and ease of surveying.

The role of magnetic and gravity methods in mineral resource exploration is somewhat different than that for oil and gas exploration. As described in Chapter 3, these methods are primarily used in reconnaissance studies and specialized detailed investigations in hydrocarbon exploration and exploitation. In contrast, gravity and magnetic methods are extensively used over a range of scales in mineral resource applications from continent-sized regions

to individual prospects. Most ore bodies occur within or in the proximity of crystalline rocks, that is igneous rocks, both volcanic and plutonic, and metamorphic rocks. Even if the ore bodies are not directly detectable, gravity and magnetic methods are extensively used in investigating these rocks as a guide to geologic mapping in three dimensions. Improved inversion techniques and enhanced computer facilities are proving to be particularly valuable in interpreting the configuration and property contrast of ore bodies using both gravity and magnetic anomaly data (Mandal et al., 2013). This is particularly true when inversion procedures consider the result of more than one geophysical method (Mandal et al., 2014). Gravity and magnetic anomaly data are particularly useful in structural mapping and under appropriate conditions can be used to identify rock types because of the strong magnetization and density contrasts in crystalline rock terranes. However, care must be used in identifying rock types from either magnetic or gravity anomalies solely on the basis of anomaly amplitudes and patterns. Strong interaction with geological and geochemical information is a necessary ingredient to achieve success in this effort.

Ore bodies may be directly related to both gravity and magnetic anomalies, but anomalies are seldom diagnostic. Anomalies vary in phase and amplitude depending on the geological, metamorphic, and geochemical history, the tectonic setting, and the depth of erosion to cite only a few factors. Commonly the anomalies are limited in areal dimensions, measured in tens or hundreds of meters, and anomaly amplitudes are rarely over a few milligals and a few hundred nanoteslas. Accordingly, seldom is it possible to directly identify an ore body anomaly in a gravity and magnetic anomaly field because there are numerous possible sources of similar anomalies. For example, circular-form magnetic minima may originate by alteration and destruction of magnetite associated with mineralization or from felsic plutons or by reversed remanent magnetization of igneous intrusives. Also, the search for ore deposits requires high precision surveys with dense observations because of the limited size and amplitude of the target anomalies.

The broad diversity of the signature of gravity and magnetic anomalies associated with ore bodies severely complicates their interpretation. Generally, exploration is focused on a single or a few types of mineral resources and survey design and interpretation are developed around a conceptual geologic model(s) of the ore body(ies) and their context within the geologic terrane. However, the ambiguity of interpretation of both magnetic and gravity methods leads to considerable uncertainty in the validity of interpretations. Accordingly, gravity and magnetic methods are seldom used without sensitivity analyses in the interpretation to evaluate the credibility

of the results and to integrate the interpretation with geologic data, physical properties preferably obtained on site either through surface collections or drillhole logging, and the results of other geophysical measurements. Seldom are gravity and magnetic methods used in the detection of ore bodies without collateral geophysical surveys and geological information. A useful approach to minimizing ambiguity of interpretations is to extrapolate known geology from outcrops or drilling into the subsurface using the magnetic and gravity data.

The primary application of gravity and magnetics in mineral resource applications is in the mapping at a range of areal scales of favorable geology for specific ore bodies and under suitable, usually restricted, conditions in the direct detection of ore bodies. With the increasing resolution, precision, and accuracy of the observation, processing, and interpretation of gravity and magnetic data, these methods are taking on an increasingly important role in the exploitation of identified ore bodies [e.g., Fullagar and Fallon (1997)]. Inverse modeling of isolated anomalies are being used to delineate ore bodies, thus guiding development drilling and maximizing ore recovery. Gravity anomalies are generally more useful in quantitative analysis than magnetic anomalies because of their lesser sensitivity to depth and the smaller range in physical property contrasts. Also, gravity anomalies can be used to estimate the tonnage of an ore body.

In addition, gravity and magnetic data can be used to evaluate potential safety and environmental concerns during the exploitation of an ore body. For example, both gravity and magnetic methods can be used to identify rock types and location of faults and alteration zones that affect rock mass characterization. This permits estimation of the strength of the rocks of the ore bodies as well as the nearby rocks that are important to optimizing the mining design and improve safety in mine operations. Gravity and magnetic data may also be used to map geological formations that are favorable for collapse over underground mining operations. Finally, gravity surveying can be used to map bedrock topography that will control the movement of waters to the mine workings and from the mine to the surrounding environment.

In the following sections of this chapter, examples are presented in brief form of the application of magnetic and gravity methods to mineral resource exploration. These have been selected from the published literature as representative of the range of uses of these methods in this application. They are neither comprehensive of the subject matter or a complete description of the case history. The reader is referred to the specific source of the case history for more details and treatment of associated geological and geophysical studies that may have had a major role in identifying the mineral deposit.

The principal purposes of the case histories are to give a representative view of the types of gravity and magnetic signatures associated with mineral resource deposits and the range of uses of these methods in resource exploration. This information should be helpful in selecting and planning gravity and magnetic surveys for mineral resource applications. Useful collections of case histories that provide further examples are available in SEG (1966); Morley (1970); Hood (1979); Hinze (1985); Garland (1989); Gubins (1997); Gunn and Dentith (1997); Gibson and Millegan (1998); Moon et al. (2006); Vallée et al. (2011). Particularly useful reviews of geophysical signatures of mineral resource deposits are given by Dentith et al. (1994); Dentith and Mudge (2014) for Western Australia and Hildenbrand et al. (2000) for the western U.S. Additional case histories are published in germane journals and textbooks.

2.3 Geological Mapping

The search for mineral resources is largely based on inductive reasoning using field experience on the occurrence of specific ore bodies to identify regions where similar deposits may be located by detailed exploration. Conceptual models of ore genesis are conceived taking into account the structure, tectonic history, rock type, age, mineralogy, and geochemistry of known ore deposits and their geological environment. These models are then used to identify analogous geological conditions favorable for similar ore deposits that are hidden from direct view. This can be accomplished by mental comparison or by more structured inductive learning systems such as decision trees, neural networks, and pattern recognition schemes. Recognizing analogous geologic terranes is usually the first step in this process; consequently reliable geologic maps are essential. In turn gravity and magnetic anomaly data are commonly an important part of mapping geology where surficial cover prevents direct mapping.

Mapping of geology with magnetic and gravity data ranges over a broad spectrum of scales from continental-sized areas to prospect level. Most countries favorable for mineral resource exploration have undertaken national gravity and magnetic anomaly mapping programs. Many of the maps and data sets of these surveys are available in the public domain to encourage mineral resource development. The magnetic mapping programs have for the most part used generally consistent magnetic survey specifications, while other programs that have used a variety of survey specifications have processed the observed data to develop merged quasi-consistent data that can be used for regional-scale investigations.

The large regional gravity and magnetic anomaly data sets have been used to construct continent-scale coverage and world data sets by supplementing continental data with marine and satellite measurements. These large scale maps have provided a new view of the structure and tectonics of the continents and are an important supplement to geological mapping [e.g., Hanna et al. (1989); Hinze and Hood (1989)] that are potentially useful in developing models for ore deposit occurrence and strategies for exploration (Fairhead et al., 1997). Although it is difficult to generalize, globally the coverage of gravity data is more complete than magnetic data, but at a continental scale magnetic data are generally more complete and detailed. The higher resolution magnetic anomaly data are particularly useful in deciphering the geology and especially the structure of the rocks at the surface of the crystalline crust. The utility of these maps in geologic mapping has been dramatically increased by improved methods of visualizing the data such as shaded relief maps and processing to emphasize gradients in the data that mark the boundaries of lithologic units [e.g., Reeves et al. (1997); Wijns et al. (2005)].

Numerous examples exist in the literature of the use of gravity and magnetic anomaly mapping to assist in geological mapping. A useful example is the mapping of the Precambrian craton in the four-state area centered along the Wisconsin/Minnesota border (Figure 2.1). This is an area of complex Precambrian geology ranging in age from roughly 3.5 to 1.1 Ga including terranes with characteristic structures and lithologies derived from several tectonic episodes. This is a mineral-rich region with world-class deposits of copper, iron, and nickel and ores of magmatic and hydrothermal origin of lead, zinc, gold, silver, and other metals (Morey and Sims, 1996). Conceptual models of these ore deposits relate them to specific metallogenic regions of characteristic age, structure, rock type, etc. Accordingly, it is important to map the Precambrian bedrock rock surface as accurately as possible. Unfortunately, Precambrian outcrops that are adequate for classical geologic mapping are limited, and are largely restricted to the general vicinity of Lake Superior. Elsewhere the Precambrian rocks shown in Figure 2.1 are largely covered by the waters of Lake Superior, Pleistocene glacial deposits, and by early Paleozoic sedimentary rocks to the south. Consequently, gravity and magnetic data have been used extensively to map the geology of the region [e.g., Klasner et al. (1985); Chandler (1996); Allen et al. (1997); Cannon et al. (2005)].

The geologic map of Figure 2.1 is a regional compilation by Chandler et al. (2007) which is based on previous geologic maps derived largely from gravity and magnetic data and recently compiled gravity and magnetic maps in

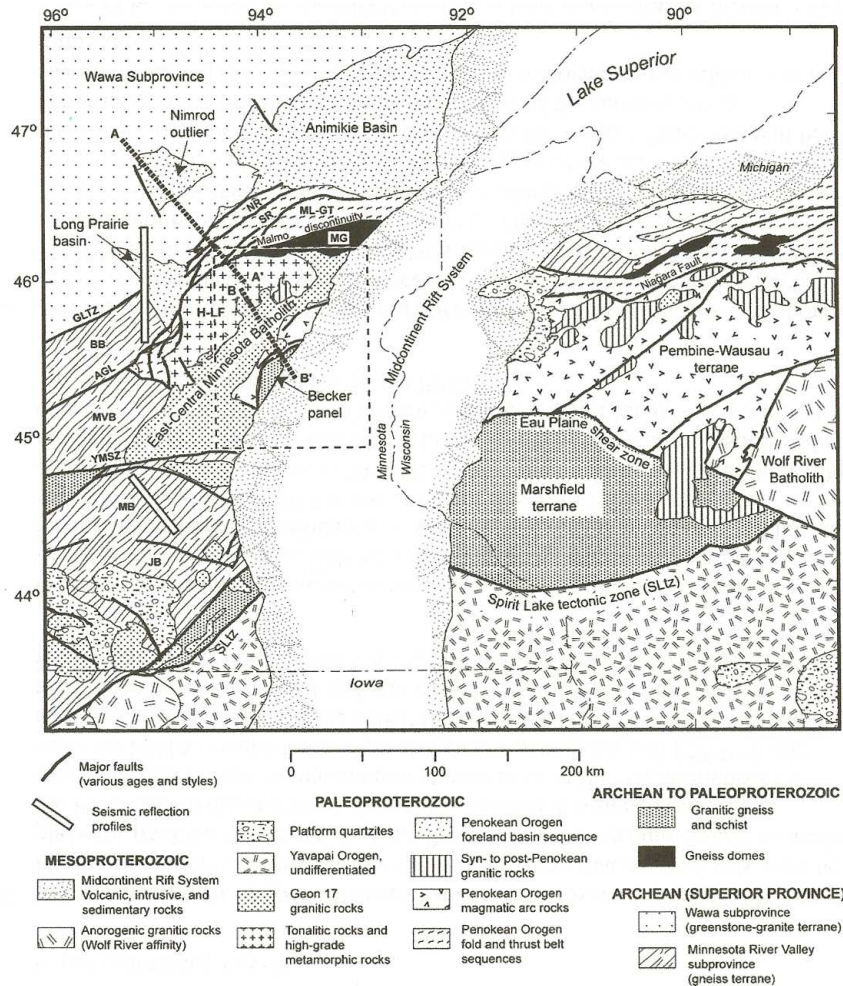


Figure 2.1 Generalized geologic map of Precambrian rocks centered on the Minnesota/Wisconsin border. This map has been prepared from mapped surface geology, drillhole lithologic logs, isotopic age dates, and magnetic and gravity anomaly data as shown in Figures 2.2 and 2.3. Adapted from Chandler et al. (2007).

combination with drillhole information and isotopic age dates. Derived magnetic and gravity anomaly maps shown in Figures 2.2 and 2.3 are particularly effective in delineating the geology shown in Figure 2.1. The aeromagnetic anomaly data were collected during several surveys of differing specifications, but generally along flight lines ranging from 0.4 to 2 km at a mean terrain clearance of 300 m or less. These data have been composited and analytically continued to a terrain clearance of 305 m and processed to de-

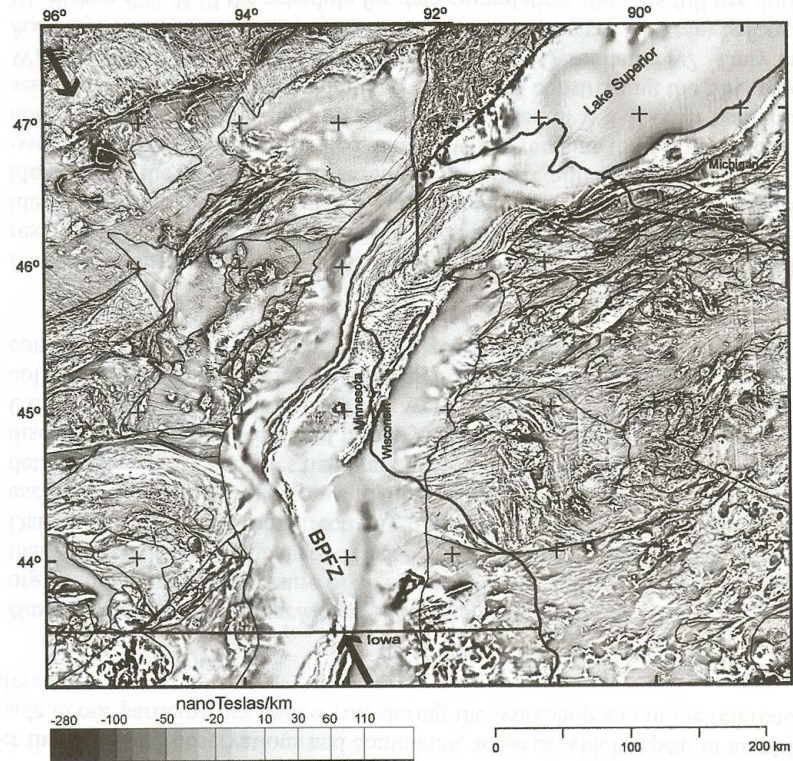


Figure 2.2 First vertical derivative map of the total magnetic anomaly data of the area shown in Figure 2.1. Thin dark lines are geologic contacts as shown in Figure 2.1. BPFZ designates the Belle Plaine Fault Zone and the bold arrows show the trend of associated anomalies extending from the fault zone. Adapted from Chandler et al. (2007).

termine the first vertical gradient of the magnetic anomaly data which is presented in Figure 2.2. The gravity data are more widely separated with stations generally spaced at 1.6 to 5 km, but at distances up to 10 km in Lake Superior, Michigan, and Iowa. The second vertical derivative of the gravity anomaly shown in Figure 2.3 was calculated after upward continuation of the gridded data to 2 km to remove local anomalies and spurious observations.

The pattern and nature of these anomalies in both the derivative maps are particularly useful in mapping the edges of the rock units, faults, dikes, and other source margins. The second derivative of gravity was used to focus on the higher wavenumber anomalies associated with the more near-surface gravity sources rather than the first derivative because the gravity

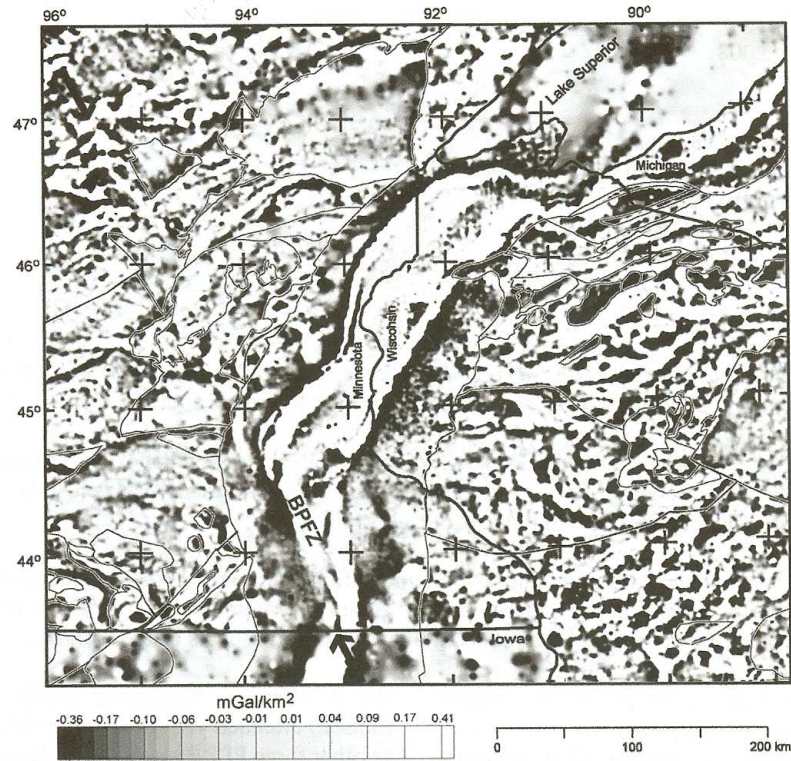


Figure 2.3 Second vertical derivative map of the Bouguer gravity anomaly data of the area shown in Figure 2.1. Thin dark lines are geologic contacts as shown in Figure 2.1. BPFZ designates the Belle Plaine Fault Zone and the bold arrows show the trend of associated anomalies extending from the fault zone. Adapted from Chandler et al. (2007).

anomaly map emphasizes the deeper-sourced components (lower wavenumber) in contrast to the magnetic anomalies. Geologic mapping in this region has depended greatly on extrapolating from and interpolating between known geologic information. The uniqueness of the results of gravity and magnetic anomaly interpretation is greatly increased when using extrapolation and interpolation from direct geologic data. The resulting map can be used in developing conceptual models of known ore deposits and locating favorable terranes for specific types of ore deposits.

In addition to mapping the geology at the Precambrian surface, gravity and magnetic data can be used to investigate the geology at depth. Forward modeling of both the gravity and anomaly data constrained by the mapping of surface crystalline rocks and physical properties measured on outcrop and drill core samples is particularly useful in this regard. An example of



Figure 2.4 Total magnetic anomaly field analytical signal image of strongly folded Proterozoic sequences in Namibia. Adapted from Hutchins et al. (1997).

two-dimensional modeling is shown in Chandler et al. (2007). The modeling provides useful insight into the nature of crust. For example, it identifies strongly magnetic granitic rocks underlying a basin of relatively undeformed Paleoproterozoic rocks (the Nimrod outlier). In addition, the modeling provides some information on the dips and depth extents of geologic bodies that subcrop at the Precambrian surface.

Mapping of interest to mineral exploration at a larger scale is conducted in much the same manner as the previous example. Because of the relationship between magnetic properties and basic crystalline rock lithologies, the ease of acquiring high-resolution magnetic data, and the relatively high-resolution of magnetic data in locating contacts between units of varying magnetization, the magnetic method is particularly useful in mapping of crystalline bedrock. To increase the resolution of these data over those of the observed total magnetic anomaly field, a wide variety of high-wavenumber pass filters are used to enhance the interpretability of the data. In the previous example from the Precambrian craton of the northern mid-continent of the U.S., the vertical derivative was used to increase the resolution. Figure 2.4 shows the analytical signal (total gradient) (see Chapter 13.4.1D) of high-resolution magnetic anomaly data over strongly folded Proterozoic sequences from a

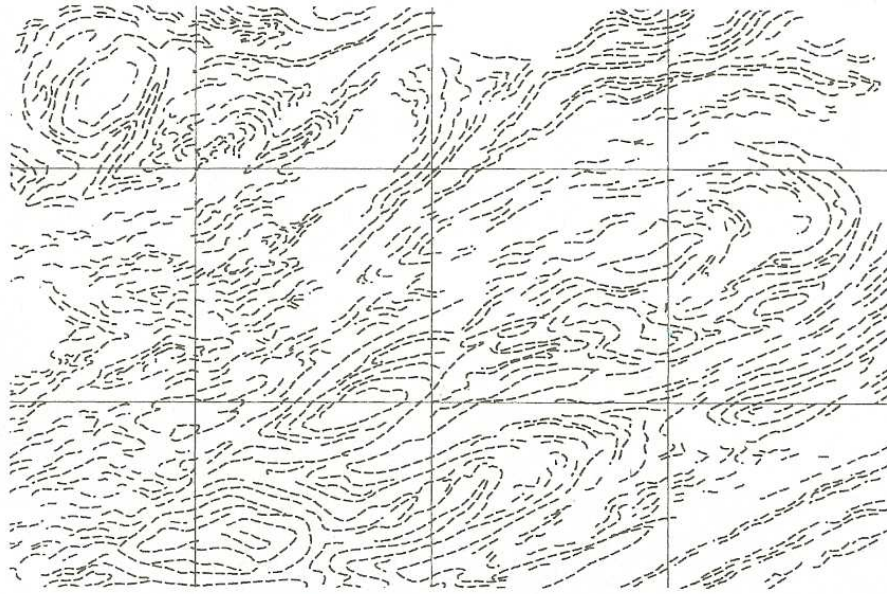


Figure 2.5 High-wavenumber anomaly trends from Figure 2.4. Adapted from Hutchins et al. (1997).

mineral-rich region of the Precambrian shield of Namibia, Africa as reported by Hutchins et al. (1997). The trends of the high-wavenumber components of this map are illustrated in Figure 2.5. Building on the discontinuities in the anomaly trends and the magnitudes of the total field anomalies, in Figure 2.6 lithomagnetic domains and magnetic pattern breaks are added to the high-wavenumber components of Figure 2.5. Finally, in Figure 2.7 a geologic map showing structural trend lines is interpreted from Figure 2.5 by extrapolation of surface geologic data. Maps of these types are an important part of a mineral exploration program.

Gravity and magnetic data have played a significant role in the recognition of geologic lineaments [e.g., Domzalski (1966)]. A lineament is a linear or curvilinear feature, pattern, or change in pattern that can be identified in a data set and attributed to geologic formation or structure. A single lineament is commonly reflected in a variety of bedrock geological features. Mapped lineaments are generally of a regional nature covering distances measured in hundreds of kilometers, but in actuality they may occur in a full range of spatial scales. Figures 2.2 and 2.3 show the position of the Belle Plaine Fault Zone and its extension to the northwest as mapped by the gravity and magnetic anomaly data. This feature is one of the many

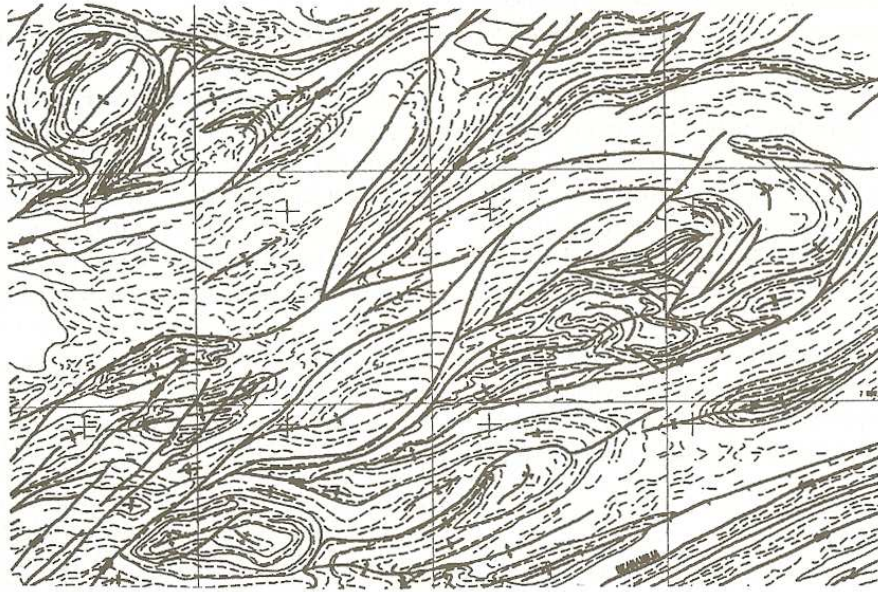


Figure 2.6 Lithomagnetic domains and magnetic pattern breaks added to the trend map of Figure 2.5. Adapted from Hutchins et al. (1997).



Figure 2.7 Interpreted geologic map of the area shown in Figure 2.4 by integrating surface geological information with Figure 2.6. Adapted from Hutchins et al. (1997).

significant lineaments in the geophysical data of the region. It is interpreted as an extensive, ancient fault zone that affected the structural development of the Midcontinent Rift Complex. Although the Belle Plaine Fault Zone has no known association with mineral deposits lineaments in gravity and magnetic anomaly data have been related elsewhere to the occurrence of mineral deposits [e.g., Mabey (1989); Reddi and Ramakrishna (1989)].

Identification of lineaments is usually a subjective process, and thus can be influenced by illusion and self-deception. As a result some identified lineaments may have limited credibility. Nonetheless, the structural control of geologic lineaments mapped by geophysical data on mineral deposits or trends (belts) of deposits has been well established. Lineaments are generally considered to be the manifestation of deep-seated, but not necessarily vertical, faults that have been reactivated throughout their history and are avenues for igneous activity and hydrothermal activity leading to ore deposits in favorable environmental settings. Increased permeability and decreased rock strength associated with fault intersections and bends in faults are particularly favorable sites for ore deposits related to igneous activity or hydrothermal activity. The source of anomalies associated with lineaments is highly varied [e.g., /citesnchez-et-al-14], however, the most common source is varying lithologies across lineaments that are related to movement along faults that bring rocks of varying composition into juxtaposition. Another significant source of lineament anomalies is the destruction of magnetite and associated decrease in magnetic susceptibility, and thus magnetic minima, caused by oxidizing waters moving through faults [e.g., Sandrin et al. (2007)].

Hildenbrand et al. (2000) have reviewed the role and importance of geophysical lineaments in the control of mineral deposits in the western U.S. They conclude that many linear trends or belts of deposits are associated with reactivated older faults as well as faulting contemporaneous with ore deposition that are related to gravity and/or magnetic lineaments. They provide numerous examples of the association of these lineaments with mineral deposits including those of the mother-lode gold belt of California, magmatic-hydrothermal (porphyry) deposit trends across the western U.S., and epithermal deposit trends in the greater Nevada region. One of the more dramatic occurrences of mineral deposits and lineaments is illustrated in Figure 2.8. O'Driscoll (1990) shows in this figure that the world-class Olympic Dam $Cu - U - Au - Ag - REE$ deposit of south-central Australia occurs at the intersection of two gravity anomaly lineaments. Geophysical lineaments thus can provide a useful guide to mineral exploration, but clearly they are

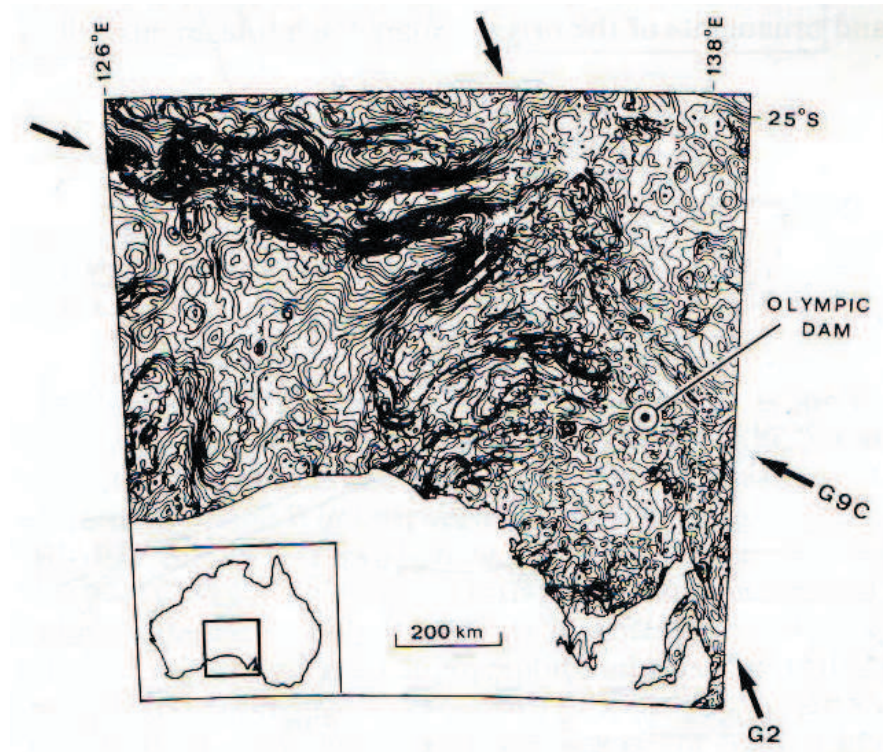


Figure 2.8 Bouguer gravity anomaly map of south-central Australia. Note that the Olympic Dam deposit is located at the intersection of the G9C and G2 gravity lineaments. Adapted from O'Driscoll (1990).

not infallible indicators and are only one of the possible considerations in delineating favorable regions for exploration.

To increase the veracity of identified anomaly lineaments, Sánchez et al. (2014) have compared magnetic anomaly lineaments with similar features in gravity, terrain, and field-based geologic maps. They found that a numerical rating system incorporating the combined results of coincident lineaments in the various spatial data useful in evaluating the reliability of the lineaments as indicators of regional geologic structural controls on hydrothermal mineral occurrences in western Yukon and adjacent eastern Alaska. The magnetic anomaly maps that well define two faults in their study area are shown in Figure 2.9.

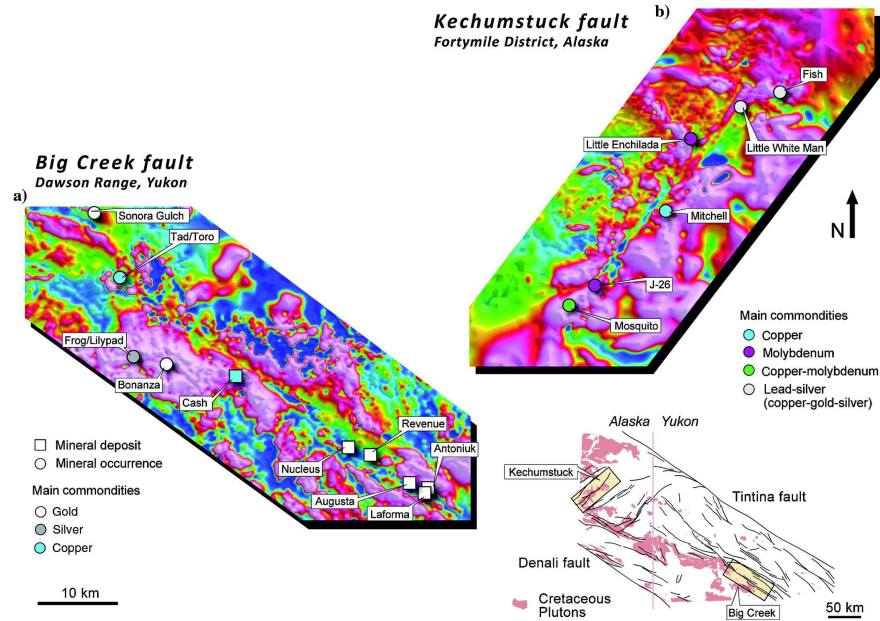


Figure 2.9 Reduced-to-pole magnetic anomaly maps of (a) the Big Creek fault in the Yukon and (b) the Kechumstuck fault in Alaska and associated mineral deposits. The magnetic anomalies increase in intensity from blue to lavender. Note the magnetic minima along the length of the lineaments and the distribution of mineral deposits along the lineaments. Adapted from Sánchez et al. (2014).

2.4 Indirect Exploration for Mineral Deposits

Magnetic and gravity methods are useful in mapping geologic terranes favorable for the occurrence of a specific ore or group of ores as described in the previous section, but they are also used in locating likely specific host rocks and structures for ore deposits even where the ore minerals are of a type or distribution that do not provide definitive anomalies. In this way the geophysical methods indirectly identify formations and features for follow-up with direct geologic exploration or more suitable geophysical methods. This is equivalent to the geologic mapping by gravity and magnetic methods described in the preceding section, but the focus is on smaller scale mapping for specific rock types or structures.

Many types of ore bodies are associated directly or indirectly with igneous rocks, both plutonic and volcanic. Ores of such elements as copper, titanium, tin, nickel, chromium, and platinum may accumulate directly in plutonic rocks. The type of ore deposits in plutonic rocks differ with the

origin and chemical composition of the intrusive igneous rock. Thus, gravity and magnetic methods are used to search for igneous intrusives ranging from ultramafic to felsic rocks based upon their distinctive anomaly signatures. For example, diamonds may occur as a primary but trace constituent in kimberlite intrusives. Although the diamonds do not impart a distinctive physical property to kimberlite intrusives, these rocks may contain sufficient original or secondary magnetite so that they can be mapped with magnetic methods. As a result, magnetic and gravity surveying are an important part of diamond exploration.

2.4.1 Diamondiferous Intrusives

Potential diamond-bearing intrusives originating from partial melts of mantle rocks at depths exceeding 150 km have a unique, but variable chemistry among rocks occurring at the earth's surface. These kimberlite and lamproite rocks, often containing an abundance of xenoliths from adjacent, intruded rocks, occur in dikes up to a few meters in width or as pipes up to, but rarely over, a kilometer and a half in diameter. The intrusives are typically cone-shaped in geometry increasing in diameter close to the surface, but they make take a variety of configurations. Their limited size and the common presence of masking overburden due in part to their rapid weathering make them a difficult target in mineral exploration. However, the tendency for diamond pipes to occur in ancient rigid craton cores suggests that favorable exploration regions that are indicative of ancient cratons may be identified by a variety of regional geophysical methods including gravity and magnetic methods Morgan (1995).

Even at the same magnetic latitude the signatures of kimberlite pipes may be highly variable (Power et al., 2004). This is illustrated in Figure 2.10, which shows the magnetic anomalies associated with four kimberlite pipes in northern Canada. Generally, the magnetic anomalies are positive with amplitudes of several hundreds of nanoteslas or more [e.g., Sarma et al. (1999)] due to a strong magnetic susceptibility of the kimberlite contrasting with the country rock, but the effect of high magnetic susceptibility may be negated by a strong magnetic remanance. Experience has shown that not all kimberlite bodies have correlative magnetic anomalies (Gerryts, 1970) and many of the anomalies are difficult to isolate from complex magnetic background anomalies without applying filters and pattern recognition schemes [e.g., Keating and Sailhac (2004)].

Gravity measurements may be useful in identifying magnetic anomalies as originating from kimberlite pipes. Typically, kimberlites are altered to

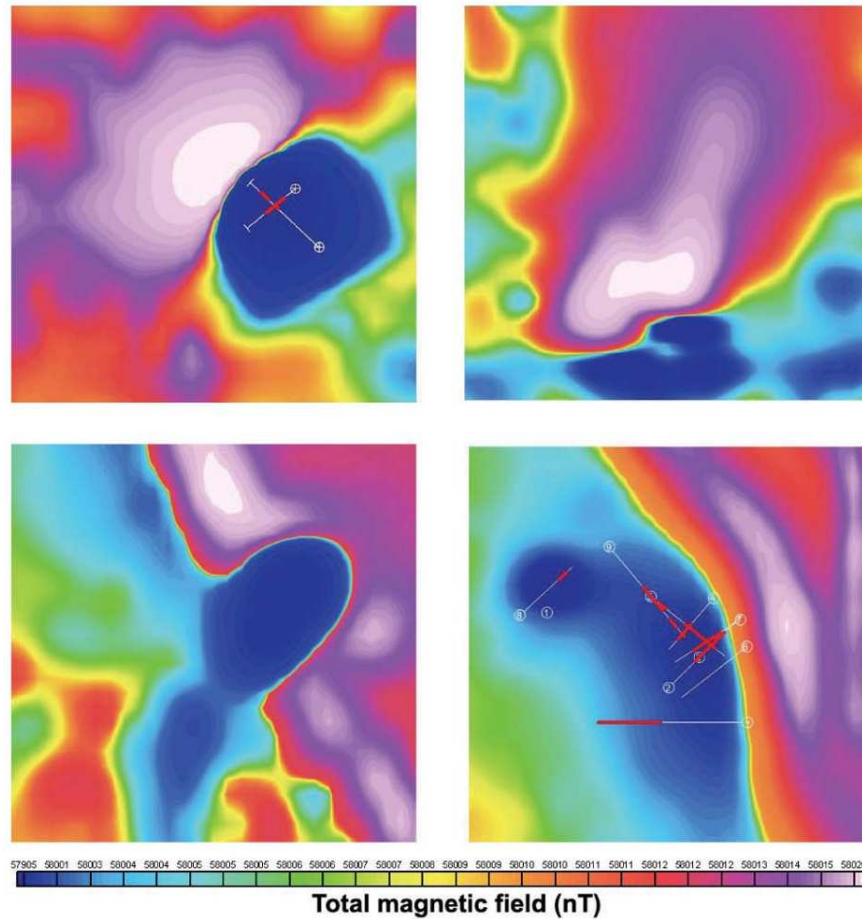


Figure 2.10 Variable magnetic anomaly signatures observed over kimberlite pipes in northern Canada. Upper left is dipole anomaly due to strong remanent magnetization of the kimberlite. Upper right is positive magnetic anomaly. Lower left is a magnetic low interrupting a positive magnetic anomaly caused by a diabase dike. Lower right is a magnetic minimum due to a kimberlite adjacent to a diabase dike. Adapted from Power et al. (2004).

densities in the range of 2200 to 2500 kg/m³, resulting in negative gravity anomalies of the order of 1 mGal or less. These negative gravity anomalies may be accentuated by negative mass effects due to craters filled with low-density sediments or lakes that often occur above kimberlite pipes. An example of the use of gravity to support identification of kimberlite pipes has been reported from the Northwest Territory of Canada (Jansen and Withery, 2004). Aeromagnetic surveying shown in Figure 2.11 mapped potential

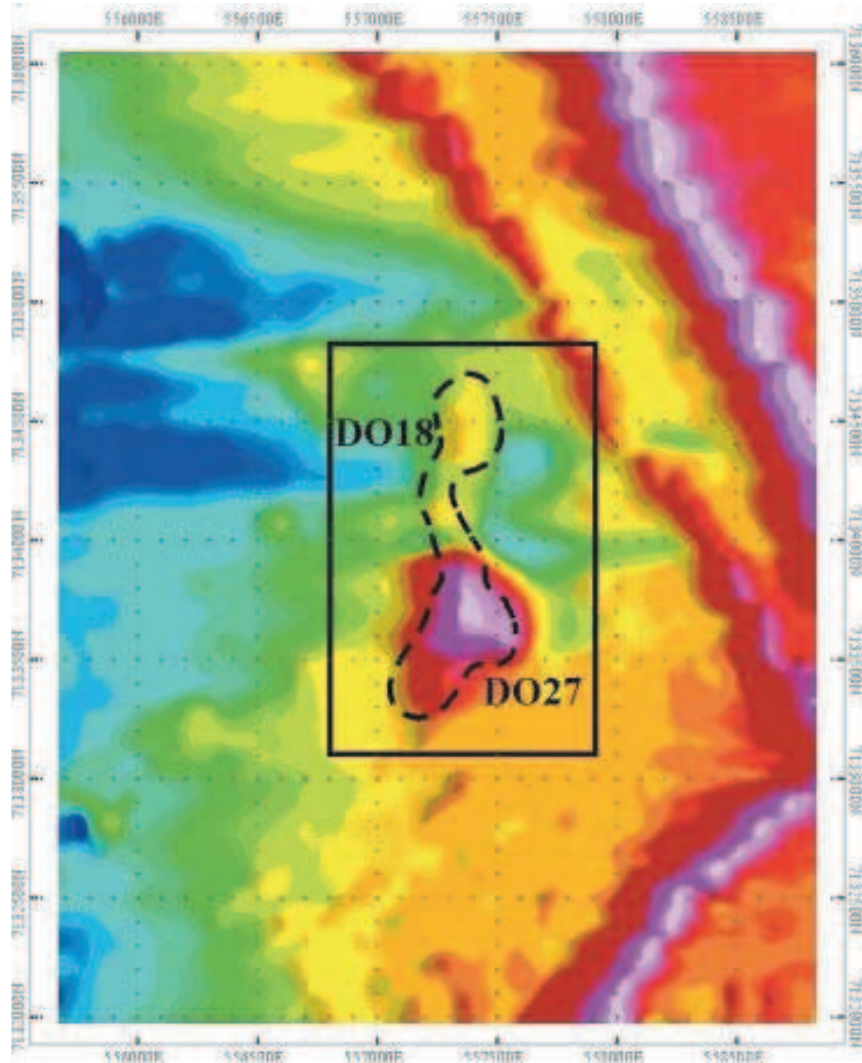


Figure 2.11 Total magnetic anomaly map over two identified kimberlite pipes (DO18 and DO27) in the Northwest Territories, Canada observed at a mean terrain clearance of 50 m. The DO27 anomaly has a positive amplitude of 240 nT. Adapted from Jansen and Witherly (2004).

kimberlite pipes within the dashed area of the figure. The pipe identified as *DO27* has a maximum amplitude of 240 nT at a survey elevation above the ground surface of 50 m. Subsequent surface gravity surveying shown in the anomaly map of Figure 2.12 shows a roughly 1 mGal negative anomaly coincident with the magnetic anomaly supporting the identification of the kimberlite pipe.

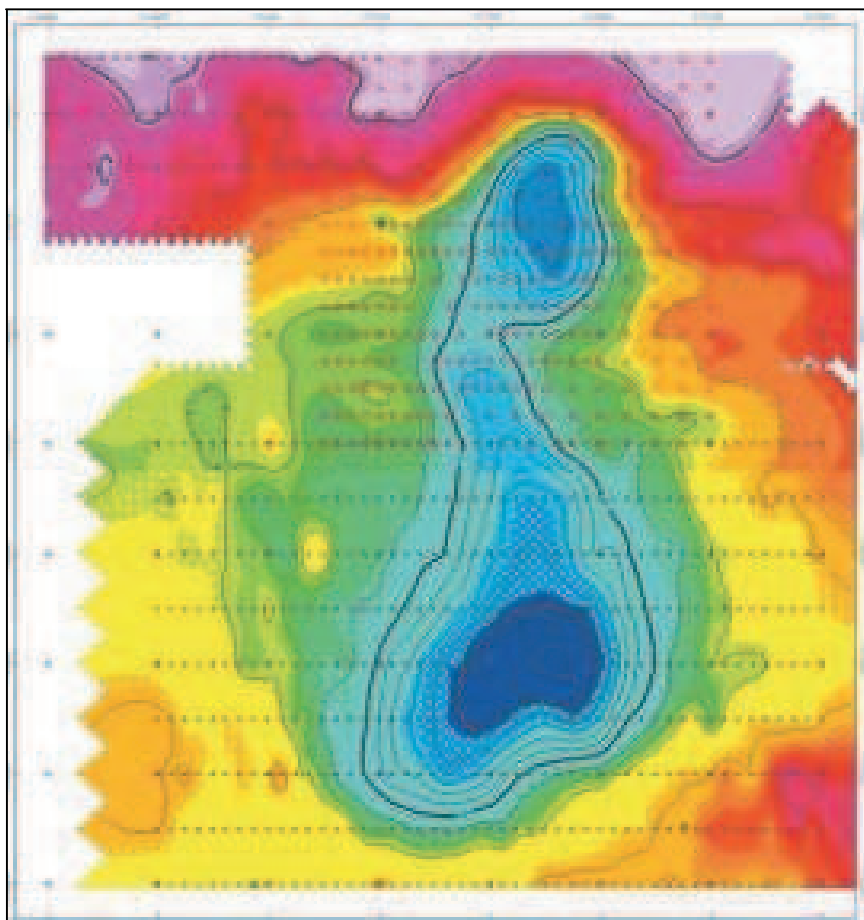


Figure 2.12 Bouguer gravity anomaly showing minimum anomalies coincident with the positive magnetic anomalies shown in Figure 2.11 that are associated with kimberlite pipes. The amplitude of the gravity anomaly minimum over the southernmost pipe (DO27) is one milligal. Adapted from Jansen and Witherly (2004).

Rajagopalan et al. (2008) report on the integrated use of magnetic, gravity gradiometer, and electromagnetic airborne surveys to identify kimberlites in the Northwest Territory, Canada. They point out that no one method definitely identifies these features, but all known pipes are discovered by integrating the interpretation of the data sets. The vertical gradient of the total magnetic intensity of a portion of the Lac de Gras kimberlite province shown in Figure 2.13 indicates a range of magnetic signatures of the kimberlites identified in the figure by the diamond symbol. For example, the

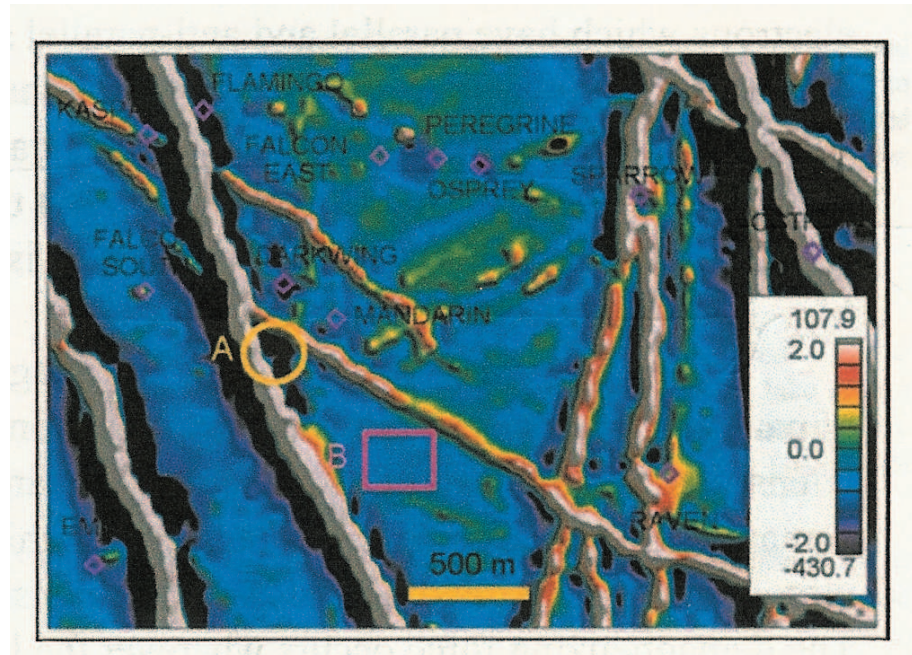


Figure 2.13 Vertical gradient of the total magnetic anomaly of the Ekati property of the Lac de Gras kimberlite province, Northwest Territory, Canada. Diamond symbols are known kimberlite pipes. Areas A and B are potential kimberlite target areas. Adapted from Rajagopalan et al. (2008). Accessible at <http://www.publish.csiro.au/nid/228/paper/PVv2008n132.htm>

Osprey deposit which has a strong remanence has an associated gradient high, while other prospects may not have a discernible anomaly or are indicated only by breaks in the linear magnetic anomalies of the dikes. The vertical gravity gradient of this region Figure 2.14 shows negative gradient anomalies associated with the pipes. These anomalies are accentuated by the decrease in gravity due to water in the lakes that commonly overlie the kimberlite pipes. Two areas associated with negative vertical gravity gradients indicated on the figures by the circle (A) and the rectangular (B) were selected as new target areas for analysis and possible investigation. Inversion of the three data sets indicated that site B was unlikely to be a pipe and not investigated further, but site A was interpreted to be associated with a viable target. Drilling of the anomaly as shown in Figure 2.15 that has been extracted from Figure 2.14 shows the drilling which encountered kimberlite deposits associated with the negative gradient anomalies.

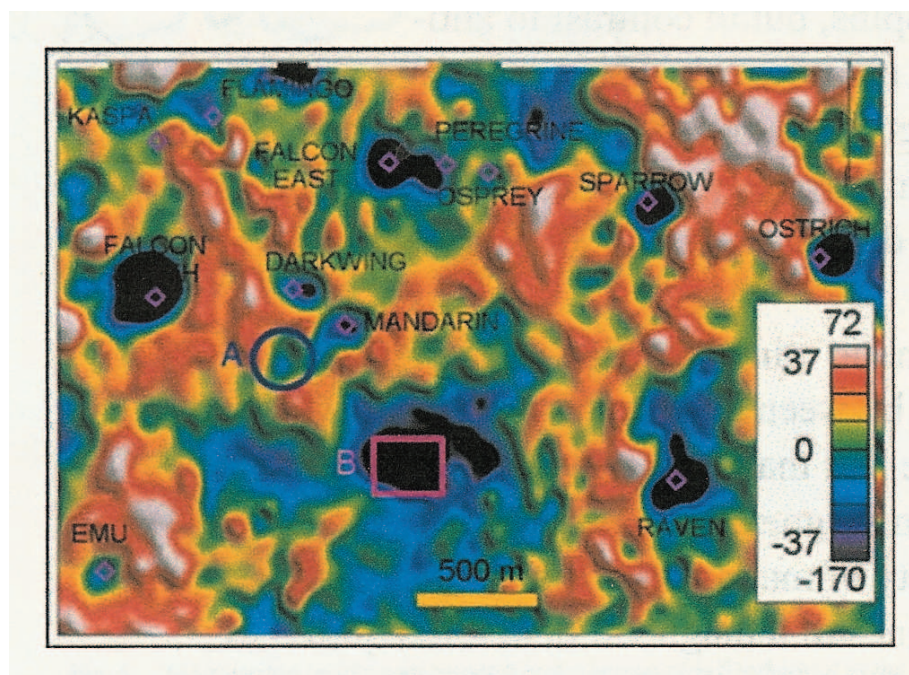


Figure 2.14 Vertical gravity gradient in Eötvös units of the Ekati property of the Lac de Gras kimberlite province, Northwest Territory, Canada. Diamond symbols are known kimberlite pipes. Areas A and B are potential kimberlite target areas. Adapted from Rajagopalan et al. (2008). Accessible at <http://www.publish.csiro.au/nid/228/paper/PVv2008n132.htm>

2.4.2 Uranium Mineralization in the Athabasca Basin, Canada

A quite different application of the gravity method to indirect exploration for mineral deposits has been documented by Wood and Thomas (2002) for uranium mineral deposits near the McArthur River uranium deposit which lies at a depth of roughly 550 m in the Athabasca Basin of Saskatchewan, Canada. Uranium oxide is concentrated in mineral deposits at and near the unconformity of the basal Athabasca sandstone of the Basin with the underlying basement rocks. The uranium deposits appear to be related to basement faults and associated alteration patterns of silicification/desilicification within the sedimentary rocks. The modification of the density of the altered sandstones is believed to be sufficient ($\approx \pm 50 \text{ kg/m}^3$) to result in positive gravity anomalies associated with silicification and negative anomalies related to desilicification.

The result of modeling a high-resolution gravity profile near and across strike of the McArthur River uranium deposit is shown in Figure 2.16. The

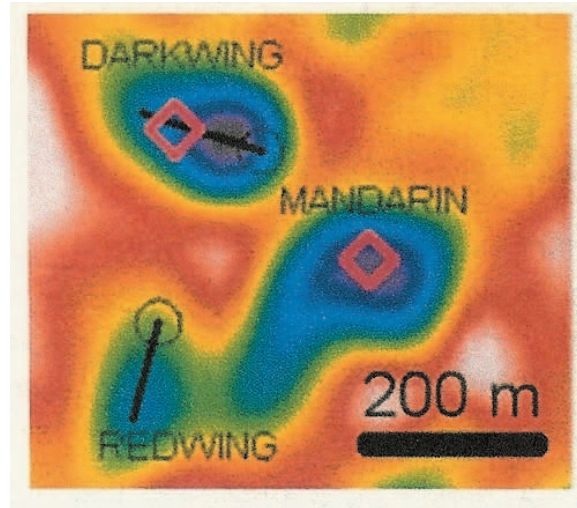


Figure 2.15 Vertical gravity gradient in Eötvös units over target A in Figure 2.14 and adjacent pipes (diamond symbol). Drill holes (circles) and traces (black lines) are shown. The southern drill hole tested target A and intersected a new kimberlite. The second drill hole tested the gravity gradient anomaly east of the Darkwing pipe and intersected a possible apophysis. Adapted from Rajagopalan et al. (2008). Accessible at <http://www.publish.csiro.au/nid/228/paper/PVv2008n132.htm>

gravity anomalies associated with the alteration zones in the sandstone are relatively minor, of the order of a milligal or less. Their width on the profile is anticipated to lie between the longer wavelengths due to intrabasement lithologic variations and basement topography and the shorter wavelengths associated with the bedrock (sandstone) surface configuration. The latter have been identified from bedrock relief mapped in drill holes adjacent to the gravity profile. The source of longer wavelength gravity anomalies are related to major intrabasement lithologic variations and basement topography which was generalized from available magnetic anomaly data. Modeling shows the presence of several intermediate wavelength gravity anomalies that may be related to alteration of the Athabasca sandstone and basement and bedrock relief perhaps associated with basement faulting. The association of these features is related to uranium mineralization elsewhere in the Basin (Wood and Thomas, 2002) suggesting that several segments of the profile shown in Figure 2.16 are potential uranium mineralization targets. More recently airborne gravity gradiometer studies of localized areas within the Basin (Witherly and Diorio, 2012) have proven useful in mapping features

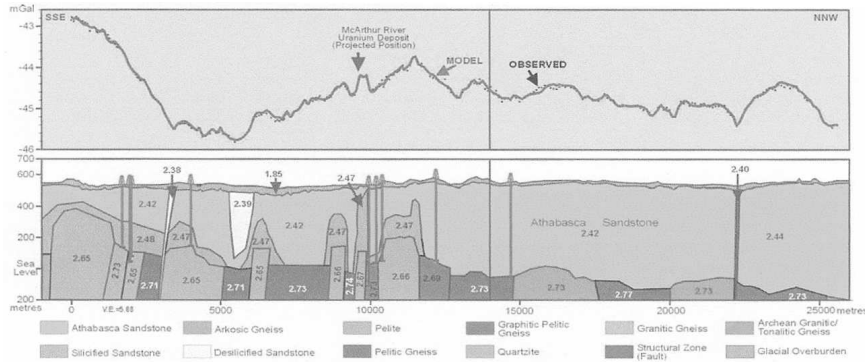


Figure 2.16 Observed and modeled Bouguer gravity anomalies along a high-resolution profile near the McArthur uranium mineral deposit in the Athabasca Basin, Saskatchewan, Canada. The profile shows the location of the McArthur deposit shifted in the plane of the profile and several zones of silicification and desilicification that may be associated with uranium mineralization. Adapted from Wood and Thomas (2002).

in the Athabasca sandstone and the basement rocks that could be related to ore-forming processes and thus a guide to exploration.

2.4.3 Olympic Dam Granite-Breccia Mineral Deposit, Australia

The giant Olympic Dam iron-oxide associated $Cu - U - Au - Ag - REE$ deposit was discovered ≈ 500 km northwest of Adelaide, South Australia in 1975 as a result of drilling on coincident gravity and magnetic anomalies observed in the regional maps of Figures 2.17 and 2.18, respectively. The roughly 1600 Ma felsic basement rocks of this region are covered by flat-lying latest Precambrian/Cambrian sedimentary rocks which attain a thickness of 300 m over the Olympic Dam deposit. There is no evidence of the mineral deposit in the overlying sedimentary rocks.

Initial consideration of these coincident gravity/magnetic anomalies as a mineral deposit target was based on a model of a sediment-hosted copper deposit from nearby basaltic volcanic rocks. The magnetic anomaly was assumed to be related to the basaltic rocks and the gravity anomaly with a horst block within the basalts (Rutter and Esdale, 1985). Drilling on the anomalies encountered hematite-rich granite breccia rather than basalt. Subsequent exploration indicated a core of hematite-silica breccia within hematite-altered breccias extending > 5 km in a northwest/southeast direction with a width of up to 3 km (Reynolds, 2001). The depth extent of the breccia is unknown, but drilling shows that it is greater than 1.4 km. The

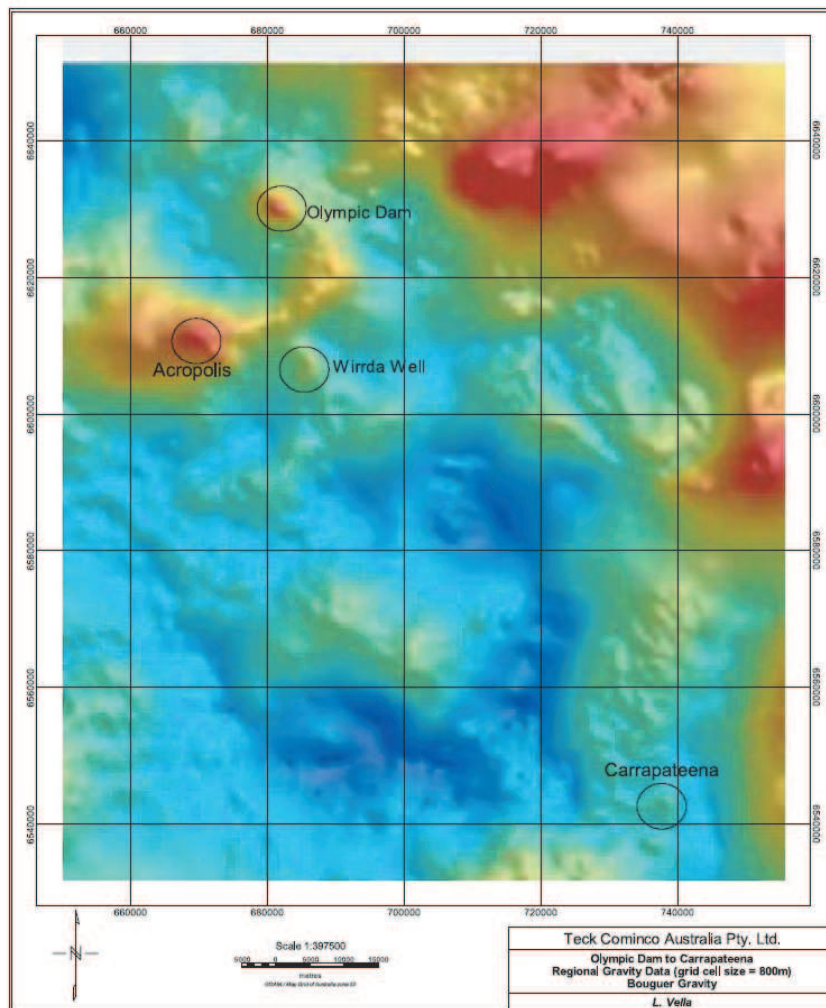


Figure 2.17 Regional Bouguer gravity anomaly map of a portion of the Gawler craton, South Australia showing the location of Olympic Dam and other mineral prospects at the intersection of the G9C and G2 lineaments. Red areas are high values and blues are low. Adapted from Vella and Cawood (2006). Accessible at <http://www.publish.csiro.au/nid/228/paper/PVv2006n122.htm>

breccia occurs within a granite and is associated with intense hydrothermal and perhaps related volcanic activity. Two periods of ore formation have been recognized (Gow et al., 1994), an early high-temperature fluid phase associated with the major granitic intrusive event which led to magnetite-rich ores distributed within the breccia complex largely at depth and a later

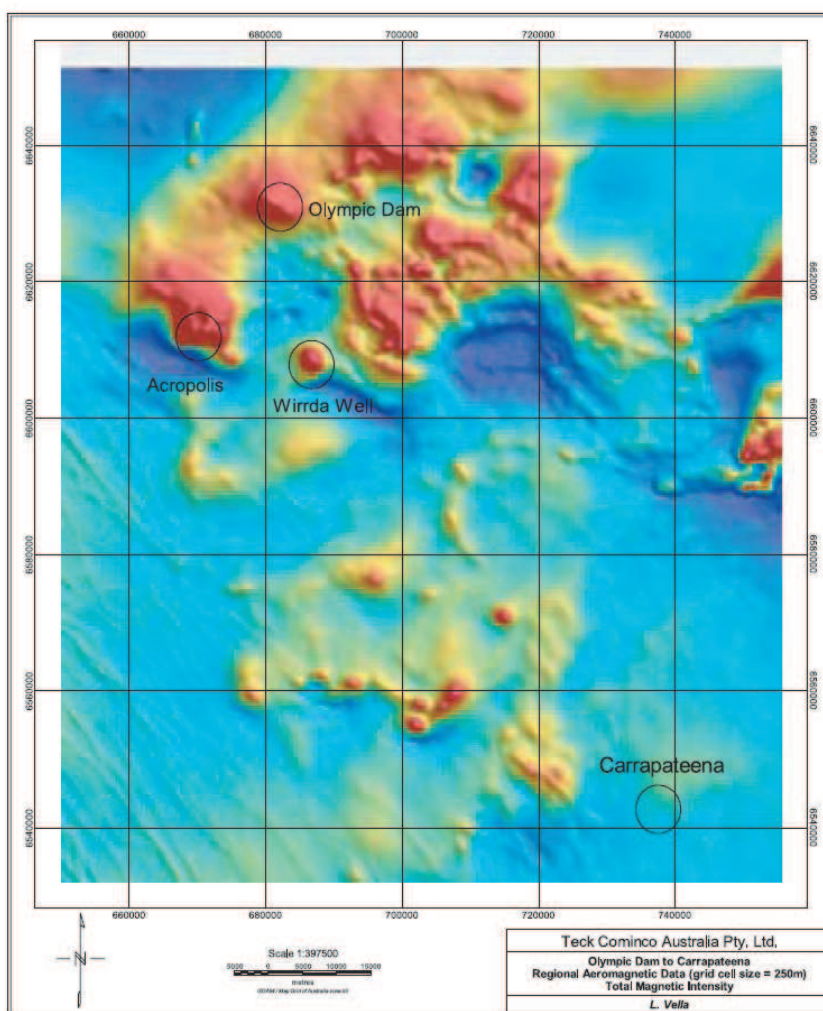


Figure 2.18 Regional total magnetic anomaly map of a portion of the Gawler craton, South Australia showing the location of Olympic Dam and other mineral prospects. Red areas are high values and blues are low. Adapted from Vella and Cawood (2006). Accessible at <http://www.publish.csiro.au/nid/228/paper/PVv2006n122.htm>

lower temperature episode of hematite-rich mineralization. The distribution of the ore is highly complex and they make up only a small fraction of the breccia zone.

Illustrations of the magnetic and gravity anomalies over the Olympic Dam deposit are shown in Figures 2.19 and 2.20. The magnetic anomaly near the

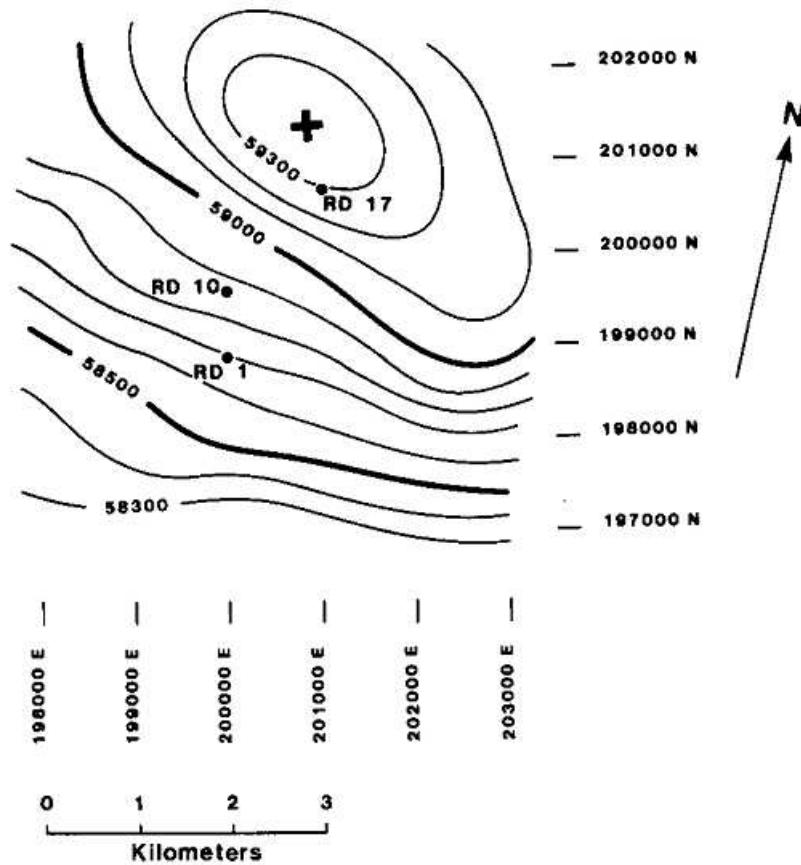


Figure 2.19 Ground total magnetic anomaly map of the Olympic Dam, South Australia, mineral deposit. Contour interval is 100 nT. Adapted from Smith (1985).

surface is of the order of 1600 nT and the gravity anomaly is roughly 17 mGal. Similar near-coincident gravity and magnetic anomalies are observed in the nearby region that are related to similar Olympic Dam-style mineralization. The ground gravity and magnetic anomalies of one of these, Wirrda Well, located 20 km southeast of Olympic Dam, is shown in Figure 2.21. The gravity anomaly attains an amplitude of roughly 6 mGal and the magnetic anomaly's total relief is of the order of 1800 nT. Modeling of the near-coincident anomalies using constraints from drillhole data and petrophysical study of cores suggests that the main source of the magnetic anomaly likely lies at depth associated with magnetite of the early hydrothermal phase of alteration. Likewise the main portion of the gravity anomaly is problematic

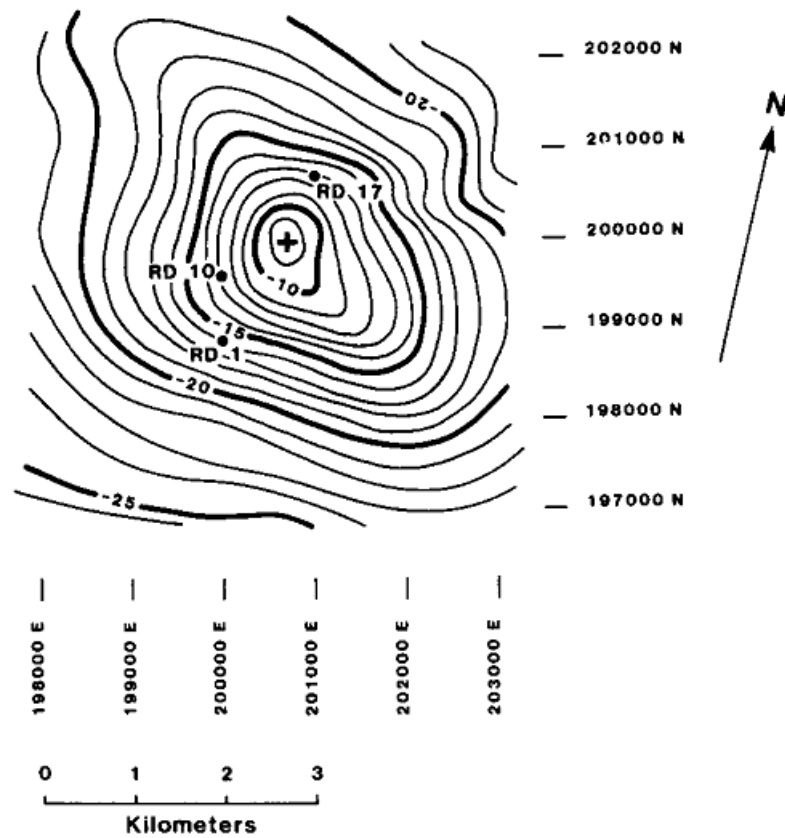


Figure 2.20 Bouguer gravity anomaly map of the Olympic Dam, South Australia, mineral deposit. Contour interval is 1 mGal. Adapted from Smith (1985).

without a deeply extending causative source (Vella, 1997). A similar Olympic Dam-style deposit, the Carrapateena prospect, has been discovered approximately 100 km southeast of the Olympic Dam deposit (Figures 2.17 and 2.18) as a result of coincident, but much lower amplitude gravity (2 mGal) and magnetic (200 nT) anomalies (Vella and Cawood, 2006). The immense economic value of the Olympic Dam deposit has encouraged exploration for similar deposits in other Proterozoic granitic terranes [e.g., Pratt and Sims (1990); Sandrin et al. (2007)].

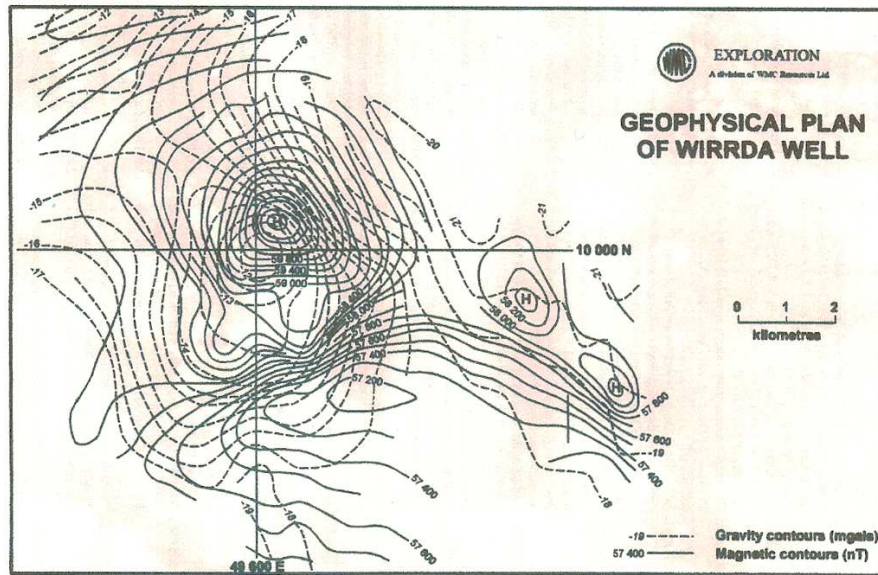


Figure 2.21 Near-coincident ground gravity anomaly and total magnetic anomaly maps of the Wirrda Well mineral prospect, South Australia near the Olympic Dam mineral deposit. Adapted from Vella (1997).

2.4.4 Porphyry Copper Deposits

Worldwide porphyry copper deposits are a major source for copper and molybdenum and to a lesser extent of gold, silver, and other base metals. These deposits occur in felsic to intermediate composition igneous plutons which commonly show a porphyritic texture. The plutons originate in igneous activity in compressive tectonic environments associated with subduction of oceanic crust beneath thickened crust that is being uplifted and subject to surface erosion. They contain disseminated metal sulfides, but may also include late stage veins of concentrated ores and intense alteration in concentric zonal patterns within the intrusive. The margins of the plutons may include magnetite-rich contact metamorphic deposits (skarns or tactites) in carbonate rocks. Geophysical methods have had an ever increasing role in their exploration as investigations have focused on the search for new deposits hidden from direct geological and geochemical exploration. Induced polarization has been particularly useful in searching for the presence of conducting disseminated sulfides, but gravity and magnetic methods have also been widely used in exploration for the intrusives and mapping related alteration patterns that may be related to porphyry copper deposits.

The gravity signature of porphyry copper intrusions is relatively simple

due to the negative density contrast between the intrusives which typically have densities in the range of 2,600 to 2,750 kg/m³ and the commonly higher-density country rock consisting of metamorphic and mafic volcanic rocks. Resulting anomalies, depending on the density contrast and the volume of the pluton, reach negative amplitudes of up to several tens of milligals. These lows may be amplified by several milligals with local fracturing, alteration, and late-stage leaching of the porphyry plutons associated with the influx of hydrothermal mineralizing solutions (Allis, 1990). Local gravity positives of a few milligals can be produced if silification extends into low density, highly porous rocks, especially volcanic rocks, which overlie the plutons.

In contrast, the magnetic signatures of porphyry copper intrusions are complex, being both positive and negative depending on the origin and alteration history of the intrusive and the character of the intruded country rock. The magnetic properties of igneous rocks to a first order increase with decreasing silica content and increasing ferromagnesian mineral content. Accordingly, the magnetization of granitic-type plutons is anticipated to be negligible or low in contrast to other igneous rocks. However, there are notable exceptions to this generality, where a minor but significant proportion of granitic plutons have associated positive magnetic anomalies which include some felsic to intermediate intrusives hosting porphyry copper deposits.

The relationship of porphyry copper mineralization to oxidized, strongly magnetic granitic rocks has been recognized in various regions [e.g., Ishihara (1981)]. Wright (1981) has noted the positive magnetic anomalies associated with these mineralized rocks in the Ely, Nevada region as illustrated in Figure 2.22. Nonetheless, negative anomalies have also been observed with porphyry copper deposits in the southwestern United States as Brant (1966) reported. The minima are related to destruction of magnetite during propylitic and phyllic alteration of the granitic rocks. The variable nature of magnetic anomalies associated with porphyry copper deposits complicates their use in identifying potential ore-bearing plutons. However, magnetic anomalies can be a useful adjunct to identifying porphyry copper deposits by the gravity method because interpretation of gravity signatures is ambiguous due to the varying density contrasts with the country rock and the multiple sources for negative gravity anomalies. Accordingly, Grant (1984a) and Grant (1984b) suggest that circular or ovoid anomalies with concentric magnetic patterns of alteration effects having diameters of 1 to 10 km along with a possible magnetic halo are suggestive of the presence of porphyry copper deposits.

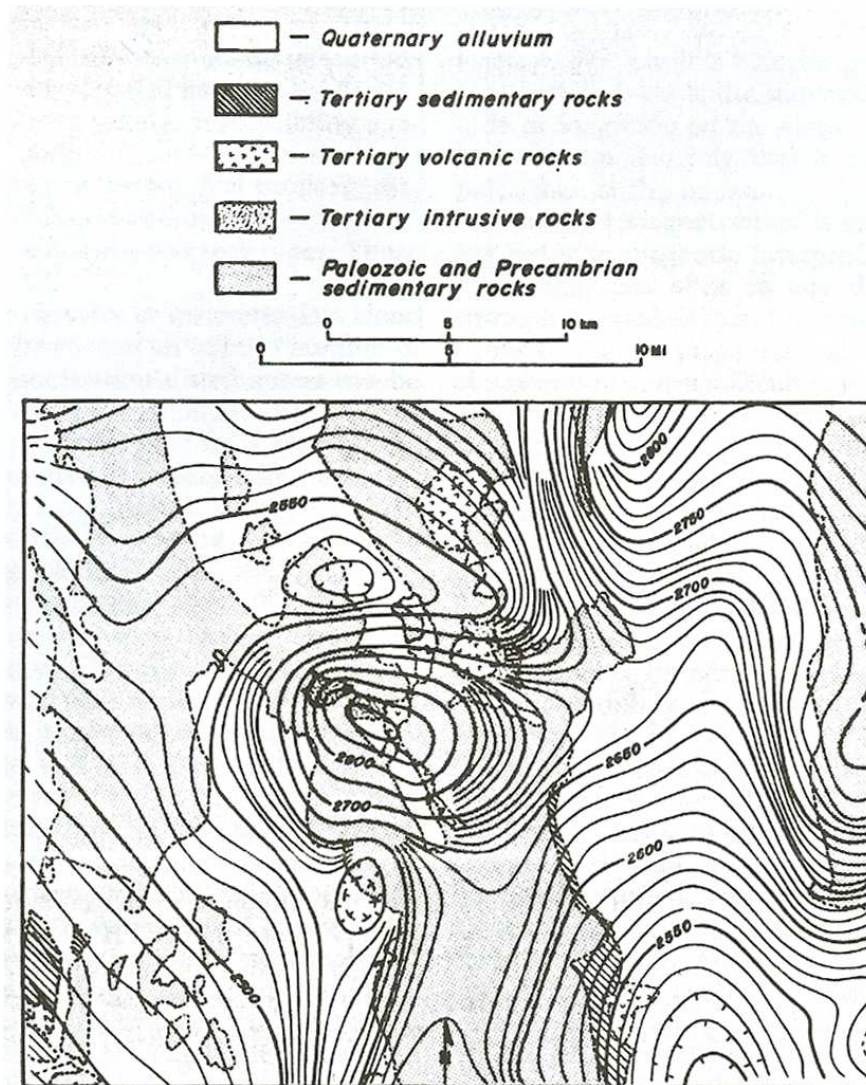


Figure 2.22 Positive total aeromagnetic anomaly centered over a porphyry copper granitoid stock in the Ely, Nevada, U.S. region. Adapted from Wright (1981).

Clark et al. (1992) have illustrated magnetic anomalies over an idealized porphyry copper system that has intruded magnetic volcanic rocks as shown in Figure 2.23 assuming vertical magnetization. The background magnetic pattern is variable as a result of heterogeneous magnetization in the volcanic rocks, whereas the porphyry pluton is a minimum caused by a total

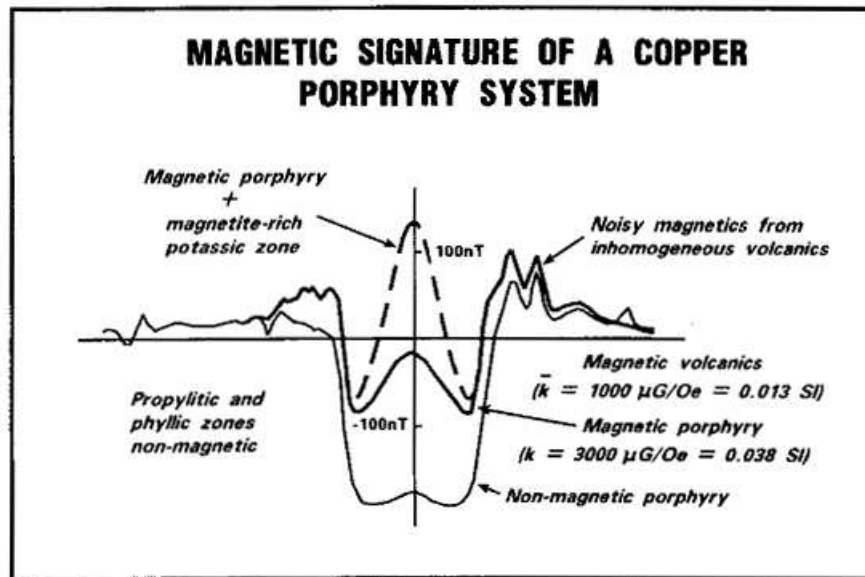


Figure 2.23 Idealized magnetic anomaly associated with a porphyry copper system assuming vertical magnetization. The irregular background anomalies adjacent to the principal anomaly are due to magnetic volcanic country rocks, the *alteration minimum* is associated with propylitic and phyllic alteration zones, and the positive arising from the magnetic porphyry plus, in the case of gold-rich copper mineralization, the magnetite-bearing potassic alteration zone. Adapted from Clark et al. (1992). Accessible at <http://www.publish.csiro.au/nid/224/paper/EG992065.htm>

magnetization which is less than the volcanic rocks which it intrudes. The central positive in the porphyry is a more intensely magnetic core related to magnetite deposited by the mineralizing solutions. Destruction of magnetite with propylitic and phyllic alteration modifies the signature of the original magnetic porphyry pluton creating a magnetic low with a central flat zone. This is similar to the magnetic anomalies described by Irvine and Smith (1990) associated with epithermal gold mineralization in silicified fracture zones, quartz-filled breccias, and silica-rich veins in felsic volcanic rocks of northeast Australia. The alteration may be reflected in annular magnetic zones reflecting the variable destruction of magnetite during alteration. If the pluton is subject to potassic alteration, magnetite in this zone will produce the amplified central high as shown in Figure 2.23.

The magnetic signatures of Figure 2.23 would be different if the porphyry pluton invaded sedimentary rocks or felsic rocks. The pluton would likely be indicated as a magnetic positive due to the magnetization contrast between

the pluton and the adjacent country rocks. Alteration accompanying mineralization would lead to destruction of magnetite and the magnetic high, but the positive anomaly would be reinforced if a magnetite-rich potassic alteration zone developed. Furthermore, a peripheral magnetic halo of highs would be associated with skarn deposits produced in adjacent carbonate rocks.

A notable example of a porphyry copper in the U.S. is the Butte, Montana mineral district. This was a very productive district for over a century that initially supported mining of late-stage mesothermal and epithermal veins rich in copper, silver, gold, and other base metals. Later, the early porphyry style mineralization consisting of largely disseminated sulfides was the principal ore. The Butte ore body occurs within the late Cretaceous Boulder batholith that has a surface area of $120 \times 40 \text{ km}^2$. The batholith is a gravity minimum of several tens of milligals as a result of the negative density contrast between the batholith and the intruded country rock and a magnetic high reflecting the significant magnetism of the dominant intrusive, the Butte quartz monzonite. However, the intense and pervasive sericite alteration of the Butte quartz monzonite in the porphyry copper deposit in the south-central portion of the batholith destroyed the original magnetite causing the porphyry copper deposit to have only negligible magnetization. As a result, the ore body is reflected in the prominent magnetic minimum (Hanna, 1969) shown in Figure 2.24 centered on the city of Butte (Klepper et al., 1971). The anomaly extends to the west, where it is associated with the generally low-magnetization, late stage quartz-latitude Lowland Creek volcanic rocks and Cenozoic alluvium. Similar magnetic minima are associated with alteration of the Boulder batholith pluton to the north of Butte roughly along the centerline of the batholith. A similar magnetic minimum is associated with porphyry copper mineralization and related alteration and mineralization with the porphyry copper deposits in the Guichon Creek batholith in British Columbia, Canada (Roy and Clowes, 2000). This zone of low magnetic susceptibility is also marked by low density and velocity rocks which host the copper deposits.

Oldenburg et al. (1997) describes an interesting example of joint inversion of magnetic and induced polarization (IP) measurements over a copper/gold porphyry deposit in British Columbia, Canada. Figure 2.25 shows the surface total magnetic anomaly data observed over the Mt. Milligan deposit that was used to interpret the 3D magnetic susceptibility of the deposit. The results in Figure 2.26 show the areal distribution of magnetic susceptibility at the depth of 80 m as well as the values obtained along three vertical sections extending to the depth of 450 m. The results from the magnetic anomaly in-

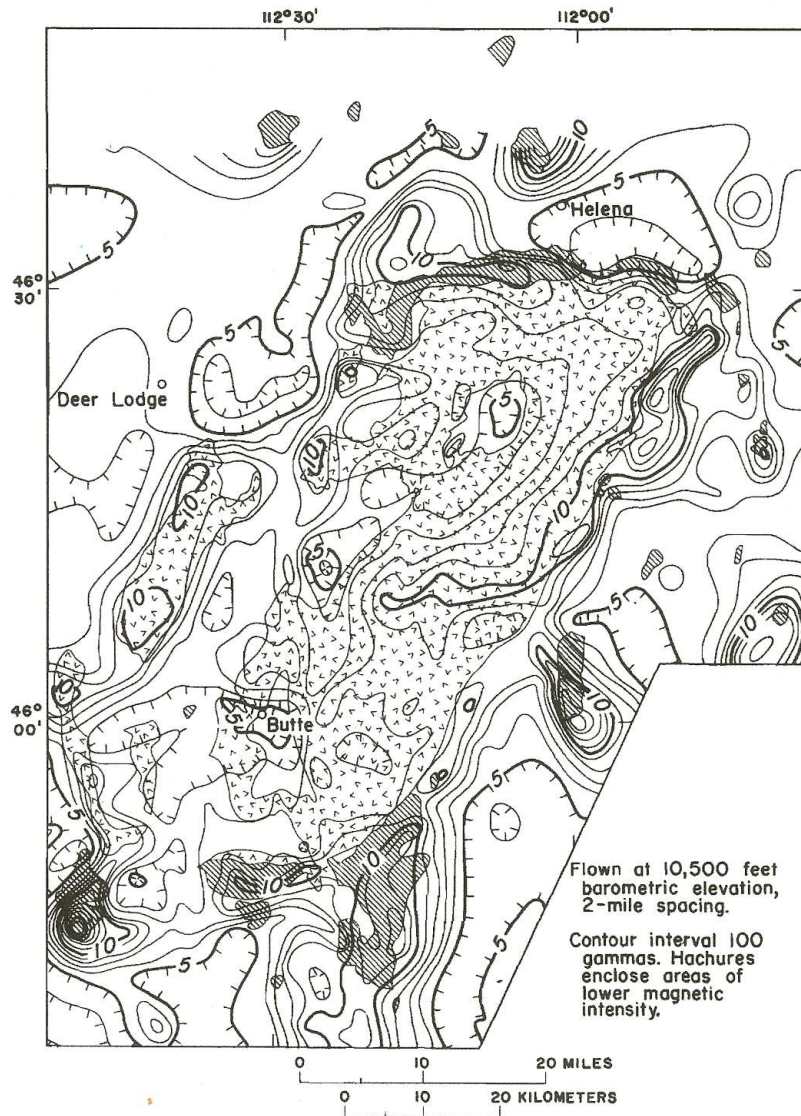


Figure 2.24 Regional total aeromagnetic anomaly map of the Boulder batholith, Montana, U.S. The negative anomaly centered on the city of Butte is associated with alteration of the Butte quartz monzonite and porphyry copper mineralization. Adapted from Klepper et al. (1971).

version as well as inversion of DC/IP and airborne EM data to chargeability and conductivity of the deposit were used with information from 600 drill holes into the deposit to determine the variation in rock properties with the gold concentration. Chargeability from IP inversion correlates with highest

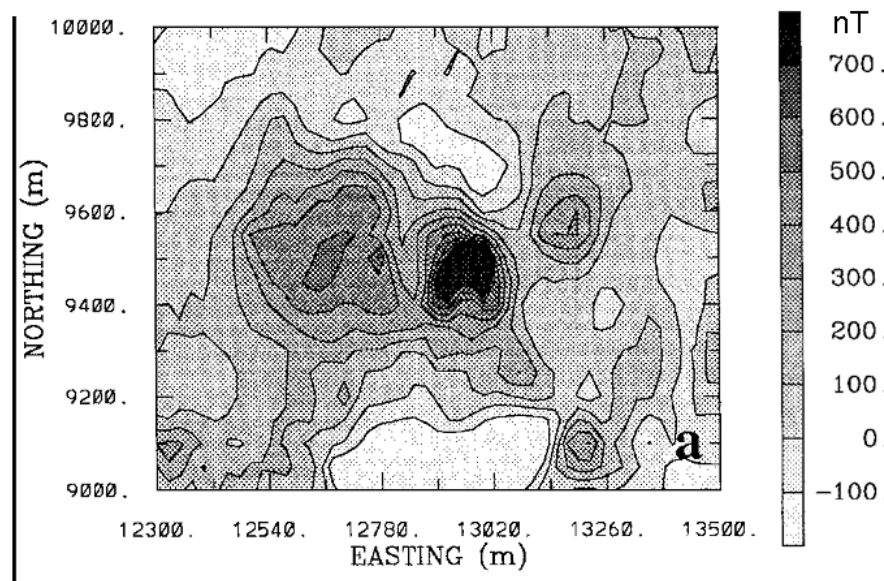


Figure 2.25 Surface total magnetic anomaly map of the Mt. Milligan copper/gold porphyry deposit in British Columbia, Canada. The darker shades are higher magnetic anomaly values in nanotesla. Adapted from Oldenburg et al. (1997).

gold concentration, while magnetic susceptibility is anticorrelated with gold concentrations. A plan view of gold concentrations at 90 m and on three vertical sections (Figure 2.27) show the gold concentrations mapped from drillhole sample geochemical data. The anticorrelation of magnetic susceptibility and gold concentration are readily observed. Accordingly, a joint "cooperative inversion" was conducted using a weighting factor determined from the results of inversion of the magnetic anomaly data set to constrain inversion of the IP data to chargeability. Oldenburg et al. (1997) indicate that drilling on the results of the joint inversion would have intersected the highest gold concentration.

2.4.5 Mafic/Ultramafic Mineral Deposits

Mafic/ultramafic intrusions are potential targets for deposits of base and precious metals. One such occurrence is the Mount Ayliff intrusion in South Africa (Sander and Cawthorn, 1996). A small nickel, copper, platinum-group metal sulfide deposit near the base of this intrusion has been mined in the past and interest continues in the detection of similar ore deposits in the in-

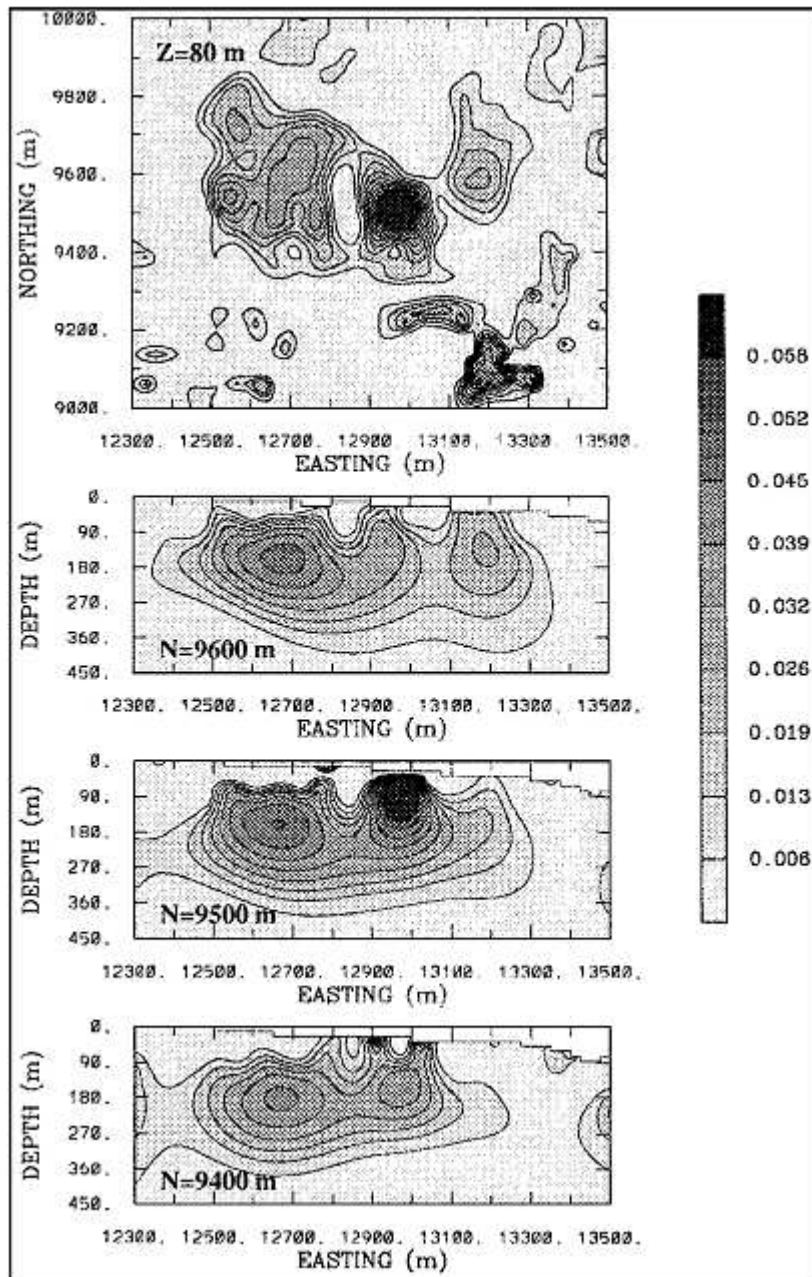


Figure 2.26 Results of inversion of the surface magnetic anomaly map of the Mt. Milligan deposit shown in Figure 2.25. The upper diagram shows the plan view of the resulting magnetic susceptibility contrast in SIu at the depth of 80 m. The panels below show successively the magnetic susceptibility contrast results on cross-sections at $x = 9400, 9500,$ and 9600 m. The darker shades are higher magnetic susceptibilities. Adapted from Oldenburg et al. (1997).

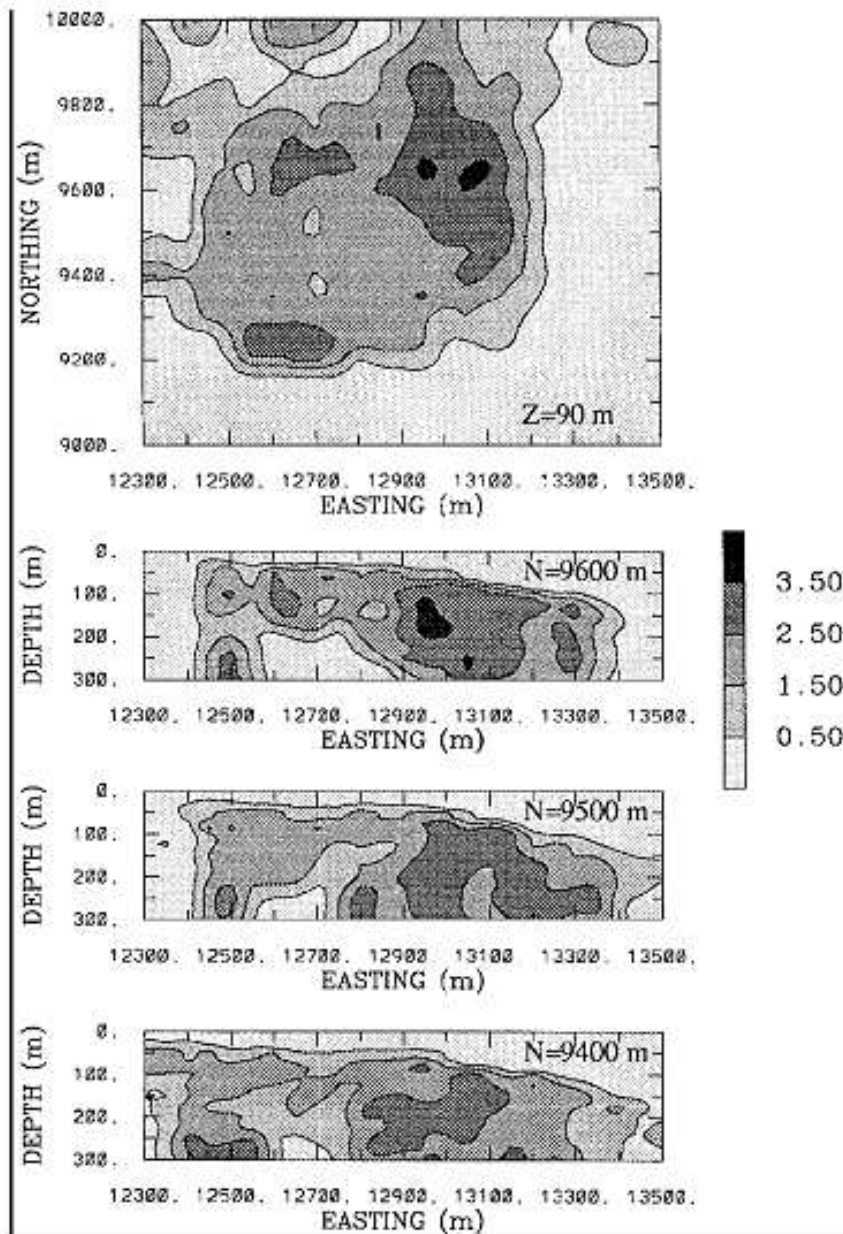


Figure 2.27 Plan view of relative gold concentrations of the Mt. Milligan deposit shown in Figure 2.25 at the depth of 90 m determined from analyses of drill core is shown in the upper map. The panels below are the gold concentrations of the cross-sections shown in Figure 2.26. The darker shades are higher gold concentrations. Note the inverse correlation between the gold concentrations and magnetic susceptibility contrast. Adapted from Oldenburg et al. (1997).

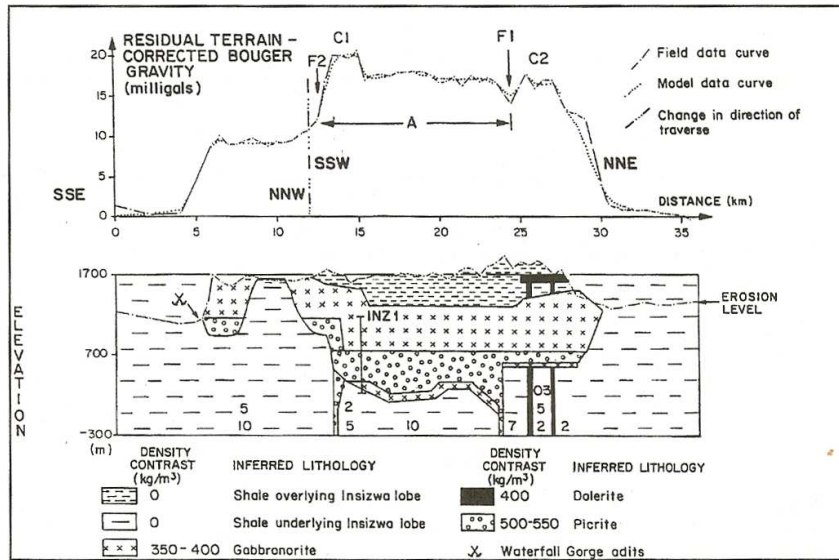


Figure 2.28 2.5D gravity model of the complete Bouguer gravity anomaly profile across the Mount Ayliff intrusion, South Africa. Numbers along the bottom of the section are strike half-lengths (in km) of overlying, or adjacent, modeled sources. Exploration drill hole *INZ1* has been projected 7.5 km into the profile along the interpreted geophysical strike. The density contrasts in kg/m^3 are referenced to the mean density of the Karoo shale of 2700 kg/m^3 . *C1, C2, F1, F2* are referenced in the text. Adapted from Sander and Cawthorn (1996).

trusion. The Mount Ayliff structure is a sill-like layered intrusion associated with the Karoo (Jurassic) continental flood basalts that intruded into Karoo shale. The ore is located within a basal zone composed of olivine-rich ultramafic rocks, largely picrite, of variable thickness that is overlain by layered gabbro/norite rocks. Exploration models require an improved understanding of the morphology of the intrusion which is largely hidden from view.

The significant density differential between the intrusion and the surrounding shale has encouraged the use of the gravity method to investigate its structure and third dimension. Gravity surveys along traverses over the intrusion have been made and interpreted based on knowledge of densities, results of available drilling, and outcrop geology (Sander and Cawthorn, 1996). A 2.5D model of one of these gravity traverses which closely matches the observed complete Bouguer gravity anomaly is shown in Figure 2.28. The profile shown is the residual anomaly profile after removal of a regional gradient determined from a smoothed profile through the observed anomaly

data, constraints from local geology, and available regional gravity anomaly mapping. Rugged topography made terrain corrections a necessity. On the profile shown in Figure 2.28, terrain corrections ranged from 1.2 to 10.6 mGal with a modal value of 3 mGal.

Modeling of the profile which reaches a maximum residual positive of 19 mGal has been constrained by the geology derived from drillhole *INZ1* which is shown on the figure as well as surface geology. The mined-out ore deposit at Waterfall gorge is also indicated on the figure. Steep anomaly gradients of anomalies *C1* and *C2* suggest shallow sources. Anomaly *C1* is related to an exposed 80 m thick dolerite (diabase) sill and is so modeled in the profile. The source of anomaly *C2* is not visible in the surface geology, but it may have a similar origin to that of *C1* or may be related to doming of the gabbro/norite in the roof of the intrusion as indicated in the model. *F1* marks the location of the mapped Blydefontein fault lineament and the possible location of a picrite feeder dike. *F2* is also interpreted as a possible picrite feeder dike, although the dikes are too small and deep to resolve in the gravity anomaly data. These dikes are potential avenues for intrusion of the several hundred meters of picrite modeled in the gravity profile and which may be a potential target for ore deposit exploration such as the mined-out deposit at Waterfall gorge. The gravity method has provided useful information on the structure and third dimension of the Mount Ayliff intrusion and the location and thickness of the potential ore horizon. The constraints of surface geology, physical property determinations, and information from drill holes have made this interpretation possible while minimizing the ambiguity of the results.

The utility of the magnetic method in the actual location of base metal deposits associated with ultramafic rocks is problematic despite the generally higher magnetization of these deposits. This is well illustrated by the investigations of, for example, McCall et al. (1995) and Peters and Buck (2000) of the nickel sulfide deposits associated with the komatiitic peridotite rocks of Western Australia. Despite the magnetization of the ores, their signature in the detailed magnetic surveys is extremely difficult to identify because of the limited thickness and depth (few hundred meters) of the ore bodies, their lack of consistent magnetic contrast with the associated ultramafic rocks, and the effect of remanence on the magnetization of the ores and ultramafic rocks which can either support or decrease the total magnetization contrast. Magnetic modeling of total magnetic intensity anomaly profiles across the Wannaway nickel sulfide deposits of Western Australia by McCall et al. (1995) as shown in Figure 2.29 illustrates the minor effect of the ore bodies and the lack of identifiable signature. Platinum group element-rich (PGE)

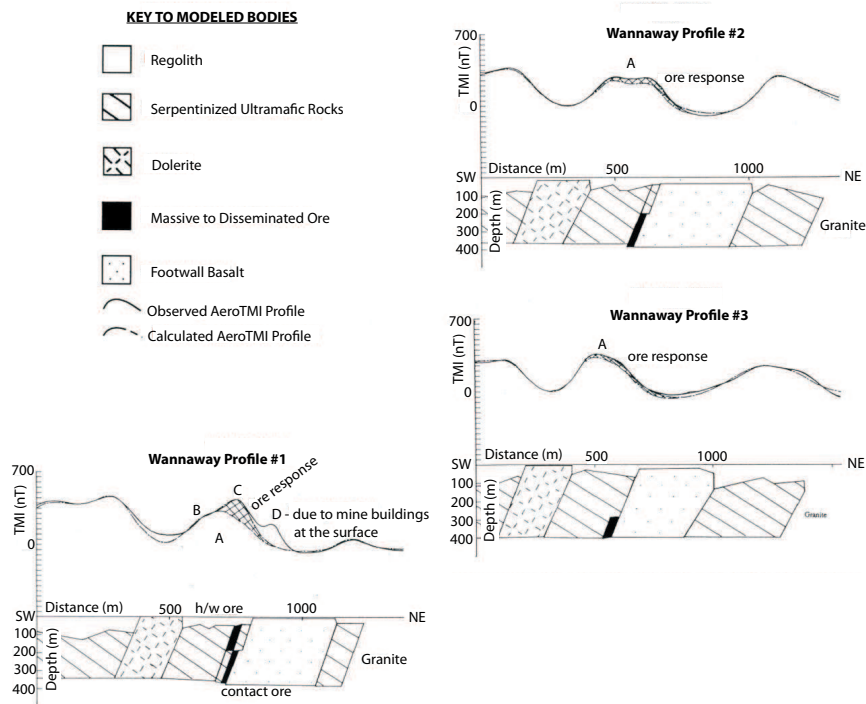


Figure 2.29 Total magnetic intensity (TMI) anomaly models of three profiles across the Wannaway nickel sulfide deposit in Western Australia. Anomaly *D* is caused by mine buildings and the cross-hatched areas on the anomaly curves are the portions of the anomalies caused by the ore bodies which are shown in solid black in the depth sections. Note the minor magnetic effect due to the ore deposit. Adapted from McCall et al. (1995). Accessible at <http://www.publish.csiro.au/paper/EG995066.htm>

disseminated *Fe – Cu* sulfide mineralization is also a significant mineral exploration target in largely layered mafic intrusives such as the Bushveld Complex in South Africa. Unfortunately the thickness and properties of these mineralized zones prevent them from having diagnostic and isolated signatures to make them viable magnetic targets. However, Larson et al. (1998) have shown that the magnetic properties of the (PGE) zones have been enhanced by magnetite enrichment in iron-rich basalt in the Archean Abitibi Greenstone Belt, Ontario. The ground magnetic signature of these zones is readily observed suggesting that high-resolution magnetics can be used for mapping potential PGE deposits. However, this methodology is likely to be successful only where geological and geochemical information is integrated with the geophysical surveys and their interpretation.

A massive major nickel/copper/cobalt ore deposit has been identified in the Voisey Bay mafic layered intrusive of Labrador, Canada. A gravity anomaly of the order of 4 mGal which has been mapped over the deposit has been subject to constrained inversion to delineate the subsurface nature and extent (Farquharson et al., 2008). A density database for the deposit obtained from samples of over 500 drill holes was used to develop reference models for constraining the inversion. This reference model has resulted in an interpretation more consistent with the known geology that would not have been obtained without it and has provided useful subsurface information for exploitation of the ore body.

One of the Earth's most interesting and mineral-rich geologic structures is the Bushveld complex of South Africa. It is a intrusive layered igneous complex of Precambrian age measuring roughly 400 km east-west and 150 km north-south. Two major components are recognized in the complex, an early mafic phase, the Rustenburg Layered Suite, and a later granitic phase. The mafic phase is a major economic mineral resource containing large reserves of chromite and platinum group elements. The mafic phase is hidden in the central part of the structure by the intruded volcanic and sedimentary rocks and upper granitic phase rocks.

Analysis of the gravity anomaly data over the complex has been used to investigate the possible occurrence of the mineral-rich mafic rocks in the central region. Early modeling suggested that the mafic rocks are largely restricted to the eastern and western ends of the complex associated with intense positive gravity anomalies derived from the mafic rocks [e.g., Cousins (2014)]. However, more recent modeling [e.g., Cawthorn et al. (1998); Webb et al. (2004)], which incorporates isostatic considerations leading to an increase in the thickness of the crust beneath the complex supported by seismic studies, shows that the mafic zone is continuous between the western and eastern limbs. The positive gravity effect of the mafic zone in the central portion of the complex is negated by the decrease in gravity due to the thickened crust. Three-dimensional gravity modeling of the complex on a west/east cross-section (Cole et al., 2014) has superseded previous 2.5D modeling. Figure 2.30 shows the profound difference between the 2.5D and 3D gravity anomaly modeling along a west/east profile across the complex. The Cole et al. (2014) study and related gravity modeling incorporating possible variations in the lower crust and upper mantle show the importance of 3D modeling and lower crust and upper mantle considerations in gravity modeling of large structural features.

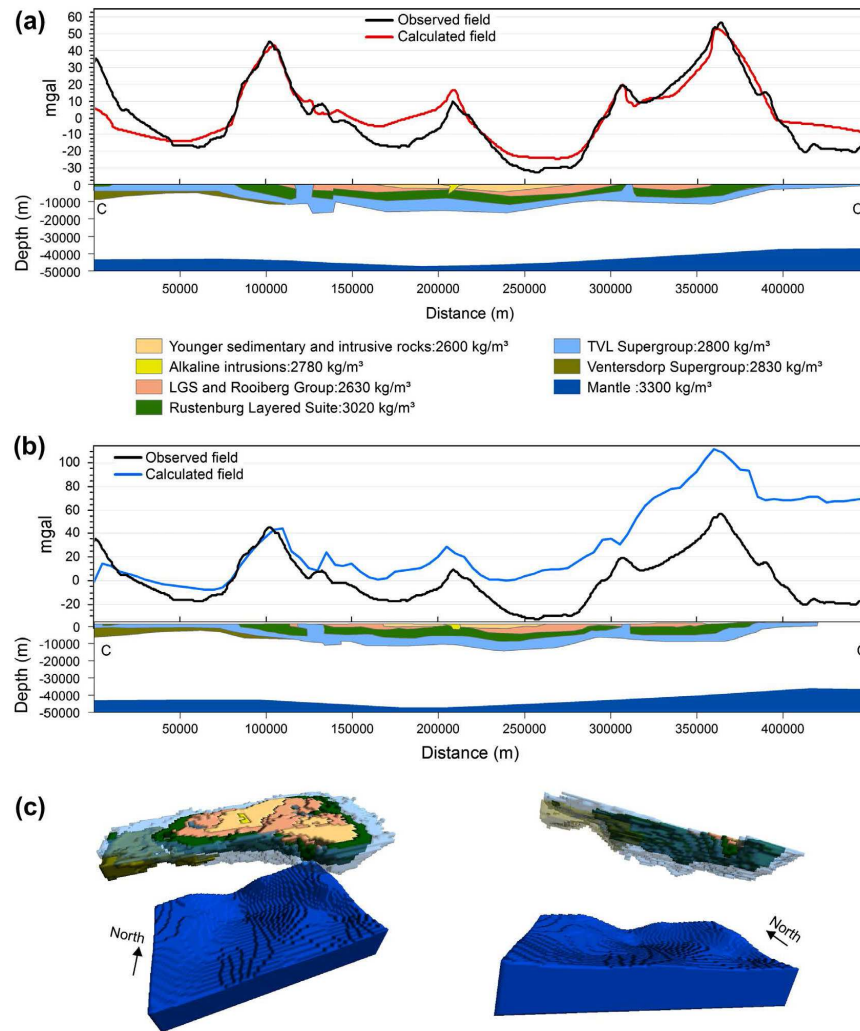


Figure 2.30 (a) Observed west/east Bouguer gravity anomaly profile of the Bushveld complex and calculated anomaly using a 2.5D model shown in the cross-section. (b) Observed west/east Bouguer gravity anomaly profile of the Bushveld complex and calculated anomaly using a 3D model with the cross-section of the 3D model shown. Note the profound difference in the 2.5D and 3D model calculated gravity anomalies. Adapted from Cole et al. (2014).

2.5 Direct Exploration for Mineral Deposits

Gravity and magnetic methods have a significant role in the indirect exploration for mineral deposits, but a more restricted role in direct exploration

because of the limited diagnostic properties of most mineral deposits and the lack of compact features which produce readily identified intense isolated anomalies. In contrast to the electrical properties of most metallic mineral deposits which foster the use of electrical exploration methods, the density and magnetization of ore bodies are in general less definitive. Nonetheless, capitalizing on the higher densities of most ore minerals compared to common rock-forming minerals, the gravity method is used to identify and map mineral deposits. In the case of magnetics, minerals with diagnostic properties useful in magnetic mapping are much more restricted. Only magnetite and less widely occurring pyrrhotite are sufficiently magnetic to be mapped by the magnetic method. Accordingly, the magnetic method is limited to iron ore deposits containing magnetite or other mineral deposits that have sufficiently significant quantities of accessory magnetite/pyrrhotite so that they can be mapped as anomalous features.

The limited physical dimensions of most ore deposits requires high-density, high-resolution investigations conducted on or near the surface to attain the precision and resolution required for mapping ore bodies, but increasingly improved airborne magnetic and gravity methods of mapping, data processing, and interpretation are being used to directly locate mineral deposits. Generally, magnetic methods are used in direct detection studies regardless of the target because seldom does magnetic mapping fail to provide useful direct or collateral information and the method is easier to implement and less expensive than other methods. The gravity method is less sensitive to source depth than the magnetic method (Hinze, 1966), and thus is commonly used to map out the depth extent of an identified exploration target and its configuration at depth. This lower sensitivity to source depth also results in a slower decrease in the amplitude of anomalies with increasing source depth, permitting enhanced detection of deeper sources by gravity over magnetic methods.

2.5.1 MacDonald Mines Property, Quebec, Canada

A useful example of direct exploration for ore deposits by the gravity method has been cited by Innes and Gibb (1970) as a result of the survey conducted by the Dominion Observatory, Canada over the MacDonald Mines property in Dufresnoy township in western Quebec, Canada. The survey was conducted to investigate the use of the gravity method in detecting near-surface ore bodies. The roughly 3 mGal gravity anomaly shown in Figure 2.31 is centered over the ore body composed of pyrite and some sphalerite with an estimated 12 million tons of ore. This deposit occurs in the near

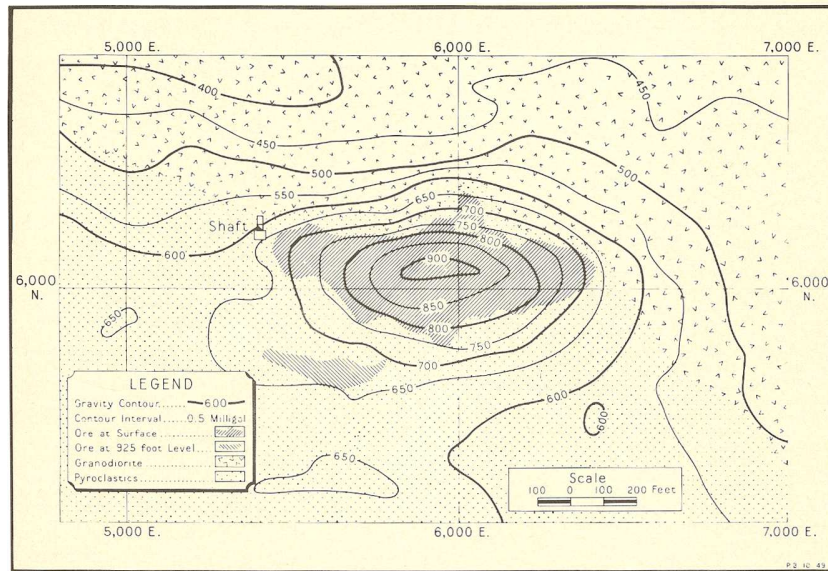


Figure 2.31 Bouguer gravity anomaly map over the MacDonald Mines property orebody in western Quebec, Canada. Adapted from Innes and Gibb (1970).

subsurface, but is completely hidden by overburden. It was discovered by drilling along the contact between volcanic rocks and a large granodiorite intrusion.

2.5.2 Barite Deposits

The high density of the ore mineral barite ($\approx 4500 \text{ kg/m}^3$) suggests that the gravity method may be used to identify and study barite deposits [e.g., Uhley and Scharon (1954)]. Accordingly Barnes et al. (1982) have used gravity to investigate the extent of a massive barite deposit that is observed in an outcrop in the western Brooks Range, Alaska. Intersecting gravity profiles across the outcrop Figure 2.32 indicate a gravity anomaly of the order of 2 mGal over the deposit. Modeling of the observed Bouguer anomaly based on a density differential of 1700 kg/m^3 derived from measurements of the density of the barite and surrounding rocks suggests that the anomaly could be accounted for by a right circular cylinder shaped source roughly 90 m in diameter and 55 m thick. These results suggest the usefulness of the gravity method in searching for and studying barite deposits.

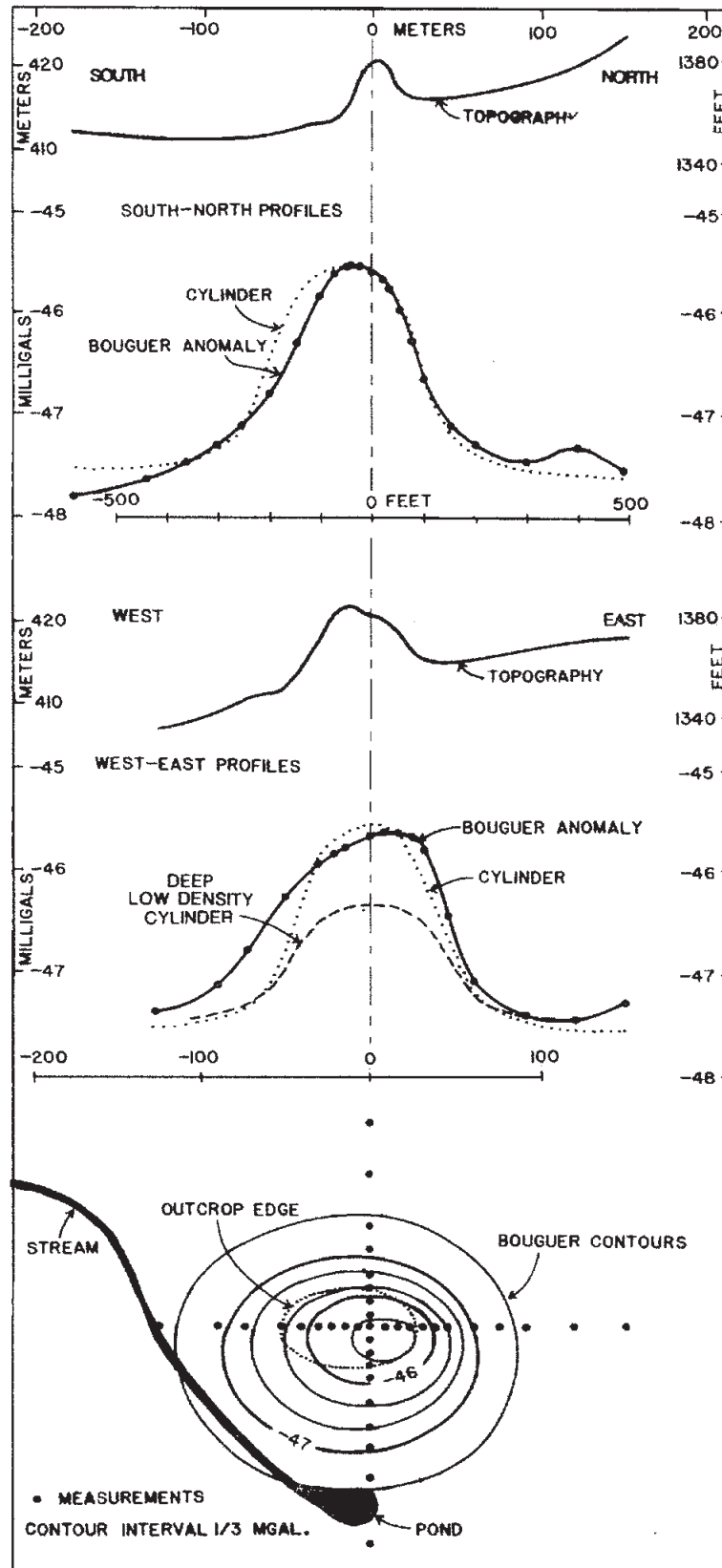


Figure 2.32 Topographic and observed and modeled Bouguer gravity anomaly profiles and map over the Nimiuktuk barite outcrop, Brooks Range, Alaska, U.S. Adapted from Barnes et al. (1982).

2.5.3 Faro Lead/Zinc Deposit, Yukon Territory, Canada

Gravity also had a significant follow-up role in the integrated airborne and ground geophysical exploration program leading to the discovery of the Faro *Pb/Zn* sulfide deposit in the Yukon Territories of Canada [e.g., Brock (1973); Tanner and Gibb (1979)]. The gravity study illustrated in Figure 2.33 was used to further define the source of the coincident magnetic and geochemical anomalies shown in the figure. The massive sulfides encountered in the drilling of the 3 mGal anomaly are shown in the accompanying geological cross-section. Gravity was useful in directing subsequent drilling of the ore body. The magnetic anomalies associated with these types of base metal deposits are generally of a subtle nature due to the occurrence of small amounts of magnetite and pyrrhotite. However, the ore bodies are commonly related to iron-rich lenses in nearby sedimentary rocks that may contain sufficient magnetite to produce diagnostic magnetic anomalies. These anomalies may suggest the nearby occurrence of base metal deposits.

2.5.4 Bathurst Mining District, New Brunswick, Canada

Thomas (1997) presented a comprehensive review of the use of the gravity method in the exploration for base metal sulfide deposits in the Bathurst mining district of New Brunswick, Canada. The ores in the district generally occur at the contact between tuffs and sedimentary rocks as layered stratiform lenses. The density of the ores range from 3600 to 4400 kg/m³ and the felsic volcanic host rocks and adjacent sedimentary rocks range from 2700 to 2850 kg/m³, although adjacent mafic volcanic rocks and iron formations have higher density. One of the more significant gravity anomalies over sulfide ores in the district is the roughly 4 mGal anomaly associated with the outcropping Brunswick #6 deposit as shown in Figure 2.34. A portion of this anomaly is caused by the adjacent iron formation (density = 4100 kg/m³). In Figure 2.34, Thomas (1997) shows that at the burial depth of 100 m the anomaly amplitude would be reduced to roughly 1 mGal and the anomaly would be smoothed making it much more difficult to relate the anomaly to an ore deposit. Figure 2.35 shows a somewhat more complicated gravity anomaly over the Brunswick #12 deposit. In this case, the presence of dense basalt on the west flank of the ore body results in a step-like anomaly. The ore body itself is suggested by a weak 0.8 mGal anomaly over the subcrop of the deposit that might be missed depending on the resolution and intensity of the gravity surveying and interpretation.

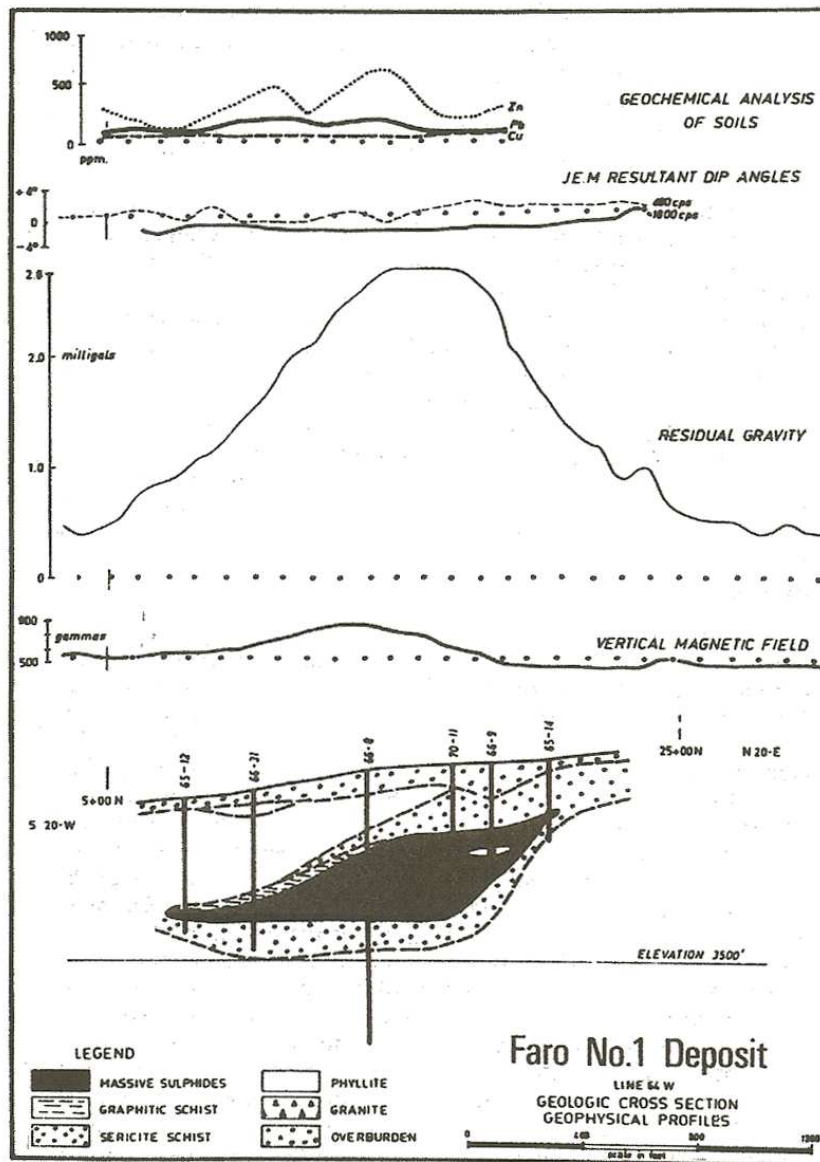


Figure 2.33 Geological cross-section of the Faro *Pb/Zn* deposit in the Yukon Territories, Canada with associated geochemical, magnetic, EM, and gravity anomaly profiles. Adapted from Tanner and Gibb (1979).

2.5.5 Volcanogenic Massive Sulfide Deposits

Although electrical methods both ground and drill hole have been important to mapping Proterozoic volcanogenic massive sulfides in Finland (Hattula

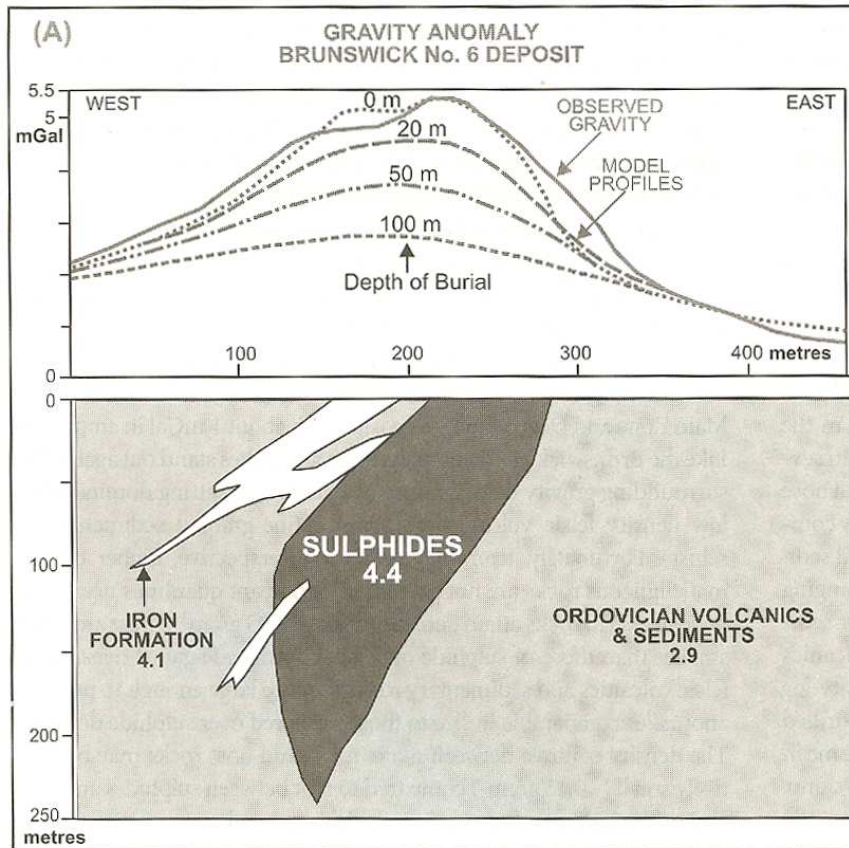


Figure 2.34 Observed and modeled Bouguer gravity anomaly profiles across the Brunswick #6 base metal sulfide deposit in the Bathurst mining district, New Brunswick, Canada. Densities are in g/cm^3 . Adapted from Thomas (1997).

and Rekola, 2000), the gravity method has also provided site-specific information for such deposits as the ores at Pyhäsalmi. The nearly vertical dipping Pyhäsalmi pyrite-rich zinc-copper-sulfur ore deposit Figure 2.36 which is 650 m long and up to 75 m wide has an associated gravity anomaly of up to 3 mGal as shown in Figure 2.37. The measured and calculated gravity anomalies over the deposit are shown in Figure 2.38 together with the ore models used in the calculations. The high density of the ores shown in the models indicates the viability of the gravity method in studying such deposits.

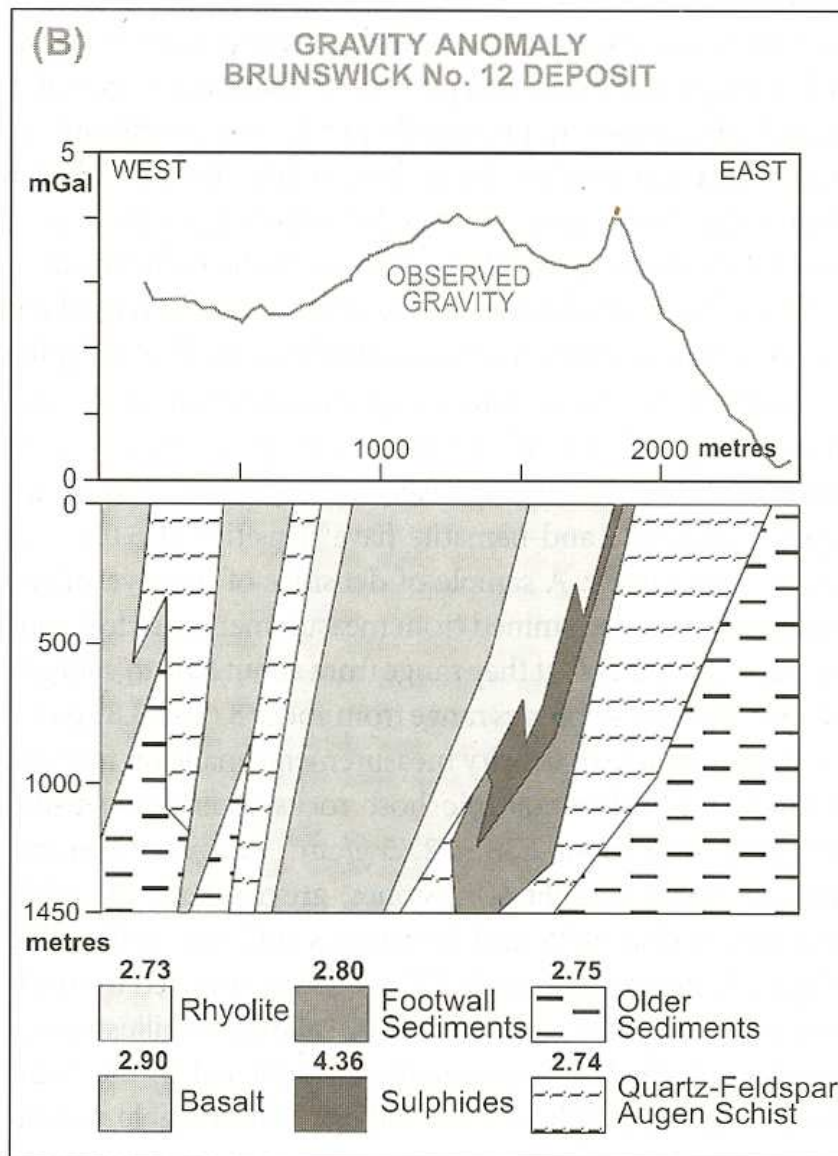


Figure 2.35 Observed Bouguer gravity anomaly across the Brunswick #12 base metal sulfide deposit in the Bathurst mining district, New Brunswick, Canada. Densities are in g/cm^3 . Adapted from Thomas (1997).

2.5.6 Rare Earth Elements

Rare earth elements (REE) are important in making many high-tech devices and thus are in great demand today. Unfortunately most of the REEs used

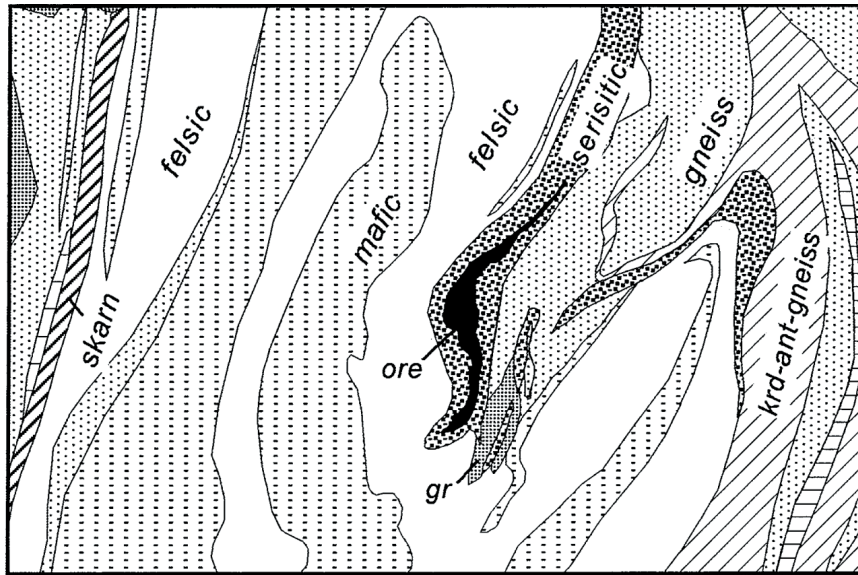


Figure 2.36 Geological map of the Pyhäsalmi zinc-copper sulfide deposit, Finland. Adapted from Hattula and Rekola (2000).

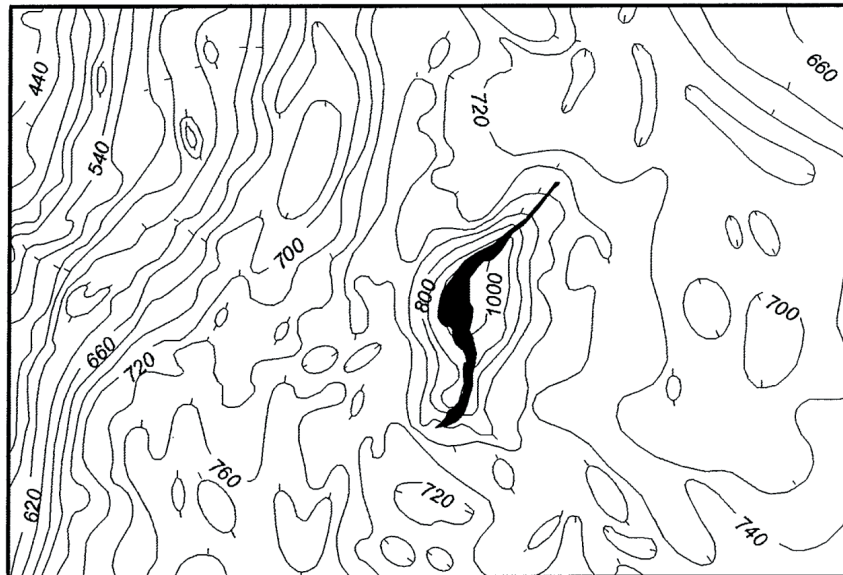


Figure 2.37 Observed Bouguer gravity anomaly of the Pyhäsalmi zinc-copper sulfide deposit, Finland shown in Figure 2.36. Contour interval is 200×10^{-2} mGal. Adapted from Hattula and Rekola (2000).

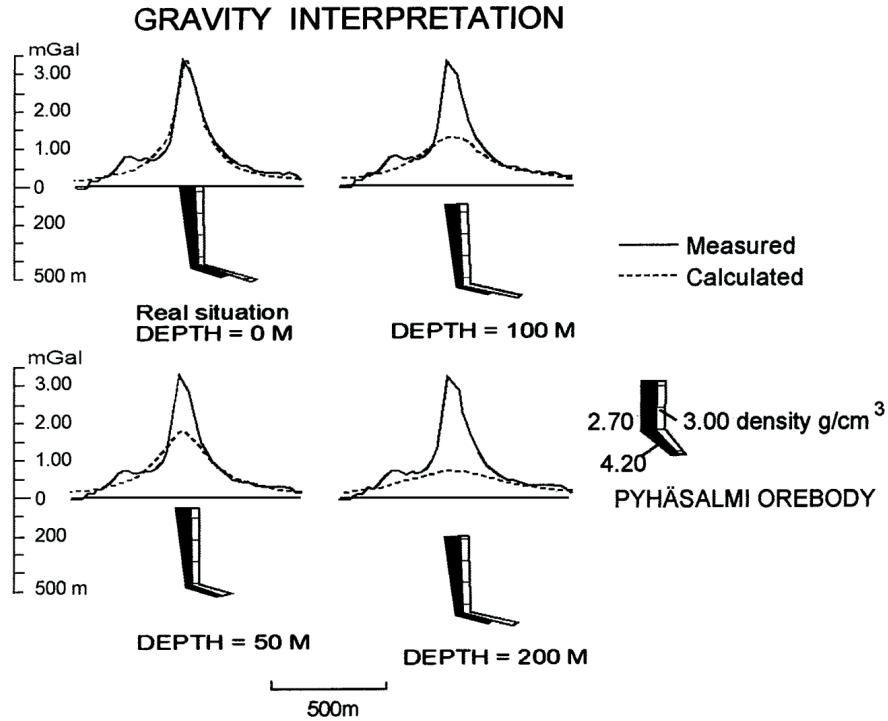


Figure 2.38 Observed and modeled Bouguer gravity anomaly profiles across the Pyhäsalmi zinc-copper sulfide deposit, Finland. Adapted from Hattula and Rekola (2000).

today are obtained from mines in China, but the Chinese have decided to limit the export of these elements. As a result, the exploration and exploitation of deposits of these elements has taken on a new urgency. One example of recent exploration for REEs is described in the report by Drenth (2012) of the lower-Paleozoic Elk Creek carbonatite identified in the subsurface of southeastern Nebraska. This complex which occurs at a depth of 200 m beneath Pennsylvanian clastic sedimentary rocks was discovered by drilling on a gravity high. The gravity high is primarily a result of a density contrast of 150 kg/m^3 between the principal lithology of the carbonate rocks and the surrounding Precambrian gneiss.

REEs are commonly associated with zoned alkali intrusive complexes such as carbonatite intrusions which consist of more than 50% carbonate minerals. The mineralogy of these intrusions is complex and their mean density is high because of the constituent mineralogy. As a result, a combined airborne magnetic and gravity gradient survey has been used to investigate the Elk

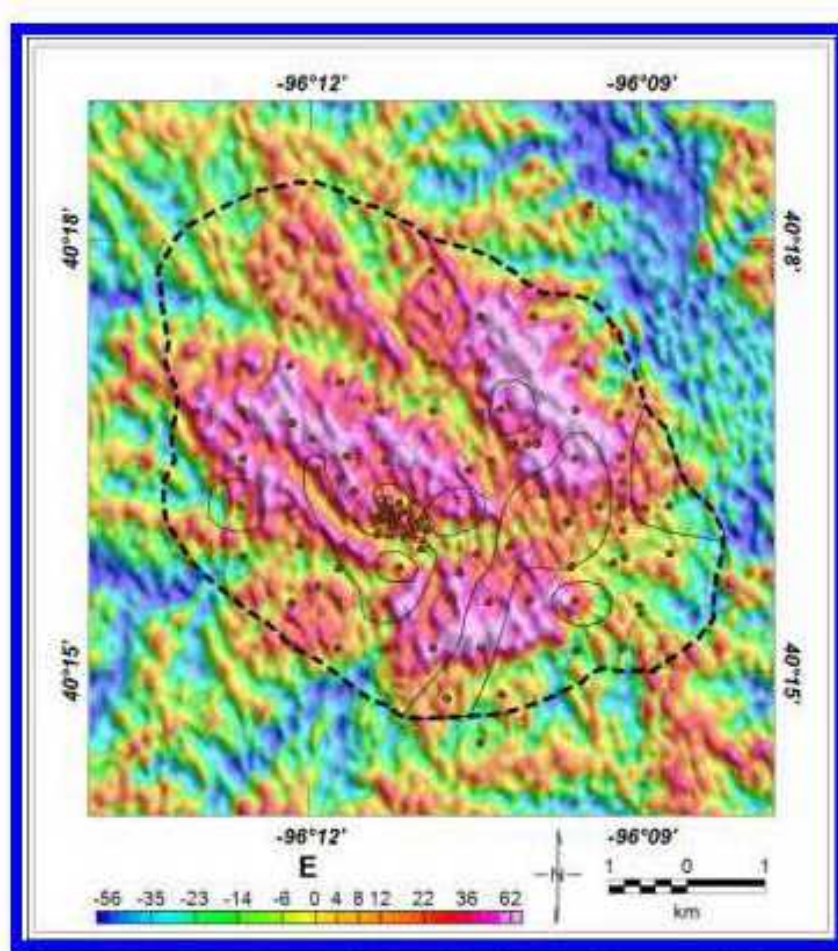


Figure 2.39 Free-air G_{zz} data over the Elk Creek Carbonatite in south-eastern Nebraska. The bedrock surface margin of the Carbonatite is shown and drillhole locations are indicated by brown dots. Adapted from Drenth (2012).

Creek deposit which is relatively rich in niobium and REEs. The results of the gradient survey shown in Figure 2.39 include the maximum amplitude of roughly 50 E.

Removal of the gravity effect of the terrain from the free-air data using a surface-terrain density of $2,270 \text{ kg/m}^3$ results in the map illustrated in Figure 2.40. The resulting map is subject to short-wavelength noise derived from reduction and geologic effects. These data were subjected to a matched filter based on spectral analysis of the gravity anomalies producing the im-

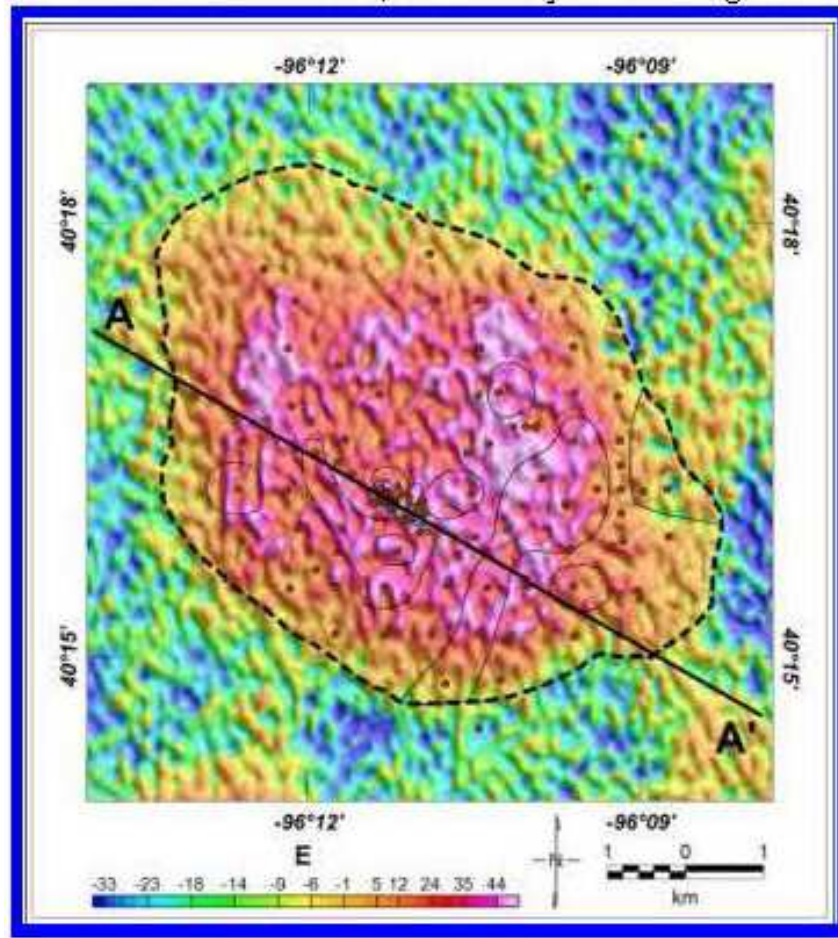


Figure 2.40 G_{zz} data of the Elk Creek Carbonatite terrain corrected using a $2,270 \text{ kg/m}^3$ density. Adapted from Drenth (2012).

proved G_{zz} map shown in Figure 2.41. A 2.5D forward model of the G_{zz} profile along AA' and the modeled geology is shown in Figure 2.42.

2.5.7 Iron Ores

The magnetic method has a long and distinguished history in the exploration of iron ore deposits (Hansen, 1970) because magnetite, one of the principal ores of iron, has a uniquely strong magnetization among minerals. As a result, generally intense magnetic anomalies are associated with magnetite ores as illustrated in Figure 2.43 over the Gruvberget and Leveäniemi

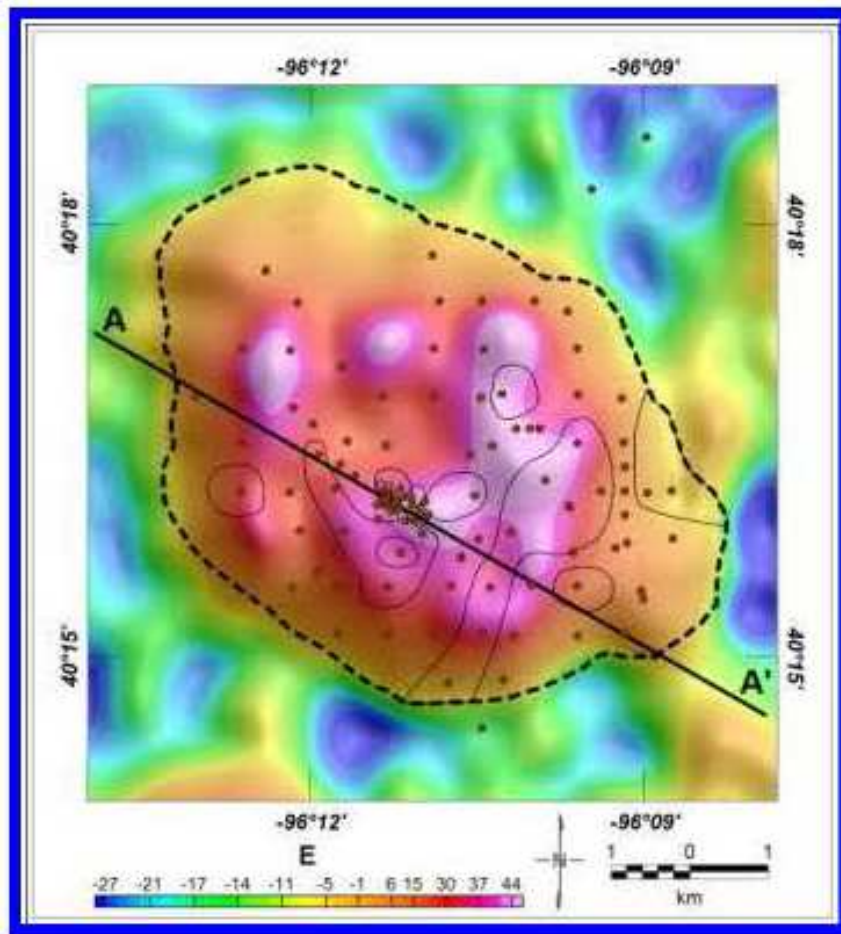


Figure 2.41 Matched filtered G_{zz} map of the Elk Creek Carbonatite. Adapted from Drenth (2012).

iron ore deposits in the Svappavaara iron ore district of Finland. However, not all ores of iron are intensely magnetic. This is true of hematite, another important iron ore mineral. Accordingly, not all iron ore deposits are related to magnetic anomaly highs. Further complicating the sign of magnetic anomalies are the effects of magnetic anisotropy and remanent magnetization.

The difference between anomalies associated with magnetite and hematite is illustrated in the magnetic anomaly over the Gruvberget iron ore deposit in the northwest quadrant of the map in Figure 2.43. As reported by Espersen (1970), the deposit that is the source of that anomaly is a N-S striking

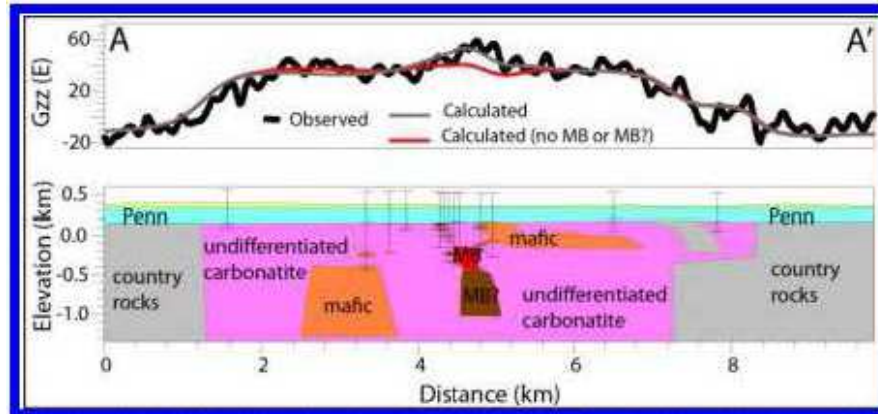


Figure 2.42 2.5D forward model along AA' across the Elk Creek Carbonatite. MB is a high density magnetite-rich lithology within the complex. No Vertical Exaggeration. Adapted from Drenth (2012).

and 65°E dipping ore sheet that is over 1 km in length and up to 70 m wide in the center with little overburden. The northern portion of this ore body is magnetite, but the southern portion is hematite and somewhat thinner than the northern part. The change in mineralogy is reflected in the termination of the 150,000 nT amplitude anomaly to the north, but the continuation to the south of the gravity anomaly high is associated with both the high-density magnetite and hematite ores. This illustrates the importance of the gravity method in support of magnetic methods in iron ore exploration (Hinze, 1966). The intense ovoid positive magnetic anomaly and associated gravity anomaly high in the southwest quadrant of Figure 2.43 is related to an irregular, roughly syncline-shaped magnetite deposit (Espersen, 1970).

An interesting example of magnetic anomalies associated with magnetite-rich iron ore deposits has been described by Riddell (1966). The Dayton iron deposit of Lyon County, Nevada originated from iron-rich solutions derived from a Cretaceous granodiorite intrusive interacting with the intruded sedimentary and volcanic rocks. Figure 2.44 is a north-south geologic and magnetic cross-section through the ore body. The magnetic cross-section is obtained from observations at the surface to a terrain clearance of 2000 feet. Of particular note are the spread of the anomaly and the decrease in amplitude with increasing terrain clearance and the shift of the peak of the anomaly to the south with increasing separation between the observation level and the source. In the southern geomagnetic hemisphere the magnetic pattern would be the mirror image of that observed over the Dayton deposit.

Hinze (1966) has described the use of the gravity method in iron ore ex-

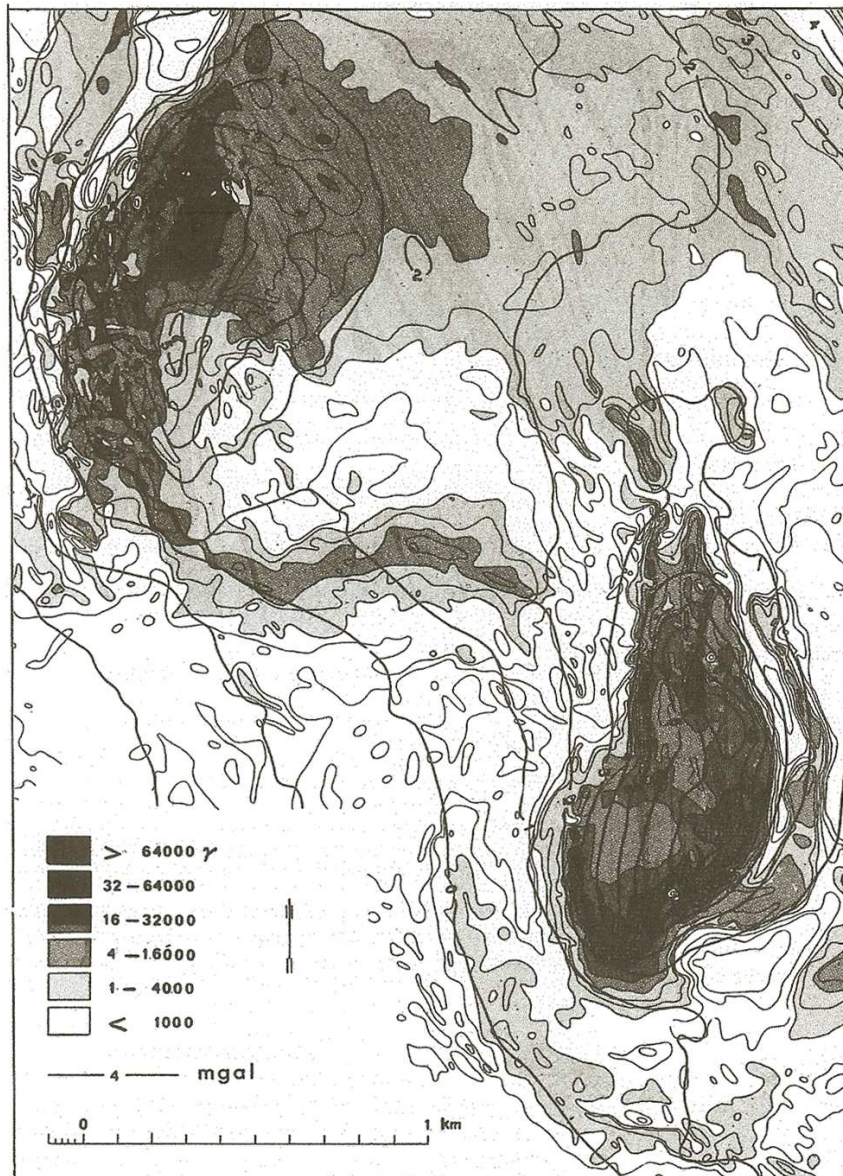


Figure 2.43 Combined magnetic and gravity anomaly map over the iron ore deposits of Gruvberget (northwest quadrant) and Leveäniemi (southeast quadrant) deposits. Adapted from Espersen (1970).

ploration and the relative merits of this method compared to the magnetic method. He points out that the gravity method has several potential advantages over the magnetic method in the assessment of identified iron ore

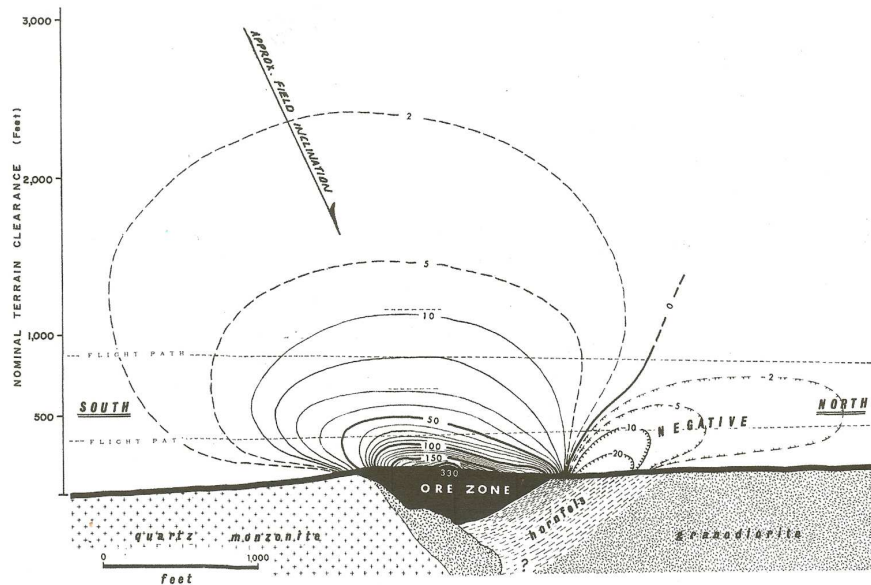


Figure 2.44 Vertical magnetic anomaly profile and geologic cross-section of the Dayton iron ore deposit, Lyon County, Nevada, U.S. Adapted from Riddell (1966).

prospects, particularly in determining the configuration and attributes of the iron ore deposit at depth. Several examples of the application of the gravity method are given including the comparative gravity and magnetic anomaly profiles over the Magnetic Center prospect of northern Wisconsin which is shown in Figure 2.45. The residual gravity anomaly separated from the regional anomaly indicates the broad extent of the iron-rich rocks compared to the limited width of the magnetic ore identified by the magnetic high.

Airborne gravity is also being used in the investigation of iron ore deposits. For example, Carlás et al. (2012) have used two different 3D inversion schemes to interpret the airborne gravity gradient tensor anomalies associated with a hematitic iron formation in the Carajás Mineral Province of Brazil. Figure 2.46 shows the observed G_{zz} component of the gravity gradient tensor. The area of the hematitic iron formation that is outlined by the black line was subject to interpretation by inversion techniques which showed that the depth of the ore body is likely deeper than indicated by drilling of the deposit.

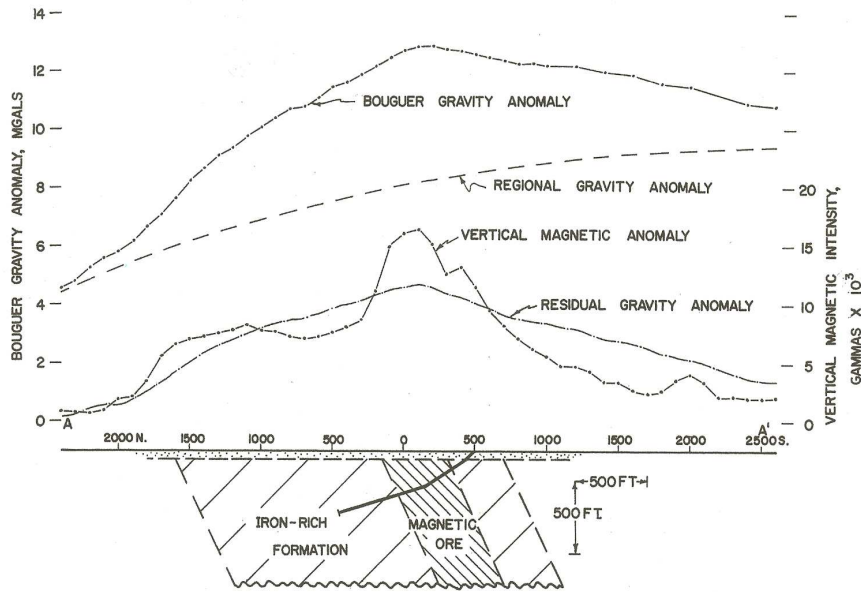


Figure 2.45 Observed regional and residual gravity and vertical magnetic anomaly profiles across the Magnetic Center iron ore prospect, Marenisco range, northern Wisconsin, U.S. Adapted from Hinze (1966).

2.6 Summary

Gravity and magnetic methods have a rich history of applications to mineral exploration, but only in special conditions with limited ores are the anomalies directly related to ore deposits. However, gravity and magnetic surveys have significant applications to regional geological mapping of favorable terranes for the occurrence of deposits and in more detailed studies for the identification of structures and rock types that host particular types of deposits. The magnetic method has particularly wide application because of the relative ease and low cost of the data acquisition and its high resolution. However, it is limited to mapping formations and detecting deposits that have magnetization contrasts associated with the generally trace minerals, magnetite and pyrrhotite. Furthermore, the magnetic method is highly sensitive to source depth which decreases the amplitude of anomalies and thus their detectability with increasing source depth. Gravity mapping is also used to identify appropriate terranes, structures, and rock types for specific types of ore deposits. The gravity method is also useful in detailed investigations of mineralized zones to locate ore bodies and to provide information on the ores and the adjacent rocks that are important in exploitation of the ore body.

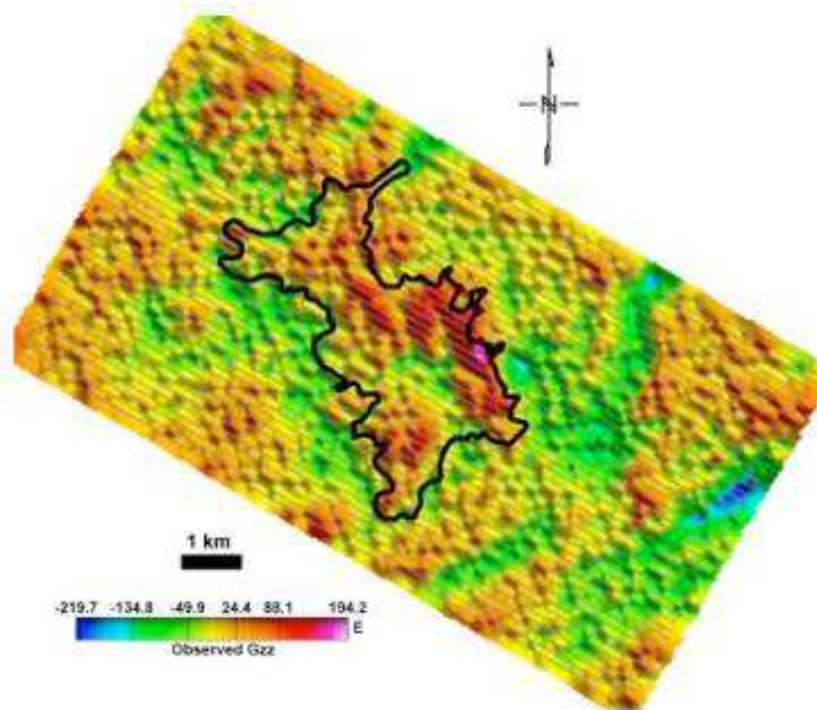


Figure 2.46 Observed G_{zz} component of the gravity gradient tensor over a hematitic iron formation (outlined by the black line) in the Carajás Mineral Province of Brazil. Adapted from Carlás et al. (2012).

Numerous examples from the published literature are given of the application of gravity and magnetic methods to and in support of mineral exploration. These are only a small but select sample of the use of these methods for geological mapping as well as indirect and direct identification and analysis of ore deposits ranging from non-metallic barite to metallic sulfides. Numerous additional examples are referenced in the cited literature. Typical examples are presented of the range of gravity and magnetic anomaly characteristics and that illustrate the importance of integrating the interpretation of the anomalies with other geophysical results and geologic information. Gravity and magnetic methods have limitations in mineral exploration preventing them from successfully delimiting ore deposits. These limitations which are described where appropriate in the examples are a result of fundamental principles of the methods, as well as the nature of ore bodies and conflicting anomalies from nearby geological variations. Under-

standing these limitations is important for effective application of gravity and magnetic methods to mineral exploration.

Energy Resource Exploration

3.1 Overview

Gravity and magnetic methods have had a primary role in hydrocarbon exploration in identifying in the subsurface the various geological conditions that are necessary for the development of commercial reservoirs. In the early days of petroleum exploration they were used both for basin studies to isolate favorable exploration regions and in the direct detection of structural and stratigraphic traps. However, over the past half century the methods have been used for only specialized studies in direct exploration and regional studies because of their ambiguity and limited resolving power in comparison to seismic reflection imaging. The advent of both high-resolution airborne magnetics and gravity and the direct measurement of their gradients have encouraged their use in regional as well as ever increasingly more detailed studies. Their efficiency and effectiveness in both regional and detailed investigations are well illustrated by a wide range of case histories. The ambiguity of the methods is well known and understood, but interpretations of their anomalies can be limited by the use of supplemental geologic and geophysical data and joint inversion of data from multiple methods. The gravity method is particularly useful when combined with the interpretation of seismic reflection data. The magnetic method is especially useful in determining the basement depth and configuration of sedimentary basins. Both methods have been used extensively in exploration for geothermal resources and to a lesser extent in coal exploration. The enhanced precision of the methods and their ease of implementation have promoted their use, particularly of the gravity method, in studies related to the exploitation of energy resources from the Earth.

3.2 Introduction

Geophysical methods have a significant role in increasing the efficiency of the exploration and exploitation of solid-earth energy resources including petroleum and natural gas, coal, and geothermal power sources. These indirect methods are particularly important in the search for and production of hydrocarbon resources because of the continuing need to discover new reservoirs at increasing depths where the deposits have limited or no surface expression.

Since the earliest days of modern exploration, gravity and magnetic methods have had an important role in the search for oil and gas. In the first half of the 20th century, the gravity method in particular played a central role in developing U.S. Gulf Coast oil fields associated with salt diapirs because of the intense anomalies resulting from the strong density contrast between the salt and the intruded sedimentary rocks. The first successful use of geophysics to hydrocarbon exploration was in 1924 when the Nash Dome in Texas was mapped by the gravity method.

The early development of portable, high-sensitivity gravimeters and magnetometers was largely in response to their success in locating new petroleum reservoirs in the first half of the 20th century. The instruments were used in regional investigations and localized studies in special geological situations. However, improvements in seismic instrumentation, recording and processing in the second half of the 20th century brought the seismic reflection method into prominence over gravity and magnetic methods in hydrocarbon exploration. Nonetheless, the gravity and magnetic methods retain an important role in providing regional tectonic and geological information for exploration planning, in complementing seismic reflection interpretation, and in acquiring detailed information on specialized geological features of interest to oil and gas exploration. In addition, recently the gravity method has become a tool for monitoring reservoir characteristics over time, thus assisting in their exploitation. The viability of the methods is in large part due to their cost effectiveness in enhancing solid-earth exploration, but also to their unique role in mapping the subsurface.

Although the primary use of gravity and magnetic methods in solid-earth energy resource applications is in the oil and gas industry, they have also been used in other energy resource studies, for example, in the exploitation of coal resources and in specialized ways to localize and study regions of high terrestrial heat flow which may serve as potential geothermal power sources.

Gravity and magnetic methods as used in the exploration and exploita-

tion of solid-earth energy resources seldom provide a complete and never a unique result. Accordingly, the interpretation of data from these methods is constrained with geologic and other geophysical information to minimize the range of possible interpretations. The usefulness and validity of gravity and magnetic interpretations therefore are determined to a significant degree on the amount and quality of auxiliary available information and the manner it is used in interpretation.

In this chapter, examples are given of the manner in which gravity and magnetic methods are used in oil and gas exploration and exploitation and to a lesser extent in the study of other solid-earth energy resources. The treatment is aimed at providing an overview of the potential application of the methods and the range of gravity and magnetic responses associated with these applications. It is not comprehensive because of the broad range of the applications and the numerous publications of case histories in scientific and trade journals. Published case histories, as those referenced in this chapter, do not necessarily represent the frontier of the application of the gravity and magnetic methods because of the delay between the actual practical application of the methods and public release and publication.

3.3 Hydrocarbon Exploration and Exploitation

Gravity and magnetic methods have proven especially useful in hydrocarbon exploration since the development of precision methods for measuring gravity and magnetic fields from ship and airborne platforms and for locating the precise position of observations. Airborne gravity and magnetic gradiometry, GPS positioning, and satellite-derived ocean gravity measurements have proved to be particularly effective in extending the range and effectiveness of gravity and magnetic methods, and thus are widely used in hydrocarbon exploration.

A number of conditions must be present to permit the accumulation of hydrocarbon deposits - sufficient volume of appropriate source rocks, thermal conditions for the generation of oil and gas from carbon-rich rocks, pathways for their upward migration into reservoirs, void space in reservoir rocks, and geological features that will trap the lighter-than-water oil and gas ascending through the Earth. As a result, essentially all hydrocarbon deposits occur in thick sequences of sedimentary rocks.

The gravity and magnetic methods can provide useful information bearing on all these necessary conditions for the accumulation of hydrocarbons although it is only in specialized situations that this information is definitive from either of the methods alone. These methods are also useful in locat-

ing and evaluating reservoir rocks that will entrap natural gas and carbon dioxide that are pumped into them providing natural underground storage facilities. Geologic storage of carbon dioxide could be an important element in mitigating greenhouse gases and underground storage provides flexibility in natural gas distribution to consumers.

Regional gravity and magnetic surveys are relatively inexpensive ways for mapping the depth and configuration of basement crystalline rocks. Magnetic methods with their higher resolving power are especially effective in this application because they can be used to map the top of intrabasement magnetic sources that often coincide with the basement surface. Mapping of the surface of the basement gives information on the overlying volume of sedimentary rocks, and thus the petroleum-bearing potential of the sedimentary basins. Also, mapping of the basement geology is important because intrabasin structures and stratigraphic features of interest to petroleum exploration commonly are related to reactivation of basement features or as a result of differential compaction within the sedimentary sequence with varying depths. Furthermore deep crustal and upper mantle studies with gravity and magnetic methods may provide clues to major tectonic controls and the temperature distributions that relate to the maturation of hydrocarbon deposits.

High-resolution, precision gravity and magnetic studies focused on higher wavenumber components of the fields are useful in studying gravity and magnetic anomalies derived from intrabasin faults, diapirs, stratigraphic variations, and alteration zones that can provide useful information related to the migration path of hydrocarbons, reservoir rock parameters, and especially structures in the sedimentary sequence that provide traps for the ascending oil and gas. Biegert and Millegan (1998) give numerous examples of how gravity and magnetics are being used in hydrocarbon exploration beyond the traditional reconnaissance uses of the methods.

In the following subsections, a selection of applications of gravity and magnetic methods to hydrocarbon exploration are reviewed. The review is not comprehensive but is sufficiently complete to show the range of applications and the character of anomalies related to oil and gas exploration and exploitation. This provides a perspective of the role and limitations of gravity and magnetics in this application and the potential for new uses of the methods.

3.3.1 Basin Studies

Regional geologic information, although not useful in a direct way in oil and gas exploration, provides important background on the geologic and tectonic framework of a potential hydrocarbon exploration target, and the broad-scale structures of a region - their type, orientation, size, depth, and relative age - which can be used in delineating prospective exploration targets and designing exploration campaigns. Among the geophysical methods, gravity and magnetic methods stand out as particularly useful in regional studies of frontier exploration areas because of the efficiency of acquiring gravity and magnetic data over broad regions, the general transparency of surface cover of water and sediments to the methods, and the increasing availability of regional data compilations from land or sea surface, airborne platforms, and satellite measurements.

Defining frontier areas for hydrocarbon exploration and the nature of potential traps is dependent on developing models for the geological evolution of the region. These models are based on available direct geologic information - lithologies, structures, and age dates - from surface exposure and drillhole samples. However, limitations in this direct information, especially in marine areas, severely restrict the credibility of the models. As a result, geophysical information often provides significant input to the models and constrains the direct information. All available regional geophysical data are used in these analyses, but gravity and magnetic information are particularly valuable especially when combined with data from the higher resolution seismic reflection and electromagnetic methods.

3.3.2 Structural Elements

Gravity and magnetic data can provide important information on, for example, structural elements and their fabric, differentiating between continental and oceanic crust, movement of lithospheric plates, the location and nature of igneous intrusions and volcanic rocks, paleo-heatflow interpretations that can be related to basin subsidence and source rock maturation, faults and fault zones, and the nature and configuration of the basement surface. This information can be interpreted in terms of the necessary elements for the development of oil and gas fields.

An example of the use of gravity and magnetic data in this regard is presented in an overview of the initial steps used in identifying new potential hydrocarbon traps in the deep water of the Gulf of Mexico Basin (Jacques et al., 2004). In this study, these data have been used to develop the plate

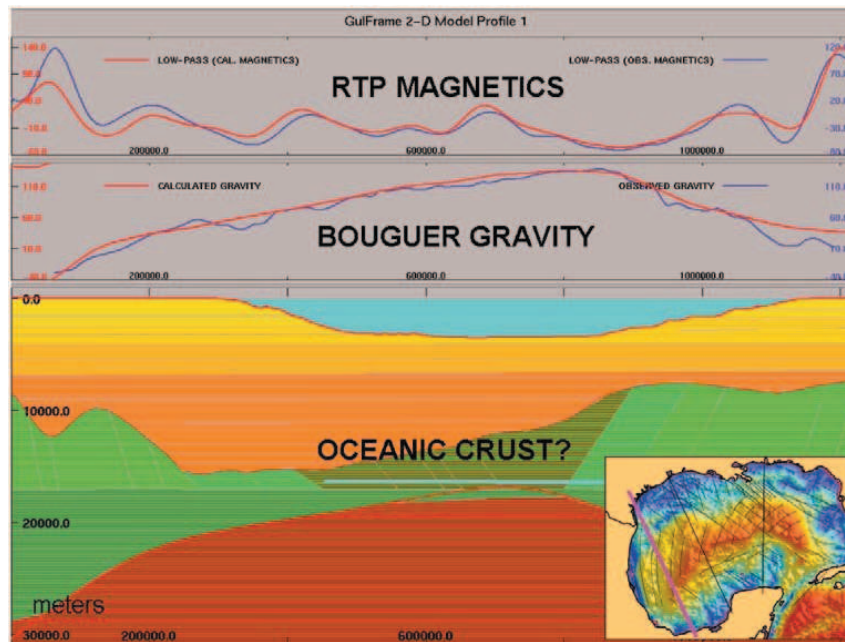


Figure 3.1 Low-pass reduced-to-pole total magnetic intensity and the Bouguer gravity anomaly profiles along the westernmost traverse of the map insert of the Bouguer gravity anomaly with matching anomaly profiles calculated from the 2D geological section shown beneath the profiles. The yellow colors of the geological cross-section represent sedimentary rocks increasing in density from 2,200 to 2,600 kg/m³ at the top of the crustal basement rocks shown in green, and the brown color is the mantle. Note the possible oceanic crust identified in the geologic section. The crustal interpretation is useful background for exploring for hydrocarbon deposits in the Gulf. Adapted from Jacques et al. (2004).

tectonic history of the region, delineate the ocean/continent crustal margin, and identify the major structural blocks which have been used to improve understanding of the distribution and nature of source rocks, reservoirs, and traps in the deep Gulf of Mexico. This information is useful in assessing the hydrocarbon potential of the region and in planning more detailed geophysical surveys to locate potential drilling sites. Figure 3.1 shows the low-pass reduced-to-pole total magnetic intensity and the Bouguer gravity anomaly profiles across the western profile indicated on the map insert of the Bouguer gravity anomaly with the profiles of these anomalies calculated from the 2D geological profile shown below the profiles. This interpretation of the gravity and magnetic anomalies is useful background for resource exploration in the Gulf.

Regional structural and stratigraphic trends in basins commonly reflect the azimuth of major structures in the basement rocks because the pre-existing features of the basement may be the foci for movements during and subsequent to basin development. The trends in the basement rocks are usually much more evident in gravity and magnetic anomaly fields than are those of the sedimentary rocks of the basins because of generally greater physical property contrasts and the larger volume of the anomaly sources within the basement. Numerous examples are available of anomaly sources in the basement that are associated with oil and gas traps in the sedimentary rock basins [e.g., Piskarev and Tchernyshev (1997)]. The magnetic method, in particular, is valuable because of its relatively high resolving power in mapping near-vertical basement faults or contacts which are related to faults within sedimentary rocks [e.g., Beaumont and Gay (1999)] that may have an important role in trapping and migration of hydrocarbons.

3.3.3 Limited Seismic Quality Regions

Gravity and magnetic methods also have been used in investigating frontier areas that are located in regions where the quality of seismic reflection data tends to be inadequate for mapping sedimentary strata. For example, Shevchenko and Lasky (2004) have used gravity mapping in the northern Perth Basin off the west coast of Australia to locate structural blocks and major fault zones important to hydrocarbon accumulation which are poorly imaged in seismic reflection data because a near-surface limestone interferes with acquisition of good-quality seismic reflection data. They find that most of the presently identified hydrocarbon fields in the Basin are correlated with positive gravity anomalies.

Similarly, Meshref and Hammauda (1982) have used gravity and magnetic anomalies to map the basement and its tectonics in the Gulf of Suez where the evaporite rocks cause severe attenuation and dispersion of seismic energy lowering the quality of the seismic reflection mapping. They used depth determinations from the magnetic anomaly data and a residual gravity anomaly map prepared by stripping off the gravity effects of the evaporites and shallower sedimentary rocks as defined by seismic and drillhole control to map the basement configuration as illustrated in Figure 3.2. The results suggest a strong correlation between positive gravity and magnetic anomalies caused by tilted fault blocks and oil reservoirs, thus providing a powerful tool for oil exploration campaigns.

Other frontier hydrocarbon areas that may be studied by gravity and magnetic methods include those that have overlying volcanic formations that can

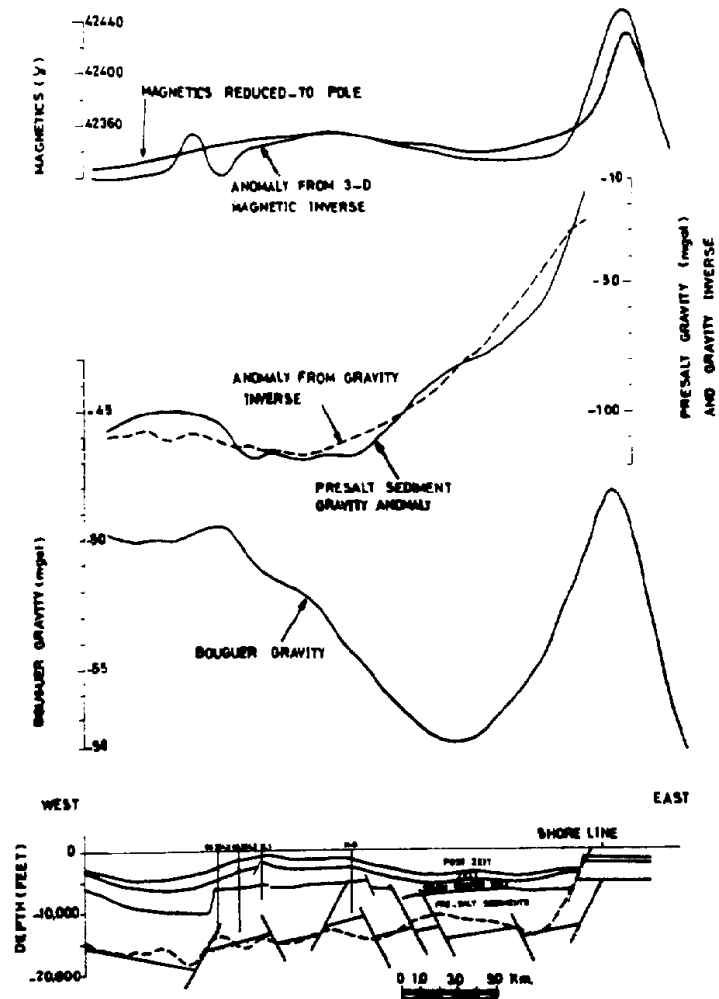


Figure 3.2 A 3D magnetic and gravity analysis of a west-east profile across the Gulf of Suez. The upper profile is the reduced-to-pole total magnetic anomaly and the anomaly computed from the inversion of the magnetics. The central profile is the Bouguer gravity anomaly of the pre-salt sedimentary rocks and the anomaly from inversion of the gravity anomaly. The lower profile is the observed Bouguer gravity anomaly. The geologic section at the bottom of the figure shows the close correlation of the basement from the inversion of magnetic anomaly (solid line) and the inversion of the pre-salt gravity anomaly (dashed). After Meshref and Hammauda (1982).

significantly decrease the quality of the results from the seismic reflection method (Rohrman, 2007). Potentially petroliferous sedimentary basins that may underlie portions of the Deccan basaltic basin of central India and the

Columbia River basalts of the Washington and Oregon, U.S. have been investigated by several geophysical methods including magnetic and/or gravity methods [e.g., Prieto et al. (1985); Withers et al. (1994); Chakravarthi et al. (2007)]. In both of these regions electrical depth sounding (either vertical electrical profiling or magnetotelluric sounding) have provided useful constraints on the gravity and magnetic methods because these soundings are sensitive to vertical variations in the rock sequence, whereas the gravity and magnetic methods are based on horizontal differences in rock properties. The interpretation of the electrical soundings, although also ambiguous as are the gravity and magnetic methods, has been used to map the base of the basalts and the depth to basement rocks. This interpretation is constrained by the nature and properties of the rocks occurring at the surface and encountered in drilling. The gravity and magnetic data have been useful in mapping the structural pattern of the subbasalt sedimentary rocks and have been used in integrated analyses with electrical soundings to map the depth and configuration of the base of the basalt and the sedimentary rock/basement interface. Heincke et al. (2006) also have used a joint inversion process combining gravity, seismic tomography, and magnetotelluric data to interpret the sub-basalt formation boundaries beneath volcanic rocks on the northwest margin of Europe.

Figure 3.3.a from Withers et al. (1994) shows an observed gravity anomaly profile striking southeast/northwest across the boundary of the Columbia River basalt in northern Oregon, U.S. Three geological models also shown in the figure match this profile. Model A is based on the basalt thickness derived from magnetotelluric studies prior to drilling of the test drill hole (Hanna #1) shown in Figure 3.3.b. Geologic models (Figures 3.3.c and 3.3.d), which also satisfy the gravity data, are acceptable alternatives that were prepared using rock densities obtained from drillhole samples. The gravity data located the sub-basalt basin of sedimentary rocks and led to an initial basin model that was refined with the constraints of electrical sounding. In this case the authors deemed the magnetic information not useful in mapping the configuration of the basement of the basin because of the interfering effect of the large magnetic remanence of the surface basalts.

The use of magnetic data in this type of terrain remains equivocal. Depending on the knowledge of the magnetic properties of the volcanic rocks, the interpretational methods used, and the effort put into the interpretation, significant information can be obtained from the magnetic anomalies and their pattern. For example, Prieto et al. (1985) have used aeromagnetic data to interpret regional structural information and basement rock compositions beneath the Columbia River basalt to the north of the region that

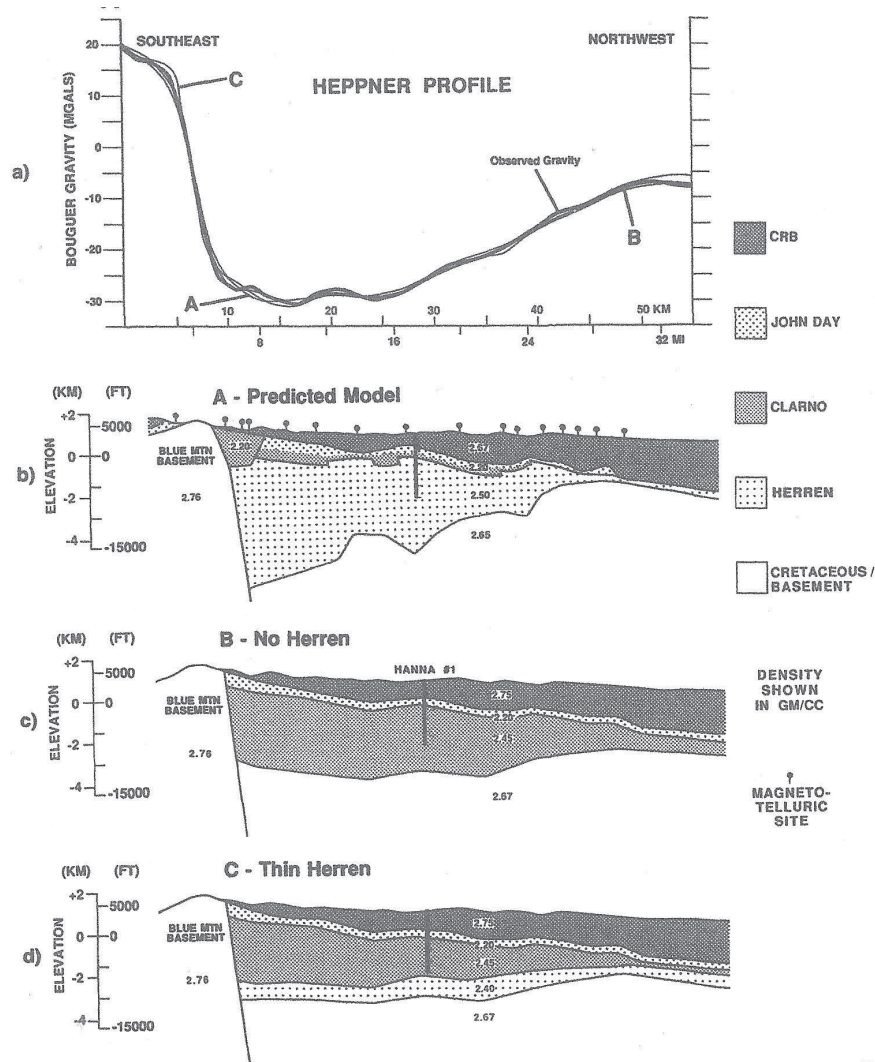


Figure 3.3 Bouguer gravity anomaly profile across the margin of the Columbia River basalt in northern Oregon, U.S. (a) together with computed profiles from the geologic models shown in (b), (c), and (d). Model A in (b) was the accepted model prior to drilling the test hole and integration with the results of the magnetotelluric interpretations. Models B (in c) and C (in d) were prepared using the results obtained from the drill hole. Each of the models match the Bouguer anomaly profile. Adapted from Withers et al. (1994).

is profiled in Figure 3.3. Their model of the sub-basalt geology based on magnetotelluric soundings and gravity data is shown in Figure 3.4 with the computed gravity anomaly based on the model. The surface volcanic rocks

Inversion of the gravity anomaly data to the basement configuration is a simple process in theory, but difficult to effect in an acceptably precise manner because of the non-uniqueness of the solution and instability of the inversion procedures. Imprecision in isolating the anomaly related to basement configuration from those derived from within the sedimentary rocks and intrabasement lithologic variations, as well as uncertainties in the density contrast across the basement/sedimentary rock interface, are major deterrents to the success of the method in this application. Constraints on the residual gravity field and density contrast from drillhole information and other geophysical data are important to improving the inversion results. For example, the location of outcrops of the basement rocks that surround a basin can be used to approximate the position of the zero residual anomaly due to the basin fill.

The procedures used in the inversion are relatively simple if a constant density differential is appropriate. However, the exponential increase in the density of the sediments as a function of their depth of burial complicates the procedures. A number of methods, both in the space and wavenumber domains, are described in the geophysical literature to treat the exponential increase in density with depth in both 2- and 3-dimensions [e.g., Cordell (1973); Pilkington and Crossley (1986); Chai and Hinze (1988); Silva et al. (2006)]. Figure 3.5 shows the results of a wavenumber domain approach to mapping the basement of the Los Angeles Basin, California from gravity data (Figure 3.5.a), compared to the basement configuration map from surface geology, drillhole data, and reflection seismic data (Figure 3.5.b). The two maps compare well, but there are unavoidable high wavenumber distortion and edge effects in the map derived from the gravity anomaly.

In contrast to the use of the gravity method in delineating geologically young basins filled with relatively low-density sediments, older basins filled with higher-density Precambrian and Paleozoic sedimentary rocks, especially carbonates, often are not evident as negative gravity anomalies. The densities of the sedimentary rocks of the older basins indicate that there is a negligible density contrast across the basement interface. In contrast to the negative gravity anomalies of young sedimentary basins, a generally direct correlation between gravity anomalies and depth to basement in Paleozoic cratonic basins in central North America is observed [e.g., Hinze and Braile (1988)]. That is, gravity anomalies (free-air gravity anomalies) increase at a rate of about 15 mGals/km with basement depth increase. This increase is due not to basement configuration, but to high-density crystalline rocks in the crust. The general relationship, however, is insufficiently precise to be used as a basement-depth mapping tool.

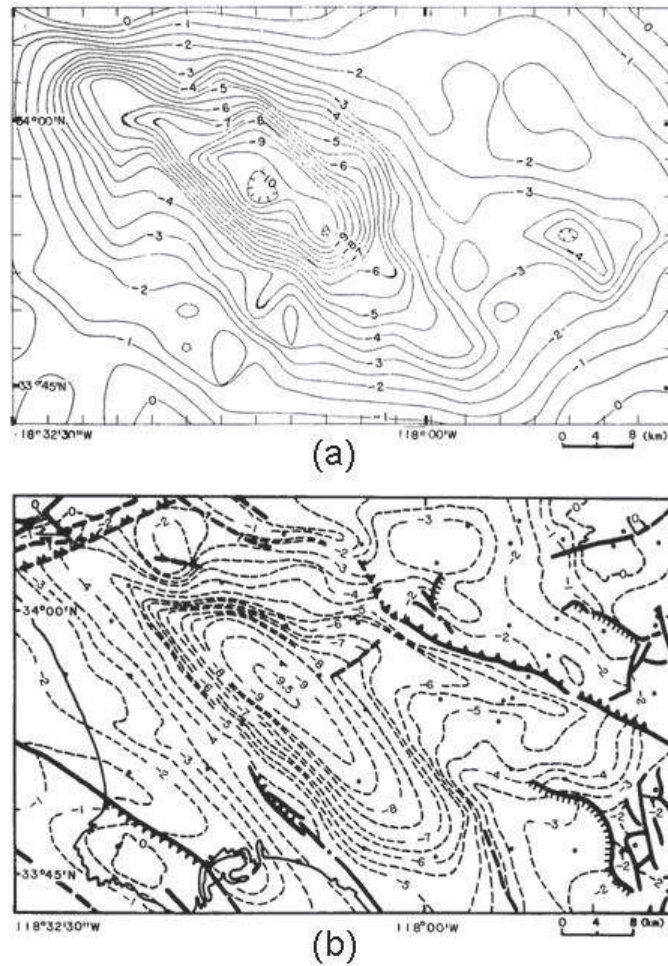


Figure 3.5 (a) Basement surface of the Los Angeles Basin, California, U.S. derived by inversion of the residual gravity anomaly in the wavenumber domain using an exponentially increasing density function with depth determined from drill hole sample density data (McCulloh, 1980). Contour interval is 0.5 km. (b) Contour map of the basement of the Los Angeles Basin determined by McCulloh (1980) from surface geology, drillhole data, and seismic reflection studies. Contour interval is 0.5 km. Adapted from Chai and Hinze (1988).

Although the gravity method has been useful in mapping basement configuration of relatively young basins, the magnetic method has been used extensively to map the basement configuration of basins of all ages, world wide. The magnetic method is particularly useful because it is more sensitive to depth to source than is the gravity method and the magnetization con-

trast between basement rocks and the low-magnetization sedimentary rocks of basins is several orders of magnitude greater than the associated density contrasts. These factors combined with the relative ease of acquiring magnetic anomaly data and its consequent low cost have favored the magnetic method as a reconnaissance tool to map basement configuration.

Magnetic depth estimates are primarily based on determining the depth to the top of intrabasement variations in magnetic polarization. Anomalies from these sources are the prominent features of magnetic anomaly maps with anomaly amplitudes commonly measured in several tens to hundreds of nanoteslas. In contrast, suprabasement anomalies caused by variations in basement relief are generally of the order of magnitude of a few tens of nanoteslas or less. Unfortunately, anomalies of similar characteristics are derived from local intrabasement variations in magnetic sources preventing these lower amplitude anomalies from being related directly to basement configuration. Magnetic mapping of the basement is based on the assumption that basement is made up of crystalline rocks, either igneous or metamorphic rocks, and that intrabasement sources exist. In some regions where low magnetization granitic or metasedimentary rocks are the basement, these assumptions will be violated, but these cases are in the minority.

The magnetic method is also advantageous because the anomalies from the basement rocks are not significantly modified by anomalies derived from within the sedimentary section. Where anomalies do arise from igneous intrusive and extrusive rocks and localized magnetization variations within the sedimentary section, these sources are readily identified by the wavelength characteristics of their anomalies and filtered from the anomaly data prior to analysis.

As explained in Chapter 13, numerous schemes have been developed for determination of source depth from magnetic anomalies. All methods are based on the evaluation of the maximum gradient of the anomalies and most assume some geometric form for the source volume and magnetization that is primarily induced by the ambient terrestrial magnetic field. Generally the methods are applied to profile data with the assumption that the sources are two-dimensional in form perpendicular to the profile. This is an acceptable assumption in most surveys, but must be considered in the final analysis and evaluation of the depth determinations.

The depth interpretation methods are applied both manually and automatically. The latter generally produce numerous solutions that may be in conflict with one another. Selection of the optimum solutions requires consideration of the methodology employed, the inherent assumptions in the method, and the geological context. Thus, selection of the optimum solutions

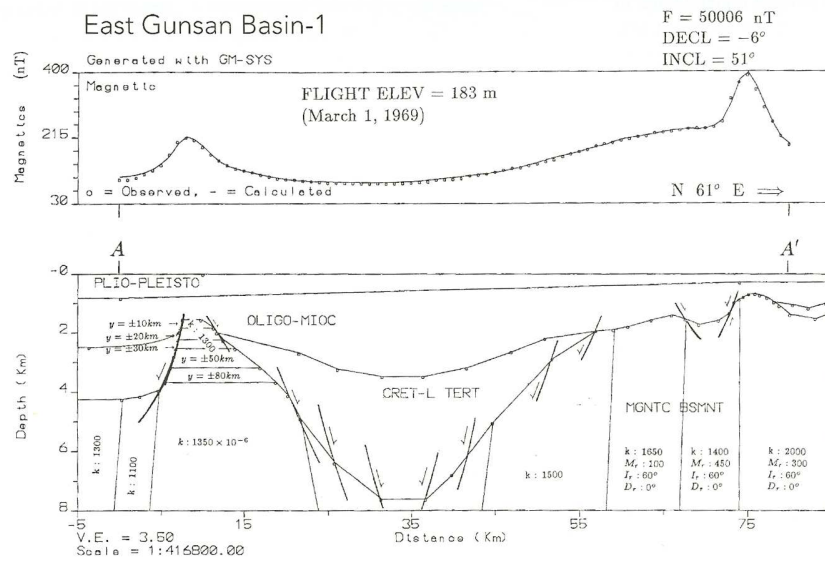


Figure 3.6 2.5D model of a total magnetic intensity profile across the East Gunsan sub-basin on the southwestern continental shelf of South Korea. The magnetic susceptibility k is in SIu; M_r , I_r , and D_r are assumed values for remanent magnetization; and $y = \pm 10$ km indicates source length perpendicular to the profile. Adapted from Baag and Baag (1998).

is very much a part of the interpretive process. Despite the mathematical sophistication of many of the depth determination methods, simplified empirical techniques are still used by many experienced interpreters. Regardless of the method(s) used in determining depths from magnetic anomalies, it is advisable to check the results by comparing anomalies calculated by simplified modeling with the observed data. Major discrepancies in the slopes of the calculated and observed anomalies suggest that further interpretational efforts are warranted.

An example of magnetic modeling to map the basement configuration is shown in Figure 3.6 after Baag and Baag (1998). This 95-km modeled profile over the southwestern continental shelf of South Korea identifies the East Gunsan sub-basin which reaches depths of the order of 7.5 km with the majority of the basin filled with Cretaceous and Lower Tertiary sedimentary rocks. The accuracy of depth determinations obtained from the magnetic method may vary significantly with the experience of the interpreter and the deviation of the geology from the assumptions made in the methods

that are used, but with care an overall error of the order of 10% or less is feasible (Bird and Nelson, 1999).

3.3.5 Integrated Interpretation with Seismic Reflection Profiling

Seismic reflection profiling is the most used and useful method of imaging the crust of the Earth. This is especially the case in sedimentary basins where the strata dip at low angles, less than a few 10s of degrees, and the interfaces of the layers are excellent seismic wave reflectors. Nonetheless, gravity and magnetic methods can have an important role in improving the interpretation of seismic profiling as for example in regions where surface formations, evaporite structures, and volcanic rocks decrease the signal to noise ratio of seismic data, thus degrading interpretation. In these cases an integrated approach to interpretation using gravity, magnetic, and other geophysical data to supplement the seismic data is most valuable.

Seismic reflection data are especially useful in mapping sub-horizontal geologic boundaries while gravity and magnetic data are particularly sensitive to sub-vertical contacts. As a result the methods complement each other. Furthermore, integration of gravity and seismic data has proven particularly useful in improving velocity models of prestack depth migration of seismic data over those derived solely from seismic data. For example, Weber et al. (2000) show how this integrated approach has been used in improving seismic data off-shore Brazil by incorporating salt deposits indicated by gravity data into the geological model. In a similar manner, Henke et al. (2005) used gravity modeling to constrain the velocity model for prestack depth migration of seismic data in the High Zagros Mountains of Iran.

Integration of interpretations takes several forms. For example, gravity positive anomalies associated with seismic highs indicate that the high is related to a basement feature, especially where magnetic data suggest associated shallow sources, rather than lower density salt or shale intrusives that may be related to hydrocarbon traps. Another approach to integration uses velocity data obtained from seismic reflection studies to determine density distributions within the study area. These densities are used as a basis for gravity modeling to test the structural and velocity data interpreted from the seismic studies. For example, Huston et al. (2004) have used a 3D distribution of velocity obtained from seismic data along with sonic well log data to prepare a density model that was used to constrain gravity modeling associated with deep salt features in the Gulf of Mexico. The result is a more accurate gravity as well as seismic interpretation than could be obtained from a non-integrated interpretation.

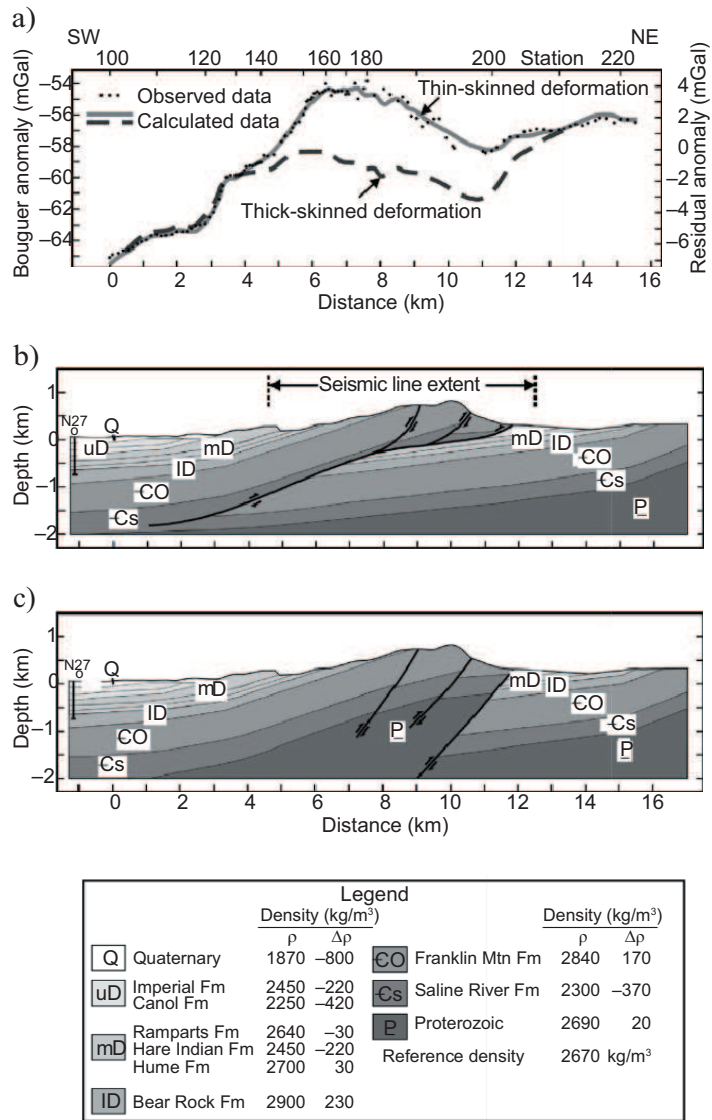


Figure 3.7 (a) Observed and calculated gravity anomaly profiles across the Norman Range in the Northwest Territories of Canada assuming a thin-skinned deformation model (b) and a thick-skinned deformation model (c). Adapted from Lawton and Isaac (2007).

The widespread use of integrated seismic/gravity interpretation is well illustrated by the study of Lawton and Isaac (2007) from the Northwest Territories, Canada. Figure 3.7 shows the results of gravity modeling (a)

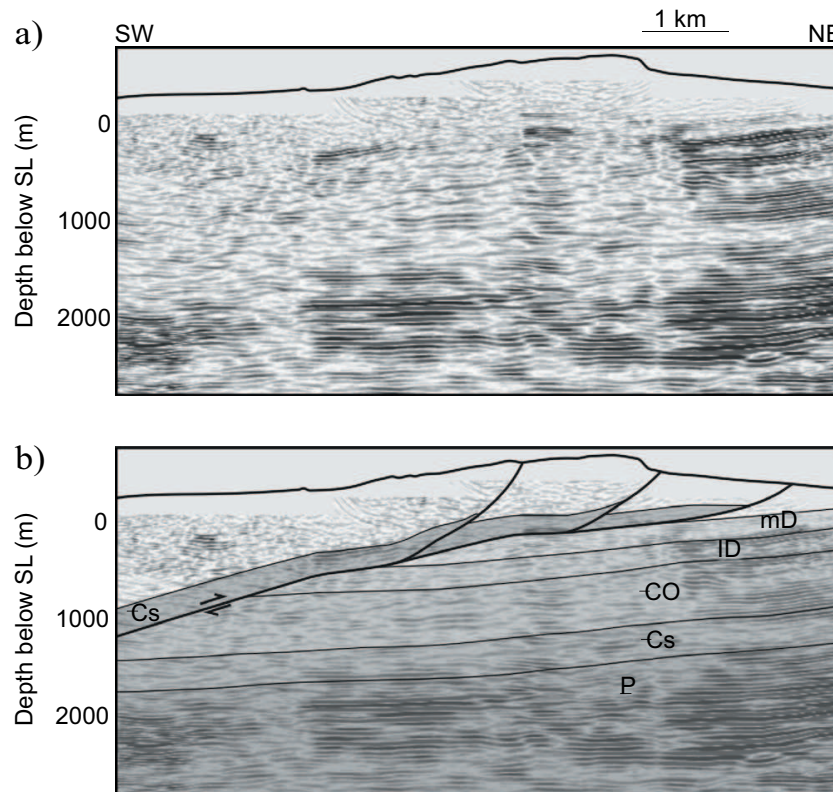


Figure 3.8 (a) Pre-stack depth migrated seismic section of the profile shown in Figure 3.7, and (b) the interpreted migrated section based on the thin-skinned deformation model. Adapted from Lawton and Isaac (2007).

along a seismic reflection profile assuming a thin-skinned deformation model (b) and a thick-skinned deformation model (c) compared with the observed Bouguer gravity anomaly. The deformation models are both possible based on surface geology, well data, interpretation of the seismic reflection profiling, and rock density data from surface samples and density logs. The thin-skinned deformation model gives a very good match with the observed gravity anomaly data. The positive anomaly effect of the thin-skinned model over that of the thick-skinned model is due to the presence of high density carbonate rocks (Franklin Mountain formation) of Cambrian/Ordovician age. The thin-skinned model was used to design a velocity model used in preparing the pre-stack migrated seismic section shown in Figure 3.8.a and the interpretation of the final depth migrated section given in 3.8.b.

3.3.6 Hydrocarbon Field Studies

Although gravity and magnetic methods find their most significant use in hydrocarbon exploration in regional studies that provide basic background geologic and tectonic information, in limited circumstances gravity and magnetic anomalies may be more directly related to oil and gas fields. In these cases, high-resolution/sensitivity observations and processing can locate favorable sites for testing for hydrocarbon traps. Gravity and magnetic methods which were intensely used in the direct study of hydrocarbon fields in mid-20th century have largely been displaced since then by the seismic reflection method because of improved resolution and decreased ambiguity. However, gravity and magnetic methods are cost effective, and thus may find use today in direct study of fields and in a supporting role to seismic reflection interpretation. Generally potential-field measurements are used in the study of fields related to structural features and to a lesser degree those associated with stratigraphic variations in sedimentary sequences that lead to the trapping of hydrocarbons. Examples of the application of gravity and magnetic methods to both types of traps are presented in the subsections below.

3.3.7 1) Structural Features

Structures in the strata of sedimentary basins are the most important trapping features for hydrocarbons. These include anticlines, faults, and piercement features that originate subsequent to the deposition of the sediments and generally after their lithification into rocks by applied orogenic or epi-orogenic stresses and the force of gravity. Often these structures result in horizontal variations of density that produce gravity anomalies and less frequently are associated with horizontal perturbations of magnetization within the sedimentary rocks.

3.3.8 a) Anticlines

Anticlinal traps are the source of much (60 – 80%) of the world's hydrocarbons. These traps may be mapped with the gravity method where the stratigraphic column includes strata of varying density. Typically higher density carbonates that have been folded into juxtaposition with lower density shales and sandstones will produce measurable positive gravity anomalies. An example of a positive residual gravity anomaly with a magnitude of roughly 5 mGal associated with an anticlinal feature with about 700 m of closure is illustrated in Figure 3.9. This anomaly closely correlates with the Horse Creek

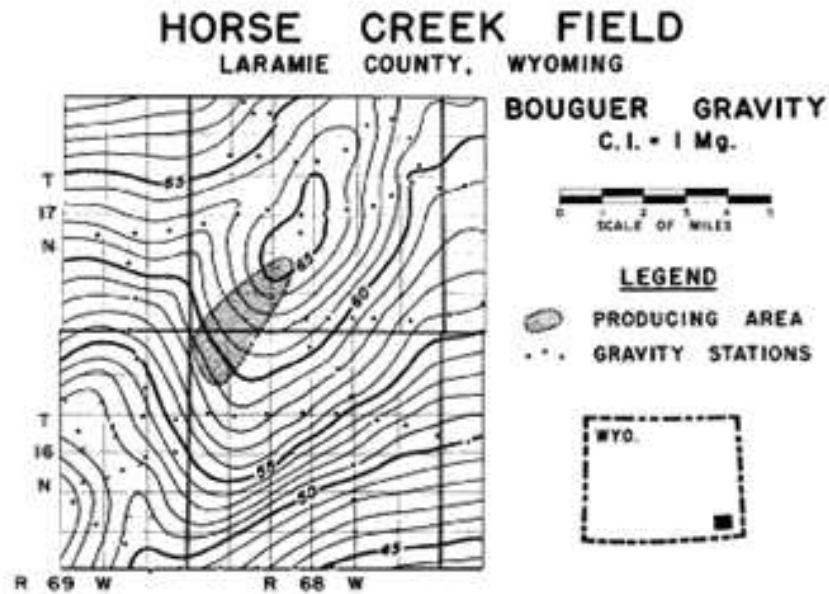


Figure 3.9 Residual Bouguer gravity anomaly of the Horse Creek oilfield with the producing area of the field (1960) shown by the shaded area. Adapted from Peters (1960).

field which was discovered in the early 1940s in the Denver-Cheyenne Basin of Wyoming, U.S. on the basis of the gravity anomaly (Peters, 1960). Similar gravity anomalies associated with anticlines are widely found in folded sedimentary basins. In many cases, the positive anomalies are intensified where the basement of the basins are related to anticlinal features either by direct structural involvement or as a result of differential compaction of sediments of varying thickness over basement topographic highs. The generally higher density of the basement highs compared to the adjacent sedimentary rocks result in positive gravity anomalies. However, it should be noted that anticlinal structures also are associated with negative gravity anomalies that originate in the negative density contrast of gas/oil reservoirs along their crests. This relationship was observed as early as the 1930s in the Tertiary basins of California.

Magnetic positive anomalies also may be associated with structural highs where sedimentary strata contain sufficient magnetic rock fragments that a lateral magnetic contrast is established by the deformed sedimentary forma-

tions. Positive magnetic anomalies also may be associated with crystalline basement highs that are related to structural highs in the overlying sedimentary rocks. Steenland (1965) has provided several examples of these magnetic anomalies that are related to known oil fields. Magnetic anomalies related to fields are typically an order of magnitude or smaller (< 20 nT) than anomalies derived from intrabasement magnetization variations that dominate the magnetic field of sedimentary basins. Thus, these anomalies are difficult to discern from minor variations in the magnetization variations within the crystalline basement rocks.

3.3.9 b) Faults

Faulting in hydrocarbon-rich sedimentary basins may lead to traps that contain significant oil and/or gas. The vertical disruption of sedimentary rocks may bring rocks of varying density into juxtaposition causing observable anomalies. Such a situation is profiled in Figure 3.10 which shows the Bouguer, regional, residual, modeled and vertical gradient gravity anomalies over the Garber field in Garber County, Oklahoma, U.S. together with a schematic cross-section of the major source of the gravity anomaly (Ferris, 1987). In this case the relatively high-density Ordovician Arbuckle limestone is upthrown by vertical faulting into contact with the lower density Pennsylvanian sedimentary rocks. Commonly, the gravity anomaly due to faulting of a sedimentary sequence of varying density layers is much more complicated than indicated by this figure as a result of the combined gravitational effect of differing signs of the density contrasts on opposite sides of the fault leading to destructive interference of the multiple anomalies.

Magnetic anomalies are also related to faulting within sedimentary basins either as a result of horizontal variations in magnetization within the sedimentary rocks of the basin or in the basement crystalline rocks. Long curvilinear magnetic anomalies with amplitudes of less than roughly 10 nT have been observed in basins containing clastic sedimentary rocks. They have been identified as originating in faulting and offset of layers of sediments with varying magnetite content derived by depositional processes from surrounding highlands. The shape and amplitude of the anomalies varies with magnetization contrast, layer thickness, fault dip, and depth. The low-amplitude of the anomalies makes them difficult to isolate particularly with increasing depth, but their continuity from profile to profile is a critical aid in identifying them as geologic sources associated with faulting. A useful illustration of these anomalies and power of the magnetic method in mapping basin faults is shown in Figure 3.11 in the Rio Grande rift south of the Albuquerque,

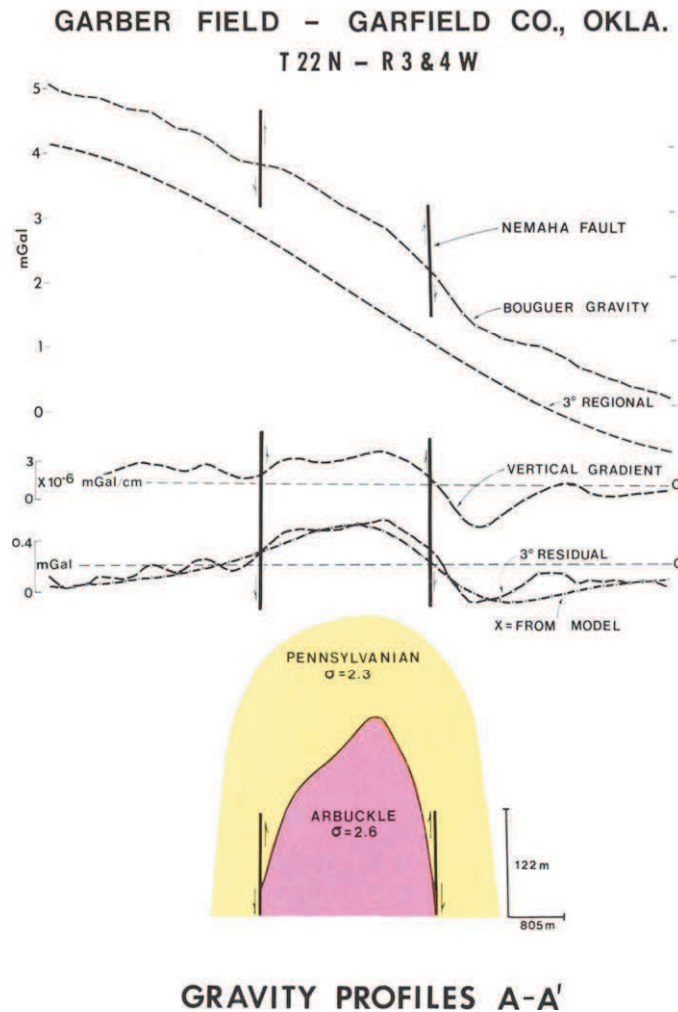


Figure 3.10 Geological cross-section of the Garber field, Garber County, Oklahoma, U.S. and the correlative Bouguer, third-degree polynomial regional and resulting residual, vertical gradient, and modeled gravity anomalies. Adapted from Ferris (1987).

New Mexico, U.S. In this figure a map is shown of the faults in the region mapped solely on the basis of geological information, as well as all faults of the area which have been mapped using both direct geological information and the presented shaded-relief aeromagnetic image.

Faults within sedimentary basins may also be identified indirectly as a result of vertical or horizontal displacement of magnetic crystalline rocks

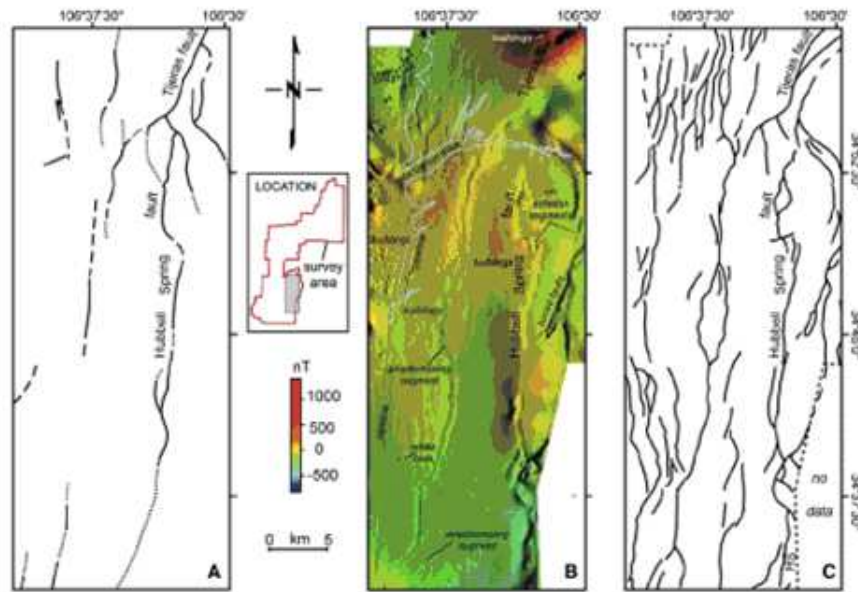


Figure 3.11 Geologically versus magnetically mapped faults of the Rio Grande rift south of Albuquerque, New Mexico, U.S. (a) Faults mapped prior to the magnetic surveying. (b) Shaded-relief aeromagnetic image illuminated from the east showing numerous subtle curvilinear anomalies that have no surface expression and are related to concealed faults in the rift basin sediments. (c) Complex fault pattern of the area as indicated by interpretation of the magnetic map in (b). Adapted from Grauch and Hudson (2007).

within the basement due to faulting which includes the magnetically transparent sedimentary section. As a result of the potentially large magnetic contrast along faults within the basement and the size of the sources, the fault anomalies are readily isolated and identified as of fault origin by their long linear or curvilinear pattern in the magnetic anomaly maps or by the displacement of patterns of anomalies on either side of the fault. Gibson (1998b) using regional magnetic anomaly data has identified rift faults in the West Siberian basin that are related to gas production. The gas traps are located in uplifted segments of the rifts that are bounded by faults. These are indicated by magnetic minima and illustrated in the magnetic profile shown in Figure 3.12.

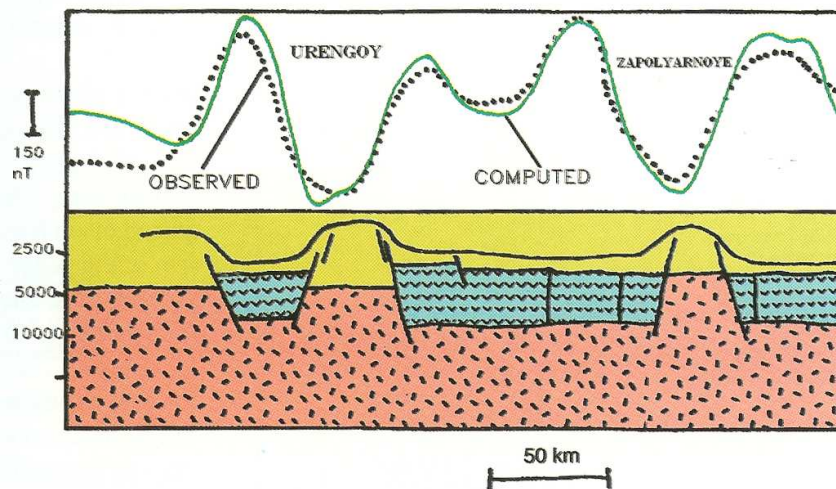


Figure 3.12 Observed total intensity magnetic anomaly profile across a portion of the Western Siberian Basin and the computed anomaly from the modeled geologic cross-section. Rift basalt (v-pattern) in grabens produce 300 to 400 nT anomalies associated with faulting leading to magnetization contrast with the basement rocks of the region (random-dash pattern) and overlying sedimentary rocks (blank). Gas fields are associated with relatively upthrown areas marked by negative magnetic anomalies. Adapted from Gibson (1998b).

3.3.10 c) Salt Features

Numerous examples exist in many hydrocarbon-rich basins of the world of gas and oil traps associated with structural features caused by the mass movement of salt within the sediments of the basin. Buried salt as a result of its plastic nature can be driven toward the surface by pressure of overlying sediments. The buoyant rising salt results in pillow, plumes or ridges of salt that disrupt the sediments and arch them upward. This structural deformation leads to traps overlying the features or along the upwarped sediments that are truncated by the impermeable salt formations. The strong density contrast and the common steep margins of salt features lead to significant gravity anomalies that are readily identified in basin gravity anomalies.

The gravity method is particularly important to studying salt features because of the difficulty in seismic reflection profiling in mapping the steep margins of the salt features and sedimentary layering beneath salt overhanging structures within the sediments. Thus, interpretation of gravity anomalies related to salt bodies is useful not only in locating these features but in mapping their three-dimensional configuration. Enhanced resolution of the

nature of the bodies can be obtained by the use of borehole gravity surveying in drill holes adjacent to or within the salt deposits.

The nature of the salt-derived anomalies is complicated by the exponential increase in density of basin sediments with depth and the varying depth to the salt features. Near the surface, sediments by virtue of their high porosity may be less dense than the salt, which typically has an average density of 2200 kg/m^3 near the surface, leading to positive gravity effects. The depth of this *density crossover* or *nil zone* from positive to negative density contrast varies even within basins, but is roughly 1.5 – 2 km in the Gulf of Mexico (Nelson, 1991). At depths greater than the density crossover the density contrast is negative and increases with depth due to the increasing density of the sediments due to compaction and lithification of the sediments and decreasing density of the salt. The density of salt decreases with depth because the effect of volume increase with increasing temperature with depth more than compensates for the effect of increasing overburden pressure (Jackson and Talbot, 1986). As a result salt densities may range from 2000 to 2200 kg/m^3 .

Further complicating the salt-derived gravity anomalies is the presence of high-density ($\approx 2950 \text{ kg/m}^3$) limestone or anhydrite formations (cap rock) at the top of some salt intrusives that have been brought to the near-surface by the action of the buoyant salt. The result is the classic salt dome anomaly (Gibson, 1998a) shown schematically in Figure 3.13.

Typically the salt dome gravity anomaly of the Gulf of Mexico is a negative anomaly of the order of 5 mGal with a central high of lesser amplitude due to the cap rock effect. Salt-derived anomalies vary widely with for example the depth of the source, cap rock effect, the depth extent of the salt feature, the change in density of the sediments with depth, and the presence of horizontal excursions (overhangs) from the apex of the salt feature. Gravity anomalies have amplitudes from zero, where the mass effect of salt bodies distributed above the density crossover cancel out the negative anomaly of the sub-density crossover salt, to greater than 10 mGal. The variation in gravity anomaly signature is typified by the results of modeling [e.g., Corrigan and Sweat (1995); Prieto (1998)] and case histories [e.g., Peters and Dugan (1945); Nettleton (1957); Austin (1998); Pratson et al. (1998); Schenk et al. (1998)].

An example of a gravity anomaly profile across a Gulf of Mexico salt dome located 125 miles southeast of Galveston, Texas, U.S. is shown in Figure 3.14 with the salt dome model anomaly that closely approximates the residual gravity anomaly. The model illustrates salt overhanging at the top of the dome and the positive gravity anomaly associated with positive

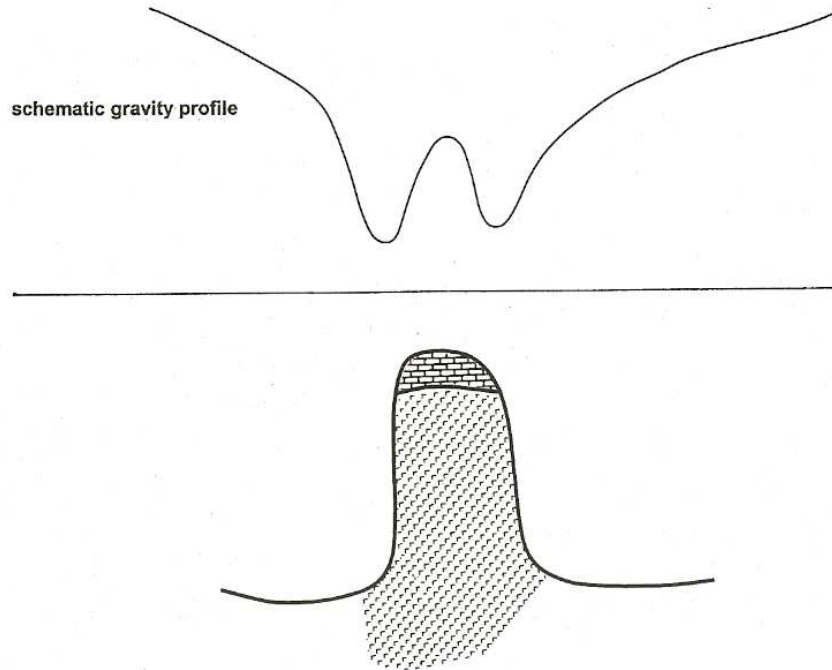


Figure 3.13 Generalized cross-section of a salt dome with cap rock and associated schematic gravity anomaly profile. Adapted from Gibson (1998a).

density contrast of the topmost layer of the dome. Increasingly, measured gravity gradients are being used to enhance the resolution and interpretation of gravity anomalies associated with salt diapirs. An example of this is given by Ennen and Hall (2011) who have mapped out the effect of the caprock of the Vinton salt dome, Louisiana, U.S. with the airborne full tensor gravity gradient measured by Bell Geospace. Figure 3.15 shows maps of the six measured gradients with the positive gravity anomaly of the caprock located in the center of each of the maps. The gravity gradients calculated by forward modeling of the effect of the caprock configuration and properties determined from extensive drilling are shown in Figure 3.16. The excellent comparison of the gradient maps illustrate the resolving power of the gravity gradients.

Magnetic anomaly data also are potentially useful in identifying the presence of salt structures that may be related to oil and gas traps. Prieto (1998) shows a high resolution magnetic anomaly map in offshore Louisiana with several obvious negative anomalies that are assumed to originate from salt domes. In Figure 3.17 the surface vertical magnetic intensity contours are shown over the Grand Saline dome in Texas, U.S. A negative anomaly of

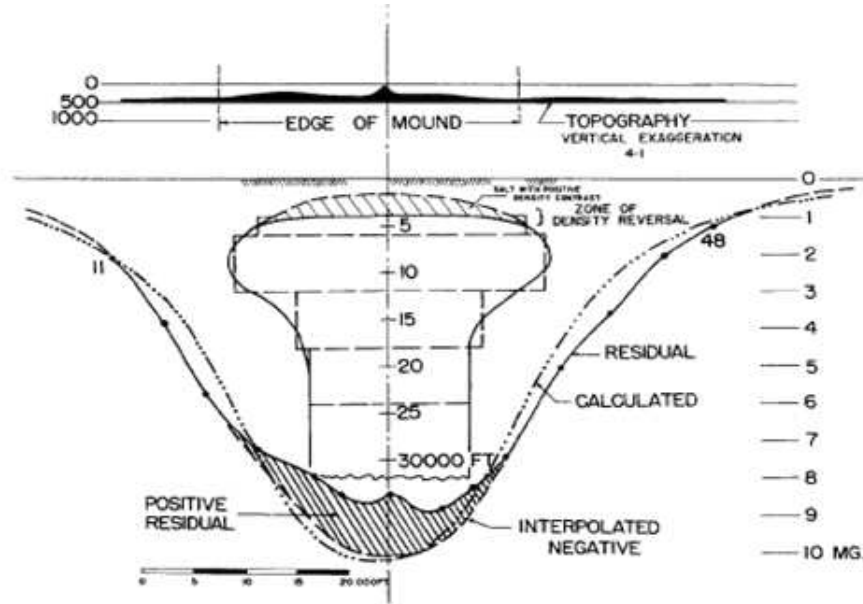


Figure 3.14 Residual gravity anomaly and calculated anomaly profile across a salt dome offshore Galveston, Texas, U.S. The structure of the salt dome used in modeling the anomaly is shown with overhanging crest and positive anomaly caused by positive density contrast of the upper portion of the dome. Adapted from Nettleton (1957).

the order of 10 to 15 nT is observed correlating with the dome, however, the amplitude and shape of magnetic anomalies related to salt domes will vary significantly with the depth to the structure and its three-dimensional configuration. Similar negative magnetic anomalies in the range from a few to 10 nT are related to salt structures in the Gulf of Mexico. The source of negative magnetic anomalies with salt structures has been the subject of discussion, but is likely due to the lack of magnetic minerals in the salt in comparison to the surrounding sediments and a slight effect due to the diamagnetic nature of salt.

3.3.11 2) Stratigraphic Features

Oil and gas may be trapped in the subsurface by changes in the sedimentary rocks due to original deposition of the sediments and by subsequent alteration with movement of fluids through them as well as thermal effects. Numerous instances of significant production from these stratigraphic traps are cited in the literature. Many of these traps are related to horizontal vari-

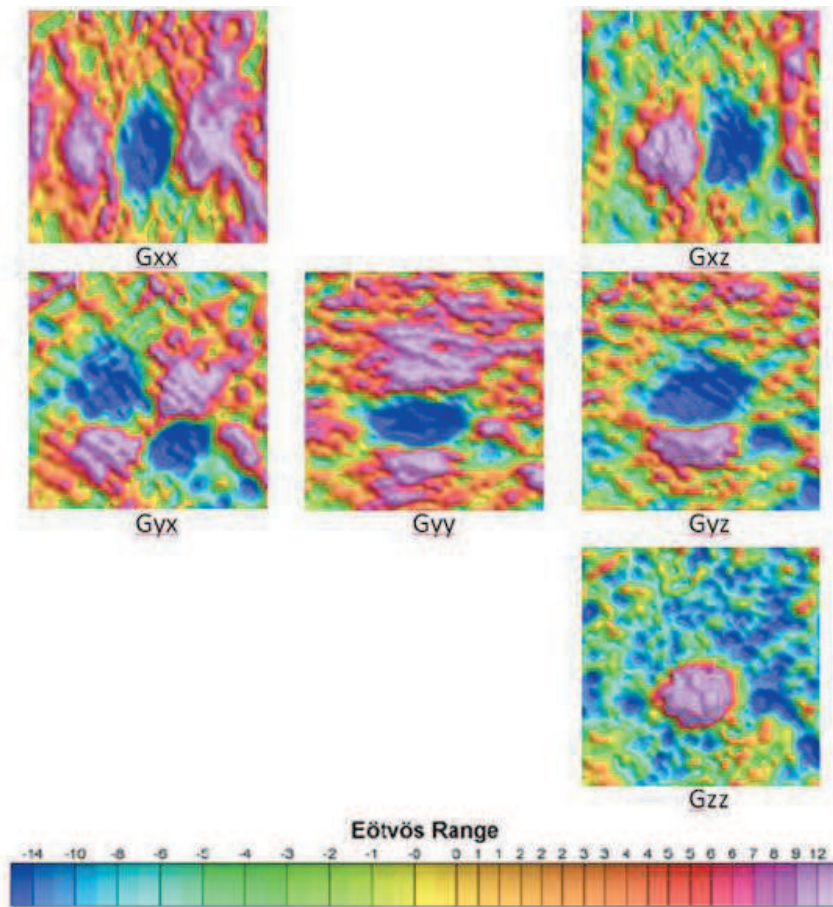


Figure 3.15 Measured airborne gravity gradients (Bell Geospace) over the Vinton salt dome, Louisiana, U.S. Adapted from Ennen and Hall (2011).

ations in density or magnetic properties of the rocks leading to measurable anomalies in gravity and magnetic fields at the Earth's surface.

The source of density variations within sedimentary rocks is well supported by a wealth of geological information (see Chapter 5). In contrast, conventional wisdom has dictated that these rocks are essentially magnetically transparent without variations that can be measured. Ground magnetic surveying which prevailed prior to the end of World War II, although sufficiently precise to measure magnetic anomalies from sedimentary rocks, generally was subject to magnetic effects from near surface sources which largely masked sedimentary anomalies. The advent of airborne magnetometry led to surveying over vast areas, but considering the height of the observations

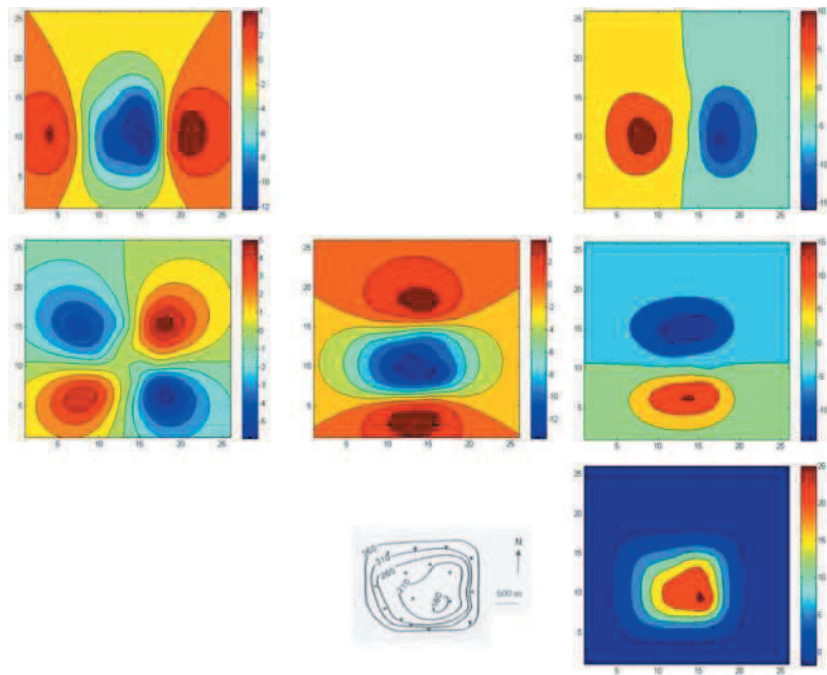


Figure 3.16 Calculated gravity gradients from the cap rock configuration of the Vinton salt dome, Louisiana, U.S. shown in the lower center map. The gravity gradients maps are positioned as they are in Figure 3.15. Note the close correspondence between the observed and calculated gradients. Adapted from Ennen and Hall (2011) and calculated by Eti (2004).

and the lack of precision in the early surveying, interpretation necessarily focused on anomalies measured in 10s and 100s of nanoteslas and not on the more subtle sedimentary rock anomalies. This situation has changed dramatically with high-resolution magnetic mapping based on improved observations, positioning, and computational methods leading to the mapping of anomalies in the few nanoteslas range and even sub-nanotesla range under optimum conditions. As a result, there are increasing opportunities for mapping stratigraphic variations in the magnetization of sedimentary rocks. The following are only a few examples of how gravity and magnetic investigations can be useful in identifying and studying stratigraphic variations in sedimentary rocks.

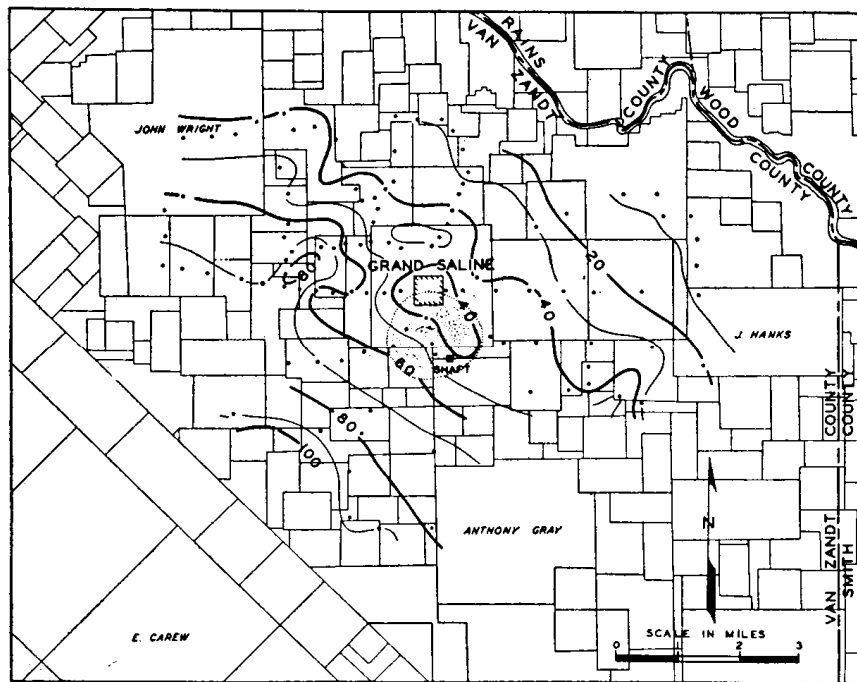


Figure 3.17 Magnetic vertical intensity contour map from surface measurements over the Grand Saline dome, Texas, U.S. Contour interval 10 nT. Adapted from Peters and Dugan (1945).

3.3.12 a) Reefs

Ancient carbonate reefs potentially are excellent oil and gas reservoirs because of their inherent porosity, which exceeds that of the adjacent sedimentary formations. As a result, they have been a notable target of geophysical exploration in the hydrocarbon exploration industry. Reefs are carbonate masses composed of the remains of fauna and flora that develop in colonies on the shallow seafloor. Where the sea floor is sinking, the colonies build upward to remain within the reach of sunlight, thus constructing isolated steeply-margined, vertically-extending masses that are subsequently buried in other sediments. Today seismic reflection is the method of choice for mapping ancient reefs, but gravity methods have had a prominent role in the past and still may be useful in exploring for these targets, particularly where the reefs are relatively shallow, within the first few kilometers of the surface. Gravity anomalies derived from reefs may have several origins and differ between basins leading to a variety of gravity anomaly signatures (Yungul, 1961).

The porosity of reefs is highly variable, but averages about 12% decreasing the density of the carbonate structure, but this decrease may be offset somewhat by the chemical alteration of limestone framework of the reef to the denser carbonate, dolomite and post-deposition filling of pore space by chemical sediments. However, reefs are commonly in juxtaposition with clastic sediments rather than carbonates. As a result, lithofacies variations marginal to reefs and differential compaction due to differing depth of sediments on and off the reef lead to a complex density contrast pattern. Yungul (1961), who concludes that the average densities of limestone and dolomite reefs are 2,500 and 2,700 kg/m³, respectively, suggests that the reef as a result of this density contrast is expressed as a positive gravity anomaly of the order of 0.5 mGal surrounded by a negative *moat* of lower amplitude than the positive. Anomalies of this type are observed over reefs in the Illinois Basin, U.S. In contrast, reefs in the Michigan Basin, U.S. are represented in the gravity field by isolated positive anomalies (< 0.5 mGal) related to the non-deposition of low density evaporates (Pohly, 1954). An example of the residual gravity anomaly associated with the Dawn No.156 reef on the southeastern margin of the Michigan basin is shown in Figure 3.18.

Magnetic methods are not used directly to search for buried reefs, but regional magnetic and gravity anomalies that isolate ancient depositional margins where reefs may be expected to occur under the proper environmental conditions are useful in isolating zones favorable for exploration. Yungul (1961) notes that reef anomalies are commonly "located near the apexes of regional gravity anomalies" and Pierce et al. (1998a) have mapped faults with magnetics that possibly are related to sea margins where reefs developed in the past.

3.3.13 b) *Direct Detection of Hydrocarbons*

The reliable direct detection of hydrocarbons in the subsurface is a goal of geophysical exploration that has largely eluded the profession despite continuing efforts. This is true of the gravity and magnetic methods, as well as other geophysical methods. Although success in the search for this goal with the gravity method has not been achieved, McCulloh (1980) describes evidence for low-amplitude, but clearly recognizable gravity minima that may be associated with petroleum and particularly gas reservoirs. Evidence of this relationship has been observed in the Tertiary basins of California [e.g., Miller (1931)]. Also, Zeng et al. (2002) describe efforts to map gravity minima within two Chinese oil fields utilizing gravity gradients. Nonetheless,

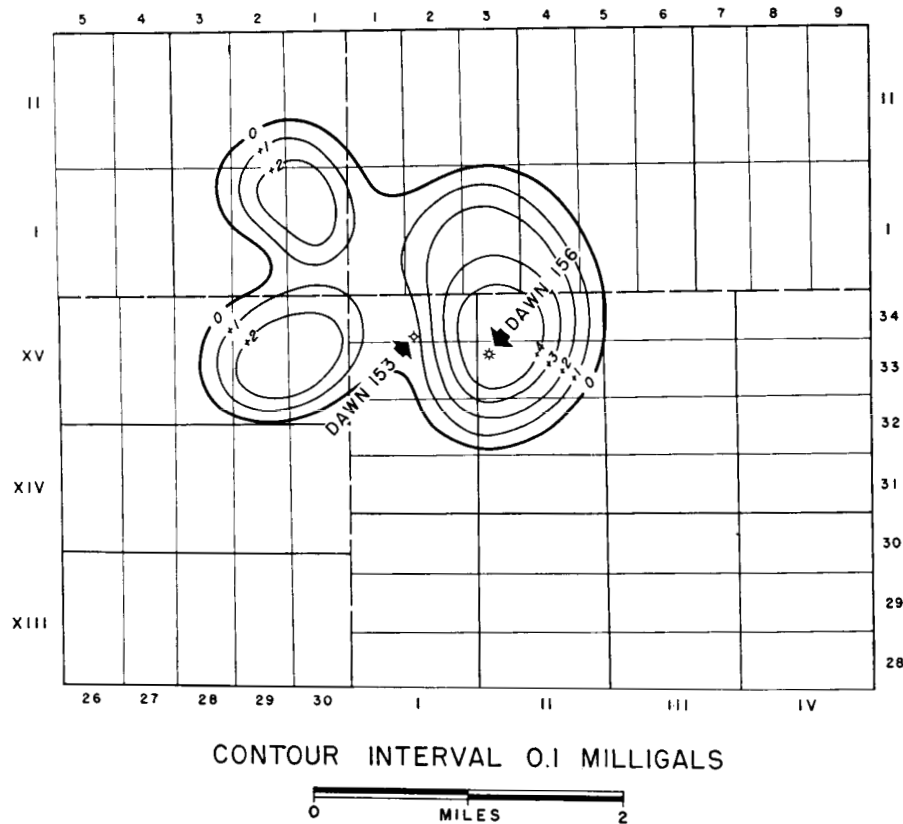


Figure 3.18 Residual gravity anomalies determined graphically from the observed gravity anomaly over the Dawn No. 156 reef in Ontario, Canada on the southeastern edge of the Michigan basin. Adapted from Pohly (1954).

the reliable direct detection of hydrocarbons by the gravity method remains problematic.

Magnetic methods have also been investigated as a technique for the direct detection of hydrocarbons dating back to the beginning of the 20th century (Becker, 1909). Numerous studies [e.g., Leblanc and Morris (1999); Phillips et al. (1998); Pierce et al. (1998b)] have been made of magnetic anomalies associated with operating oil fields, magnetic properties of sedimentary rocks, and theoretical models. Donovan et al. (1979) mapped near-surface magnetic anomalies over the Cement oil field, Oklahoma, U.S. that they ascribed to epigenetic (secondary or post-deposition) magnetic minerals in the overlying sedimentary rocks. Subsequent laboratory and field studies have recognized the existence of geochemical reactions, sometimes enhanced

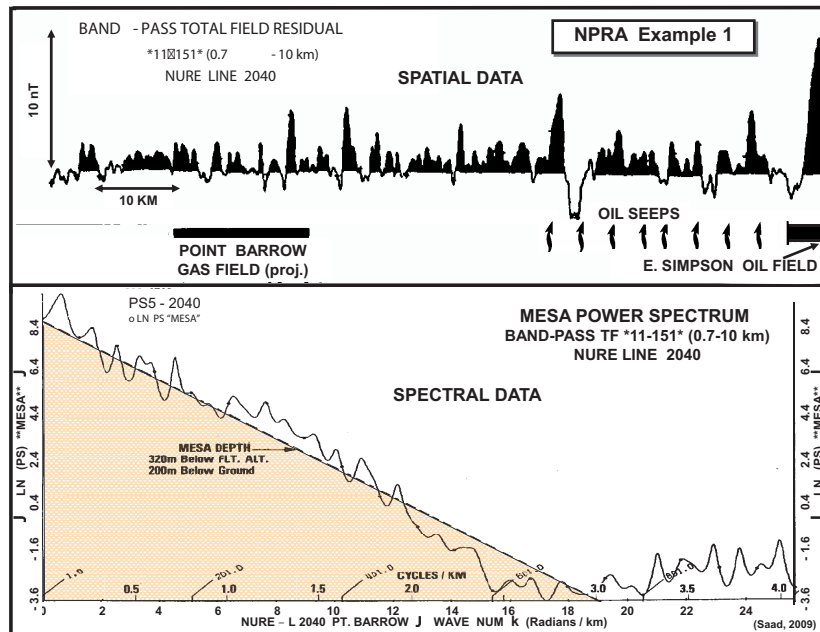


Figure 3.19 Band-pass filtered total magnetic intensity profile showing a population of short-wavelength sedimentary magnetic anomalies (top) and their MESA power spectrum (bottom), over an area of oil and gas production and seeps in the NPRA, North Slope, Alaska. Adapted from Saad (2009a).

by biological activity in the sedimentary rocks overlying oil fields, involving the reduction of iron in the rocks from the ferric to the ferrous soluble state in reducing conditions associated with escaping hydrocarbons and sulfur compounds. The ferrous iron can be redeposited as iron-rich minerals of relatively high magnetic susceptibility or remanent magnetization near the surface where an oxidizing environment exists. It is these epigenetic minerals, such as magnetite (Fe_3O_4), pyrrhotite (Fe_7S_8), and greigite (Fe_3S_4), that have been proposed as the source of the magnetic anomalies over oil fields.

Figure 3.19 shows an example of several high-frequency magnetic anomalies obtained by band-pass wavelength (0.7 – 10 km) filtering of a total magnetic intensity profile from the public domain NURE survey data (Saad, 1986, 2009a). The survey was flown in 1980 over the NPRA, Alaska at an altitude of 120 m above the ground surface. The profile used in this figure is located in the northern part of the NPRA over the Point Barrow-East Simpson area. The wavelength of the anomalies is typically 1 to 5 km, while

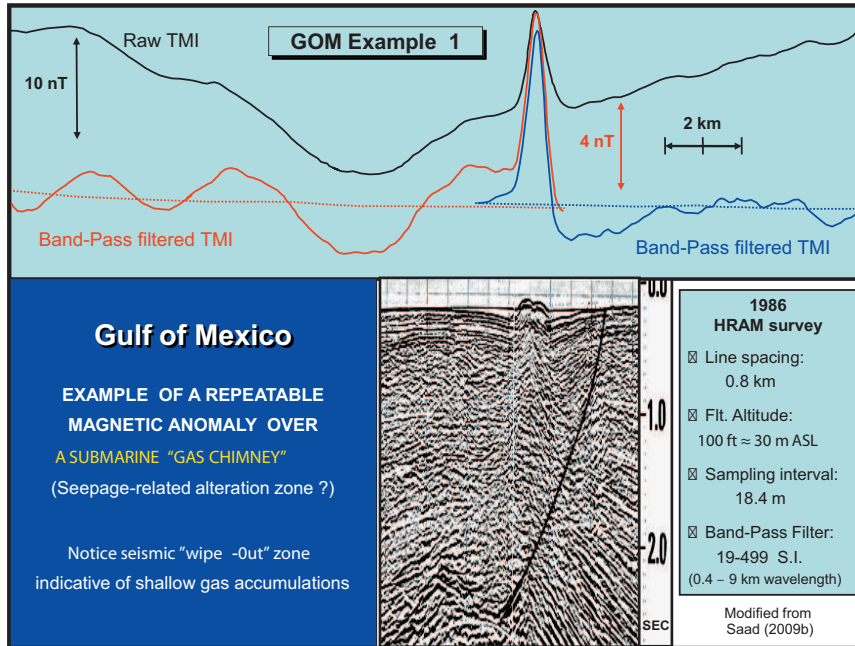


Figure 3.20 Example of a repeatable short-wavelength magnetic anomaly over a submarine "gas chimney" in the Gulf of Mexico; the anomaly most likely is due to seepage-related alteration of shallow sediments and *in-situ* formation of iron sulfides magnetic minerals. Adapted from Saad (2009b).

their amplitudes range from 2 to 10 nT. The source of these anomalies is relatively shallow. Using the MESA spectral depth estimation technique on these data (Figure 3.19, bottom), the average depth to the sources of the anomalies, obtained from the slope of the straight line fitted to $\ln(PS)$, is about 200 meters below the surface. The spatial band-pass filtered data (Figure 3.19, top) clearly show a number of short wavelength anomalies that appear to correlate well with hydrocarbon production or seeps. The least intense anomalies occur over or near the E. Simpson oil field and Point Barrow gas field and over areas with known oil seeps. The source of these micro-magnetic anomalies has been postulated to be diagenetic magnetic minerals (such as magnetite, pyrrhotite, greigite, and maghemite) that may be related to chemical changes of the sediments at shallow depths caused by micro-seepage of hydrocarbon reservoirs (Reynolds et al., 1991). Both induced and remanent (CRM) magnetizations most likely produce the magnetic anomalies.

Figure 3.20 is an interesting example from the Gulf of Mexico (GOM - Example 1) of a high-frequency magnetic anomaly having an amplitude of 8

nT and is due to a shallow source (Saad, 2009b). This non-cultural anomaly is repeatable on a re-flight of a portion (blue) of this line. A close look at the seismic section in this area (Figure 3.20) shows the sharp positive magnetic anomaly coincides exactly with a seismic "gas" anomaly where gas seems to be seeping all the way to the ocean floor. The noticeable seismic "wipe-out" zone is indicative of shallow gas accumulations. It is possible that gas seepage may chemically alter the sediments resulting in the formation of magnetic iron sulfide minerals such as pyrrhotite (Fe_7S_8) or greigite (Fe_3S_4) within the shallow sediments (Saad and Sisemore, 1988). The ferrimagnetic mineral greigite forms in a reduced sulfur-rich environment. It has been identified in some offshore samples over hydrocarbon-producing areas in the Gulf of Mexico and other areas such as the Alaska North Slope (Reynolds et al., 1991).

Several additional studies indicate correlations between magnetic anomalies and oil fields such as observed at the Cement field in Oklahoma, U.S., but none have provided definitive evidence that the origin of the anomalies is epigenetic mineralization. Reynolds et al. (1990) have located the ferrimagnetic pyrrhotite in the shallow sedimentary rocks over the Cement field, but the anomalies resulting from the presence of this mineral are an order of magnitude less than the observed anomalies and the spectra of the anomalies differ. The consensus of opinion on the source of the Cement field anomalies is that they are related to cultural features associated with the field (Phillips et al., 1998). It is likely that other correlations between oil fields and magnetic anomalies have a similar origin. Gay (1992) in a study of the literature of magnetic anomalies and sedimentary rocks concludes that no definitive evidence exists that anomalies are due to epigenetic minerals, although clearly there are numerous examples of syngenetic (primary or detrital) magnetic anomalies over sedimentary basins. However, in specialized conditions highly magnetic epigenetic minerals may be formed by the heating effects of spontaneous combustion of fine pyrite (FeS_2) in marine rocks. This combustion metamorphism maybe associated with oil fields (Cisowski and Fuller, 1987), and thus under the proper geological conditions, can be useful in detecting hydrocarbon accumulations.

In summary, gravity methods have not found a use in the detection of the presence of oil or gas as a result of associated changes in density of the reservoir or adjacent rock formations. The geochemical effects of hydrocarbons on the magnetic properties of reservoirs and adjacent rocks have been extensively investigated without definitive associations being found that indicate the viability of the magnetic method to directly detect hydrocarbon fields.

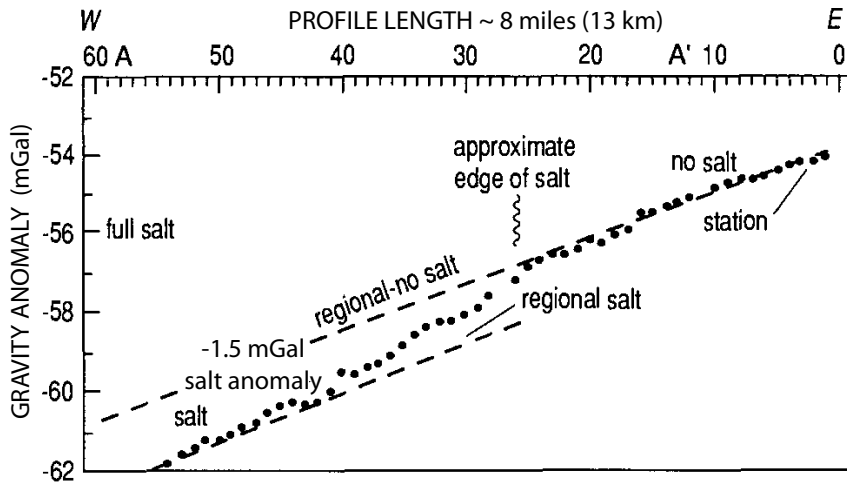


Figure 3.21 Bouguer gravity anomaly across an updip salt-dissolution edge in west-central Saskatchewan, Canada showing an approximate -1.5 mGal negative anomaly associated with the edge between the regional-no salt and the regional salt anomalies. Adapted from Anderson and Cederwell (1993).

3.3.14 c) Stratigraphic Lithologic Variations

Gravity and magnetic anomalies originate from lateral variations in sedimentary rock basins caused by structural activity as explained above, but also by stratigraphic effects originating from original deposition or subsequent diagenetic processes. Stratigraphic sources generally are of lower volume and have less sharp boundaries than those associated with structural disturbances. As a result, the anomalies have lower amplitudes and gradients than those derived from structures, making them more difficult to identify in the background potential field, and require high precision and resolution investigations for their detection.

The subtle nature of gravity anomalies associated with stratigraphic lithologic variations is illustrated by the gravity anomaly over the salt dissolution boundary associated with the Westhazel General Petroleum's oil field in west-central Saskatchewan, Canada (Anderson and Cederwell, 1993). The petroleum trap is caused by reversal of dip caused by an updip dissolution edge of Devonian rock salt. Data presented by Anderson and Cederwell (1993) show that the seismic reflection signature of the salt-dissolution feature can be complex, thus it is useful to seek confirmatory evidence in the gravity anomaly data. A Bouguer gravity anomaly profile across the salt edge is shown in Figure 3.21 together with regional gravity anomalies with

and without the salt. A negative gravity anomaly of roughly -1.5 mGal amplitude is shown west of the approximate edge of the salt due to an assumed density contrast of -400 kg/m³ (2200 kg/m³ for the salt and 2600 kg/m³ for post-Paleozoic clastic rocks). The subtle nature of the anomaly requires intense integration of the analysis with available geologic data and care in the isolation of the anomaly.

Hammer and Anzoleaga (1975) have shown that both horizontal and vertical gravity gradients can be used to assist in the isolation and evaluation of anomalies associated with pinchouts of sedimentary formations that may serve as hydrocarbon reservoirs. Rose et al. (2006) illustrate the use of the higher sensitivity of airborne gravity gradients at shorter wavelengths to hydrocarbon exploration. One example is the mapping of a shallow subsurface channel in the Gippsland basin in the Bass Strait offshore Australia that is a hydrocarbon exploration target.

Magnetic anomalies associated with sedimentary rocks of varying magnetizations are also potentially useful in mapping of sedimentary formations. The presence of detrital magnetite, that is magnetite grains deposited by wind and water, is well known in sedimentary rocks. Depositional or erosional processes that lead to varying concentrations of magnetite in specific zones and lithologies of sedimentary basins can cause sufficient magnetic susceptibility variations for magnetic mapping at the surface. In addition, secondary processes, such as chemical remanent magnetization, occurring after sediment deposition may strongly influence magnetization. For example, Flanagan et al. (1988) show that by taking into account both the susceptibility and remanent magnetization of the sediments in the Gulf of Mexico Basin, magnetic modeling can be a powerful independent tool for evaluating seismic reflection interpretations in the region. They find limited differences in susceptibility of the sediments, but the magnitude of the remanent magnetization varies quite widely. Phillips et al. (1998) have reached a similar conclusion in modeling the primary and secondary magnetizations of sedimentary rocks in the Arctic Wildlife Refuge of Alaska, U.S. Figure 3.22 shows the result of modeling along a seismic profile using the indicated magnetizations for the sedimentary formations.

Figure 3.23 shows an example of sedimentary magnetic anomalies from the Gulf of Mexico (GOM - Example 2) whose sources are shown on the seismic section (Saad, 1993). The classic well-defined 2 nT positive anomaly in the middle is observed over a mapped shallow sand channel of Upper Pleistocene (Wisconsinan) age at a subsurface depth of about 1000 ft (305 m) in water depth of 300 ft (91 m). The anomaly is flanked by two distinct magnetic lows of about 4 to 7 nT in magnitude associated with shallow salt structures. The

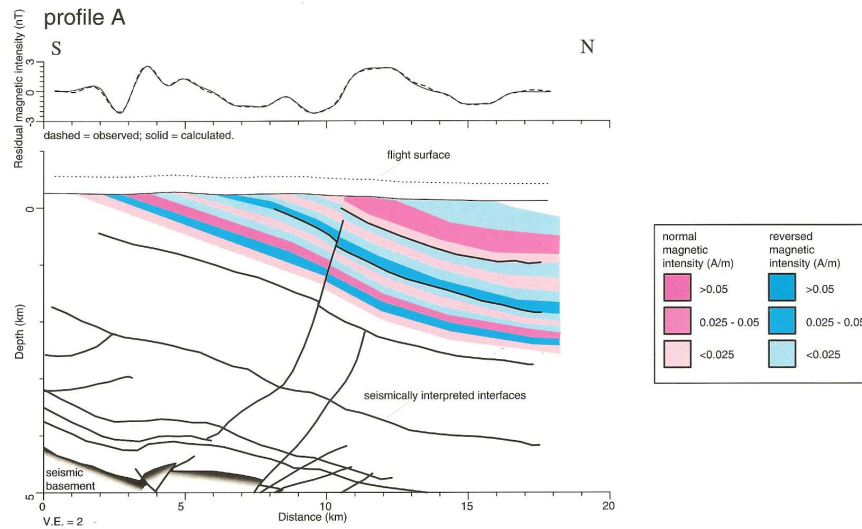


Figure 3.22 Observed and calculated total intensity magnetic anomalies in the Arctic Wildlife Refuge of Alaska, U.S. based on both normal and reversed magnetizations as indicated. Heavy lines on the cross-section are stratigraphic and structural boundaries interpreted from the seismic reflection profiling. Subhorizontal boundaries are representative of many parallel reflections. Adapted from Phillips et al. (1998).

sand anomaly is also located in the middle of a broader magnetic low which is apparently due to a deeper salt structure directly below the sand channel at a depth of about 2400 m. Saad (1993) shows additional examples of high resolution aeromagnetic anomalies due to a deeper Lower Pleistocene sand channel near the same area of the Gulf of Mexico.

The GOM-Example 3 in Figure 3.24 shows a 2 nT anomaly located offshore the Texas-Louisiana coast line on the outer continental shelf of the Gulf of Mexico. The anomaly is repeatable on four adjacent east-west magnetic lines, 0.5 mile (0.8 km) apart, flown at 100 feet (30 m) above sea level. The magnetic anomaly has been interpreted (Saad, 1987) to be due to a sand channel at a depth of about 2,000 to 3,000 feet (610 to 914 m). The existence of this channel was confirmed by the exploration geologists working in the area and by its seismic expression highlighted in Figure 3.24. The channel is Wisconsinan (Upper Pleistocene) in age and located on the slope just south of the shelf edge in deep water, 600 ft (183 m).

GOM-Example 4 in Figure 3.25 shows a portion of a stacked-profiles map displaying band-pass filtered total magnetic intensity anomalies due to sedimentary sources in the Gulf of Mexico (Saad, 2009b). The high resolution

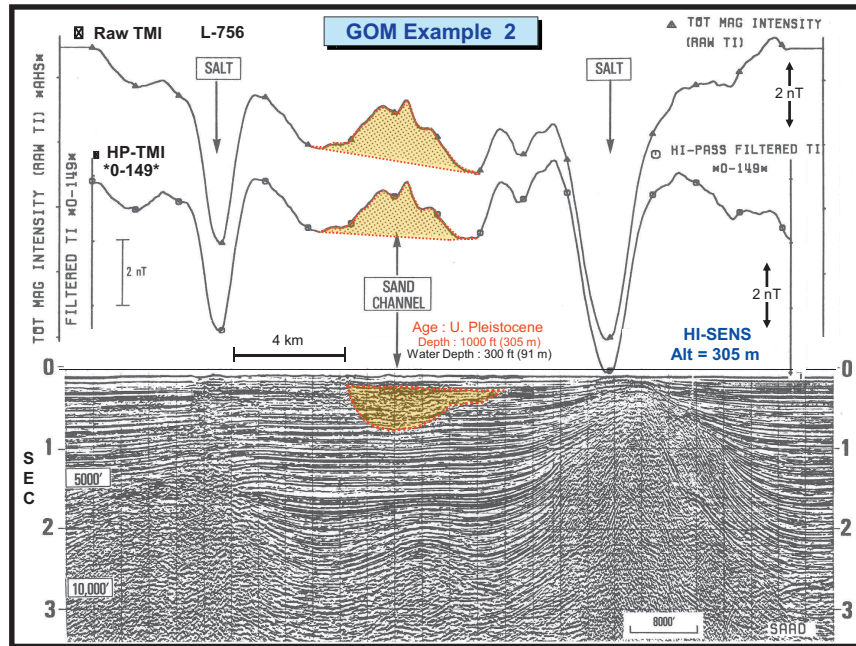


Figure 3.23 Sedimentary magnetic anomalies due to known shallow sand channel and salt structures in the Gulf of Mexico. Adapted from Saad (1993).

aeromagnetic data were observed at an altitude of 30 m above the Gulf with 0.8 km line and tie-line spacing. The survey was designed for the primary purpose of detection and delineation of sand channels and other sedimentary structures. To preserve the integrity, amplitudes, and shapes of the sedimentary micro-anomalies, special techniques for profile data processing, enhancement, and display were used. These included space-domain wavelength band-pass (0.5 – 9 km) filtering to remove high-frequency random noise and low-frequency basement and deeper anomalies (Saad, 2009b). The MESA technique was used for filter design and testing and estimation of average depth to the sources. Finally, the stacked-profiles color map format was found to be most effective for optimum display, preservation and line-to-line correlation of the anomalies. Figure 3.25 displays two prominent trends of anomalies: a subtle positive (blue) trend "1" interpreted to be due to a sand channel, and a strong negative (red) trend "2" due to a mapped salt ridge in this area.

Sand channels provide locales for minor concentrations of heavy minerals, very much similar to alluvial deposits and buried placers. The heavy

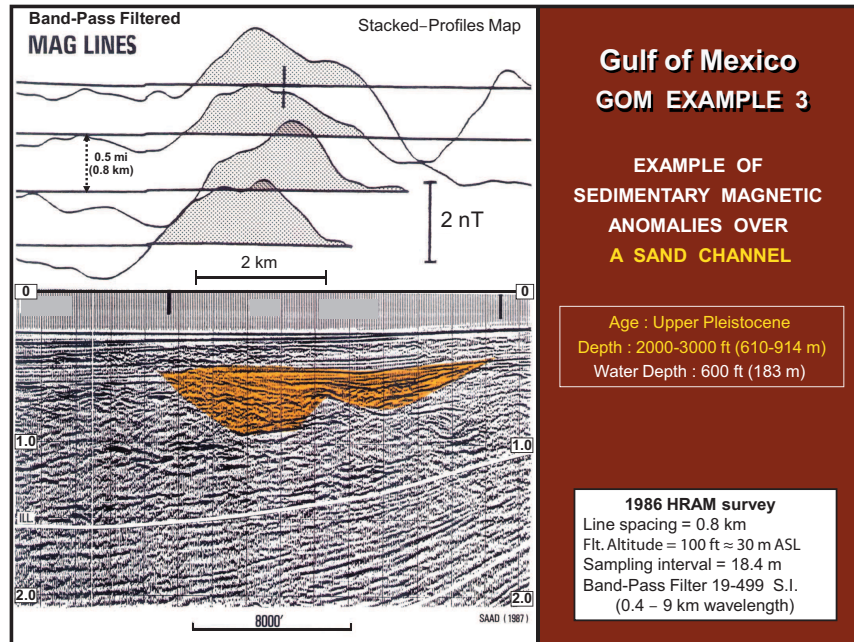


Figure 3.24 Example of band-pass filtered sedimentary magnetic anomalies on four stacked-profiles over a sand channel in the Gulf of Mexico. Adapted from Saad (1987).

mineral content most likely includes detrital magnetite and/or other magnetic minerals. The magnetite enrichment in a channel can cause a high enough magnetization contrast with the surrounding sediments to produce detectable magnetic anomalies. Modeling has shown that only 0.05 – 0.1% by volume increase in magnetite content within a channel is sufficient to cause measurable anomalies. In fact, examination of subsurface sand samples of Sangamonian and Illinoian age suggests that some of the sands in the offshore Gulf of Mexico may contain a high percentage (greater than 0.5%) of black minerals mostly magnetite (Crane, 1989).

Similar magnetic anomalies associated with sand channels relatively enriched in detrital magnetite have been observed in other basins where they are potentially important to hydrocarbon exploration. As in the case of gravity anomalies, increasing attention is being given to observed magnetic gradients useful in studying intrabasin sources of magnetic anomalies [e.g., Mushayandebvu and Davies (2006); Schmidt and Clark (2006)].

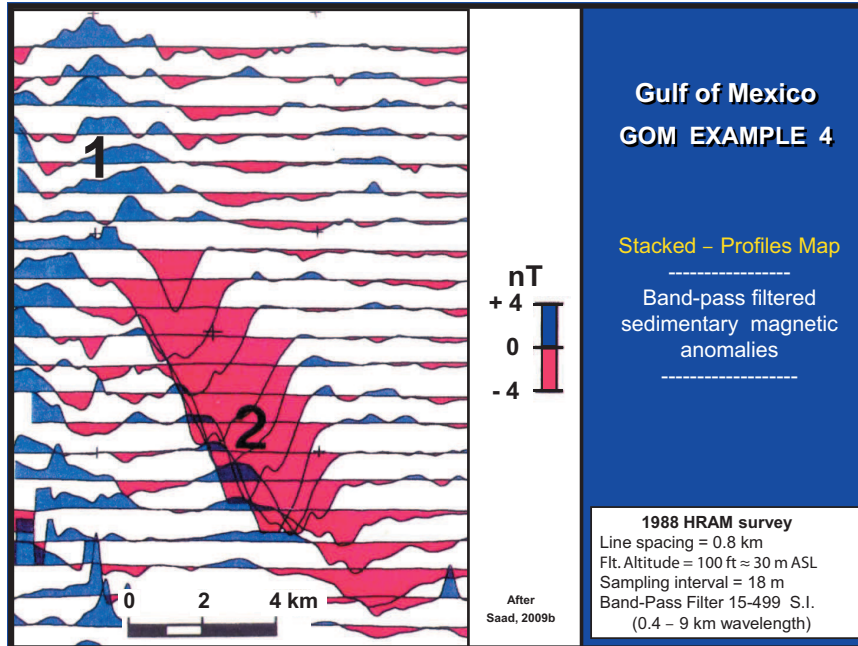


Figure 3.25 Stacked-profiles map of band-pass filtered sedimentary magnetic anomalies over (1) an interpreted sand channel and (2) a known salt ridge in the Gulf of Mexico. Adapted from Saad (2009b).

3.3.15 Exploitation

Gravity and magnetic methods are commonly thought of in the hydrocarbon industry as reconnaissance techniques for isolating regions for more intense exploration largely by other geophysical methods. However, the above case histories convincingly show that they are useful beyond this simple view and in fact have found an increasing role not only in exploration, but also in the exploitation of oil and gas fields.

One of the ways that gravity and magnetics can be used in hydrocarbon exploitation is identifying potential subsurface hazards to drilling. A useful example is the unfortunate failure to use regional gravity and magnetic anomaly mapping to aid in the location of a multiple-company drill hole in the St. George Basin southwest of Alaska, U.S. in the Bering Shelf as described by Chapin et al. (1998). Instead of drilling a thick sedimentary rock sequence as expected the well drilled through more than a kilometer of volcanic rocks before being abandoned. Yet published regional marine gravity (Figure 3.26) and magnetic data (Figure 3.27) clearly show significant positive gravity (20 mGal) and magnetic (700 nT) anomalies at the drill site

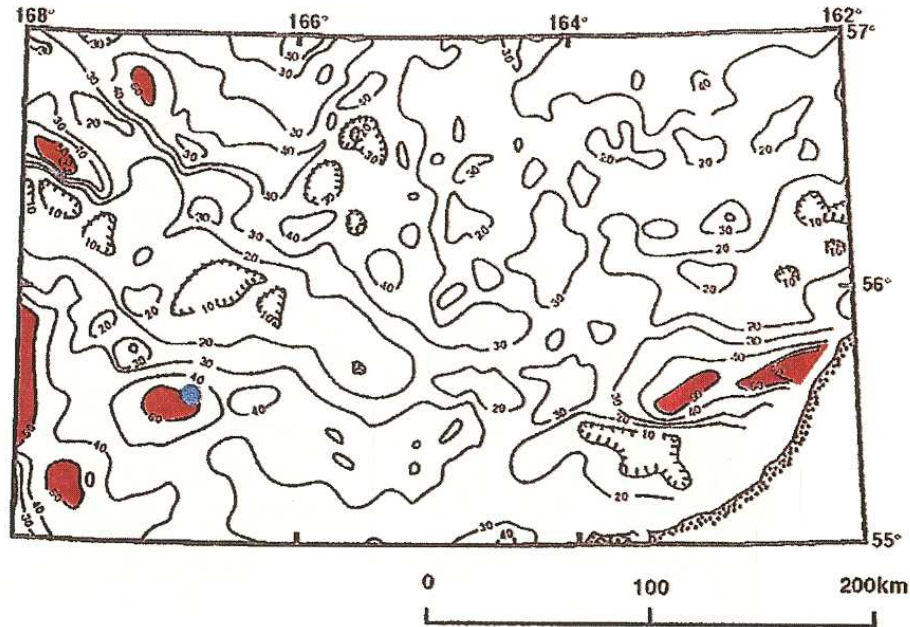


Figure 3.26 Free-air gravity anomaly map (contour interval 10 mGal) off southwestern Alaska, U.S. showing the roughly 20 mGal positive anomaly in the southwestern quadrant associated with the 1976 multi-company drill site indicated by the filled circle. Adapted from Chapin et al. (1998) and Pratt et al. (1972).

indicating the presence of the volcanic rocks. If these data would have been integrated into the placement of the drill hole, failure of the drilling to meet its objectives could have been prevented.

Another example of the use of gravity data integrated with seismic data is to identify gas accumulations in the sedimentary formations of the near-seabottom surface that could lead to catastrophic blowouts if the gas were unexpectedly drilled into during hydrocarbon exploration. Bauer and Fichler (2002) have illustrated the application of this integrated interpretation based on a high-resolution gravity data (accuracy estimated of the order of 0.02 mGal) and post-stack seismic data from the central North Sea. Figure 3.28 shows the free-air gravity anomaly and the similar anomaly calculated from the model that identifies the gas *chimney* that is visible, but not well defined in the seismic section. It should be noted that these near-surface gas pockets can be indicators of migration of gas from deeper, more extensive gas fields.

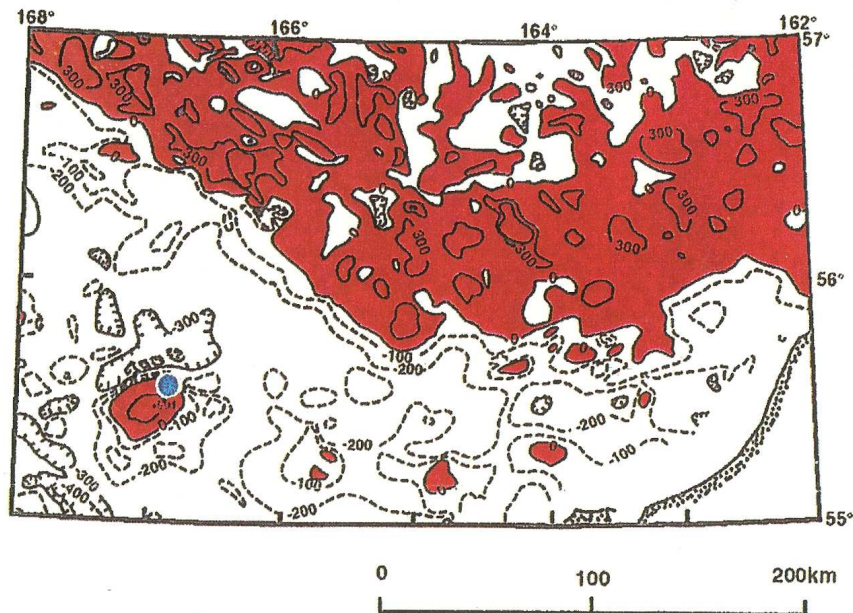


Figure 3.27 Marine magnetic (total intensity) anomaly map (contour interval 100 and 300 nT) off southwestern Alaska, U.S. showing the roughly 700 nT positive anomaly in the southwestern quadrant associated with the 1976 multi-company drill site indicated by the filled circle. Adapted from Chapin et al. (1998) and Pratt et al. (1972).

Subsurface natural gases may in the appropriate environment crystallize into gas hydrates that can be a hazard to hydrocarbon exploration drilling as well as a potential source of hydrocarbons. The density of hydrates is estimated to be of the order of $800 - 900 \text{ kg/m}^3$, thus gas hydrate-rich sedimentary zones are a potential target for gravity exploration providing confirmatory evidence to the results of other geophysical methods.

Borehole gravity data can also be used to exploit oil and gas subsurface traps because of the enhanced resolution achieved by increasing the proximity of the observations to the source, and also by using the data to calculate the density of the adjacent sedimentary strata. Bradley (1974) has shown that the use of the densities obtained from borehole gravity measurements when compared with averaged densities from gamma-gamma (FDC) logs can be successful in isolating high porosity zones in Niagaran reefs in the Michigan Basin too far from the bore to be detected by the FDC log. This is illustrated by FDC and borehole gravity logs in a reef well drilled by Amoco

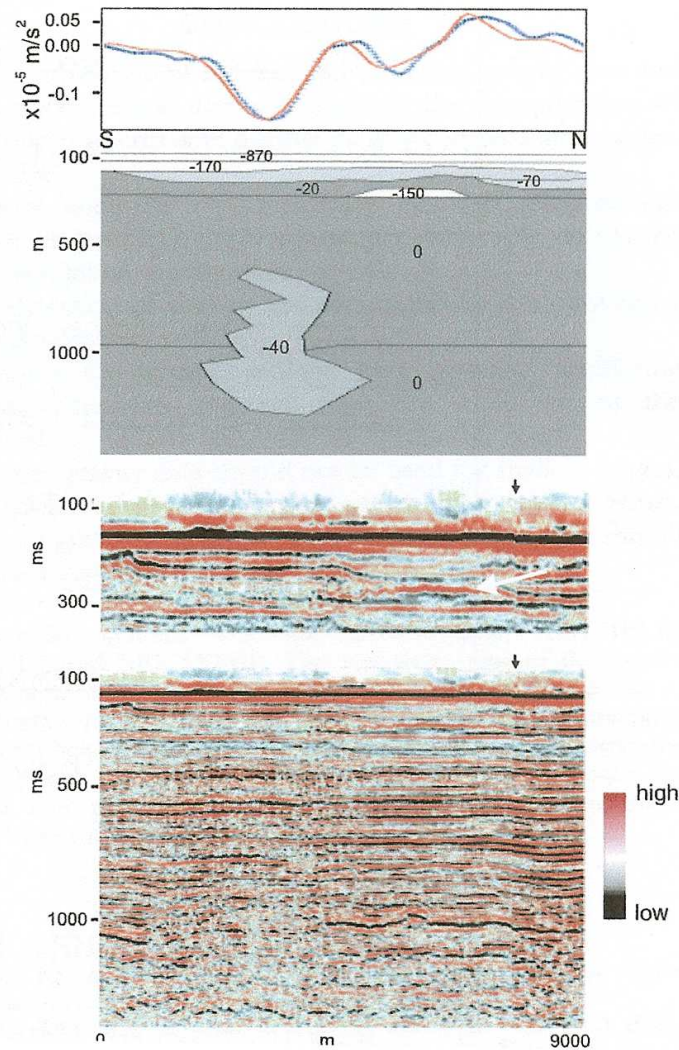


Figure 3.28 Observed (crosses) and calculated (continuous line) free-air gravity anomaly based on the geologic model with density contrasts in kg/m^3 in the central North Sea. The gas chimney modeled with a -40 kg/m^3 density contrast (light gray) has an anomaly of -0.15 mGal ($1 \text{ mGal} = 10^{-5} \text{ m/sec}^2$) and is suggested in the seismic data by the strong negative amplitude reflection off the top of the chimney. Adapted from Bauer and Fichler (2002).

Corporation in Kalkaska County, Michigan, U.S. shown in Figure 3.29. The FDC and borehole gravity logs indicate a potential productive zone from

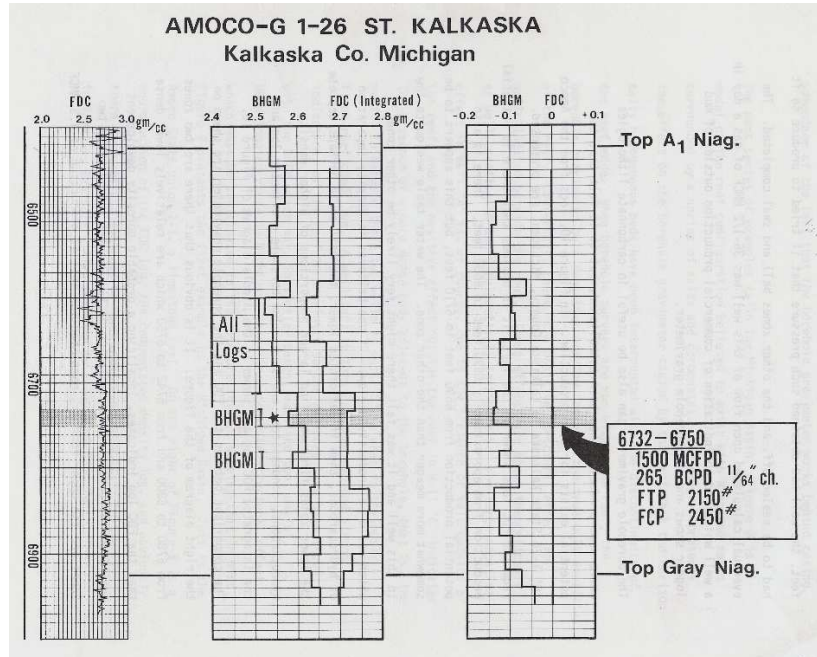


Figure 3.29 Compensated formation density (FDC) log and borehole gravity (BHG) log through a Niagaran reef in the Michigan Basin, U.S. The difference between the logs shown on the right indicates a potentially productive oil and gas zone between 6,732 and 6,750 feet which upon development led to gas production of 1.5 MMCFPD and 265 BCPD. Adapted from Bradley (1974).

about 6,590 to 6,710 feet which was developed, but the difference between these two logs shown on the right indicates other *hidden* zones between 6,732 and 6,750 feet and 6,780 and 6,800 feet. The upper zone was perforated and completed with an initial production of 1.5 MMCF of gas per day and 265 BCPD showing the utility of combined borehole gravity measurements with the traditional density logs in enhancing well productivity. Borehole gravity measurements as shown for example by Schultz (1989) may have additional uses in developing hydrocarbon wells as in monitoring fluid or gas movement in reservoirs adjacent to the measured wells.

Interest has developed in time-lapse or *4D* gravity using surface measurements made over a breadth of time to monitor changes in hydrocarbon reservoirs as a result of density variations in the fluids/gases filling the reservoir pore space. High precision measurements have been made with relative and absolute gravimeters that show a repeatability of the order of $5 \mu\text{Gal}$ and a total error budget of roughly $12 \mu\text{Gal}$ over the Prudhoe Bay reser-

voir, Alaska, U.S. (Ferguson et al., 2007). Theoretical modeling shows that progress of a gas cap waterflooded in the Prudhoe Bay reservoir at a depth of ≈ 2.5 km should produce changes of $100 \mu\text{Gal}$ after 5 years of flooding (Hare et al., 1999), and thus should be mappable by time-lapse gravity.

Eiken et al. (2004) report on the use of time-lapse ocean bottom gravity measurements over the Troll gas field in the North Sea that attain a repeatability as measured by the standard deviation of $4 \mu\text{Gal}$. These measurements are useful in mapping the water influx as the gas is drained from the field, perhaps to a resolution of the order of $1 - 2$ m. Additional numerical experiments indicate that high-sensitivity 3D full tensor gravity gradiometry (Droujinine et al., 2007) should be useful in applications including direct monitoring of a gas/oil contact and temperature front expansion during steam injection in heavy-oil reservoirs at shallow and moderate depths. Time-lapse gravity also has potential application to monitoring the subsurface plume of CO_2 injected into subsurface reservoirs at sequestration sites (Sherlock et al., 2006). In many applications surface gravity measurements are incapable of mapping the change in the gravity signal due to modifications in the reservoir because of the depth of the source, the density contrast, and amplitude of the various noise sources. As a result consideration has been given to measuring the change in gravity at depth using borehole gravimeters [e.g., Gasperikova and Hoversten (2006)] because the decreased distance to the reservoir will significantly increase the signal, permitting the mapping of the time variation in the reservoir.

3.4 Coal Exploration and Exploitation

Coal is an important energy resource in many regions, especially as fuel for stationary electrical power plants. Most of the world's resources of coal in its various forms are reasonably well known. None-the-less in some remote areas, the specific location of coal deposits, particularly in the near surface where they can be readily exploited by surface mining, is still an objective of resource exploration. Furthermore, studies of underground coal strata are conducted to aid in planning mining activities of known coal deposits and detecting hazards that may exist as a result of past underground mining of coal. The occurrence of coal beds within sections of sedimentary strata of modest structural complexity makes the seismic reflection method the optimum geophysical technique in their exploration and exploitation. However, under specialized circumstances gravity and magnetic methods can also be useful in coal exploration and exploitation.

Interpretation of gravity and magnetic anomaly data may provide valu-

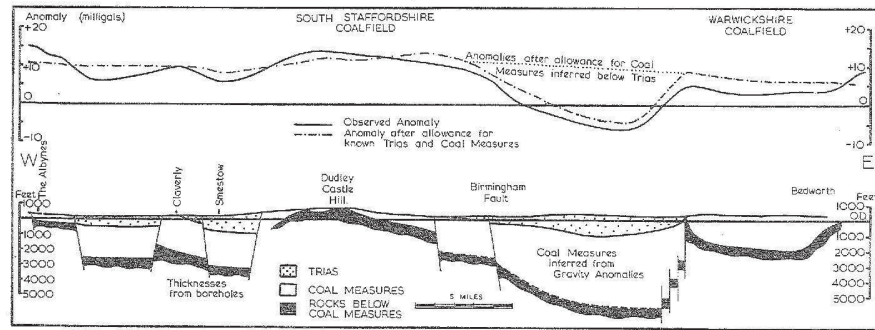


Figure 3.30 Gravity mapping of coal measures in West Midlands, England (Cook et al., 1951). Bouguer gravity anomalies (top) in mGal with the profile (dot-dashed line) modeled by the crustal cross-section shown at the bottom. The black-shaded units in the cross-section are Silurian and Cambrian strata that underlie the inferred coal measures. Adapted from Parasnis (1979).

able insight into the structure of sedimentary basins that can prove useful in exploration for and exploitation of coal deposits in much the same way they are used in studies of hydrocarbon fields. They may be used either directly through the physical property contrasts between the sedimentary rocks and the enclosing basement or indirectly as a result of mapping basement structures, particularly faults, that are reactivated subsequent to development of the basins [e.g., Lyatsky (2000)]. Faults are especially important to identify and map because of their possible relationship to lithofacies variations within the sedimentary rocks and their potential to cause difficulties in coal mining.

Figure 3.30 gives an example of using Bouguer gravity anomalies to infer the distribution of coal measures within Triassic marls and sandstones of West Midlands, England (Cook et al., 1951). Figure 3.30.A shows a map of the anomalies obtained on extensively faulted, generally flat-lying strata that outcrop in the Arden forest and between the Wyre forest and South Staffordshire coalfields. The thicknesses and densities of the surface rocks and underlying coal are known at numerous locations so that their gravity effects are well constrained and may be compared with the Bouguer anomalies at the other locations to establish effective coal thickness estimates. Figure 3.30.B shows profiles of the Bouguer anomalies (solid line) and the modeled gravity anomalies (dot-dashed line) after adjustment for the known geology along the profile from Albynes to Bedworth in Figure 3.30.A. The relative minima in the anomalies east of the Birmingham fault

may be interpreted for the thickness variations of coal measures in the underlying cross-section that include the roughly 4,000-foot deposit beneath Trias cover.

The availability of gravity modeling constraints on the detailed spatial variations of the measures from outcrops and drilling greatly facilitated the gravity mapping of the West Midlands' coal measures. However, where these detailed constraints are lacking, coal deposits are usually not attractive targets for gravity surveys because their density contrasts with the surrounding sedimentary rocks are typically low. The corresponding magnetic property contrasts also are relatively low and limit the role of magnetics in coal exploration.

The presence of coal burns, however, is a notable exception because the associated heat significantly modifies the magnetic properties of coal and commonly those of the surrounding sedimentary rocks. Coal burns may be initiated by spontaneous combustion of pyrite or underground and surface fires. Some coal fires have been burning for thousands of years, destroying a useful resource, and emitting great volumes of carbon dioxide into the atmosphere. Notable examples are found in western North America and Asia.

Thermal metamorphism associated with coal burns results in a range of magnetic minerals in the burnt rocks (clinkers) depending on among other factors their original composition, maximum temperature attained during burning, and the oxidation state [e.g., Cosca et al. (1989)]. Common magnetic minerals produced are magnetite, hematite, and maghemite [e.g., Cisowski and Fuller (1987); de Boer et al. (2001)]. As a result burning of coal produces a strong increase in the natural remanent magnetization and magnetic susceptibility of the burned rocks. de Boer et al. (2001) cite natural remanent magnetizations in the range of 0.1 to 10 A/m and magnetic susceptibilities of 100×10^{-4} to $1,000 \times 10^{-4}$ SIu for these rocks which are several orders of magnitude greater than the original rocks. These magnetizations lead to intense magnetic anomalies of the order of thousands of nanoteslas at the surface and observable anomalies from airborne platforms. Gay and Hawley (1991) describe several coal burns associated with the Cretaceous Straight Cliffs formation in Utah, U.S. from magnetic anomalies of the order of a few tens of nanoteslas in amplitude observed at terrain clearances of 1,000 to 1,500 feet (Figure 3.31). These magnetic anomalies may be useful in exploration for coal, identifying coal fires that should be put out, and isolating zones of potential surface subsidence associated with the removal of coal seams by combustion.

Coal burns may lead to voids in the subsurface that are potentially subject

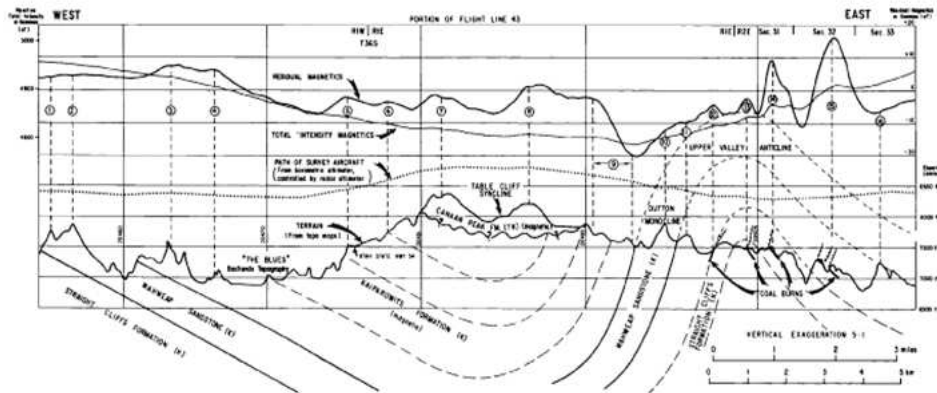


Figure 3.31 Magnetic/topographic/geologic profile across a portion of the Kaiparowits Plateau, Utah, U.S. Note the residual magnetic anomalies derived from a smooth profile through the observed magnetic anomaly that correlate with the coal burns of the Cretaceous (K) Straight Cliffs formation in the right portion of the figure. Adapted from Gay and Hawley (1991).

to subsidence that reaches through to the surface. Subsidence of other voids due to mining of coal seams is also a potential surface hazard. Detection of these voids is important to hazard mitigation where accurate mining maps are unavailable or where the voids are due to burns. Magnetic mapping of voids is impractical considering the low magnetization of coal and the shape and volume of the voids except where the void is related to burns. Coal burn voids are indicated by anomalies associated with thermal metamorphism of the adjacent sedimentary rocks.

In contrast, the gravity method is potentially useful in mapping voids due to removal of coal seams regardless of the cause of this removal. The density contrast between an air-filled void and the surrounding sedimentary rocks is particularly intense, but even where the void is water filled, a marked density contrast will exist. The gravity method has a long and useful history of mapping subsurface voids (see Chapter 14 and Chapter 1 of the website) and several case histories evidence the practicality of mapping coal voids in the subsurface [e.g. Lyness (1985)]. However, the amplitude of the gravity anomalies is small, usually only at most several tenths of a milligal. This requires great care in the observation and reduction of the gravity data to isolate void anomalies and even then the shape of the void and its limited volume make the associated gravity anomalies difficult to observe in the anomaly field [e.g., Miller (1988)].

3.5 Geothermal Exploration and Exploitation

Geothermal resources are increasingly used worldwide for electrical power and direct applications such as space heating [e.g., Bertani (2005); Lund et al. (2005)]. Approximately 25 countries now use geothermal resources as part of their energy mix with Italy, Mexico, Indonesia, and the U.S. among those with the highest production. Geothermal sources occur in numerous geological environments. They include convective vapor (steam) and hot water systems driven by heat emanating from magma chambers or by heating of waters circulating to depths in faults, fracture, and sedimentary aquifers where they are exposed to high temperatures by abnormally high temperature gradients. As a result of the diverse conditions numerous geophysical methods have been used for exploring and exploiting this natural resource. Thermal and electrical methods have been particularly useful in a variety of geological terranes [e.g., Wright et al. (1985)], but gravity and magnetic methods have an important secondary role in both regional and detailed exploration and in evaluating geothermal systems.

Regional magnetic anomaly data have been used to map the depth to the Curie point within the earth. At the Curie point temperature, spontaneous magnetization of minerals vanish, thus by mapping the bottom of magnetic sources in the lithosphere it is possible to estimate the depth to this temperature. The Curie temperature of magnetic minerals vary with composition, but is generally assumed to be of the order of 580°C , the Curie point temperature of magnetite. Regions of decreased depth to the Curie temperature are thus fertile areas for the existence of exploitable, shallow geothermal resources. Unfortunately, the inversion of magnetic anomaly data to bottom depths of magnetic sources is difficult because of the low amplitude and long wavelength of the signature of the bottom of the sources and requires numerous assumptions (Blakely, 1988). Inversion is performed either by determining the shape of isolated magnetic anomalies or by evaluating the statistical properties of the power density spectrum of patterns of magnetic anomalies within a specified region. Both methods have their advantages, but the latter is the preferred method in most recent studies largely because of the problems in isolating anomalies of individual sources in the former.

Curie isotherm mapping has been used over extensive regions [e.g., Okubo et al. (1985); Blakely (1988); Ross et al. (2006)] using analyses of the power density spectra of overlapping regions. The results of the study of California (Ross et al., 2006) are generally confirmed by direct geothermal measurements and related geophysical phenomena. Bhattacharyya and Leu (1975) have used analysis of individual magnetic sources mapped by low-pass filter-

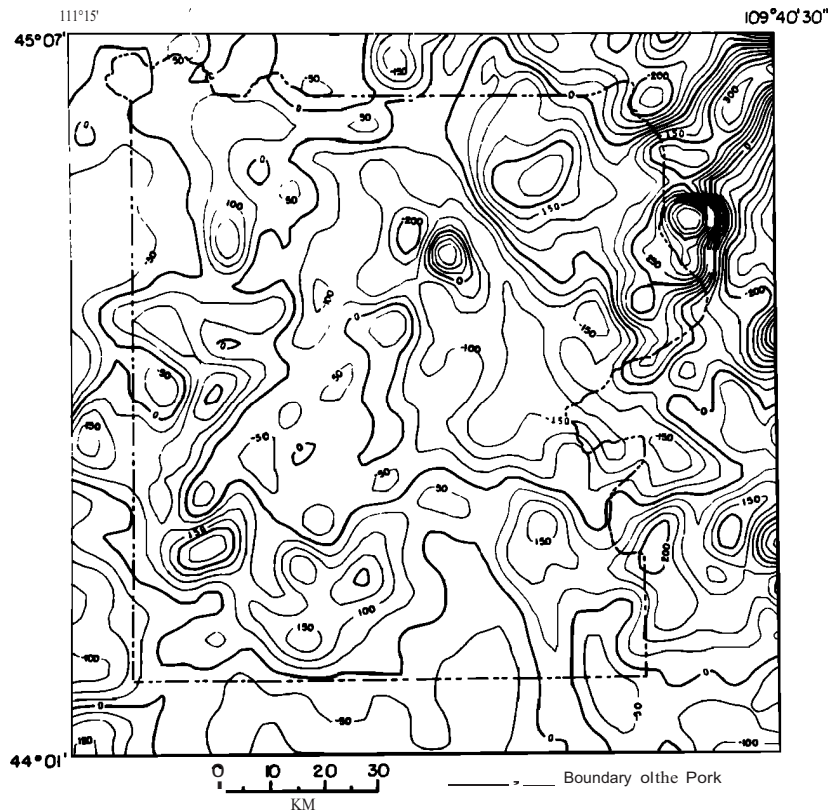


Figure 3.32 Filtered magnetic anomaly map of the Yellowstone National Park, U.S. region passing wavelengths greater than 10 km. The contour interval is 50 nT. Adapted from Bhattacharyya and Leu (1975).

ing of an aeromagnetic survey of the Yellowstone National Park, U.S. (Figure 3.32). Their results shown in Figure 3.33 reveal shallow Curie temperature isotherms (5 – 6 km) associated with the central part of the Yellowstone caldera with narrow extensions to the southwest and east.

Both gravity and magnetic anomaly data have been used to investigate the geologic formations and structure of a variety of terranes that are potential systems for developing geothermal resources. These include mapping magma bodies, faults and other structural disturbances of both igneous and sedimentary terranes, and igneous plutons. The latter are of interest as *hot dry rock* resources because of their remaining original heat or heating by decay of radioactive minerals. Massive hot dry rocks can be hydrofractured by inserting water into the hot rocks under pressure. The fractures can be

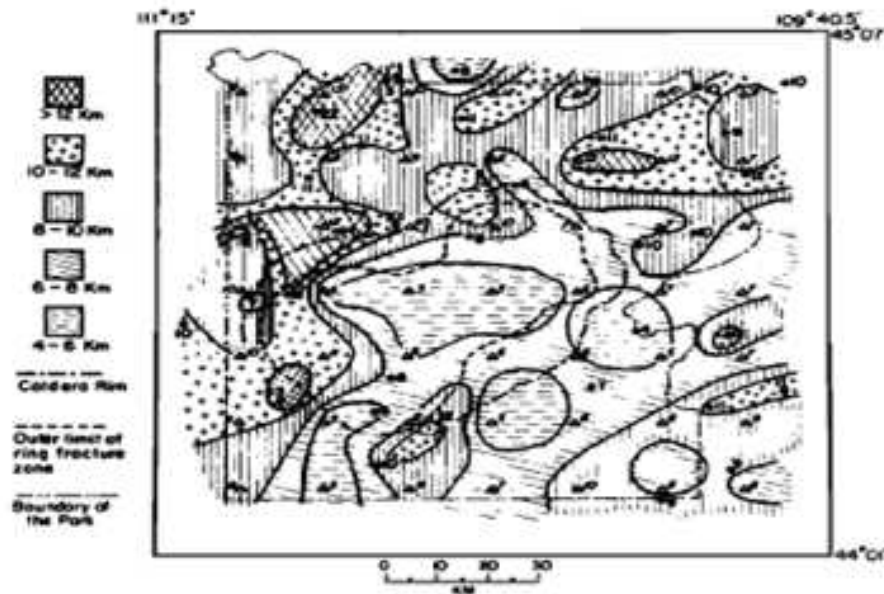


Figure 3.33 Contour depths of the Curie temperature isotherm from analysis of Figure 3.32. The contour interval is 5 km. Note the location of the rise in the isotherms in the center of the Yellowstone caldera. Adapted from Bhattacharyya and Leu (1975).

used in a closed water system to bring hot waters to the surface for direct exploitation.

The wide variety of geological terranes and sources of geothermal systems lead to a broad array of associated anomalies. For example, gravity lows are often related to radioactive-rich plutons and hydrothermally altered rocks, while positive anomalies may be related to deposition of minerals by circulating hot waters filling void spaces and structural highs related to intruded magma. Figure 3.34 shows the results of a gravity survey in the Tertiary Rio Grande Rift in New Mexico, U.S. In this figure, which is the residual gravity obtained by subtracting the 3rd order polynomial from the Bouguer gravity anomaly, a gravity high is associated with the region of high heat flow that isolates the McGregor geothermal system. The high that is related to a basement structural rise in the Rift corroborated by a seismic reflection study is believed to originate in the uplift associated with the intrusion of an underlying laccolith.

Generally magnetic lows are associated with geothermal systems by virtue of destruction of magnetic minerals and remanent magnetization by the high

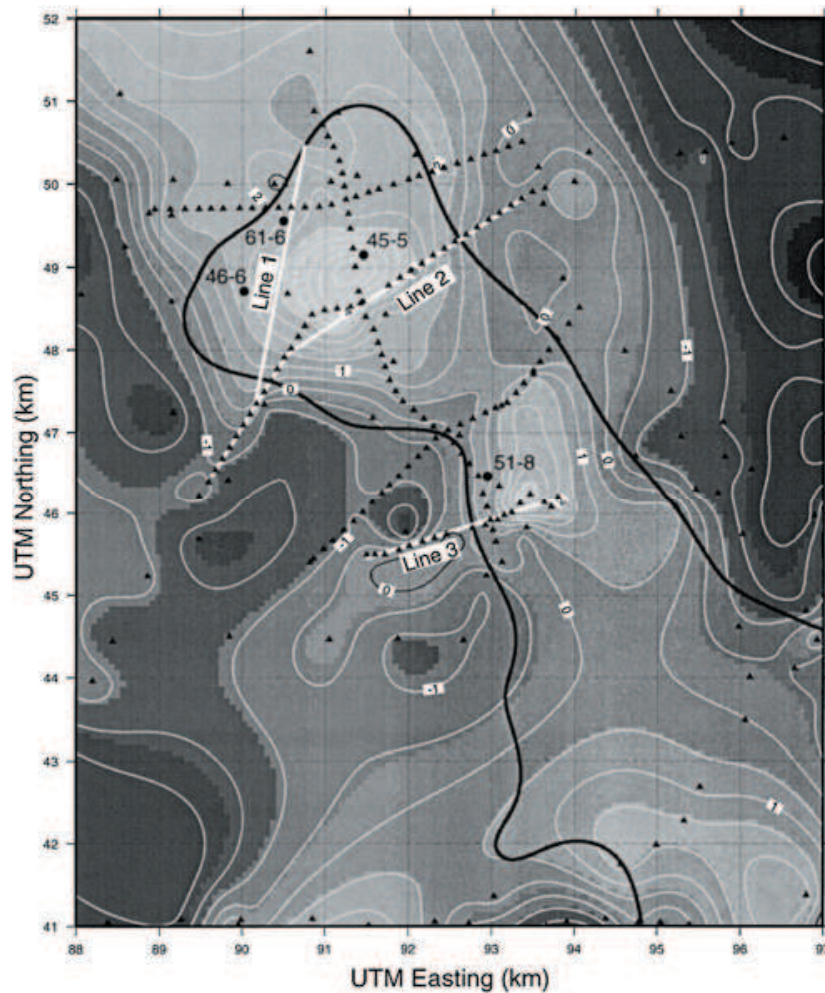


Figure 3.34 Residual gravity anomaly map created by removing a best fitting third-order polynomial surface from the Bouguer gravity anomaly to remove regional effects. The contour interval is 0.5 mGal. Triangles are gravity stations, large black circles are wells, thick white lines are seismic lines, and the thick black line is the 400 mW/m² heat flow contour outlining the McGregor geothermal system in the Rio Grande Rift in New Mexico, U.S. The gravity high coincides with the heat flow high. Adapted from O'Donnell et al. (2001).

temperatures and circulating hot waters, but magnetic highs may be found on the periphery of geothermal systems as a result of deposition of magnetic minerals and associated with some radioactive-rich plutons. A useful example of a magnetic anomaly minimum (Figure 3.35) associated with hy-

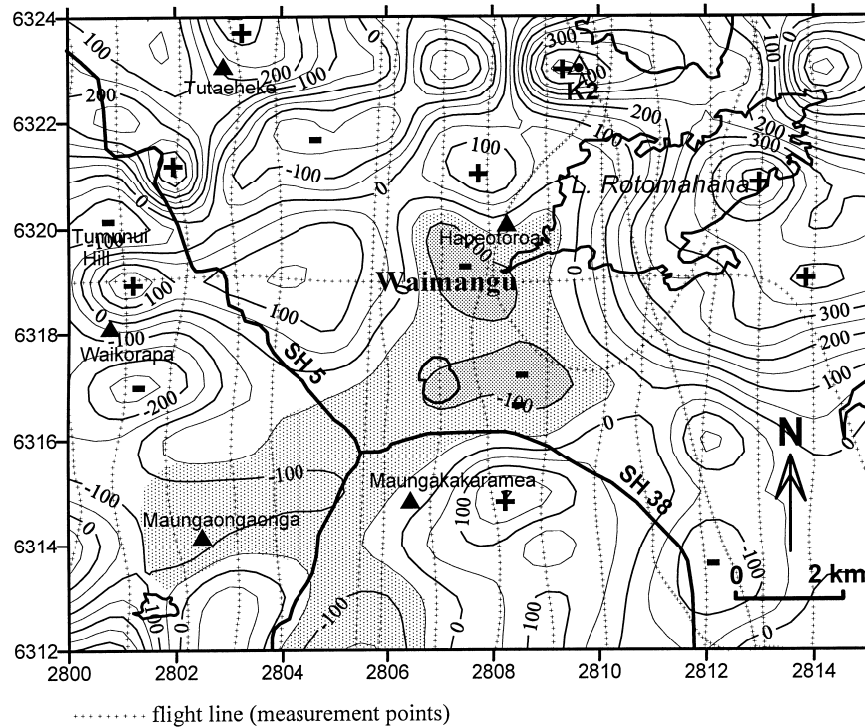


Figure 3.35 Total field magnetic anomaly map of the Waimangu geothermal region on the North Island of New Zealand. The minimum associated with the geothermal area is shaded in the figure. The contour interval is 50 nT. Adapted from Soengkono (2001).

drothermally altered volcanic rocks is presented by Soengkono (2001) over the Waimangu geothermal area of the North Island of New Zealand. In this case, the magnetic minimum is believed to result from alteration of magnetite in the country rocks to an essentially non-magnetic mineral by circulating hot waters. The minimum shown by the shaded area in the figure correlates with other evidence of the presence of circulating hot waters.

Both gravity highs and lows have been observed over geothermal systems as a function of the density of the host rock and the maturity of the geothermal system. As pointed out by Williams (1997) early in the history of the system, fracture porosity and clays are formed in the generally volcanic host rocks leading to a decrease in density of the rock resulting in negative gravity anomalies. Later as the rocks of the geothermal system cool they are flooded by silica and calcite resulting in densification of the rocks and po-

tential positive gravity anomalies as observed in the Imperial Valley and Salton Trough, California.

High-precision repeat gravity measurements have been successfully employed to study the subsurface effects of exploitation of geothermal systems. Typically, these measurements indicate anomalies of the order of several hundreds of microgals with standard errors in the ten microgal range. Gravity effects from the mass changes in the subsurface must be isolated from the repeat measurement variations caused by surface subsidence due to withdrawal of fluids from the system. Precision evaluation of the subsidence effect must consider changes in the vertical gradient of gravity over the survey area (Hunt et al., 2002). Both positive and negative gravity changes have been observed over New Zealand geothermal reservoirs. Negative gravity changes of up to 1,000 μGal have been mapped over the production area of Wairakei geothermal field (Allis and Hunt, 1986) due to deep liquid pressure draw-down resulting in a steam zone, changes in saturation in the steam zone, and groundwater level variations. In contrast, at the Rotokawa geothermal field in which the water production has been reinjected into the field, positive gravity effects are observed in the repeat measurements (Hunt and Bowyer, 2007) as a result of liquid resaturation of near-surface parts of the system.

Applications to Lithospheric Studies

4.1 Overview

The crust and upper mantle make up the lithosphere with notable variations in density and magnetization. Accordingly, the gravity and magnetic methods have a rich history and important uses today in studying the nature, composition, and structure of the Earth. This is particularly true in the crystalline portion of the lithosphere where structural deformation and intrusive events are more likely to result in near vertical contacts between rocks of varying physical property contrast than exist in the largely near horizontal layering of the overlying sediments and sedimentary rocks. These near vertical contacts lend themselves to producing much more identifiable gravity and magnetic anomalies than do horizontal interfaces.

Large regional geologic features produce relatively intense and readily mapped and identified gravity anomalies. Thus, historically, gravity anomalies have been used to map continental and sub-continental scale geologic structures, such as orogens, sedimentary basins, and intrusive complexes, despite less sensitive measurements made at wide spacing that were dictated by the limits of historic instrumentation. Significant advances in gravity data acquisition in terms of sensitivity and the use of marine, airborne, and satellite platforms as well as in anomaly processing have made it possible to investigate ever smaller and more detailed geological features and achieve dense coverage over regions not favorable for ground-based, dense measurement networks. Furthermore, these investigations are being made efficiently and effectively using gradient and tensor observations as well as vertical acceleration measurements. As a result, new applications have opened up for gravity investigations which include more detailed studies of individual geologic features.

In contrast the early magnetic investigations were largely limited to detailed studies of localized geologic features, but with the increasing sensitivity

of magnetic instrumentation particularly in shipborne, airborne, and satellite platforms and major improvements in processing of the data, there has been an increasing number of applications of the method to regional studies. These regional studies have made it possible in marine and airborne measurements to map detailed features over broad regions of the Earth. This is particularly advantageous because of the high resolution obtainable from magnetic measurements especially when using measurements of gradients and tensors. As a result, for example, magnetic mapping of the oceanic crust from both ships and aircraft have observed the magnetic lineations and their disruptions that were the prime driver in developing the plate tectonics paradigm and deciphering the history of the oceans and their interaction with the continents. Furthermore, these regional magnetic studies have found significant applications in mapping ancient crustal sutures, individual igneous plutons, faults, volcanoes, ancient impact structures, and a broad variety of other structures and geologic terrains that have had a marked impact on our knowledge of the makeup of the Earth, its history, and geologic processes.

In addition, satellite surveys have mapped the global gravity and magnetic fields of the Earth, Moon, Mars and other mass-differentiated planets that facilitate studies of lithospheric processes across the solar system.

4.2 Introduction

Gravity and magnetic studies have had a broad and distinguished role in investigating the nature and processes of the Earth's crust and uppermost mantle that make up the lithosphere. The lithosphere is the rigid outer layer of the earth which overlies the mobile asthenosphere. It is not a petrologic boundary, but rather is the lower limit of the relatively strong outer shell of the Earth which differs in thickness between oceanic and continental plates [e.g., see Fig. 1.1]. Along the axis of the mid-ocean ridges it may be as thin as the crust, but generally in the oceans it is from 50 to 100 km thick. In the continental regions it typically is thicker, ranging from 100 to 200 km. This zone preserves the history of the Earth processes, both the products of and the structural results of asthenospheric movements and thermal perturbations resulting in interaction with the overlying plates and the processes of erosion of the plates and the sedimentation of the detritus resulting from erosion. Accordingly, geologists study the nature of the lithosphere, its petrology, structure, and processes to decipher the Earth's history. The limited deep drilling and widespread surficial cover of sediments derived from erosion as well as terrestrial waters make it necessary to remotely sense the nature of the lithosphere.

The scale of lithospheric applications includes all geologic and geophysical investigations that are not considered as part of resource investigations and studies of the near-surface for engineering, environmental, and archaeological purposes. As a result the scale of these studies varies greatly, from the fine structure and properties of sedimentary basins to continental and oceanic plates.

Gravity methods were initially used to investigate the isostatic state of the Earth based on a relatively few, widely spaced observations. Then beginning in the first half of the 20th century and especially after World War II, advances in gravity instrumentation for both land and marine observations allowed the gravity method to be applied to studies of a wide range of lithospheric features. More recently the advent of airborne and satellite observations have opened up new vistas for the gravity investigation of the lithosphere. The method is based on observing the spatial or temporal change in gravity. Spatial changes in gravity are based on horizontal changes in the mass of the lithosphere as a result of lateral changes in density brought about by structural, lithologic and thermal changes. Temporal changes are largely based on changing fluid content within relatively near-surface rocks which cause mass variations.

Although observations of the spatial variation in the magnetic field of the Earth have been made for centuries, they were largely restricted to areally-limited studies for resource exploration until the advent of airborne magnetometry after World War II. Airborne and related marine magnetic observations have opened up the use of the magnetic method to regional studies useful in mapping the lithosphere. Today this mapping supplemented with satellite measurements have made it possible to map the magnetic field of the entire earth in useful detail. Mapping of the magnetic stripping in the ocean basins has been particularly important because it is recognized as providing the critical information that has led to the theory of plate tectonics which has synthesized a wide range of geological observations and theories into a coherent view of Earth processes. As in the gravity method, spatial magnetic observations are primarily focused on horizontal variations in the magnetization of the earth, particularly on near vertical contrasts. As a result both the gravity and magnetic methods complement seismic and electrical methods of investigating the Earth which are largely focused on mapping horizontal variations in rock properties, rather than vertical variations.

The interpretation of both gravity and magnetic anomaly data are problematic because of the inherent ambiguity of the methods, that is anomalies cannot be identified with a unique source without collateral information.

As a result successful gravity and magnetic anomaly interpretation involves constraints placed on the anomalous sources by direct geological information or supplemental geophysical data. Magnetic data are particularly useful in mapping of crystalline geological terranes which commonly include a variety of rock types with a range of magnetizations because of the enhanced resolution of the magnetic method in comparison to the gravity method. Furthermore because of the greater sensitivity to source depth over the gravity method, the magnetic method is particularly useful in mapping the geology of the crystalline rock surface and less capable of mapping the depth extent of the sources. As a result although the gravity and magnetic methods are similar in theory, they each have their particular utility in lithospheric mapping.

In this chapter, examples from the published literature are given of the use of the gravity and magnetic methods in studying the nature and processes of the lithosphere. These are obviously only a limited example of the use of the methods in lithospheric investigations, but they should provide the reader insight into the advantages and limitations of the methods for these types of studies and the possible range of their application.

4.3 Impact Craters and Basins

Numerous craters on the Earth's surface have been generally recognized for the past half century as having an external source due to the impact of meteoroids (asteroids and comets). Similar craters cover the surface of the inner bodies of the Earth's solar system where they have been largely preserved, contrary to the situation on the earth, by the lack of tectonic and surface processes for the past hundreds of millions of years. Many of these craters record an intense period of meteoroid bombardment at approximately 4 Ga, but impacts of these bodies have continued to the present day albeit at a decreasing rate since then.

Increasing interest in craters has developed since the dawn of the space age as an analog to the surface craters of the Moon and the inner planets and as a source of catastrophic effects on the Earth and its environment, and thus potentially their importance on the evolution of the Earth and life on the Earth. Furthermore, there is continuing growth of interest in economic natural resource deposits associated with terrestrial impact structures. Grieve (2005) has described mineral resources such as diamonds, *Cu*, *Ni*, platinum group elements, and base metals that are derived from the actual impacts, as well as subsequent hydrothermal alteration in the fractured rocks. He also points out that roughly 50% of the identified impact

structures in hydrocarbon-bearing sedimentary basins in North America are oil and/or gas reservoirs, and estimates that the value of natural resources taken from impact structures was \$18 billion in 2005. This interest has led to the identification of roughly 180 terrestrial craters ranging in age from 2.4 Ga to the present. By analogy with the flux of meteoroids on the inner planets, this number must represent only a fraction of the impact structures on the Earth. Terrestrial craters have been modified or destroyed by erosion and tectonic activity or are hidden from direct view by water, ice, and later sediments and sedimentary rocks. As a result, the vast majority of identified structures occur on ancient cratons and numerous additional hidden terrestrial impact structures await identification. This is largely the task of geophysical exploration methodologies, especially the gravity and magnetic methods.

Impact craters are produced by the shock wave accompanying the extraterrestrial bodies impacting at hypervelocities of the order of 10s of kilometers per second onto the surface (Melosh, 1989). At impact a tremendous amount of energy is released essentially instantaneously causing the destruction of the meteoroid and excavating a surface crater many times the dimensions of the impactor. In this process, the target rocks are fractured and ejected into the atmosphere and may be melted. Additionally rock formations may be flexed downward and subsequently rebounded above their original stratigraphic level. As a result of these numerous processes, variables in the velocity, composition and size of impactors, and differences in the nature of the target rocks, the morphology and structure of terrestrial impact features are highly varied, but if not modified by subsequent, unrelated tectonism, they are all roughly circular in plan view.

Craters are classified into two broad categories, simple and complex. In their pristine form both consist of a bowl-shaped depression with a narrow uplifted rim which is surrounded by an ejecta blanket that thins away from the crater. The rocks bounding the crater are intensely fractured and brecciated by the shock wave traveling into the Earth. The excavated material is thrown out of the crater by a rarefaction shock wave generated by the impact of the compressional shock wave upon the surface. If the impactor generates sufficient energy a portion of the target rocks may be melted forming lenses within the crater which is covered by ejecta falling back into the depression and sliding of fractured crater walls into the interior of the crater. Simple craters, which have a maximum diameter of 4 km, or less when the target rocks are sedimentary, are limited to a simple depression and have a depth to diameter ratio of 1/5 to 1/7. In craters exceeding this dimension additional processes come into play beyond the excavation of debris from

the crater. Notably among these is the presence of a central high within the crater caused by rebounding of sub-crater rocks that are flexed downward by the shock wave accompanying the impact. Additionally, annular rings of topographic highs may occur within a complex crater as a result of failure of the margins of the crater and slumping into the interior of the depression. The depth to diameter ratio of complex craters (1/10 to 1/20) is less than that of simple craters. Useful recent reviews of the occurrence, origin, and nature of impact craters and a description of several impact structures have been prepared by Plado and Pesonen (2002) and Grieve (2006).

The catalogue of the Earth's 180 known impacts [e.g., <http://www.unb.ca/passc/ImpactDatabase>] is dominated by craters which are classified as circular crustal impact depressions with diameters under 300 km. Larger impact structures are called impact basins of which the only one verified for the Earth is the South African 300-km diameter, ≈ 2.2 Ga Vredefort basin (Carpenter et al., 2005). However, impact basins are prominent crustal features of the Moon [e.g., Spudis (2005)] and Mars [e.g., Schultz and Frey (1990)], where they are commonly characterized by multiringed topography overlain by inversely correlated, ringed satellite gravity anomalies.

4.3.1 Gravity Anomaly Signatures

Localized highly disturbed surface features have long been recognized by geologists as indicative of meteorite impacts. However, it was not until the post-World War II era that it has been generally accepted that many of these, particularly those associated with circular surface depressions (craters), were caused by extra-terrestrial impacts. In addition to evidence related to morphology and structural deformation, critical support for an extra-terrestrial origin of craters has been identified in the micro and macro shock effects in the target rocks. Geophysical investigations, particularly gravity and magnetic methods, have played an important role in mapping the three-dimensional structure of impact craters and in identifying them where they are hidden from direct observation. It is likely that these methods will be even more important in the future in locating new impact structures as the emphasis moves toward identifying impact structures not visible on the surface.

Initially geophysical methods were used in crater investigations to search for buried meteoroids, but when it was realized that the impacting bodies do not survive the collision because they are vaporized or fractured and dispersed around the crater, geophysics was used to study the interior structures of the craters. Gravity and magnetic methods have proven particularly

useful in mapping impact structures because of the strong physical property contrasts associated with craters and the fact that these relatively inexpensive methods can be used for mapping regional-sized areas. However, it is not surprising, in view of the widely varying morphology and structure of terrestrial impact structures, that gravity and magnetic anomaly signatures cover a broad range. Nonetheless, there are generalities in the signatures that are useful in identifying the structures [e.g., Pilkington and Grieve (1992); Grieve and Pilkington (1996); Grieve (2006)].

A gravity minimum is generally associated with impact craters with the amplitude increasing with the diameter of the crater. Typically the minimum reaches a maximum value of approximately -30 mGal over craters with diameters in excess of 30 km. The 65 Ma Chicxulub crater in the Yucatan Peninsula of Mexico which has a diameter of 180 km has an associated -30 mGal gravity anomaly (Figure 4.1), whereas the 50 Ka Barringer (Meteor) Crater of Arizona (Figure 4.2) has a diameter of 1.18 km and only a -0.6 mGal gravity anomaly (Figure 4.3). The negative gravity anomaly is caused by the lower density of the ejecta fall-back and slip-back within the crater, the fracturing of the rocks making up the crater floor, and any sediments subsequently deposited in the crater. If impact melt sheets occur within the crater they too may have a lower density than the surrounding target rocks, thus contributing to the negative anomaly. However, the gravity anomaly is more complicated over complex craters. In this case the central uplift is often marked by a positive anomaly and the central minimum may be disturbed by annular rings. These features are evident in the horizontal gradient gravity anomaly map of the Chicxulub crater (Figure 4.4), which emphasizes density contacts within the crater.

Inversion of the gravity anomaly data by various techniques including comparison of the anomaly from conceptual forward models constrained by morphological, geologic (outcrops and drill holes), and other geophysical data with observed data are used to determine the third dimension of the crater's structure. This is illustrated in (Figure 4.5), which compares the calculated and observed gravity anomaly over the complex 35 Ma Popiai impact structure of Siberia that has a diameter of 100 km. Consideration of geologic controls and petrophysical data has led to an acceptable geologic model for this crater including the surface suevite/tagamite formation consisting of impact related breccias and crystallized melt formations, allogenic breccias, and fractured crater floor that contrast with target rocks consisting of surficial sedimentary rocks overlying Archean basement rocks (Pilkington et al., 2002). The topography of the crater floor reflects an annular ring. This is one of the few studies that has documented in a quantitative way

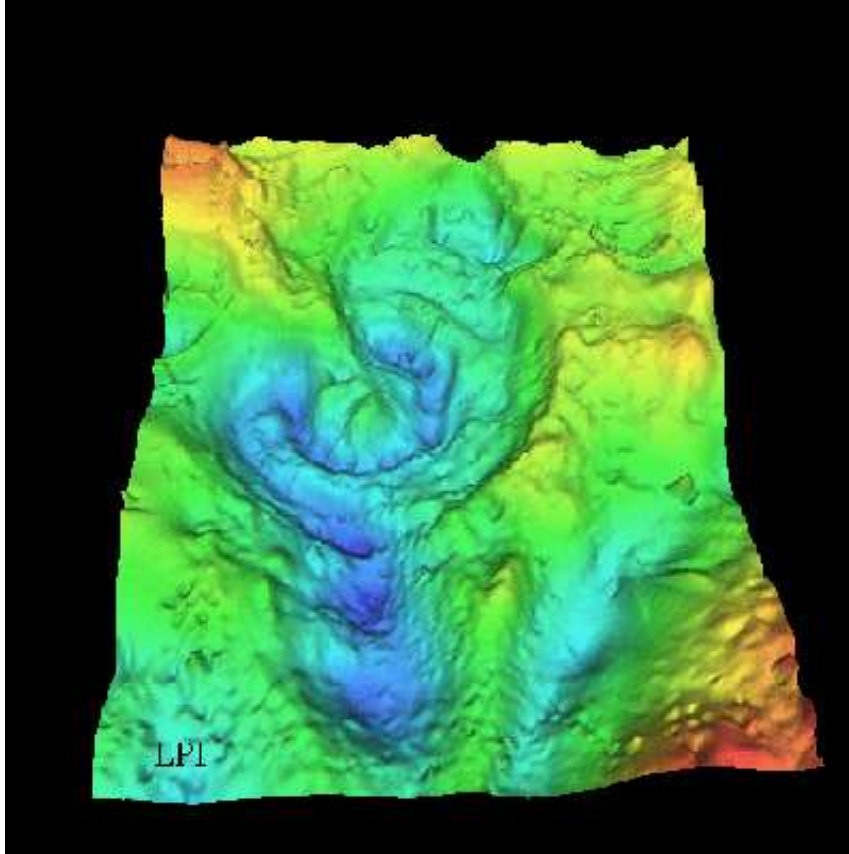


Figure 4.1 Three-dimensional gravity anomaly map of the Chicxulub crater straddling the northwestern shoreline of the Yucatan Peninsula, Mexico. Gravity highs are in red and lows in blue, with north to top of image. Prepared by V. Sharpton, LPI.

the decreased density of the floor of the crater due to fracturing associated with the impact event.

Although a gravity minimum is the typical anomaly over terrestrial impact craters, there are variations from this. For example, a positive anomaly may be associated with structures that have been deeply eroded removing the allogenic breccias, melt lenses, and fractured crater floor. The positive density contrast is due to the upwarping of deeper, higher density rocks in the central uplift of complex craters. Examples are the Upheaval Dome in Utah (Joesting and Plouff, 1958) and the Kentland complex in Indiana (Tudor, 1971).

Impact basins on the Moon and Mars (Figure 4.6), by contrast, are com-



Figure 4.2 Aerial view of the Barringer (Meteor) crater, Arizona looking southwest with horizontal scale centered over the crater. Adapted from Regan and Hinze (1975).

monly overlain by ringed positive satellite gravity anomalies that may be attributed to the effects of uncompensated concentrations of mass produced within the crust from the impact [e.g., Muller and Sjogren (1968); Wise and Yates (1970); von Frese et al. (1997); Potts and von Frese (2003a,b); Potts et al. (2004)]. The central anomaly peak is taken to reflect primarily the enhanced mass concentration or mascon of an uplifted, relatively dense mantle plug that was suspended in the crust when it recoiled from the meteorite impact. In the lunar craters, post-impact basaltic fill or mare also has been inferred to make additional minor contributions to the peak anomalies [e.g., von Frese et al. (1997); Potts and von Frese (2003a,b)]. The flanking negative ring anomaly, on the other hand, can be readily interpreted as the effect of uncompensated crustal thickening around the margin of the impact basin [e.g., von Frese et al. (1997); Potts and von Frese (2003a,b)]. Thus, the strength of the lithosphere is presumed to maintain the higher density

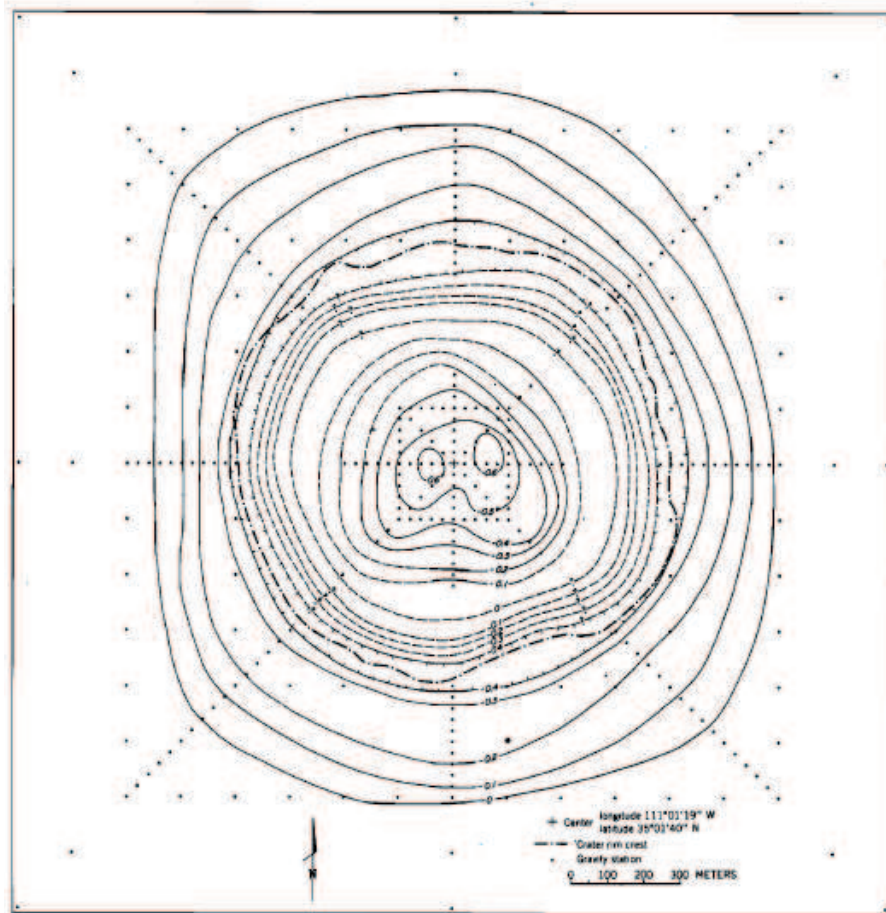


Figure 4.3 Residual Bouguer gravity anomaly map of Barringer (Meteor) crater, Arizona. Contour interval is 0.1 mGal and dashed or queried contours are inferred from gravity models. Dash-dot line marks the rim of the crater. Adapted from Regan and Hinze (1975)].

mascon (and mare fill if any) and the surrounding excessively thickened, lower density crust against isostatic forces to produce the central positive and flanking negative ring anomalies, respectively.

von Frese et al. (2009) noted an analogous inverse correlation between a circular 500-km diameter depression in the subglacial topography of Wilkes Land in East Antarctica and an overlying ringed positive anomaly in the GRACE satellite gravity observations (Figure 4.6) that may mark a giant impact basin beneath 2 – 3 km of glacial ice (von Frese et al., 2009). They relate the impact to the greatest mass extinction of life on Earth at the end

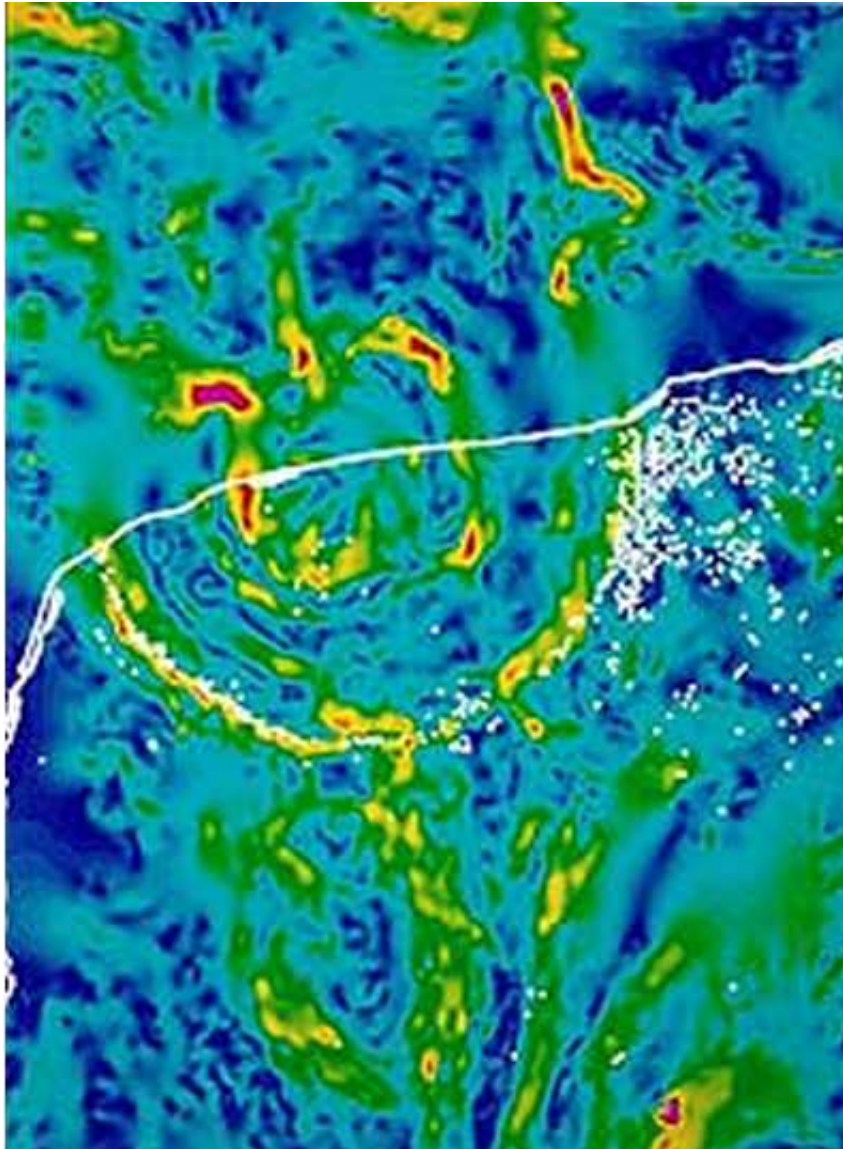


Figure 4.4 Horizontal gravity anomaly gradient map of the Chicxulub crater, straddling the northwestern shoreline of the Yucatan Peninsula, Mexico (white line). Cenotes (sink holes) in the carbonate bedrock are shown by white dots. Courtesy of soundwaves.er.usgs.gov.

of the Permian based on micrometeorite evidence from Graphite Peak in the Transantarctic Mountains, and the impact's striking antipodal relationship to the Siberian Traps in reconstructed P-Tr coordinates that accords with

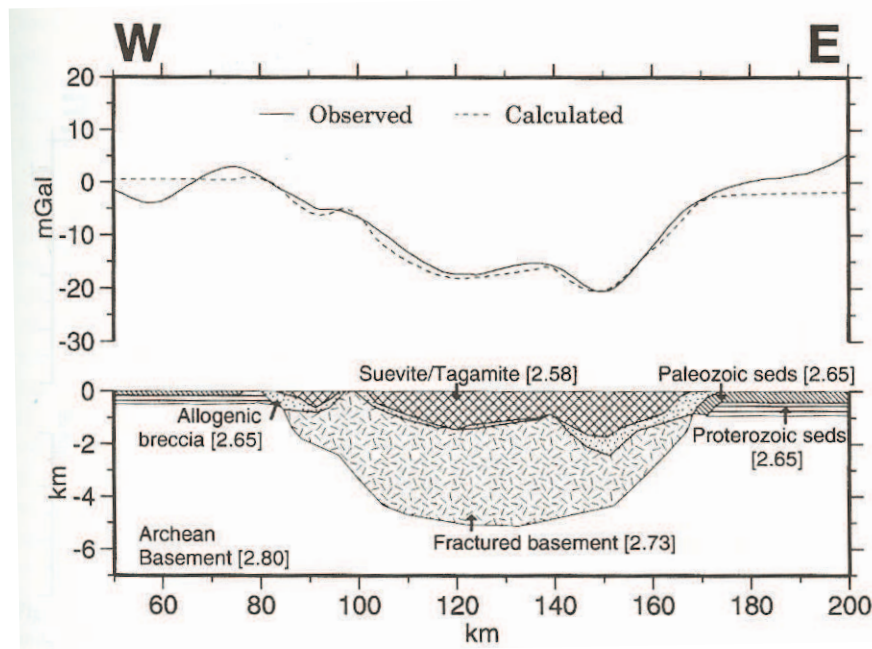


Figure 4.5 Comparison of observed residual and calculated gravity anomalies from the illustrated geological model of the Popigai impact structure of Siberia. Densities are given in units of 10^{-3} kg/m^3 . The allogenic breccia and the impact melt rocks (suevite/tagamite) fill the crater and the extent of the fractured Archean basement rocks caused by the impact is shown. Adapted from Pilkington et al. (2002).

antipodal crustal disturbances of large impacts on the Moon, Mars, and the Earth [see von Frese et al. (2009) and references therein].

4.3.2 Magnetic Anomaly Signatures

Magnetic anomalies over both simple and complex impact craters are typically minima, but these anomalies are even more complex than those associated with gravity anomalies. Numerous impact processes may lead to modification of the magnetization of the target rocks and the crater infill resulting in a variety of types of anomalies and anomalies will differ depending on the depth of erosion at the crater. Also, the magnetic signature is dependent on the types of target rocks. Craters in crystalline rocks which generally have a greater magnetization due to both induced and remanent magnetization are generally more complex than are craters in sedimentary rocks which have significantly lower magnetizations.

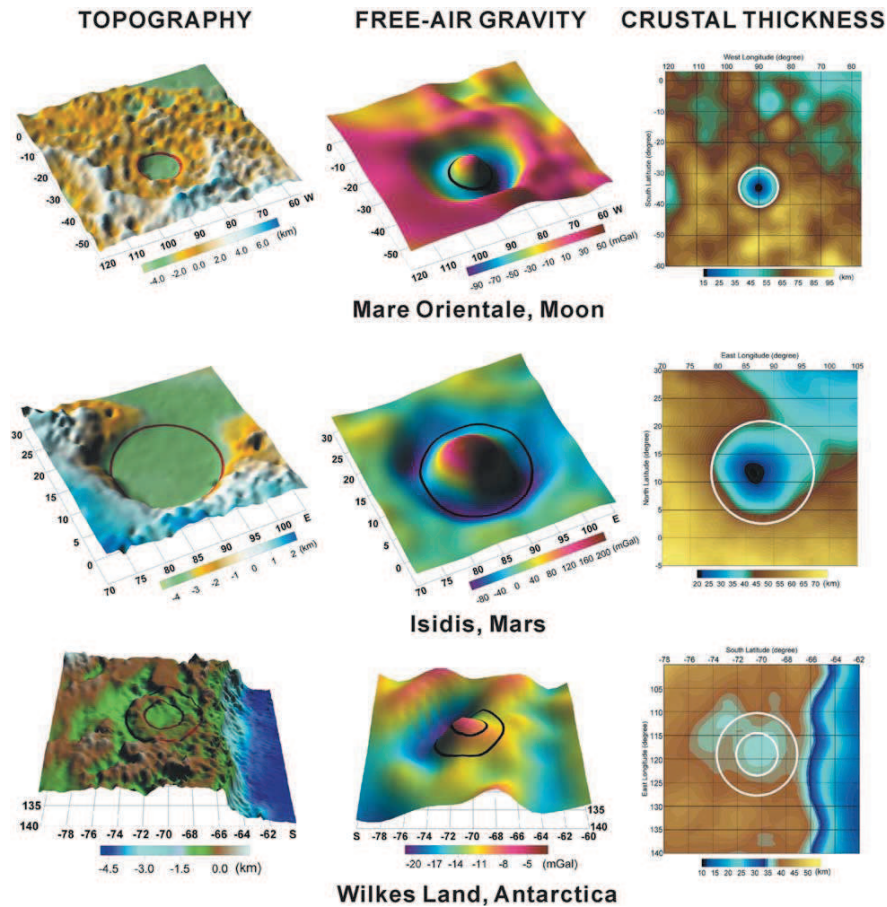


Figure 4.6 Generalized crustal properties for the lunar Mare Orientale basin (von Frese et al., 1997), the Isidis basin of Mars (Potts et al., 2004), and the Wilkes Land impact basin reveal common effects of giant meteorite impact. The lunar and Martian spherical patches list degrees latitude and longitude along the respective left and bottom axes, and vice versa for the Wilkes Land basin of East Antarctica. The circles broadly outline the topographic boundaries of the central basins. Adapted from von Frese et al. (2009).

Magnetic minima over craters in crystalline rocks are believed to be caused by alteration of the crater fill and the surrounding rocks which modifies the magnetic minerals to a non-magnetic form. The magnetic lows are seldom obvious in map form but are observed in smoothing of the anomaly contours and subdued magnetic trends that extend through the anomaly. The subdued anomalies are a result of the greater depth to the crystalline mag-

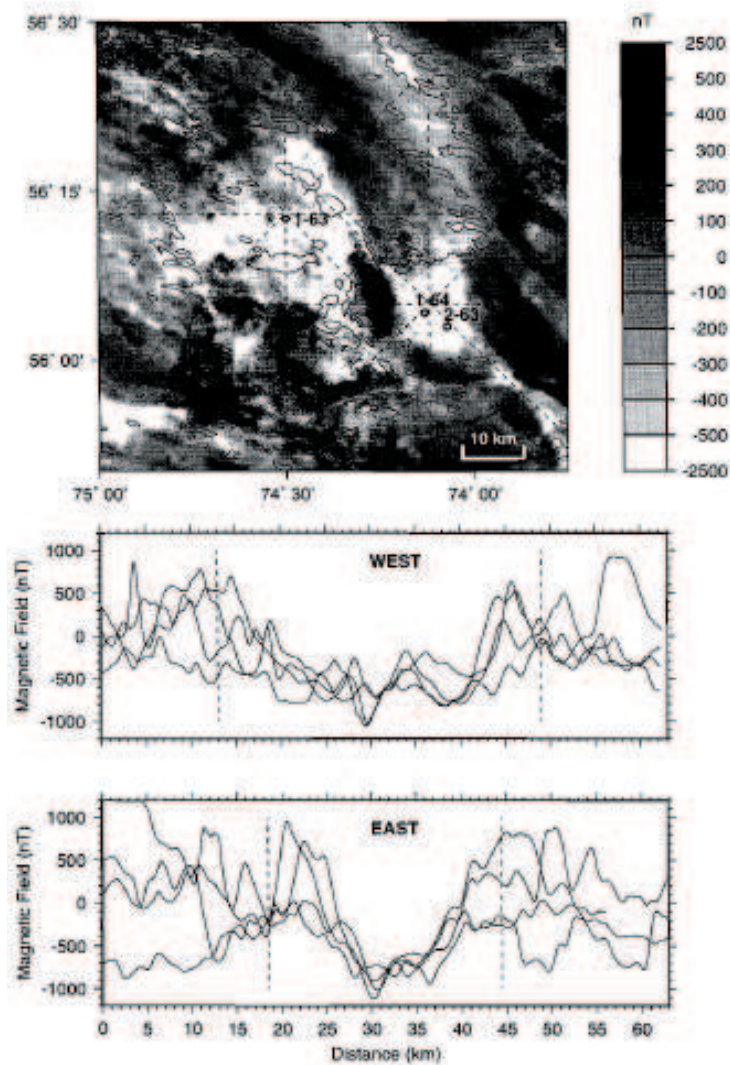


Figure 4.7 (top) Gray shade total magnetic intensity map of the Clearwater impact structures, Canada showing the location of drill holes used to obtain constraining geological and petrophysical data. Dashed lines show positions of magnetic field profiles. (bottom) Reduced to pole magnetic anomaly data along profiles passing through the center of the structures. Vertical dashed lines are the limits of the structures. Adapted from Scott et al. (1997).

netic anomaly sources due to the overlying relatively non-magnetic crater fill. Figure 4.7 shows the total field intensity map of the Clearwater structures within the crystalline rocks of the Canadian Shield in northern Que-

bec. The geophysics of the western-most crater, which is 36 km in diameter, and the eastern 26-km diameter crater are described and analyzed by Scott et al. (1997) and Grieve (2006). The minima associated with both craters attain amplitudes of greater than 500 nT at the observation height of 300 m which are especially evident in the profile form (Figure 4.7). Modeling of the anomalies using rock magnetic data obtained from crater drill core samples indicate that the observed anomalies cannot be satisfied by the lower magnetization of the crater rocks, suggesting that a zone of reduced magnetization occurs in the floor of the crater due to shock demagnetization at the time of the impact (Scott et al., 1997) or alternatively by a decrease in magnetic susceptibility of the floor rocks by hydrothermal alteration. The shock wave associated with the impact may randomize the directions of the remanent magnetization leading to demagnetization. However, it is also possible under extreme shock wave pressures that the directions of the remanance may be aligned in some craters causing an increase in the magnetization and intensity of magnetic anomalies.

In complex craters, Grieve (2006) observes that for crater diameters of less than 10 km the magnetic anomaly is a simple low or a subdued zone, but a central zone of sometimes intense short wavelength anomalies is possible for diameters from 10 to 40 km and probable for diameters greater than 40 km. These central zones which are generally less than a half crater diameter in size may be caused by the magnetic pattern of the rocks of the central uplift or by remanently magnetized impact melt rocks within the crater. These melt rocks have been observed to acquire an intense thermal remanent or chemical magnetization in the direction of the Earth's ambient magnetic field (Grieve and Pilkington, 1996). As a result these anomalies may be either positive or negative depending on the polarity of the Earth's magnetic field when the magnetization was acquired. An example of the magnetic anomalies associated with remanent magnetization of impact melt rocks is shown in Figure 4.8 of the Ries crater in Germany. The central high is due to remanently magnetized impact melt rocks while the positive magnetic anomaly in the southwestern part of the crater is due to a basement mafic rock in the floor of the crater.

The origin of magnetic anomalies associated with craters in sedimentary rocks is more problematic than in the case of those in crystalline rocks [e.g., Ugalda et al. (2005); Hawke et al. (2006)]. The Barringer (Meteor) crater which occurs in sedimentary rocks has a minimum of 20 nT which extends beyond the crater rim (Figure 4.9) while other craters such as the Yallalie impact structure in the Perth Basin of Western Australia have a central high surrounded by sub-circular concentric anomalies (Figure 4.10). The

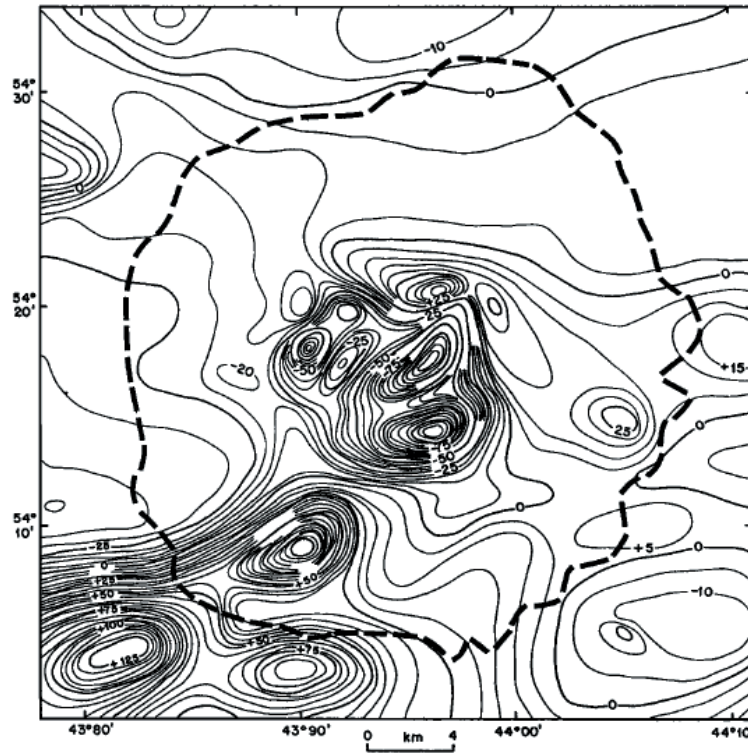


Figure 4.8 Residual total magnetic intensity anomaly map over the Ries crater, Germany [after Pohl et al. (1977)]. Contour interval is 5 nT and the flight elevation of the survey is 1,000 m. Dashed line marks the position of the crater rim. The intense positive magnetic anomaly in the southwestern quadrant is not of impact origin, but rather due to lithologic variations within the basement rocks. Adapted from Pilkington and Grieve (1992).

minimum related to the Barringer crater may be caused by demagnetization of the remanent magnetization of the sedimentary rocks by the impact shock wave (Regan and Hinze, 1975) and the anomalies of the Yallalie structure are related by Hawke et al. (2006) to remanent magnetization of the impact breccia acquired during impact or magnetic minerals formed as a result of impact-related hydrothermal activity in crater floor faults.

The intense magnetic anomalies at the northern shoreline of the Yucatan Peninsula as shown in Figure 4.11 were the first indication of the presence of the Chicxulub crater. This crater which is now buried by approximately a kilometer of Tertiary sedimentary rocks was formed in bedrock of several kilometers of carbonates and evaporites. The sources of the intense magnetic anomalies (> 500 nT) have been the subject of study by several investiga-

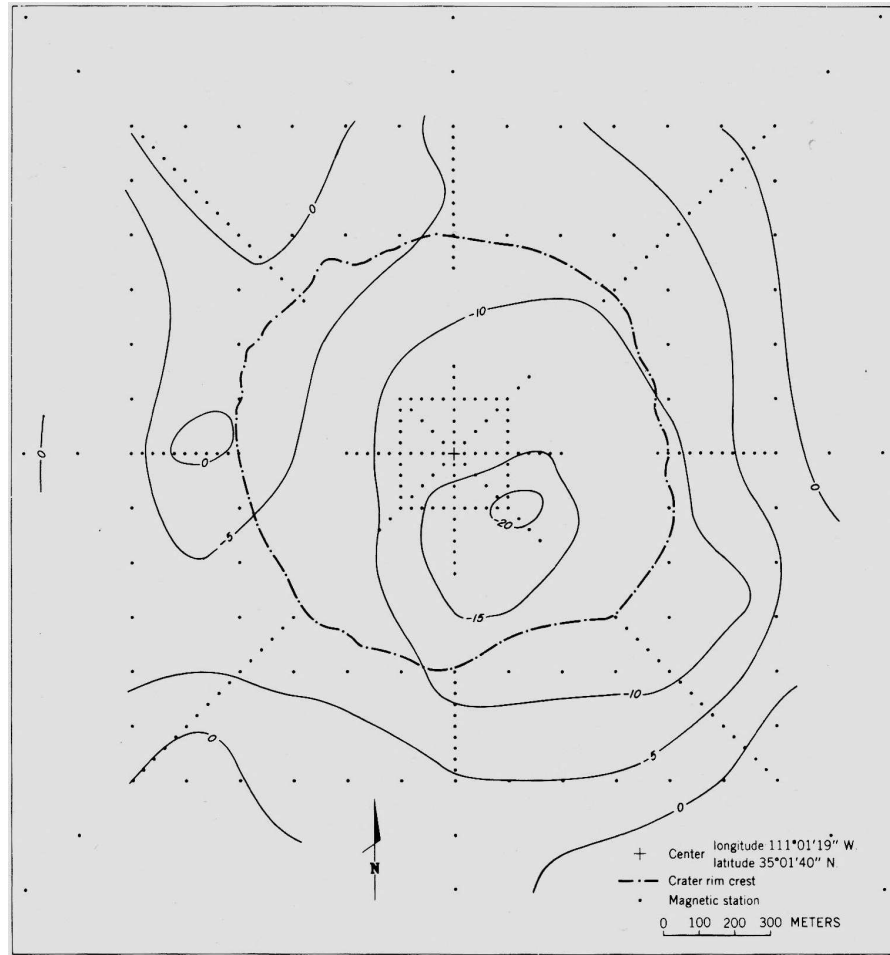


Figure 4.9 Residual vertical magnetic intensity anomaly map over the Barringer (Meteor) crater, Arizona. Contour interval is 5 nT. Dash-dot line marks the rim of the crater. Adapted from Regan and Hinze (1975).

tors. Pilkington and Hildebrand (2000) have modeled the magnetic anomalies using a 3D inversion method on a two layer model. They conclude that an upper layer at a depth of roughly 2 km is associated with crater impact melt zone that produces two generally concentric anomalies at radii of 20 and 45 km localized by the crater structure. Longer wavelength magnetic anomalies within the crater are related to topography on the magnetic crystalline basement at an average depth of about 5 km which is uplifted to a depth of about 3.5 km beneath the roughly 50-km diameter central uplift of the crater.

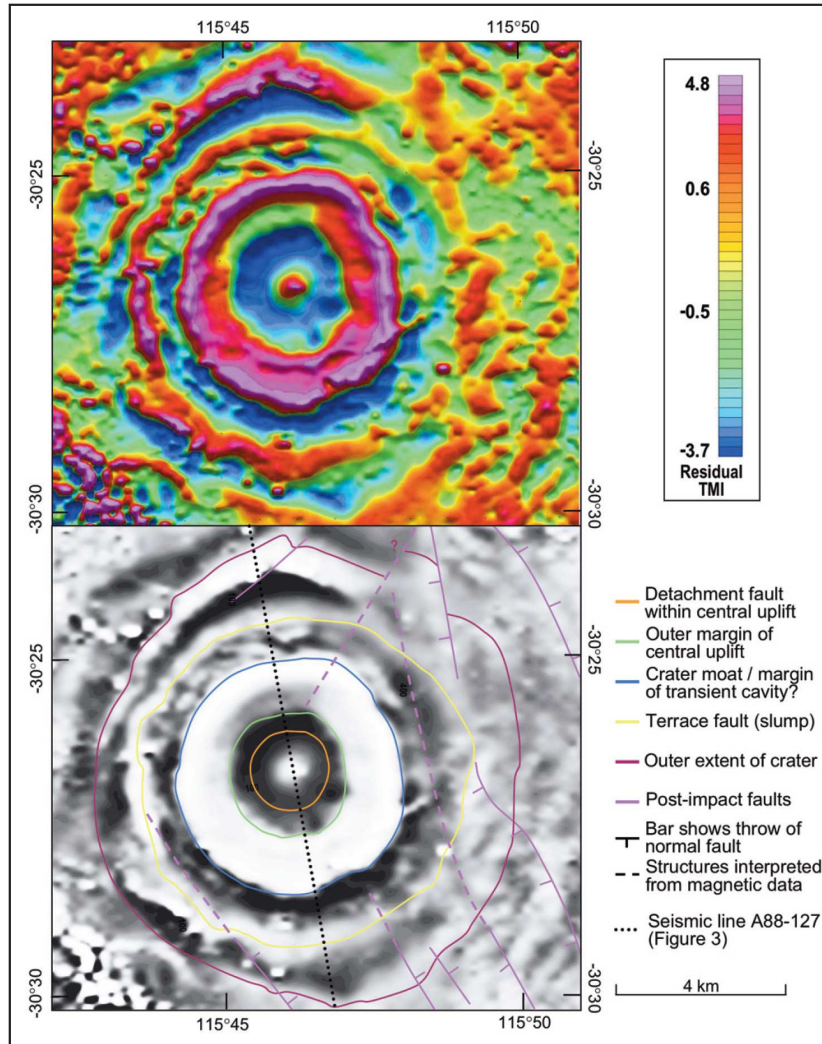


Figure 4.10 Residual total magnetic intensity map of the Yallalie impact structure, Western Australia based on results of removing a one-dimensional regional from the results of an aeromagnetic survey flown along flight lines spaced at 200 m (N-S) and 200 m above the ground surface. Top is the shaded-relief residual anomaly map in color with the color bar in nanoteslas. Bottom is the same map in grayscale overlain with a structural interpretation from seismic reflection profiling. Adapted from Hawke et al. (2006).

The magnetic signatures of lunar impacts are quite weak and difficult to relate to crustal magnetization properties [e.g., Hood (2010)], whereas the giant impacts on Mars appear to have mostly demagnetized by shock

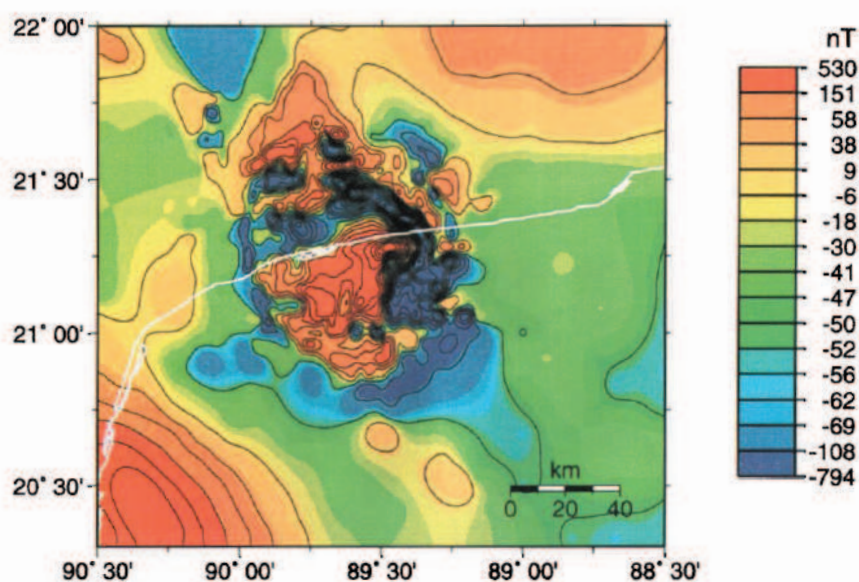


Figure 4.11 Total magnetic field intensity over the Chicxulub crater, Yucatan, Mexico after removal of a 48,380-nT base-level. Based on a 1-km gridded Pemex aeromagnetic survey flown at an elevation of 450 m along 6-km spaced flight lines. The contour interval is 50 nT and the white line marks the northern shoreline of the Yucatan Peninsula. Adapted from Pilkington and Hildebrand (2000).

metamorphism some of the strongest crustal remanent magnetic anomalies of the solar system [e.g., Connerney et al. (2005)]. On Earth, however, the putative Wilkes Land impact basin appears to be associated with the largest satellite-observed, positive crustal magnetic anomaly of Antarctica as shown in Figure 4.12 (von Frese et al., 2013). In reconstructed Gondwana, the Wilkes Land magnetic anomaly (WLMA) extends the prominently magnetized crust into south-central Australia. The strongly enhanced crustal magnetization may reflect the impact's thermal enhancement of lower crustal viscous remanent magnetization, as well as the production of positively magnetized igneous rocks within the fractured crust. In addition, the WLMA suggests a normal polarity crustal magnetization that is consistent with an end-of-Permian impact.

The modeling of the satellite gravity and magnetic anomalies of Wilkes Land clearly lack uniqueness due to the inherent source ambiguity of potential fields. However, significant additional crustal constraints on the putative Wilkes Land impact basin will result as the anomaly data from on-going

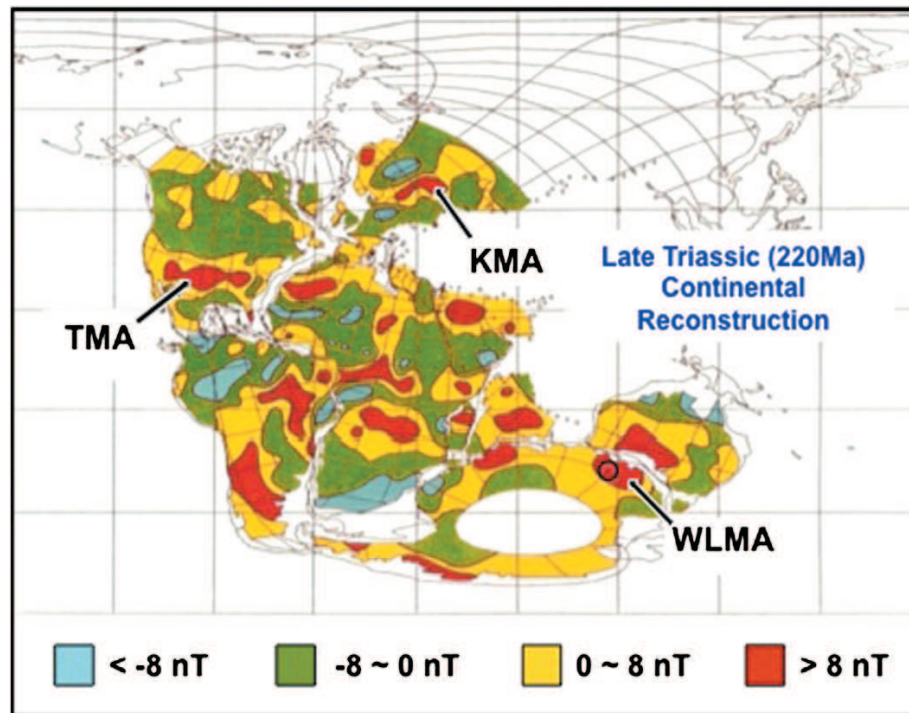


Figure 4.12 Pangea (Smith et al., 1981) and Magsat scalar total magnetic field anomalies reduced to 400 km altitude and 60,000 nT radial polarization intensity [adapted from von Frese et al. (1986)]. The Transcontinental Magnetic Anomaly (TMA) of the conterminous US and the Kursk Magnetic Anomaly (KMA) are highlighted. The black circle in the Wilkes Land Magnetic Anomaly (WLMA) outlines the 500-km diameter central crater of the putative impact basin. Adapted from von Frese et al. (2013).

near-surface gravity and magnetic surveys become available [e.g., Golynsky et al. (2013)].

4.3.3 Summary

The above brief description of gravity and magnetic anomalies of impact structures and the descriptions of a few examples from the published literature of anomalies associated with specific structures show how these anomalies can be used to identify and study the nature of impact craters and basins. These objectives can best be accomplished by a combined analysis of both gravity and magnetic field analysis in concert with other geophysical data as well as geologic and petrophysical information. Examples of this synergistic

approach include papers by Hildebrand et al. (2005); Tsikalas et al. (1998); Ormö et al. (1999); von Frese et al. (2009, 2013), and the description of numerous impact structures in Canada by Grieve (2006).

4.4 Continent-Ocean Boundaries

The major division in the Earth's topography is between the continents and the oceans. The elevation variation between them which is approximately 6 km is a result of the lower density of the continental rocks and isostasy which leads to the Earth processes seeking to bring about a level of hydrostatic equilibrium or constant mass per unit surface area at a level within the Earth. The margin between these two major topographic elements, commonly referred to as the continent-ocean boundary (COB), is one of the most significant geologic boundaries. It takes on a wide variety of forms depending on the nature of the processes that are involved in its formation. Most of the Earth's COBs are passive margins, such as those that surround much of the Atlantic Ocean, which are derived from disruption of continents leading to the construction of intervening ocean basins. This type of boundary may be accompanied by voluminous extrusion of largely mantle-derived magma, but other segments of the margin along the same continental edge may be essentially devoid of volcanic rocks. As a result a broad range of structures and rock types occur at passive margins, but all have sedimentary cover derived from the volcanic rocks of the margin and the adjoining continental rocks. Other COBs are active margins that involve subduction of oceanic lithosphere beneath the lighter continental lithosphere. Such is the case along the western edge of South America where the Nazca plate dives below the South American plate. Still other margins called transform margins involve oblique or strike-slip movement between plates with no present-day continent or ocean destruction or construction as occur along portions of the western coastal boundary of the U.S.

Investigation of COBs has been a major component of geologic/geophysical studies since the advent of marine geophysical studies that largely developed after World War II. These studies have been advanced by worldwide marine seismic reflection profiling, but also by the ready access to shipborne and airborne gravity and magnetic data and satellite observations. The nature of these observations and their processing are described in the text of the accompanying book. The study of these boundaries has been fostered by interest in the destruction and construction of plates that makeup the Earth's surface and form the backbone of plate tectonic processes, and also because of their importance as a source of hydrocarbons. Roughly a third

of the world's petroleum reserves are located within the sedimentary rocks of the COBs making them attractive targets for regional and detailed studies by both industry and governmental agencies. The acquisition of gravity and magnetic anomaly data is particularly efficient, encouraging their widespread use for studying continental margins.

4.4.1 Gravity Anomalies

Not only are continental margins the major subdivision of the Earth's topography, they are a major boundary between global gravity and magnetic anomalies. Gravity anomalies of the COB originate in a wide variety of sources the effects of which are superimposed upon each other to produce a complex array of anomalies. Sources of anomalies include the difference in the density between the waters of the ocean covering the oceanic crust and the enclosing continental rocks, the contrast between the average thickness of the continental crust, ≈ 35 km, and that of the oceanic crust, ≈ 6 km, the presence of thick wedges of clastic sedimentary and evaporite rocks deposited on the attenuated continental crust, differences between the oceanic and continental crust compositions, the occurrence of mafic intrusives and extrusive volcanic rocks as well as underplating of the crust by rising magma from the mantle, isostatic disturbances commonly related to plate tectonism, and possible effects due to the effect of temperature variations between the continental and oceanic lithosphere on the density of the rocks. Typically passive margins are associated with positive free-air gravity anomalies with a maximum generally near the continental edge shelf and a seaward minimum, the so-called "edge effect anomaly." This is commonly interpreted as the combined gravitational effect of deepening of the Moho from the ocean to the continent and the shallowing bathymetry. In addition to the passive margin anomalies, significant gravity anomalies and to a lesser extent magnetic anomalies originate along active margins where oceanic lithosphere dips below the continental lithosphere where it is consumed.

The horizontally contrasting Earth materials at the COB host some of the largest density contrasts in the lithosphere resulting in major amplitude gravity anomalies. For example, the Bouguer anomaly is of the order of +300 mGal or more in the ocean contrasting with near zero or slightly negative anomalies (< -50 mGal) in most continental areas and anomalies up to -300 mGal in mountainous regions (see Figure 4.13).

Useful reviews of the sources of gravity anomalies over the continents are given by Simpson et al. (1986); Hanna et al. (1989) and Simpson and Jachens (1989). Subduction zones are typically negative gravity anomalies attaining

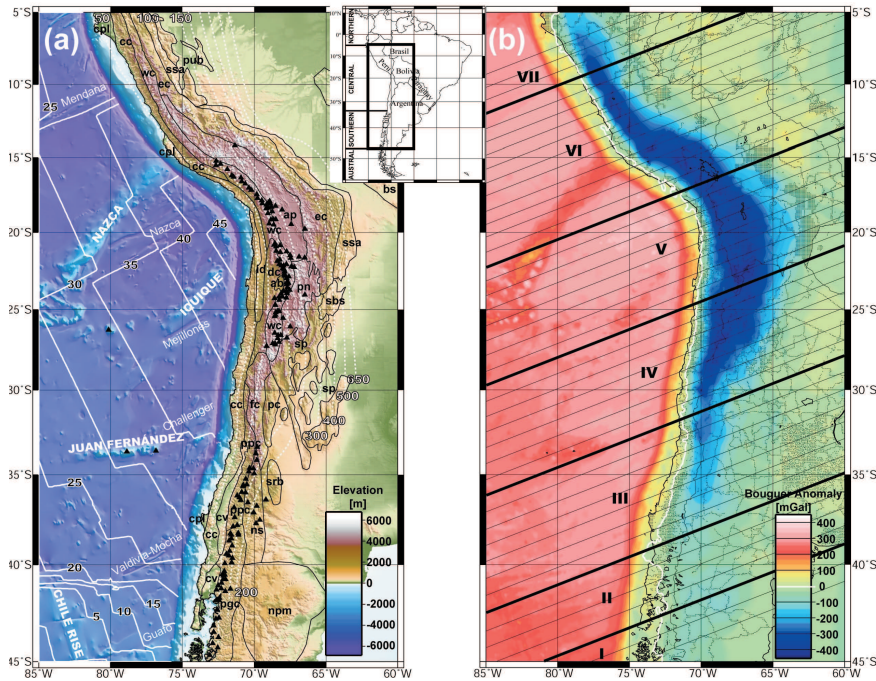


Figure 4.13 Geotectonic and topographic setting (a) and Bouguer gravity anomaly (b) of a portion of the western continent-ocean boundary region of South America. Note the amplitude of the Bouguer gravity anomaly in relation to the boundary and the topographic elevation. Additional details of the maps (a) and (b) are presented in Figure 1 of Tessara et al. (2006). Adapted from Tessara et al. (2006).

values of roughly -200 mGal or more due to the higher density oceanic lithosphere dipping beneath the lower density continental lithosphere and deeper rocks.

A major source of gravity anomalies is the density contrast between the crust, either oceanic or continental, and the underlying mantle. This boundary, the Moho, is commonly portrayed and evaluated as a distinctive interface, but it may be transitional over a depth range of several kilometers. The evidence for the density contrast between the crust and the upper mantle is described in Chapter 4 of the accompanying text. Suggested density contrasts range from 200 to 450 kg/m^3 or more depending on the region and the vertical range over which the contrast is used. Typically values of 350 kg/m^3 are used suggesting that a Moho depth change of a kilometer results in an anomaly of approximately 15 ± 3 mGal. As a result the decrease in the thickness of the crust from roughly 12 km, including the water, in the

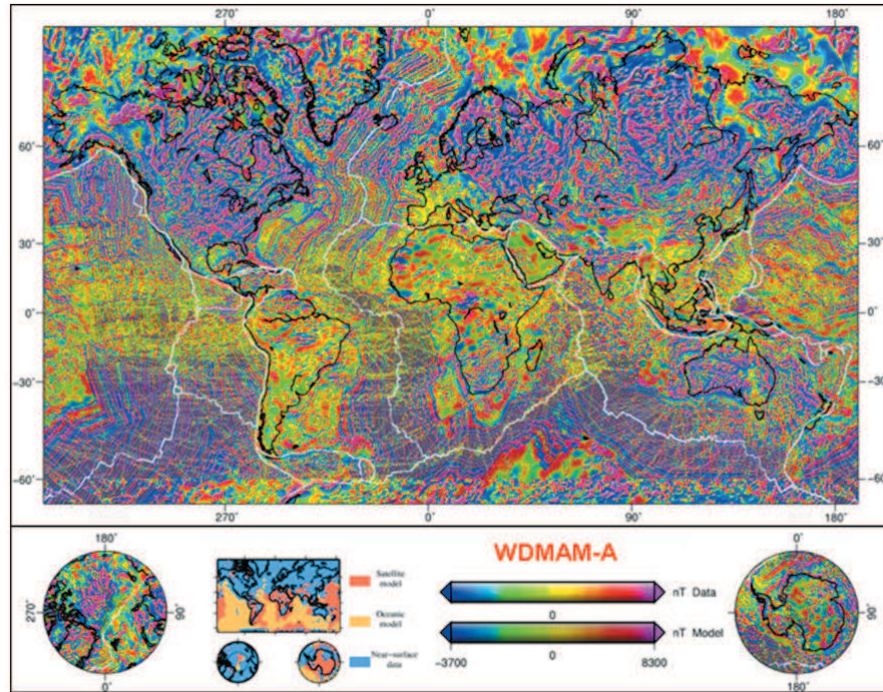


Figure 4.14 World magnetic anomaly map from Mercator and polar projections of the EMAG2 global magnetic anomaly grid. The grid has a resolution of 2 arcmin and is referenced to an elevation of 4 km above the geoid. Adapted from Maus et al. (2009).

oceans to 35 km in the continents produces an anomaly of approximately 350 mGal.

Unfortunately the superposition of the anomalies from the various sources produces a complex anomaly that cannot be interpreted without ambiguity unless geological and geophysical information are available to constrain the interpretation. Accordingly, gravity anomalies are commonly interpreted in concert with seismic reflection profiling with the gravity providing important insight into a more complete interpretation of the reflection profiling and extending the interpretation beyond the limits of the seismic studies.

4.4.2 Magnetic Anomalies

As in the case of gravity anomalies, magnetic anomalies differ between the oceans and continents with the contrast particularly evident at the COB. However, as shown in Figure 4.14 the differences are primarily in the pat-

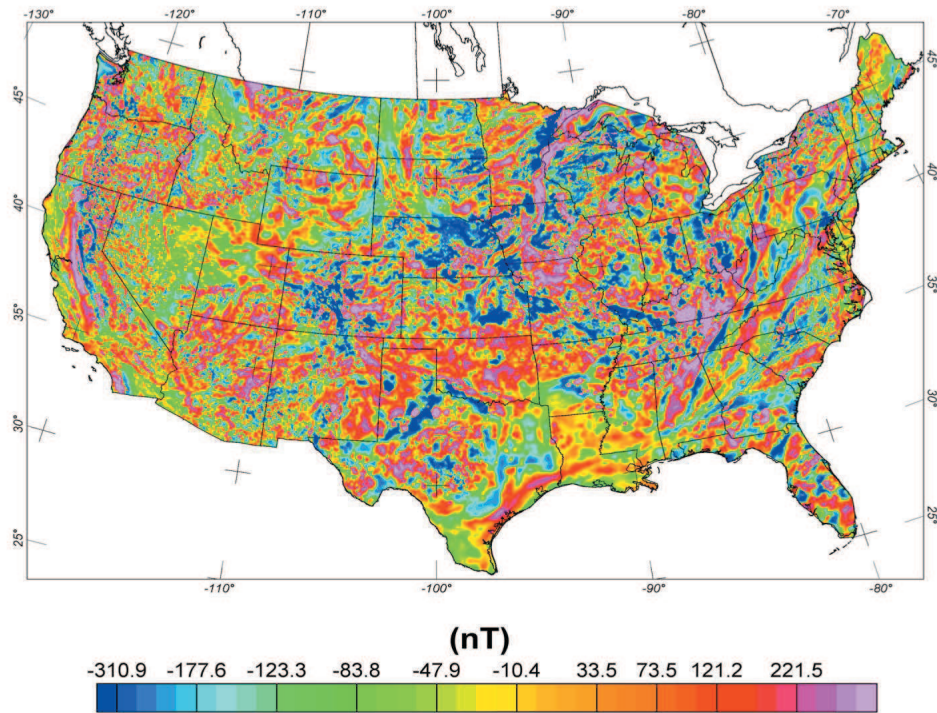


Figure 4.15 Reduced-to-pole magnetic anomaly map of the conterminous United States. Adapted from Ravat et al. (2009).

tern of anomalies in contrast to their amplitude. The oceans are dominated by magnetic stripping anomalies that roughly parallel the mid-ocean ridges where the sources of the anomalies originate. Whereas the magnetic pattern of the continents, for example the conterminous U.S. (Figure 4.15), is dominated by anomalies derived primarily from the crystalline basement rocks and have a pattern controlled by the complex tectonic history of these rocks. The oceanic anomalies are primarily caused by remanent magnetization while the continental anomalies originate largely in, but certainly are not restricted to, induced magnetization in the magnetite content of the rocks. The anomalies of the ocean generally are more subdued than continental anomalies with gentler gradients because the sources are typically at a depth of 6 km or more. This is in contrast to the continental anomaly sources that are buried at these depths only in the limited deeper sedimentary basins of the continents. Typically the magnetic stripping of the oceans becomes more subdued as the continent-ocean margins are approached as a result of the increased depth to the sources due to the thickening sediment

accumulation until they disappear entirely due to the overwhelming effect of the marginal anomalies and the anomalies of the continents (Heirtzler, 1985).

There are several potential sources of magnetic anomalies associated with the COB, however, the number of magnetic anomaly sources that can be resolved in surface mapping is considerably less than are pertinent to gravity mapping. Magnetic interpretation is less sensitive to depth extent of the source and to deep sources than in gravity analysis. This is, of course, a disadvantage because there is less to interpret in the magnetic method, but it also can be turned to an advantage because there are fewer potential sources of the anomalies. The magnetic method is particularly useful in depth determination and in isolating and interpreting anomalies related to mafic intrusives and volcanic rocks that occur in many COBs. However, the magnetization of volcanic rocks, in particular, is dominated by remanent magnetization of unknown intensity and direction that increases the ambiguity of the interpretation.

Magnetic anomalies are restricted in their depth sounding range because of the effect of the Curie point temperature ($\approx 560^{\circ}\text{C}$ for magnetite, the principal magnetic mineral of lithospheric rocks) on the magnetization of the rocks. Above the Curie temperature rocks lose their ferrimagnetism, and thus are only weakly magnetic, incapable of producing mappable magnetic anomalies. The Curie point is reached in normal continental lithosphere at approximately the depth of the Moho and somewhat shallower depths in the ocean. As described in Chapter 10 of the accompanying text, there has been considerable discussion regarding the magnetic nature of the Moho. The arguments in favor of the Moho as a lower boundary of lithospheric magnetization put forward by Wasilewski et al. (1979) and subsequent workers have been generally accepted, but more recent studies by Ferré et al. (2013) on fresh mantle xenoliths have raised new questions regarding the potential for sub-Moho magnetic sources.

Useful reviews of the origin of crustal magnetic anomalies are presented by Hinze and Zietz (1985); Blakely and Connard (1989), and Harrison (1989).

4.4.3 Passive Margin Examples

4.4.4 a) North American Atlantic Margin

The magnetic anomaly pattern of the COB off the Atlantic coast of the U.S. is dominated by a linear positive magnetic anomaly that roughly coincides with the continental slope over much of its 3,000-km length from Newfound-

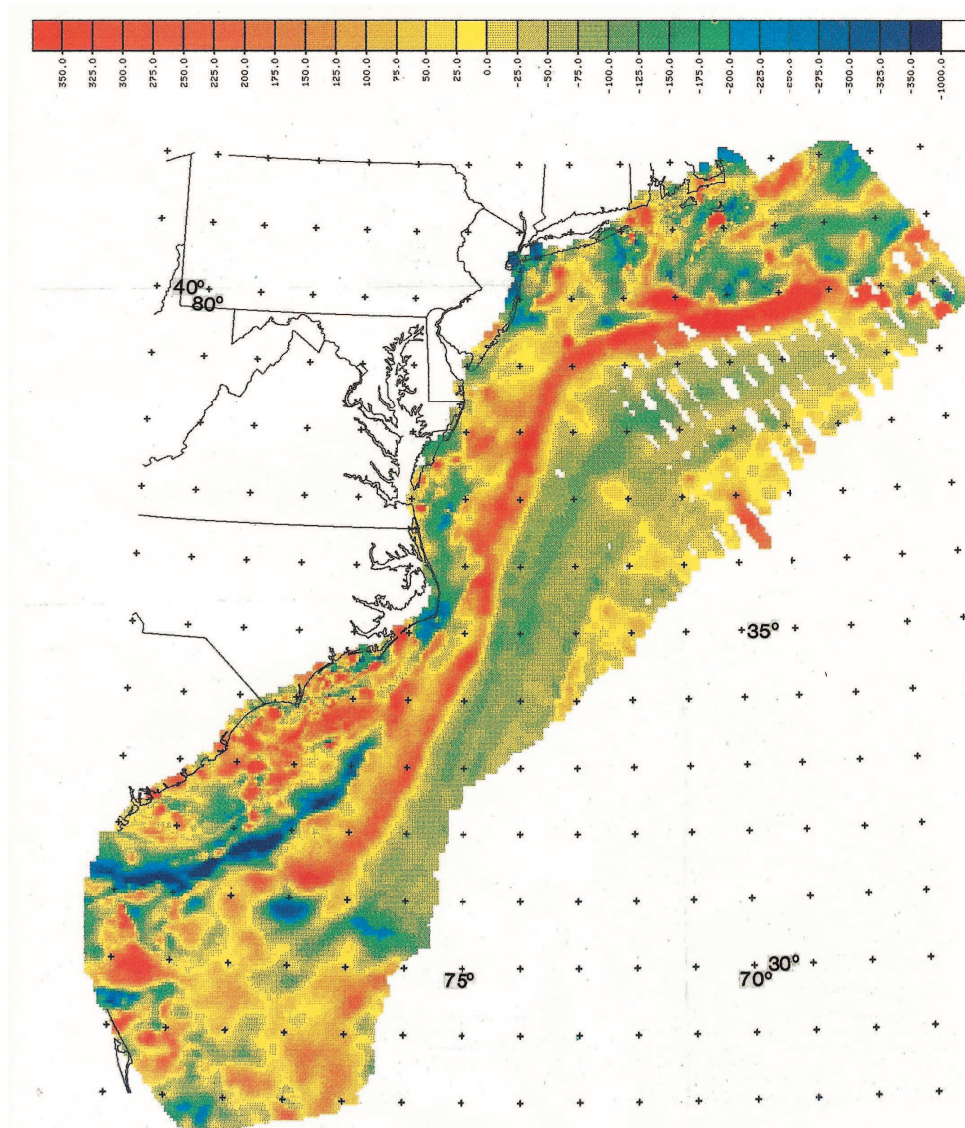


Figure 4.16 Total magnetic intensity magnetic anomaly of the Atlantic margin. The contour interval is 25 nT and the red colors are highs and the blues low anomaly values. Adapted from Behrendt and Grim (1985).

land to Georgia (Figure 4.16). This East Coast Magnetic Anomaly (ECMA) is similar to others observed along other passive COBs. Oceanward the principal positive anomaly of the ECMA is paralleled by highly-subdued, positive and negative anomalies until the oceanic magnetic stripping anomalies become prominent. In contrast, to the west, the anomaly pattern is complex

and relatively higher wavenumber reflecting the magnetic heterogeneity and proximity to the surface of the continental crust. The anomaly splits off the North Carolina coast into two segments separated by an intense minimum that turn into Georgia and northern Florida as an irregular series of positive anomalies that are highlighted in the second vertical derivative map (Figure 4.17). The anomaly was extended by Hall (1990) across Florida into the eastern Gulf of Mexico and southern Louisiana, and southwestwards into southern Texas.

The source of the ECMA has been the subject of much investigation and conjecture since it was first recognized by Keller et al. (1954). For example, Taylor et al. (1968) favored an origin related to an intrusive source. Behrendt and Grim (1985) suggested that an edge effect associated with the oceanic crust may account for most of the ECMA, but that the shorter wavelength components of it are perhaps caused by igneous intrusions. More recently seismic reflection profiling has shed more light on the possible origin of the anomaly. For example, Holbrook et al. (1994) mapped a lateral velocity change in the deep crust across the ECMA that may be related to extensive intrusions and extrusion of mafic magma associated with the anomaly. Alsop and Talwani (1984) suggested a transitional zone of thinned crust with a composite model including a normal fault correlated with the landward gradient of the ECMA and associated crustal mafic intrusives and extrusive rocks. A contrasting interpretation by Hall (1990) involves modeling of magnetic anomaly profiles across the ECMA and its extension into the Gulf Coast (Figure 4.18). associated with a northwest dipping suture consisting of mafic and ultramafic rocks. Behn and Lin (2000) have processed the gravity data along the Atlantic margin and have found a correlative gravity anomaly with the ECMA (Figures 4.19 and 4.20). indicating a common source for the gravity and magnetic positive anomalies.

A comparison of the EDGE-801 seismic profile (Figure 4.19) (Holbrook et al., 1994) with the observed gravity and magnetic anomalies as well as the modeled gravity anomaly considering differing interpretations of the lower crusts is shown in Figure 4.21). The maximum residual isostatic gravity anomaly and the reduced-to-pole magnetic anomaly (RTP) coincide with the thick, high-velocity lower crust. The exact nature of the origin of the ECMA remains a matter of conjecture, but probably involves a composite model involving volcanic rocks, a mafic intrusive basement, and an edge effect bringing into juxtaposition rocks of differing magnetic properties.

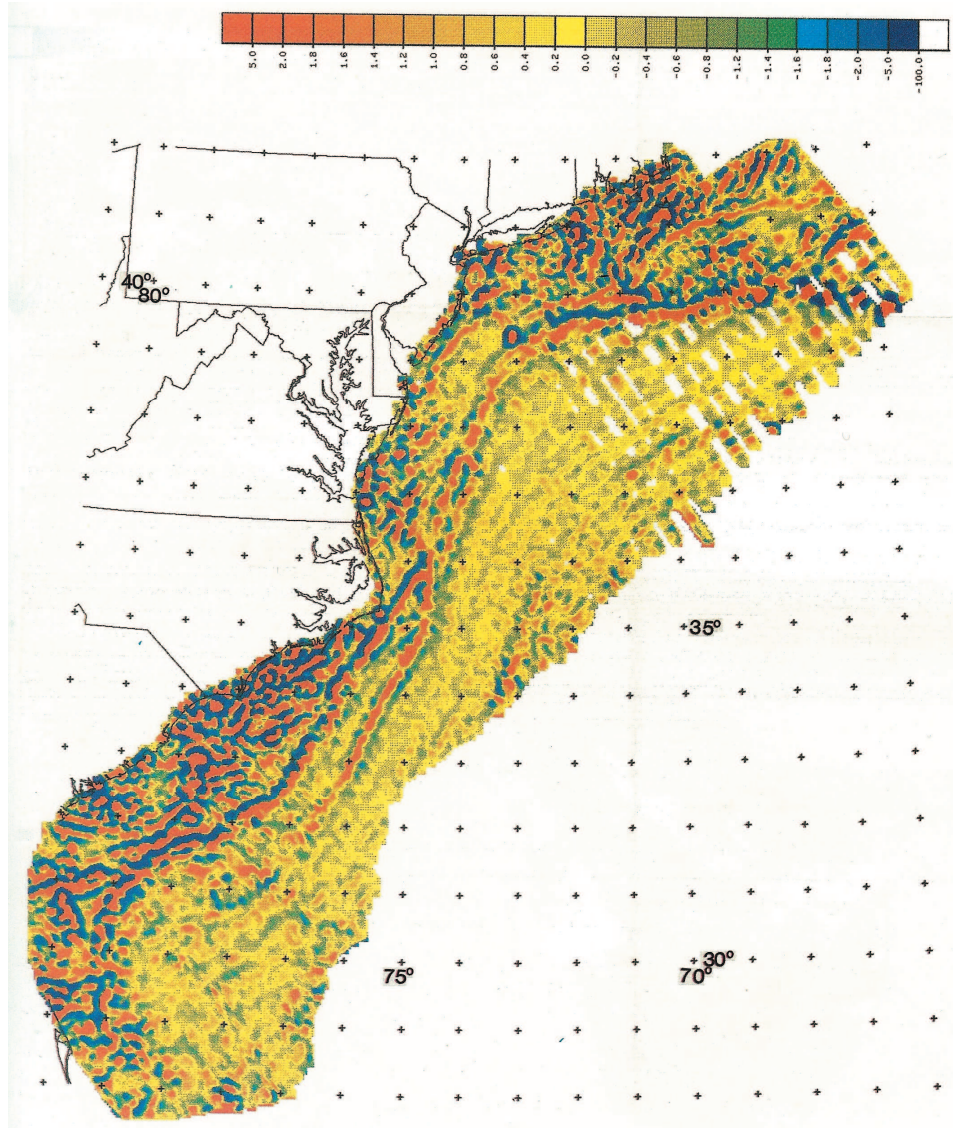


Figure 4.17 Second vertical derivative of the total magnetic intensity anomaly shown in Figure 4.16. The yellow regions are underlain by thick sedimentary rocks. The red colors are high second vertical derivative magnetic anomalies and the blues are lows. Adapted from Behrendt and Grim (1985).

4.4.5 b) Africa and South America Atlantic Margins

The Atlantic margin of Africa and South America have been the subject of considerable interest because of their potential for hydrocarbon resources.

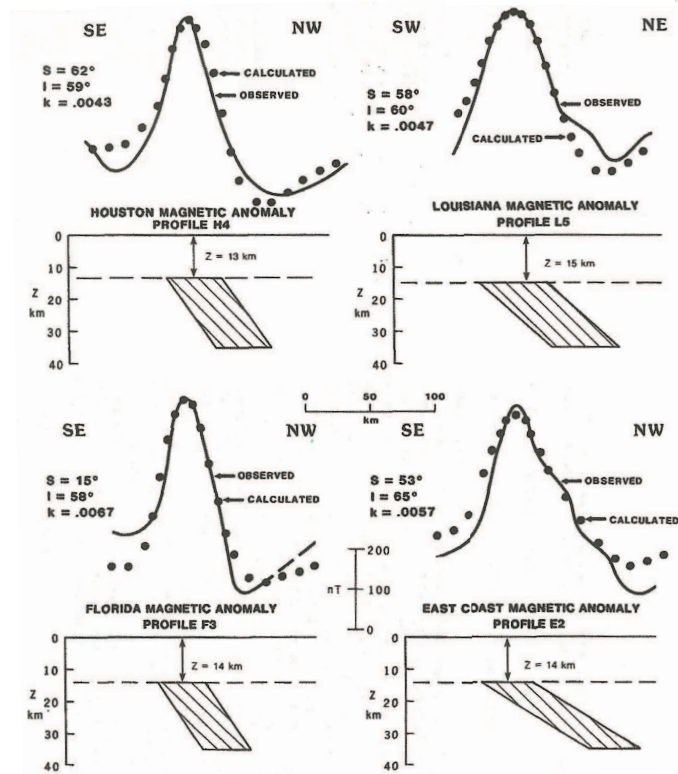


Figure 4.18 Two-dimensional prism magnetic models for four representative profiles across the ECMA and its extension into the Gulf Coast region. The prisms are interpreted by Hall as sutures with mafic and ultramafic rocks magnetized by induction. I = magnetic inclination, S = strike of profile azimuth from magnetic North, and k = magnetic susceptibility contrast in EMu. Adapted from Hall (1990).

For example, Pawlowski (2008) has described the application of gravity anomalies to identifying the Atlantic continental margin of southwest Africa. He illustrates the gravity and magnetic anomalies along the seismic profile AM-01 that is located on the Bouguer gravity anomaly map in Figure 4.22. Figure 4.23 shows the horizontal gradient of the Bouguer gravity anomaly map, and Figure 4.24 illustrates the associated reduced-to-pole magnetic anomaly map. In Figure 4.25(a) the observed Bouguer gravity anomaly profile is closely duplicated by the gravity anomaly calculated from the Moho (density contrast of 350 kg/m^3) indicating that the dominant contributor to the anomaly is the crustal thickness. Figure 4.25(b) shows that the gravity gradient maximum closely correlates with the COB, but that the gradient

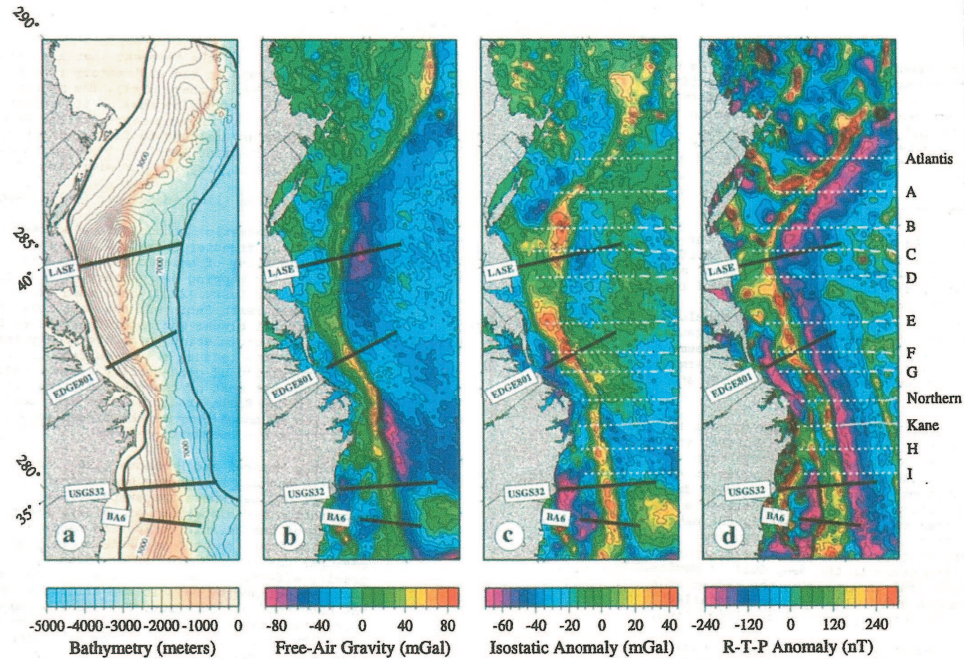


Figure 4.19 (a) Shaded bathymetry of the Atlantic coastal margin. Contours are the thickness of the sedimentary rocks. (b) Free-air gravity anomaly map of the Atlantic coastal margin. (c) Residual isostatic gravity anomaly of the Atlantic coastal margin. (d) Reduced-to-pole (RTP) total magnetic intensity anomaly map of the Atlantic coastal margin. Adapted from Behn and Lin (2000).

high is not completely satisfied by the effect of the Moho. Figure 4.25(c) reveals that the COB closely coincides with magnetic anomaly M4.

Another example of interpreting the COB offshore Gabon, West Africa using both gravity and magnetic enhanced anomaly patterns has been presented by Goussev et al. (2008). The data used included public domain satellite-derived free-air gravity and a merged set of aeromagnetic survey data. The enhancements applied to the gravity data included 3D Bouguer correction, isostatic correction, and calculation of horizontal gradient (HG). Figure 4.26 shows the interpreted COB superimposed on the isostatic gravity, horizontal gradient of the isostatic gravity, and horizontal gradient of the Bouguer gravity. The enhancements applied to the aeromagnetic data included differential reduction to the pole (DRTP), downward continuation (DWC) to the sea floor, and calculation of horizontal gradient (HG) of the DRTP DWC field. Figure 4.27 shows the interpreted COB superimposed on the regional basement depth map (120 km low-pass filtered) interpreted from

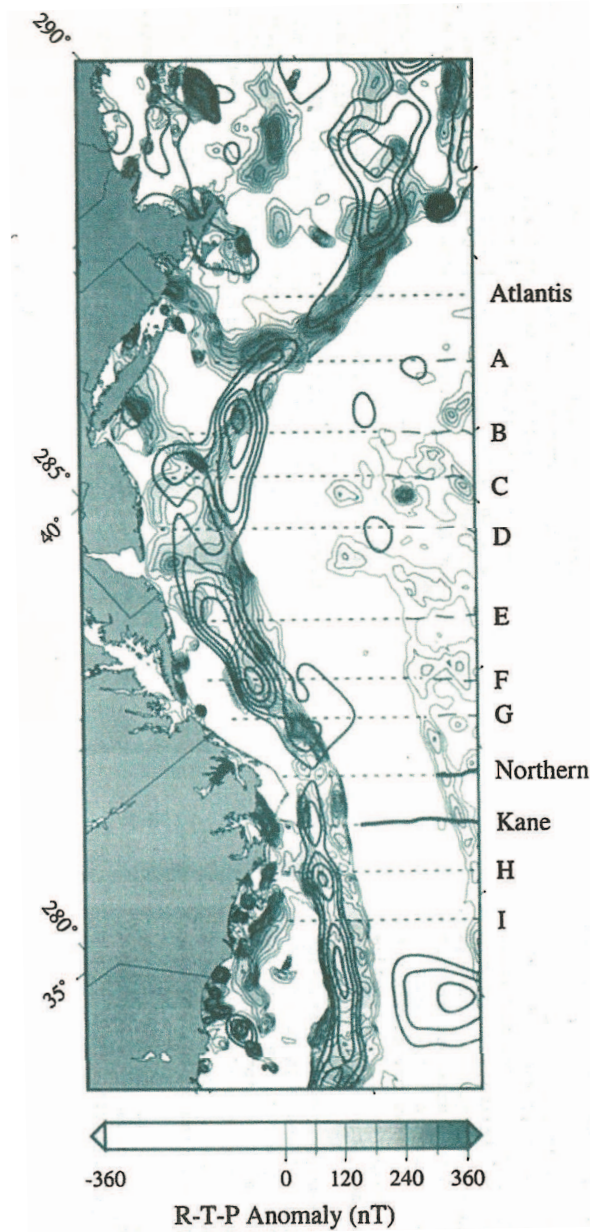


Figure 4.20 Comparison of RTP magnetic and isostatic gravity anomalies. Thin shaded contours illustrate RTP magnetic anomaly > 0 nT with a contour interval of 60 nT. Thick contour lines without shading show filtered isostatic gravity anomaly greater than 0 mGal with a contour interval of 10 mGal. Isostatic anomalies have been low-pass filtered using a cosine cutoff taper to remove wavelengths $< 50 - 100$ km. Note the strong correlation between the peak of the RTP anomaly and the isostatic gravity high along much of the East Coast margin. Adapted from Behn and Lin (2000).

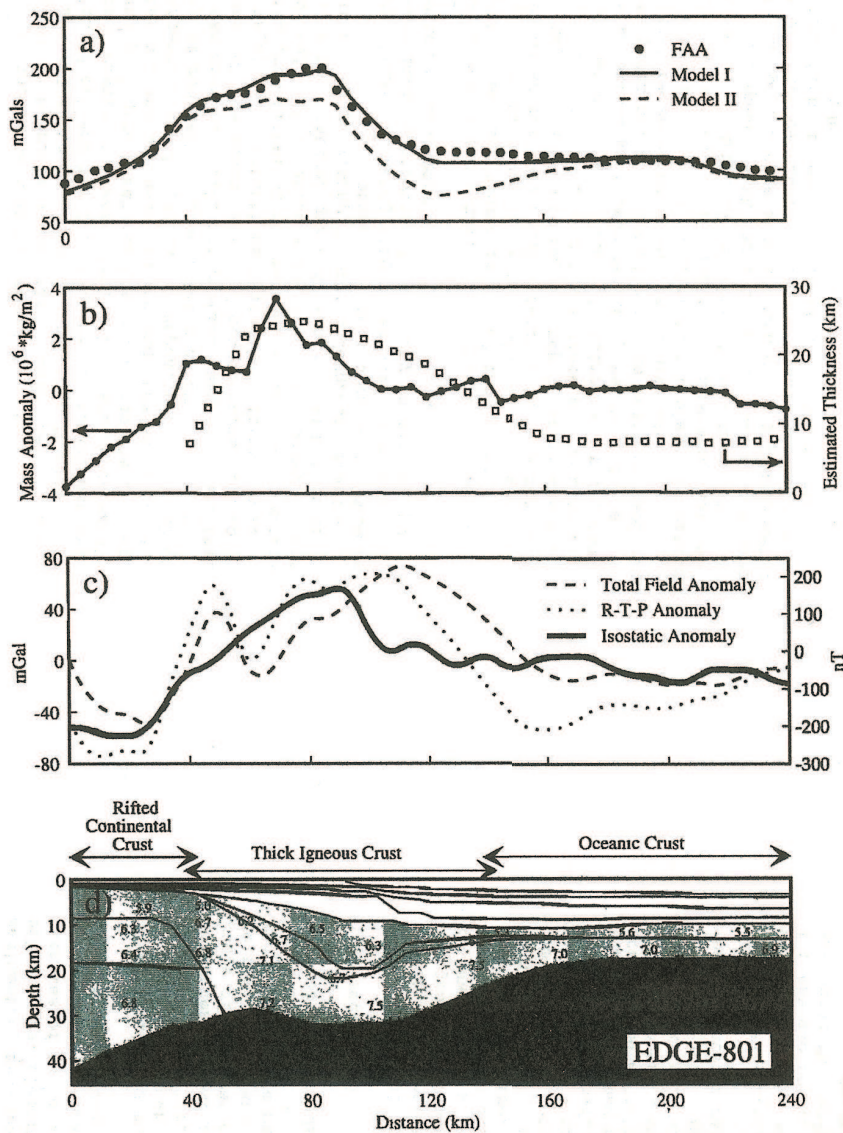


Figure 4.21 Comparison of the EDGE-801 seismic profile (Holbrook et al., 1994) whose location is indicated in Figure 4.19 with observed and modeled gravity and magnetic anomalies. (a) Observed free-air gravity anomaly and modeled gravity anomalies. Model I is based on density structure of Holbrook et al. (1994) and Model II uses a reduced lower crustal density of $3,030 \text{ kg/m}^3$. Note that without the higher lower crustal densities used in Model I, unreasonably high densities would be required in the upper crust. (b) Mass anomaly (solid circles) that results from (Holbrook et al., 1994) s density structure. Open circles are the estimated thicknesses of the emplaced igneous rocks. (c) Residual isostatic gravity, total field magnetic, and RTP anomalies. (d) Crustal velocity model of the EDGE-801 seismic profile. Adapted from Behn and Lin (2000).

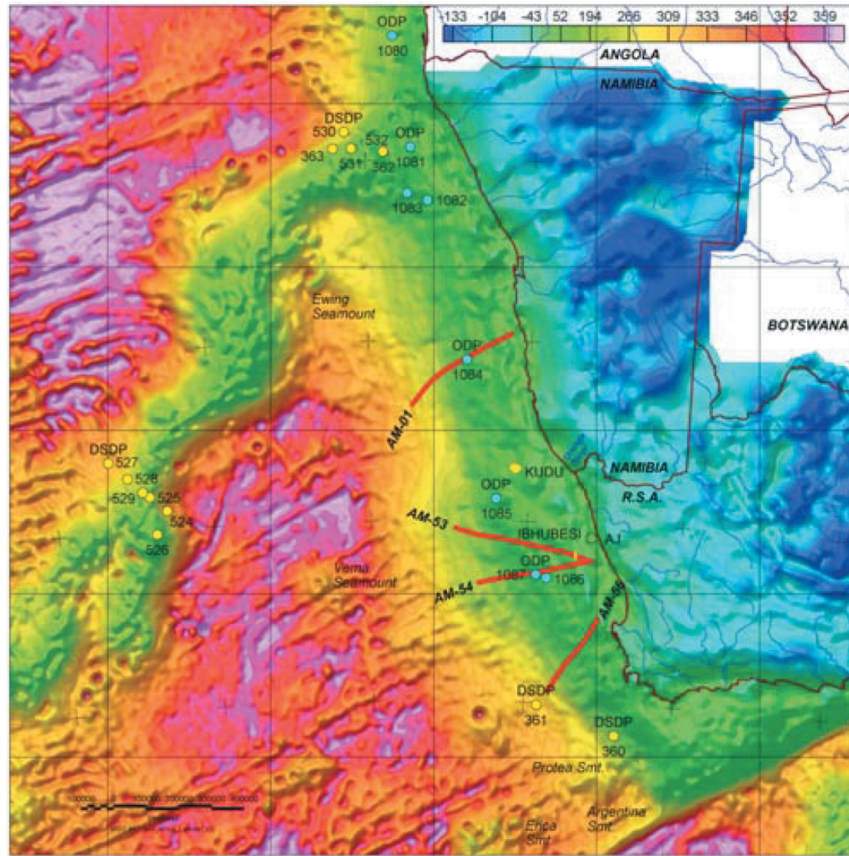


Figure 4.22 Observed Bouguer gravity anomaly map in milligals of southwest Africa. Adapted from Pawlowski (2008).

the magnetic data, the DRTP DWC minus DRTP difference map, and the horizontal gradient of the DRTP map. According to Goussev et al. (2008), these enhancements provide the most efficient enhancement and visualization of changes in anomalous signatures of the filtered gravity and magnetic fields on both sides of the COB in this area.

Investigation of conjugate margins of Africa and South America with gravity and magnetic fields and seismic reflection profiling show highly variable tectonic development and resulting crustal geology on the two sides of the South Atlantic Ocean [e.g., Dragol-Stavar and Hall (2009); Blaich et al. (2010)] reflecting the asymmetric rifting process. Accordingly, the gravity and magnetic anomalies vary both across conjugate positions of the margins and along the individual COBs. Figure 4.28 illustrates this in a segmented

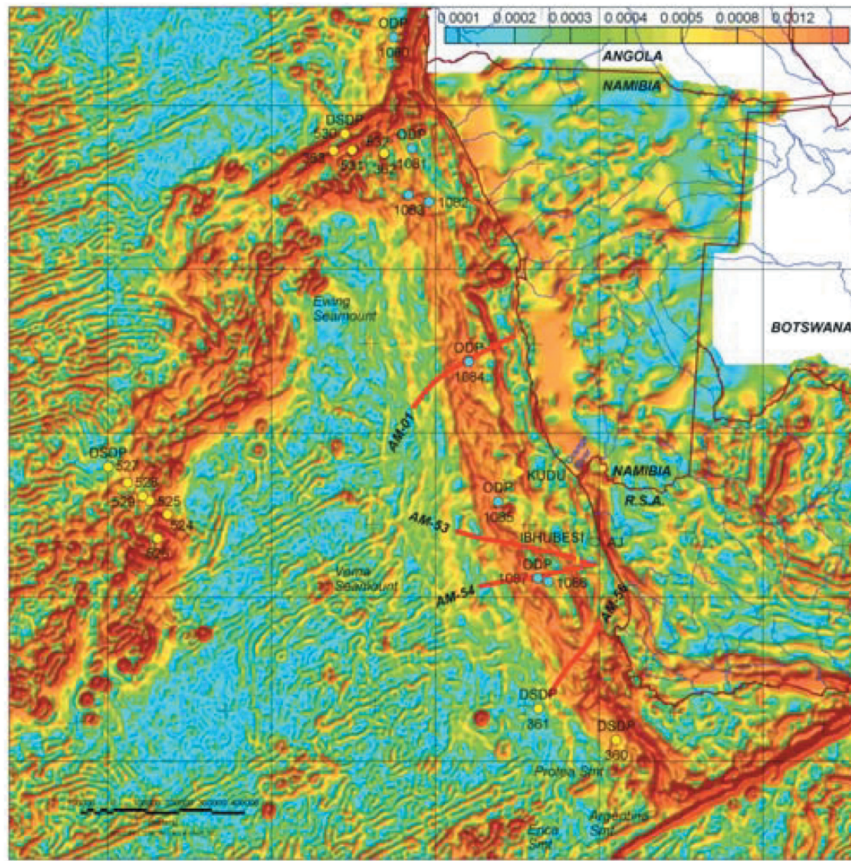


Figure 4.23 Horizontal gradient of the Bouguer gravity anomaly map in Figure 4.22 in mGal/m. Adapted from Pawlowski (2008).

crustal and gravity and magnetic anomaly profile across the South Atlantic Ocean margins. The observed and computed free-air anomalies over the eastern and western margins shown respectively in Figures 4.29 and 4.30 show the use of the gravity data together with the seismic reflection profiling in interpreting the nature of the COB.

Studies of the gravitational effect of COBs commonly do not consider the thermal effect on the densities of the hotter oceanic lithosphere contrasting with the cooler continent. However, others have incorporated this effect into their analyses [e.g., Karner and Watts (1982); Kuo and Forsyth (1989), and Chappell and Kusznir (2008)]. Breivik et al. (1999) has made the case for taking into account thermal effects of the lithosphere on gravity modeling of the relatively recent - early Tertiary - western Barents Sea passive margin

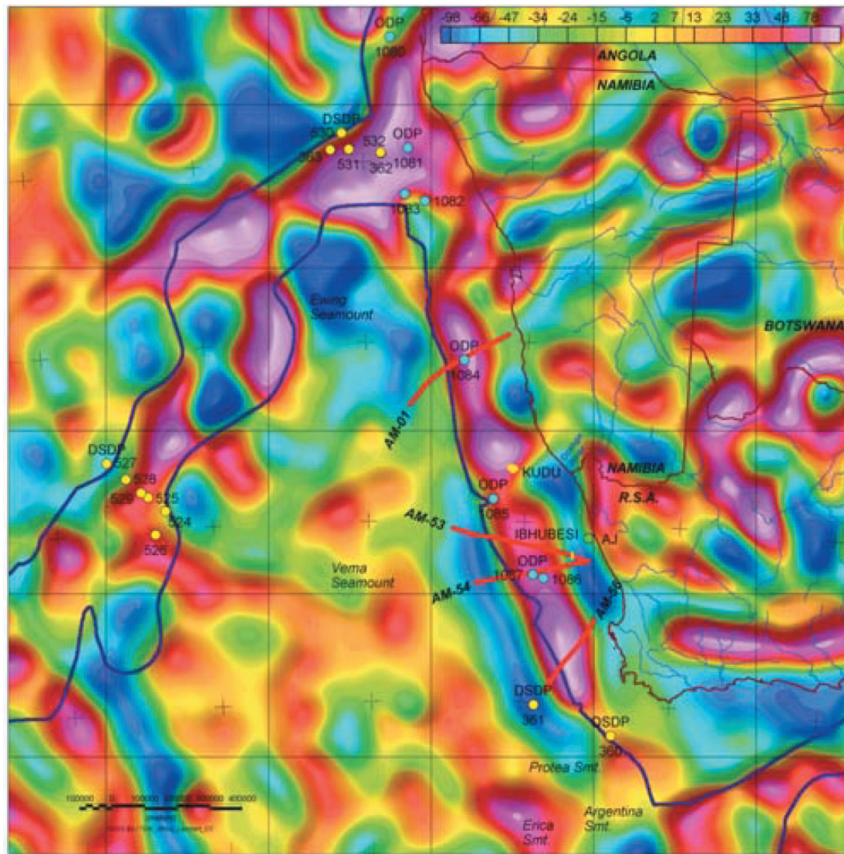


Figure 4.24 Reduced-to-pole total magnetic intensity anomaly map of region shown in Figure 4.22 in nT. Adapted from Pawlowski (2008).

off the northwest coast of Norway. They model the thermal effect of the 125 km thick lithosphere as shown in Figures 4.31 and 4.32. The thermal effect in their modeling leads to anomalous changes of the order of 150 mGals with the resulting models comparing much better with the observed gravity. As they point out, the effect of the thermal variations will decrease with the age of the rifting and, of course, it will vary with distance from the current location of the rift, and thus care needs to be used in applying thermal effects.

4.4.6 Active Margin Examples

Active margins involve the destruction of oceanic crust with the higher density oceanic lithosphere dipping into the Earth's mantle beneath continental

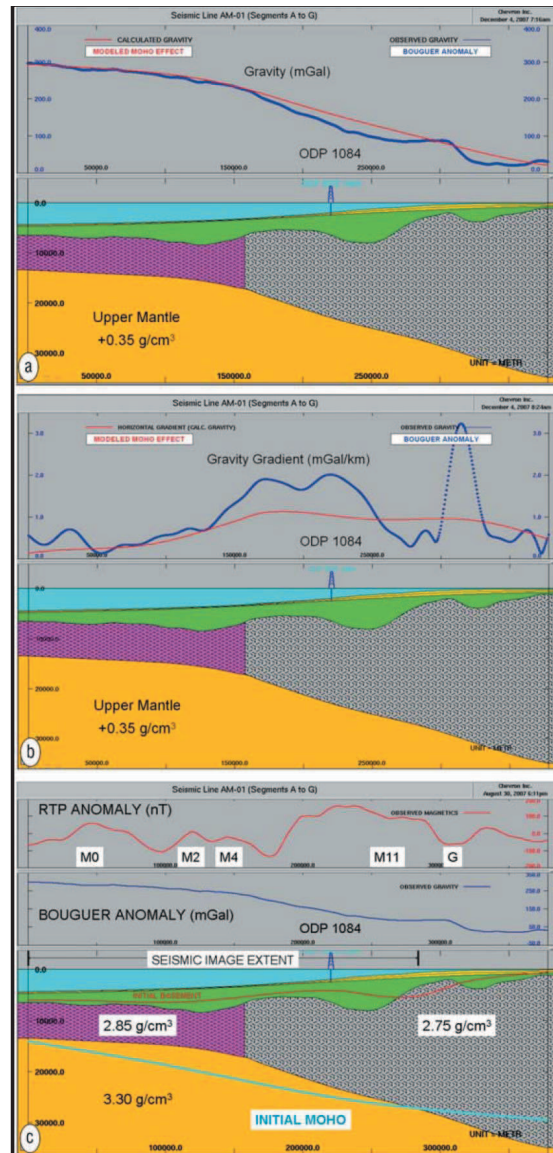


Figure 4.25 Observed and modeled gravity and magnetic anomaly profiles along seismic profile AM-01 that is located on Figure 4.26. Continental-type crust is gray and oceanic crust is magenta. Sediments are green and yellow and the ocean water is cyan. (a) Observed and modeled Bouguer gravity anomaly. The model only considers the effect of the density contrast across the Moho (350 kg/m^3). The close correspondence of the profiles indicates the dominant effect of the change in crustal thickness on the anomaly. (b) Horizontal gradient of the Bouguer gravity anomaly with the maximum closely approximating the position of the COB. (c) Reduced-to-pole (RTP) total magnetic intensity anomaly profile. Magnetic anomaly M4 approximates the location of the COB on this profile. Adapted from Pawlowski (2008).

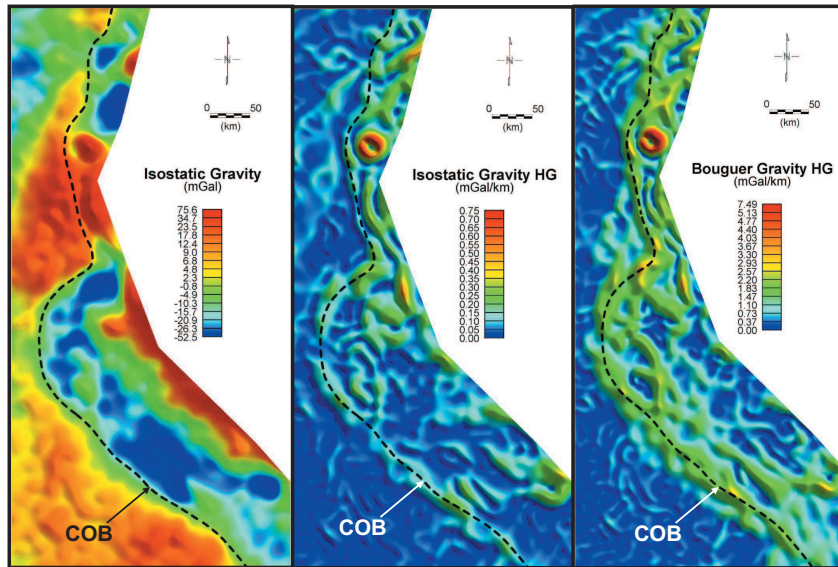


Figure 4.26 Interpreted COB, offshore Gabon, superimposed on satellite-derived isostatic gravity, horizontal gradient (HG) of isostatic gravity, and HG of Bouguer gravity. Adapted from Goussev et al. (2008).

lithosphere. Examples of these boundaries exist along the margin of the Pacific Ocean, the Caribbean Sea, and the Mediterranean Sea and are commonly related to oceanic trenches filled to varying amounts with sediments. Typically, these margins are characterized by intense parallel, paired anomalies as observed in Figure 5.22 of the accompanying text and illustrated over the Japanese island of Honshu in Figure 4.33. The total amplitude of the minimum/maximum may range up to 500 mGal and are separated by a 100 to 150 km. The minimum is located over the bathymetric trench and the maximum lies seaward over a broad bathymetric ridge. The minima located over the oceanic trenches were mapped by Vening Meinesz (1948) originate largely by the trenches and their sediments. Watts and Talwani (1974, 1975) find that the downgoing lithospheric slab contributes little to the anomaly and is limited to the region of the island arc and trench as shown in Figure 4.34. Any effect of the downgoing slab is largely compensated by variations in density lower in the mantle. Thus, Watts and Talwani (1974, 1975) show that gravity modeling can do little to determine the nature of the downgoing slab. The seaward gravity maximum, the so-called Outer Gravity High as described by Watts and Talwani (1974) is not related to the downgoing

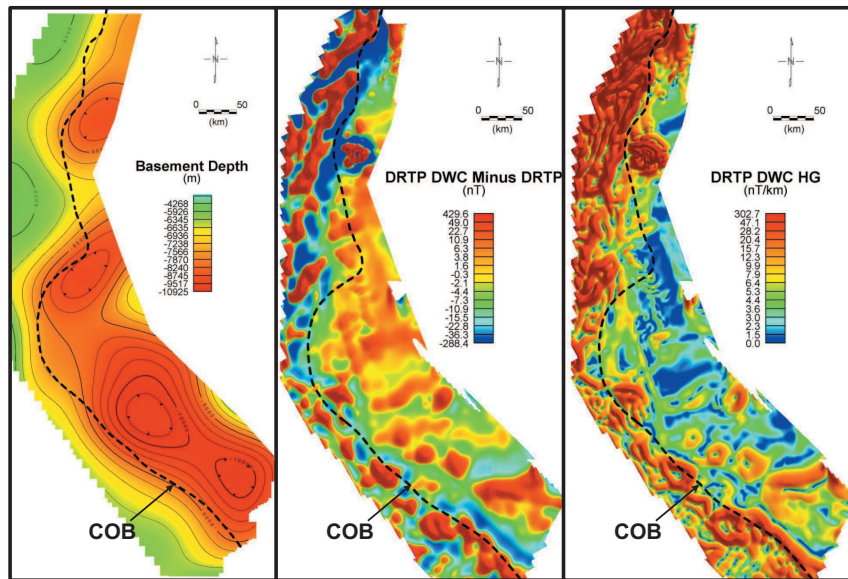


Figure 4.27 Interpreted COB, offshore Gabon, superimposed on regional basement depth interpretation map, difference between downward continued differentially reduced-to-pole (DRTP DWC) data and original DRTP data, and horizontal gradient (HG) of the DRTP DWC data. Adapted from Goussev et al. (2008).

slab, but is a result of structures produced by the stress system related to the convergence of lithospheric plates at island arcs.

Magnetic maxima may be associated with active margins involving the lower temperature downgoing slab [e.g., Schubert et al. (1975)] because of the increase in the thickness of the magnetic lithosphere related to deepening of the Curie point isotherm where the magnetic minerals lose their ferrimagnetism. For example, Clark et al. (1985) have modeled the magnetic anomaly mapped by the MAGSAT satellite over the Aleutian arc with a slab-like source as shown in Figure 4.35. However, Blakely et al. (2006) have shown that long-wavelength positive magnetic anomalies (and to some extent gravity anomalies) are caused by mantle hydration by the release of water from the downgoing oceanic plate. Magnetite is an important product of this hydration resulting in enrichment that causes magnetic highs. This is shown by Blakely and his co-authors for the Cascadia convergent zone in the northwest U.S. Figure 4.36 shows the magnetic, gravity, and generalized geology of the region. It is important to note that the positive magnetic anomaly in (A) (horizontal ruled pattern) has no comparable grav-

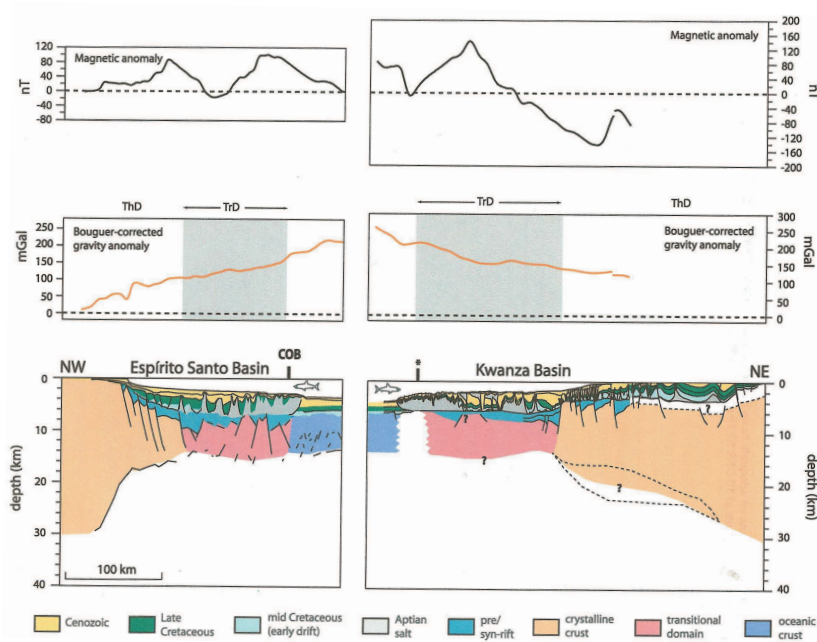


Figure 4.28 Gravity and magnetic anomaly profiles over conjugate COBs in the South Atlantic as interpreted from seismic profiling and gravity modeling. Adapted from Blaiçh et al. (2010).

ity anomaly in (B) as would normally be anticipated. Thus, it is concluded taking into account depth determinations on the magnetic anomaly, that deep-seated, highly magnetic, low-density rocks associated with hydration of rocks overlying the downgoing slab of Cascadia are the source of the magnetic positive. A gravity and magnetic profile (Figure 4.37) with the associated geologic model shows the relationship of the anomalies and their sources.

A comprehensive three-dimensional model of the western COB of South America has been prepared by Tessara et al. (2006) to a depth of 410 km. A typical vertical cross section across the COB is shown in Figure 4.38. It illustrates the nature of the sources that together with their densities are described by Tassara and his co-authors. The densities of downgoing slab sections (a-d) increase with depth with slight variations for the segments of the boundary (I-VII) shown in Figure 4.13. The densities of segments (a-c) of the slab are decreasingly less than the surrounding mantle until segment (d) whose density exceeds the mantle. The results of the modeling showing the resulting depth to the slab, the lithosphere-asthenosphere boundary and

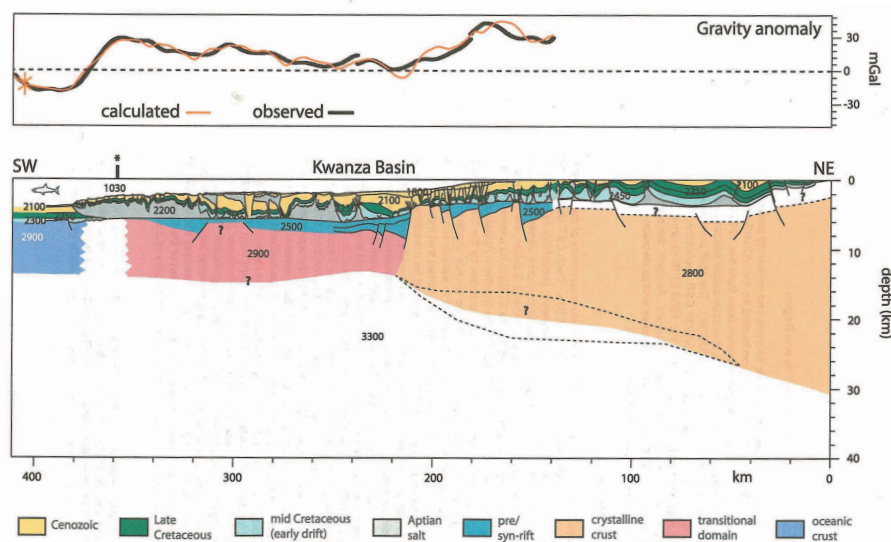


Figure 4.29 Gravity modeled transect over the Kwanza Basin, South Atlantic African margin. Densities are in kg/m^3 . Adapted from Blaich et al. (2010).

the Moho over a 3,000 km length of the western South American COB are illustrated in Figure 4.39.

4.5 Continental Rifts

Continental rifts, both modern and ancient, are widespread over all the continents with fossil (ancient or paleo) rifts occurring over an extensive range of Earth's history. They are evidence of significant horizontal extensional forces either present or past. Some current rifts may evolve into oceanic basins by continuing extensional forces, while ancient continental rifts indicate that the stresses causing them were aborted after only a relatively few to a few tens of kilometers of extension. Morphological continental rifts are commonly manifested as graben-like structures, typically asymmetric, filled with sediments, and tectonically they are defined as long narrow depressions. Olsen and Morgan (1995) have discussed the definition of various types of rifts and restricted the term continental rift to those in which the entire lithosphere has been modified in extension. Modern rifts are tectonically and/or magmatically active, and are subject to transient thermal phenomena. In contrast, paleorifts are tectonically inactive with respect to the extensional forces that originated them and without transient thermal phenomena.

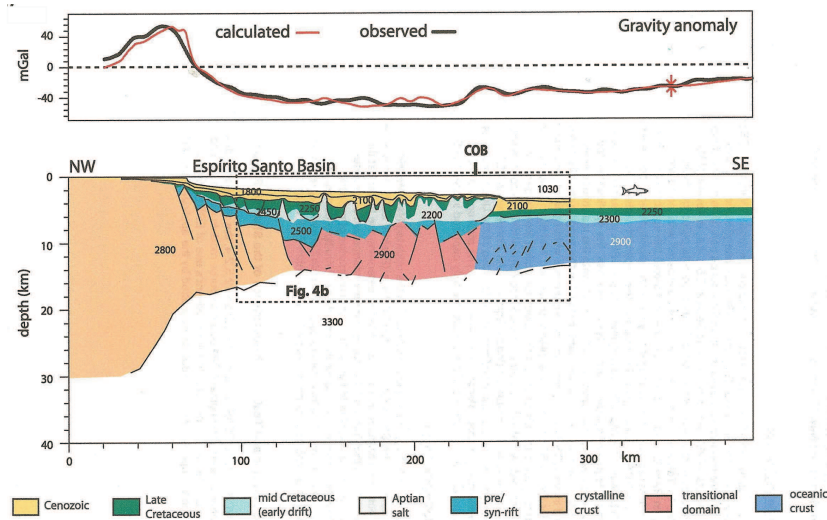


Figure 4.30 Gravity modeled transect over the Espírito Santo Basin, South Atlantic South American margin. Densities are in kg/m^3 . Adapted from Blaich et al. (2010).

The restriction of the term continental rift to those grabens involving the entire lithosphere is critical to their origin and important to their characteristics. Modern continental rifts are typically characterized by volcanism, high heat flow, anomalous crust and underlying mantle, regional uplift, and seismicity, while paleorifts have the resulting effects of rift-related magmatism in both the upper and lower crust, and possible seismicity associated with their ancient zones of crustal weakness that are reactivated in the modern stress field. In addition, modern rifts are typified by linear, surface, fault-bounded troughs filled with sediments. In paleorifts these trough sediments have been lithified, but may have been largely removed by erosion. Furthermore, paleorifts may be buried beneath sedimentary basins [e.g., DeRito et al. (1983); Hinze and Braile (1988)] as a result of subsidence shortly following the rifting event in accordance with the Earth's effort to achieve isostatic equilibrium or much later related to the densification of the crust by rifting magmatism.

The origin of continental rifts has been and remains a subject of considerable conjecture [e.g., Morgan and Baker (1983); Crough (1983); Robbins (1983b) and Bott (1995)]. However, there is general agreement that rifts may form either actively or passively in regard to the germane forces causing them. In simplified terms Olsen and Morgan (1995) differentiate between

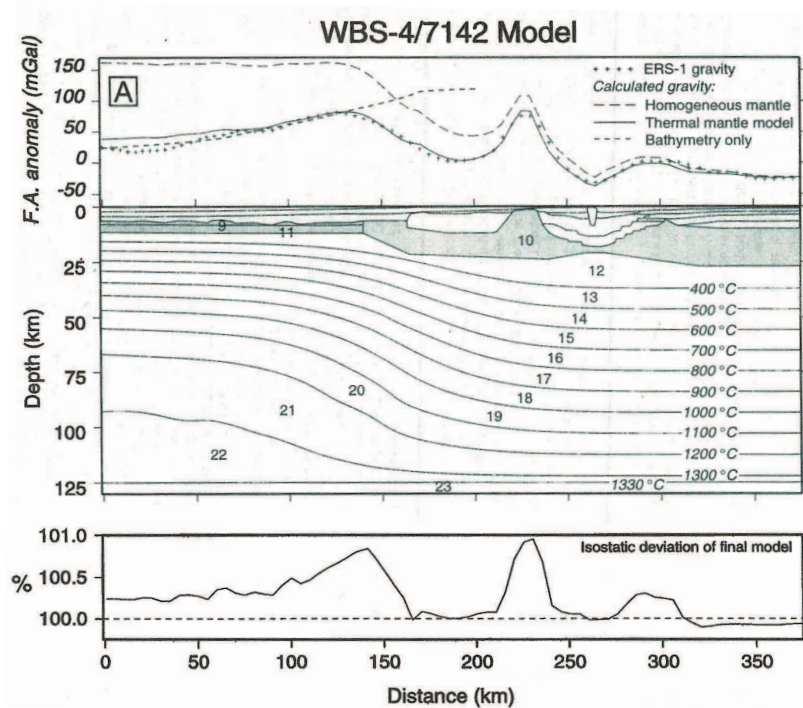


Figure 4.31 Comparison of observed free-air gravity anomalies along the WBS-4/7142 seismic profile with gravity models with differentiated crust and with and without thermally differentiated lithosphere mantle density. Isostatic deviations above the lithosphere boundary at 125 km are shown in the lower panel. Note the improved comparison of the observed and thermal model gravity anomalies over the homogeneous model. Adapted from Breivik et al. (1999).

these rifts on the basis of the origin of the causative stress field. Active rifts are caused by rifting (extension) in response to thermal upwelling in the asthenosphere, while passive rifting is in response to a remote stress field. Thus, active rifts are due to a (relatively) local stress field and passive rifts are caused by a regional stress field. Active rifting involves the interaction of a rising mantle plume on the lithosphere causing thinning of the lithosphere and tensional forces leading to rifting (Figure 4.39). Passive rifting (Figure 4-34) is caused by lithospheric tension from a distant source that leads to extension of the crust. Bott (1995) describes various alternatives associated with each type of rifting. It is notable that the uplift in response to the thinning of the crust and mantle lithosphere is unlikely to be the source of the tensional forces (Crough, 1983).

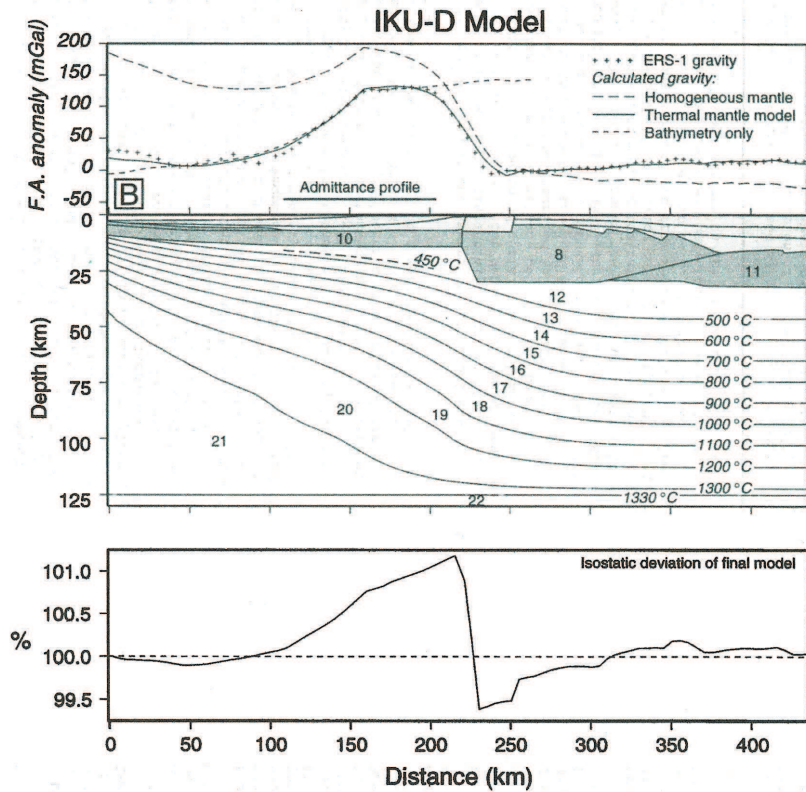


Figure 4.32 Comparison of observed free-air gravity anomalies along the IKU-D seismic profile with gravity models with differentiated crust and with and without thermally differentiated lithosphere mantle density. Isostatic deviations above the lithosphere boundary at 125 km are shown in the lower panel. Note the improved comparison of the observed and thermal model gravity anomalies over the homogeneous model. Adapted from Breivik et al. (1999).

Continental rifts have drawn the attention of geoscientists for many years because of their striking geology and topography. However, this interest has risen markedly because of their role in global evolution that has become apparent since the advent of plate tectonic concepts and the description of the Wilson cycle. Olsen and Morgan (1995) have described the significance of continental rifts. Basically, continental rifts provide insight to the origin of tensional forces in continental crust and their manifestation, they provide a window to the mantle geology and geochemistry via their igneous intrusions and volcanic rocks, they provide important information on the structure and nature of the rocks of a widespread tectonic feature of the continen-

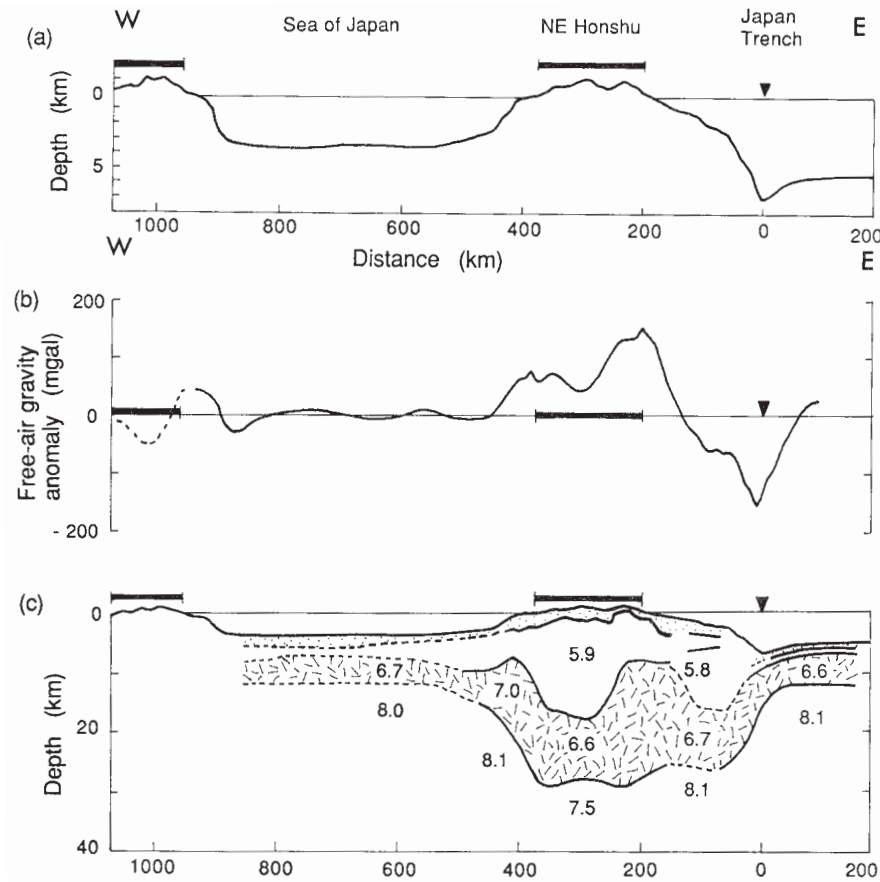


Figure 4.33 Cross-sections across the Japan Trench and Arc over the island of Honshu. (a) The topography and bathymetry profile. (b) The free-air gravity anomaly profile. (c) Crustal section with p-wave velocities. Adapted from Fowler (1990).

tal crust, and they are the site of both important natural resources and potential natural hazards including earthquakes and volcanoes. The latter significance has fostered much recent investigation of continental rifts. For example, the Mississippi embayment with its underlying rift has been the site of some of the highest magnitude intracratonic earthquakes (Stauder et al., 1977), and thus is the subject of continuing study. In addition, numerous mineral resources are associated with the sedimentary and igneous rocks of continental rifts [e.g., Robbins (1983a)], and in recent years have become important potential sources of hydrocarbons accumulating in rift sediments and geothermal power in active continental rifts.

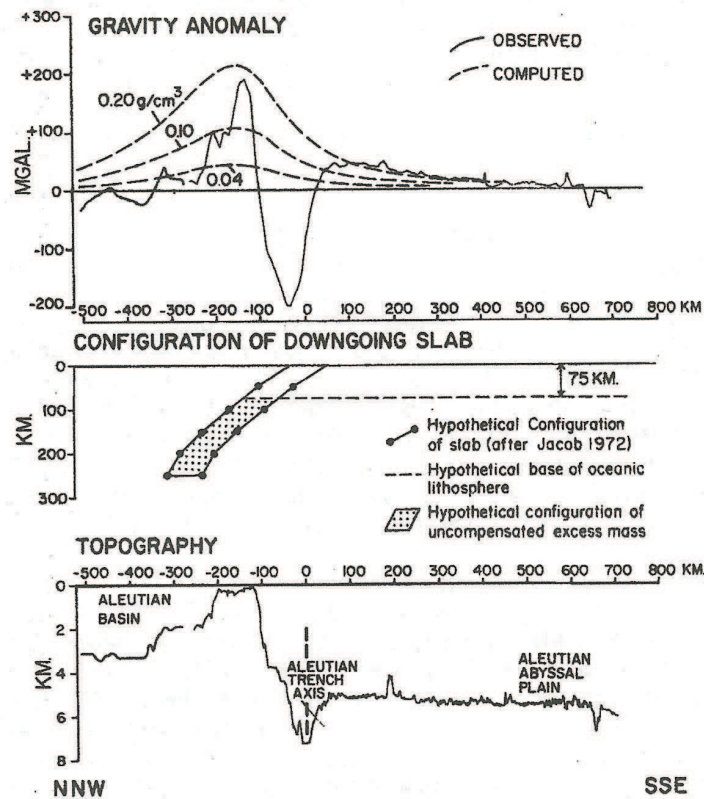


Figure 4.34 Computed gravity effect of a dense downgoing slab beneath the Aleutian Arc compared to the observed free-air gravity anomaly. Computations are shown assuming uniform densities of +0.04, +0.10, and +0.20 g/cm³. Note that to explain the positive anomalies forward of the trench, a uniform density of at least +0.20 g/cm³ is required. Adapted from Watts and Talwani (1974).

4.5.1 Gravity Attributes

Density contrasts between crustal rocks of continental rifts are among the highest on the continents. The density contrast between the sediments and sedimentary rocks and the enclosing rocks of the shoulders of rift grabens, the volcanic rocks and sediments, and the igneous intrusions, which are generally mafic due to their origin in the mantle, with the enclosing crystalline rocks of the crust are all significant. As a result of these contrasts and the intense structural deformation of continental rifts, gravity anomalies of rifts are among the most intense on the continents. These anomalies, that commonly transect older anomalies at high angles, cause patterns of anomalies

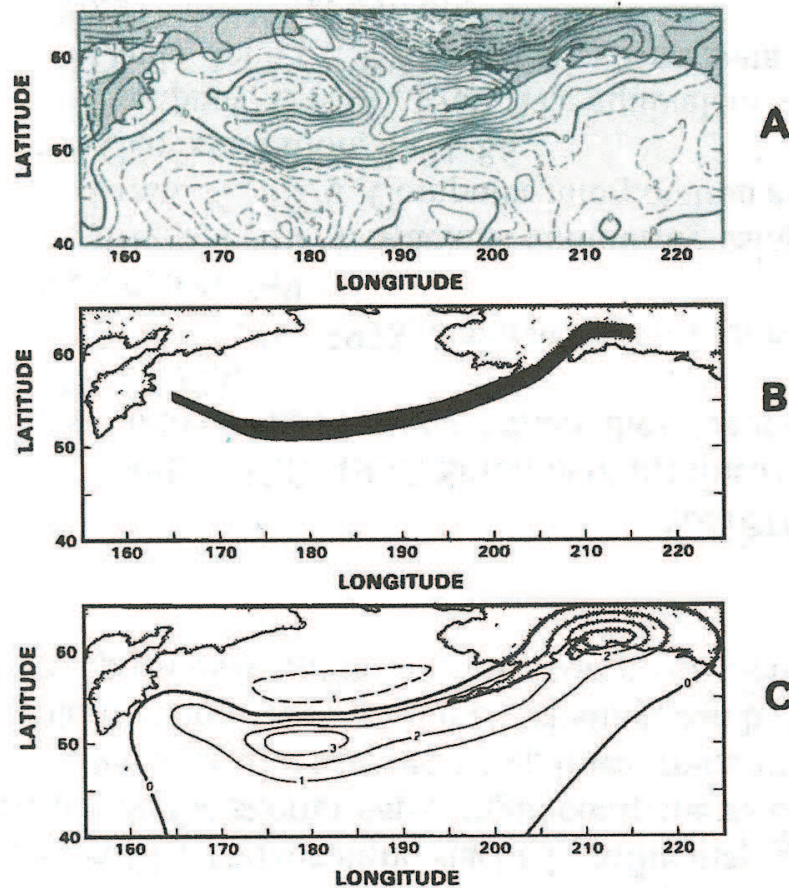


Figure 4.35 MAGSAT scalar magnetic anomaly and model calculations for the Aleutian Arc. (a) Averaged scalar magnetic anomaly in nanotesla from MAGSAT data. (b) Plan view of model body for downgoing slab. (c) Modeled magnetic anomaly in nanotesla at 400 km altitude. Adapted from Clark et al. (1985).

that commonly have offsets of several tens of kilometers or more between separate linear segments of the crude linear pattern. As a result gravity anomaly patterns are highly diagnostic of the location of rifts. This is illustrated in Figure 4.41 that is the Bouguer gravity anomaly map of the midcontinent of North America. The positive anomalies (red color) of the Midcontinent Rift System are highly visible cutting across the regional gravity anomalies. The rift anomaly extends northwesterly for over 2,000 km from Kansas in the southwest, through Lake Superior, and southeasterly to the southeast corner of Michigan.

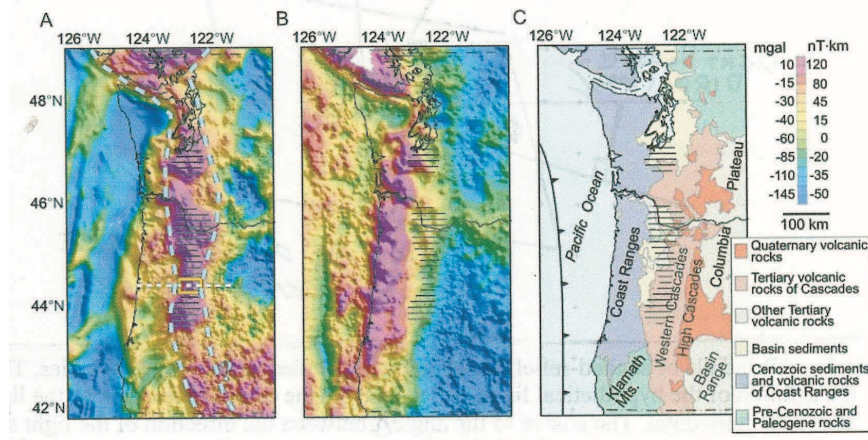


Figure 4.36 Cascadia potential-field anomalies and geology. (A) Aeromagnetic anomalies, transformed to magnetic potential (in nanotesla-km). (B) Bouguer gravity anomaly on shore, free-air anomalies offshore. (C) Generalized geology. Black horizontal line pattern shows location of magnetic anomalies of highest amplitude. White dashed line is the seismic profile. Adapted from Blakely et al. (2006).

It is impossible to present a characteristic gravity anomaly associated with continental rifts because of differences between modern and paleorifts, the range of structural disturbance, the extent of surface volcanic rocks, the depth of erosion, and the differences in the volume, location, and lithology of associated magmatic activity. Furthermore, there are numerous superimposed rift-related anomalies making it difficult to isolate anomalies from specific sources. This makes the ambiguity limitation of gravity interpretation even more difficult to overcome. For example, the negative gravity anomaly of a sediment-filled graben may be negated by the positive anomalies due to the positive anomalies of surface volcanic rocks or igneous intrusive rocks beneath the graben. Furthermore, negative anomalies due to thinning of the crust in modern rifts may be difficult to resolve because of positive anomalies from igneous intrusions or magmatic underplating of the crust and thickening of the crust in paleorifts may be superimposed on anomalies of similar wavelengths and amplitude from sedimentary rocks in overlying basins that developed after the primary rifting event. As a result the successful interpretation of gravity anomalies observed over modern or paleorifts is highly dependent on constraining geological information which in part is obtained from surface geology, but most importantly from supplemental geophysical data, primarily from crustal seismic and magnetotelluric profiling (Bott and Hinze, 1995).

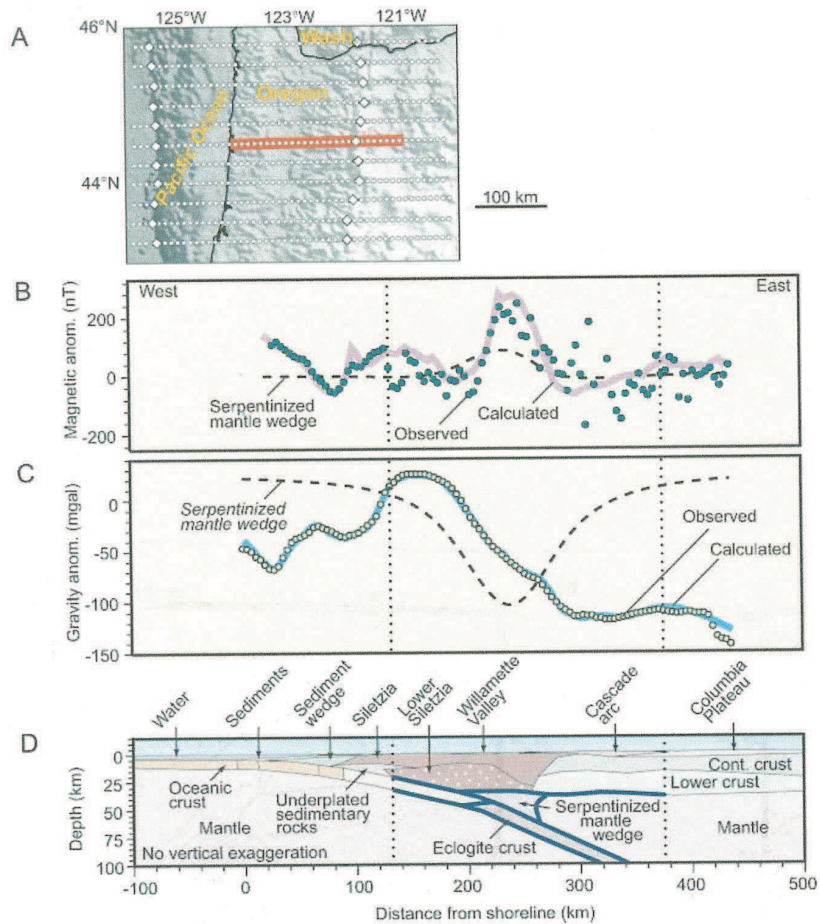


Figure 4.37 Simultaneous observed and modeled gravity and magnetic anomalies of Oregon forearc. (A) Topography and bathymetry of the western Oregon and offshore regions. Red line is seismic profile. (B) Stacked magnetic anomaly profile of 11 profiles shown by east/west white dotted lines in (A). (C) Stacked gravity anomaly profile. (D) Crust and upper mantle used in modeling results shown in (B) and (C). Physical properties of components of this profile are given in Table 1 of Blakely et al. (2006). Adapted from Blakely et al. (2006).

Nonetheless some generalities can be made regarding gravity anomalies. Broad, regional negative Bouguer gravity anomalies are observed over the regional topographic swells associated with modern continental rifts, but the free-air anomalies tend to average out to zero reflecting that isostatic equilibrium is approached. These rifts typically have intense negative grav-

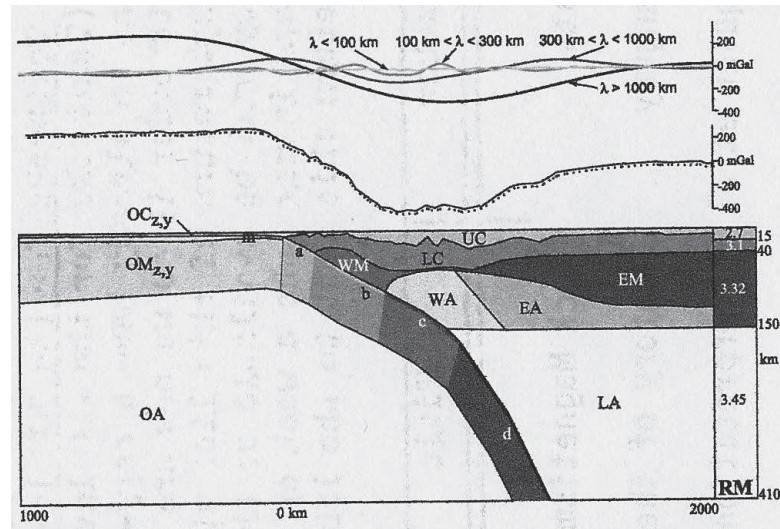


Figure 4.38 Typical observed and modeled Bouguer gravity anomaly used by Tessara et al. (2006) to map the nature of the crust and upper mantle at the western South America COB to a depth of 410 km. Densities used are discussed in the text and given by Tessara et al. (2006) in Table 1. Adapted from Tessara et al. (2006).

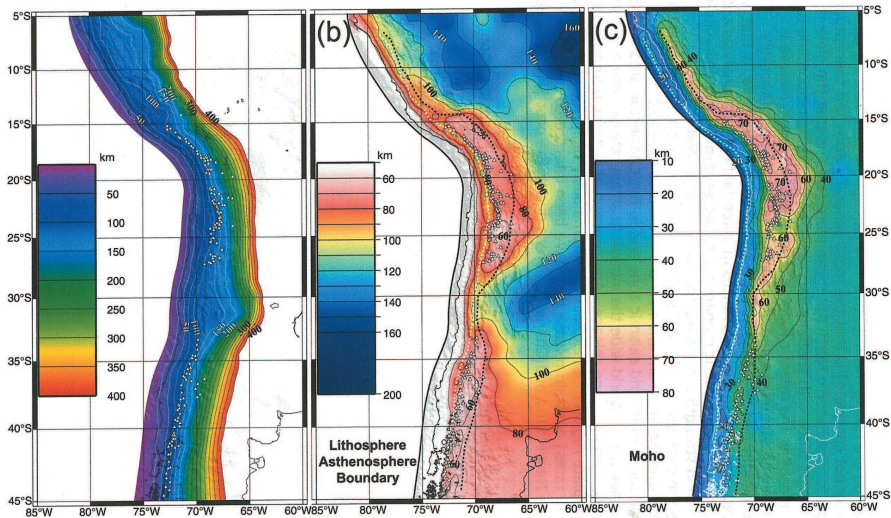


Figure 4.39 Contour maps of the depth to the downgoing slab with 25 km contours (a), lithosphere/asthenosphere boundary (b), and Moho depth (c) resulting from the gravity anomaly modeling along a 3,000 km length of the western South American COB. Adapted from Tessara et al. (2006).

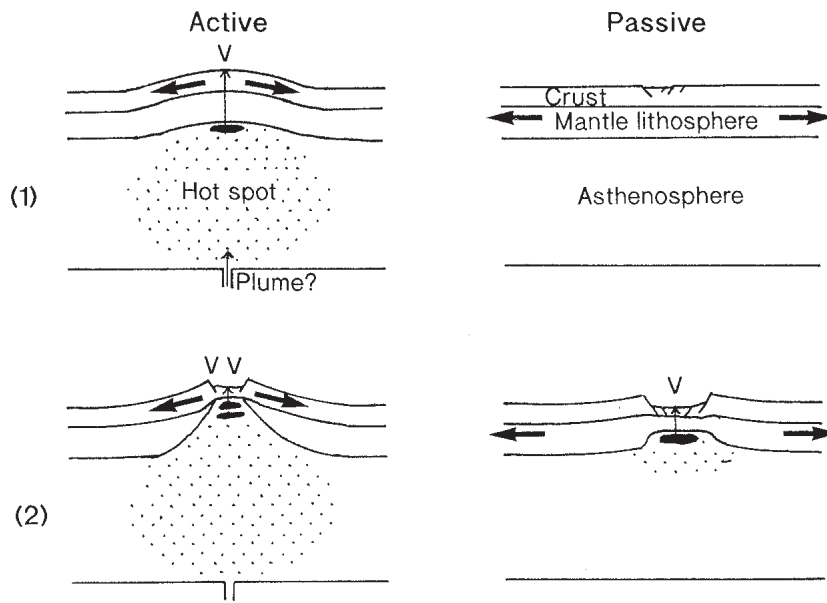


Figure 4.40 Idealized diagrams of a cross-section of the crust, mantle lithosphere, and asthenosphere comparing the results of active and passive rifting at the initial stage (1) and a subsequent stage of development (2). The stippling indicates hot, low-density regions of the crust that rise by buoyancy. V denotes volcanism and black components are magma. Adapted from Bott (1995).

ity anomalies over the grabens, but the anomalies are complicated by the amount of magmatism leading to mafic intrusives, as well as extrusive rocks, and their associated positive anomalies, as well as the lower density of the mantle material in the rising plume of active rifts. In paleorifts the crust is generally thickened, producing a regional negative Bouguer gravity anomaly, but the free-air gravity anomalies typically tend to zero because of the compensating positive anomalies from mafic intrusives into the lower and upper crust and volcanic rocks. Commonly, but not necessarily paleorifts are identified by positive anomalies because of the abundance of magmatic intrusions and extrusions and minimal sedimentary rocks as a result of non-deposition or erosion. A typical gravity anomaly over a paleorift (the Midcontinent Rift of the U.S. midcontinent) is illustrated in Figure 4.42 together with a crustal section.

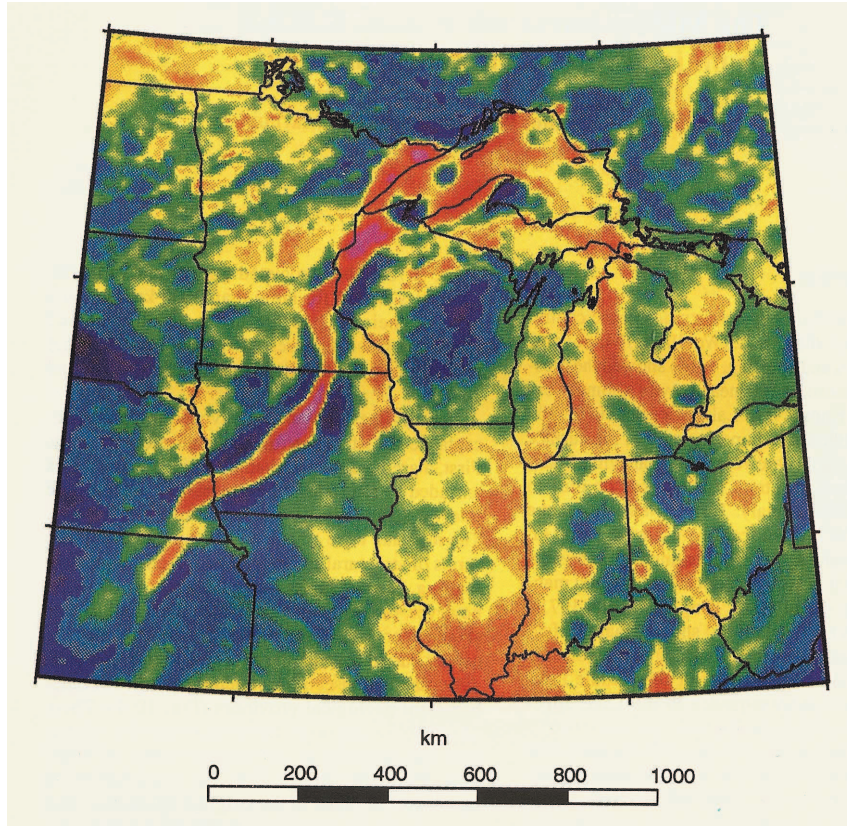


Figure 4.41 Bouguer gravity anomaly map of the midcontinent of North America. Note the positive (red) anomaly that follows the Midcontinent Rift System from Kansas in the southwest to Lake Superior and then southeasterly through Michigan. Adapted from Allen et al. (1995).

4.5.2 Magnetic Attributes

Magnetization contrasts of continental rifts, like density contrasts, are intense, but unlike density contrasts they are limited. Nonetheless, the distinctive magnetic anomaly patterns of crystalline crustal rocks are disrupted by anomalies derived from rift rocks readily locating the linear grabens of rift systems that cut them at obtuse angles (Figure 4.43). The abundance of magnetic anomaly maps that cover most continental regions has greatly improved the identification of continental rifts. These disrupting anomalies in both modern and paleorifts arise primarily from the subdued nature of the magnetic anomaly pattern of basement rocks which are buried at much greater depths than they are on the rift shoulders and the presence of mafic

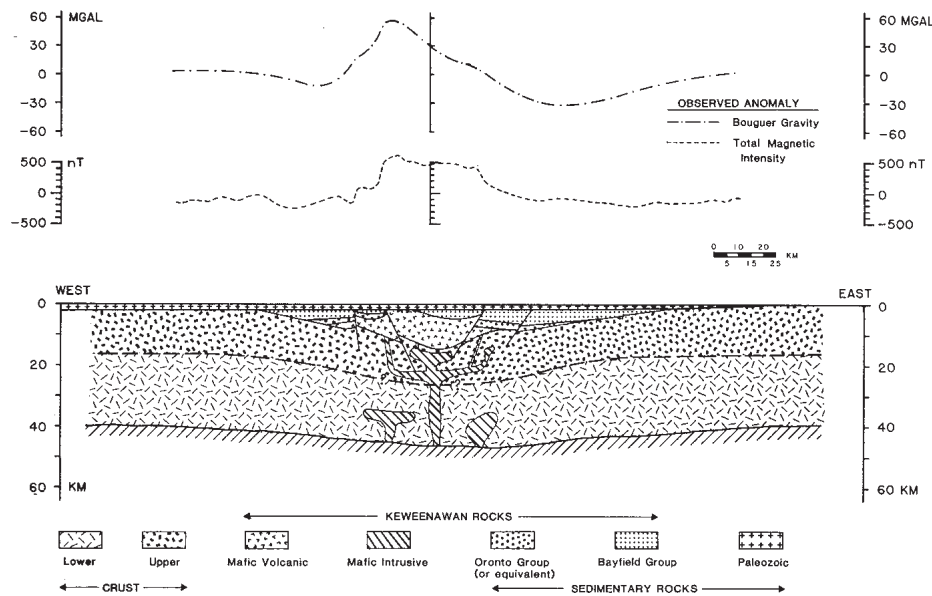


Figure 4.42 Hypothetical idealized crustal cross-section and Bouguer gravity and total magnetic intensity anomaly profiles across the western limb of the Midcontinent Rift System. Adapted from Hinze and Kelly (1988).

volcanic rocks that commonly carry an intense remanent magnetization and to a lesser extent mafic intrusives unless they are near the surface (Figure 4.41). The anomalies associated with lower crustal intrusives are difficult to observe. An additional anomaly source in modern rifts is the rise of the Curie point isotherm ($\approx 560^{\circ}\text{C}$.) due to enhanced heat flow which results in a broad, regional magnetic minimum that is difficult to discern in a complex array of anomalies.

4.5.3 Examples of Modern Continental Rifts

4.5.4 a) European Cenozoic Rift System

One of the more extensively studied modern continental rifts is the European Cenozoic Rift System (ECRS) that extends for 1,100 km across western Europe from the North Sea to the Mediterranean Sea (Figure 4.44), although it is likely to extend across the Mediterranean Sea into North Africa. It consists of a series of more or less linear rift structures that developed during the main and late Alpine orogenic phases (Ziegler, 1992). The central part of the zone is made up of the Rhine Graben that has been intensely studied both geologically and geophysically and has been recognized as a rift since

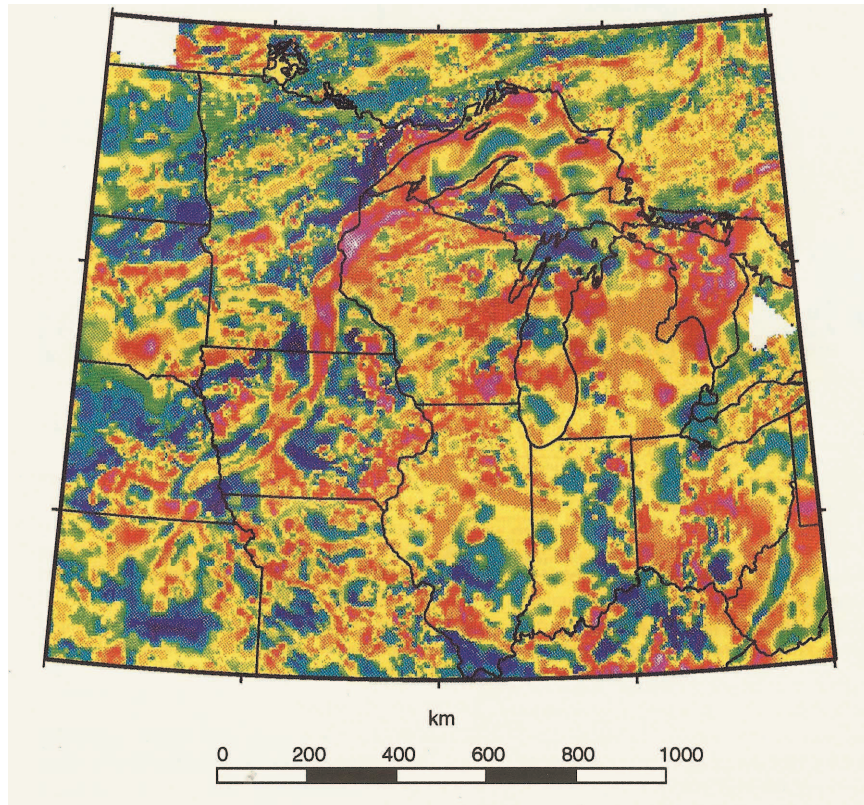


Figure 4.43 Total magnetic intensity anomaly map of the midcontinent of North America showing the position of the Midcontinent Rift System by the positive (red) magnetic anomalies transecting the regional anomaly trends extending from Kansas in the southwest to Lake Superior, and then with less continuity than the Bouguer gravity anomaly (Figure 4.41) across Michigan. Adapted from Allen et al. (1995).

the mid-1800s. The rift started to develop during the late Eocene as a result of NNE Alpine compression. The deepest portion of the Rhine Graben lies north of the bounding Black Forest and Vosges Mountains where it is filled with more than 3.5 km of sediments (Figure 4.45).

The Bouguer gravity anomaly map of the Rhine Graben (Figure 4.46) shows the intense minimum especially in its northern half cutting across the regional gravity anomaly pattern. The vertical gradient of this map (Figure 4.47(a)), clearly indicates the boundary and intra-graben faults as illustrated in Figure 4.47(b). Modeling of the Bouguer gravity anomaly profile by Rotstein et al. (2006) identified as AA on Figure 4.47(a) is shown in Figure 4.48. A significant component of this modeled anomaly is derived from

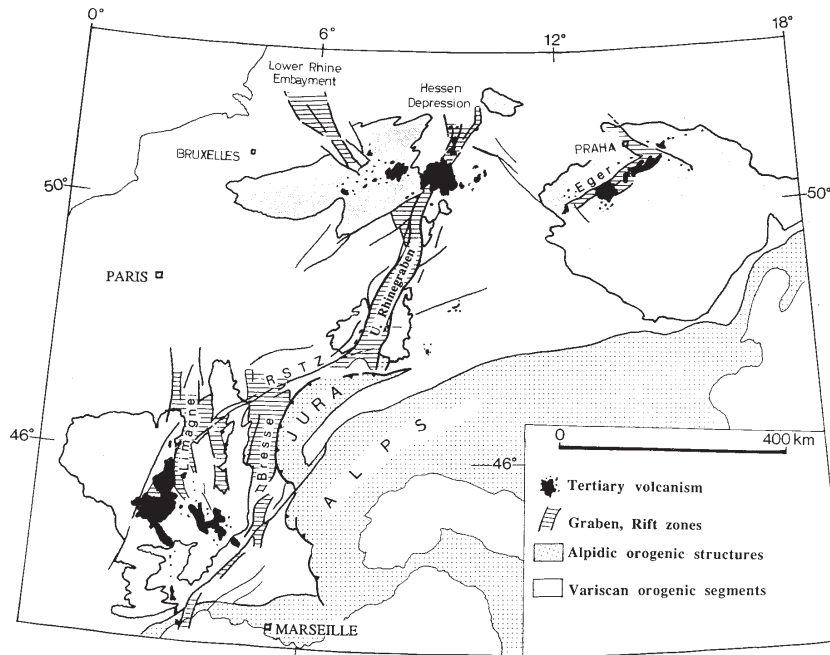


Figure 4.44 The European Cenozoic Rift System between the North Sea and the Mediterranean Sea. Adapted from Prodehl et al. (1995).

density contrasts placed within the basement rocks. However, other workers [e.g., Rousset et al. (1993)] have found significant anomaly components related to a thinning of the crust along the rift, intra-crustal sources, and a regional lower density upper mantle. Prodehl et al. (1995) provide an extensive overview of the use of geophysics, including gravity and magnetic data, in studying the ECRS, and the Rhine Graben in particular. Their review supports the association of the rift with a thinned crust and lithosphere and lower density upper mantle that are primary characteristics of modern rifts. The magnetic studies of the rift system have largely focused on mapping the intense anomalies associated with the related volcanic rocks.

4.5.5 b) East African Rift System

The East African Rift System (EARS) extends through a topographic swell in east Africa from roughly 15°S (Malawi) to the Red Sea at 15°N (Figure 4.49) as a series of long, linear, disjointed troughs. It has been extensively investigated since the late 1800s to the present day. It was here that the gravity method was first applied to rifts (Bullard, 1936). It is identified as

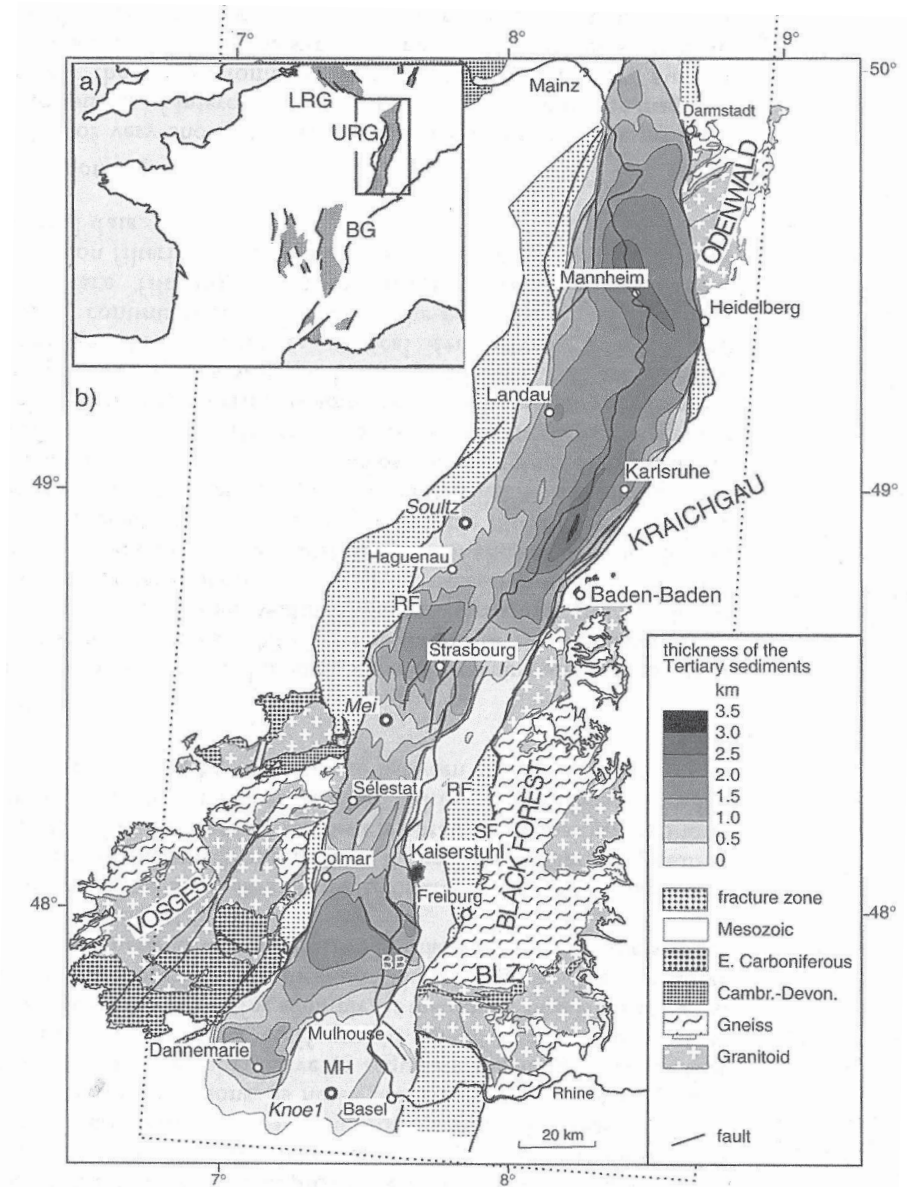


Figure 4.45 Geological map of the upper Rhine Graben (URG) of the European Cenozoic Rift System. Adapted from Rotstein et al. (2006).

an active rift and is the benchmark rift with which other rifts, modern and paleorifts, are compared. It has evolved since the early Tertiary, generally advancing south from the Red Sea. The EARS is commonly divided into

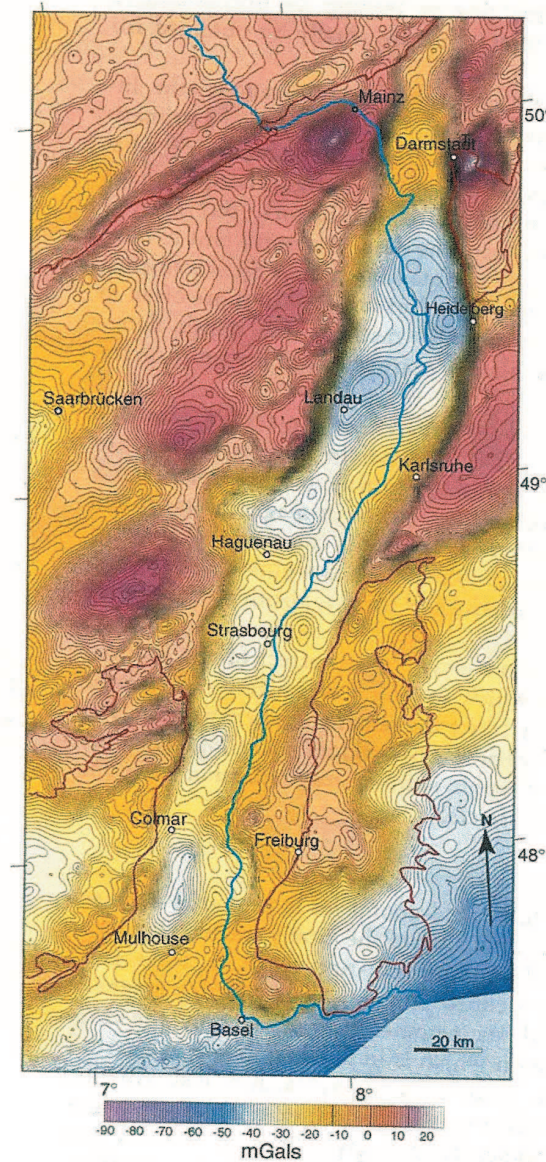


Figure 4.46 Complete Bouguer gravity anomaly map of the upper Rhine Graben. Contour interval is 1 mGal. Adapted from Rotstein et al. (2006).

at least three segments: the Western rift, the Kenya rift that lies to the east, and the Ethiopian rift to the north that intersects with the Red Sea rift. All of these segments developed at somewhat different times and involve variable magmatic activity. The Western rift has significantly less rift-related

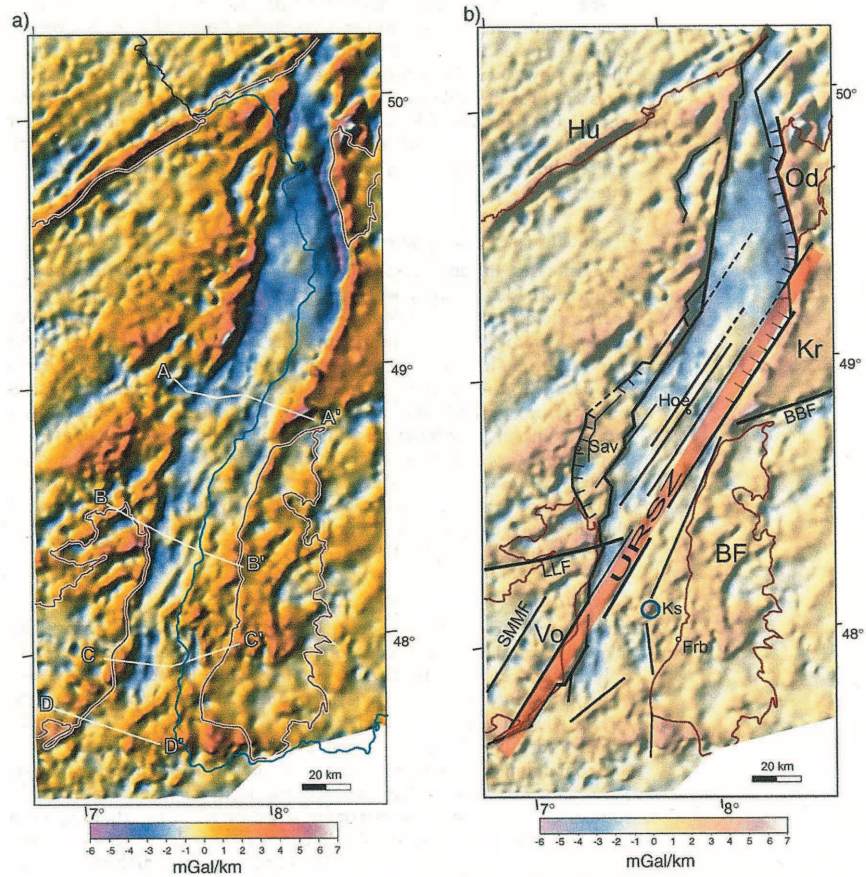


Figure 4.47 (a) Vertical gradient gravity anomaly map of the gravity anomaly shown in Figure 4.46. Profile AA is modeled in Figure 4.48. (b) Figure 4.47(a) with faults superimposed. URSZ is the Upper Rhenish Shear Zone. Adapted from Rotstein et al. (2006).

volcanic rocks than the other segments and the original crust of the northern portion of the Ethiopian rift (the Afar segment) has been largely replaced by magmatic products.

The Bouguer gravity anomaly of the topographic swell is a large regional gravity anomaly minimum while the free-air gravity anomaly averages close to zero indicating that the topography is compensated at depth leading to an isostatic equilibrium state. Superimposed upon these regional anomalies are a variety of local anomalies associated with the rift structures. They change with location, reflecting the crustal separation, magmatic activity,

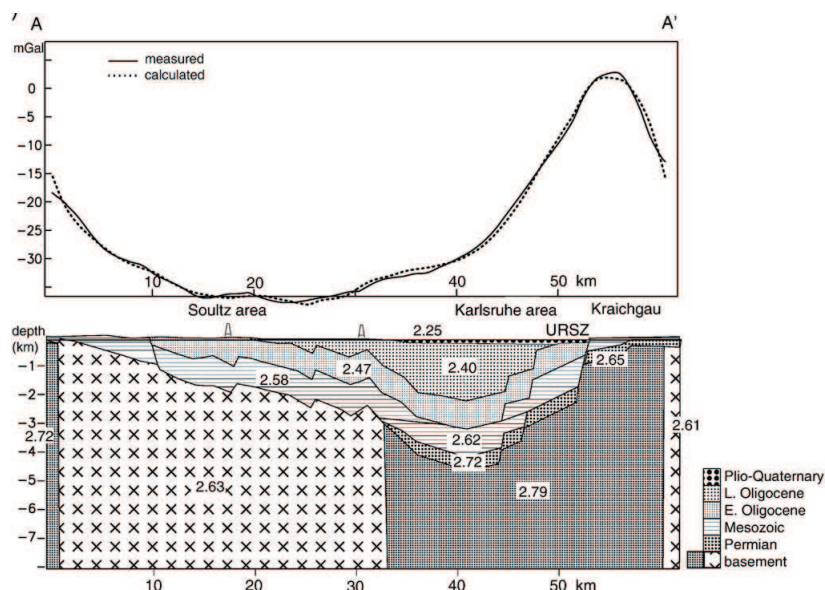


Figure 4.48 Observed and modeled Bouguer gravity anomaly profile of AA on Figure 4.47(a) and modeled crustal section. Adapted from Rotstein et al. (2006).

lithospheric modifications, and the variable depths of the sediments and their structure in the rift troughs. Crustal separation and intense magmatic activity in the Ethiopian rift results in positive anomalies. The rifts farther south are noted for their intense negative anomalies and local positive anomalies associated with the prominent mafic volcanic rocks of the rift system. However, the anomalies derived from surface rocks and the upper crust are complicated by the effects of intrusions into the lower crust, thinning of the crust, and modifications in the upper mantle due to partial melting of the rising, more buoyant rocks of the mantle plume as illustrated in Figure 4.50. The Kenya Rift has an axial positive anomaly of about 50 mGal superimposed on the regional minimum. The source of the axial high is subject to controversy, but is likely associated with magmatic activity in the crust. A comprehensive gravity anomaly model across the Kenya rift near the equator taking into account pressure-dependent velocity-density relationships for the crustal rocks and mantle densities derived from seismically measured velocities is presented in Figure 4.51. Of particular note in this model is the thinning of the crust and the low-density mantle plume beneath the rift.

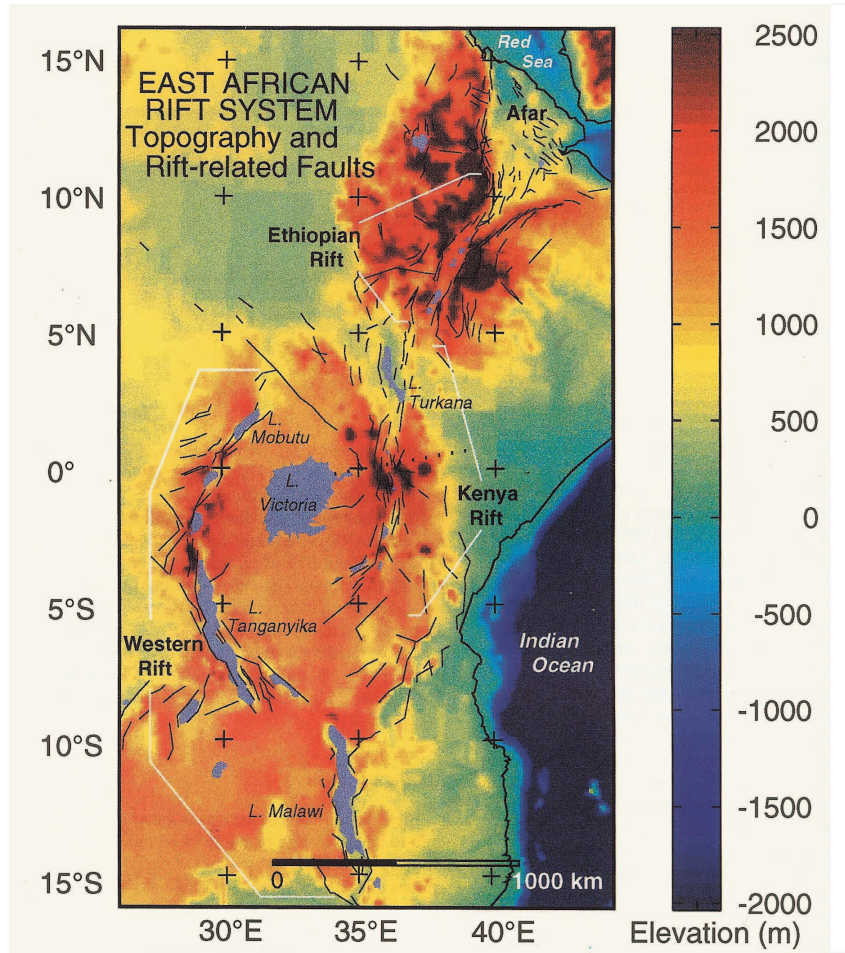


Figure 4.49 Topographic map of East Africa. Elevations higher than 2,500 m are shown in dark red. Lakes irrespective of elevation are shown in blue. The major faults are indicated by thin black lines. Adapted from Braile et al. (1995).

4.5.6 c) Rio Grande Rift

The Rio Grande Rift is one of the more striking active rifts of North America. It lies on the western margin of the broad region of uplift, the Colorado Plateau that bounds the Basin and Range province that makes up much of the southwestern U.S. The rift that extends as a series of north-south trending, interconnected, asymmetrical basins from southern Colorado to the Rio Grande River in Texas has undergone lithospheric thinning and crustal extension during the middle to late Cenozoic (Figure 4.52). Its origin

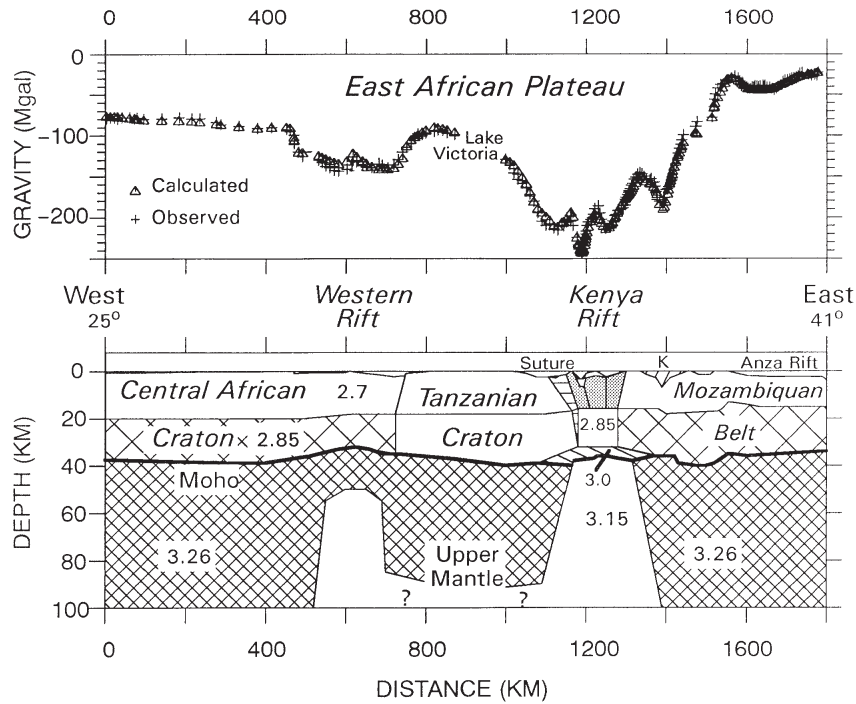


Figure 4.50 Regional Bouguer gravity anomaly model across the Western and Kenya rifts along the equator. Numbers indicate densities in g/cm^3 . Upper crustal densities in the Kenya rift valley are slightly ($0.01 - 0.02 \text{ g}/\text{cm}^3$) higher than in the adjacent areas. Adapted from Braile et al. (1995).

is generally related to plate boundary forces of the southwestern margin of the North American Plate (Baldrige et al., 1995).

The gravity pattern of the central portion of the rift is shown in the residual isostatic gravity anomaly map of Figure 4.53. The most obvious anomalies are the minima over depositional centers in the rift due to the density contrast between the low-density sediments and the surrounding basement rocks. Cordell (1982) has observed that these relative short-wavelength minima are superimposed, as in other active rifts, on a long-wavelength gravity low associated with a broad zone of low-seismic and density upper mantle and intermediate-wavelength anomalies due to crustal thinning and/or crustal intrusions. Accurate use of gravity to map the configuration of the basins requires identification and removal of these secondary components of the gravity field.

Magnetic anomaly data of the rift region primarily provide information on the surface volcanic rocks and the pre-rifting structures. Cordell (1976) has

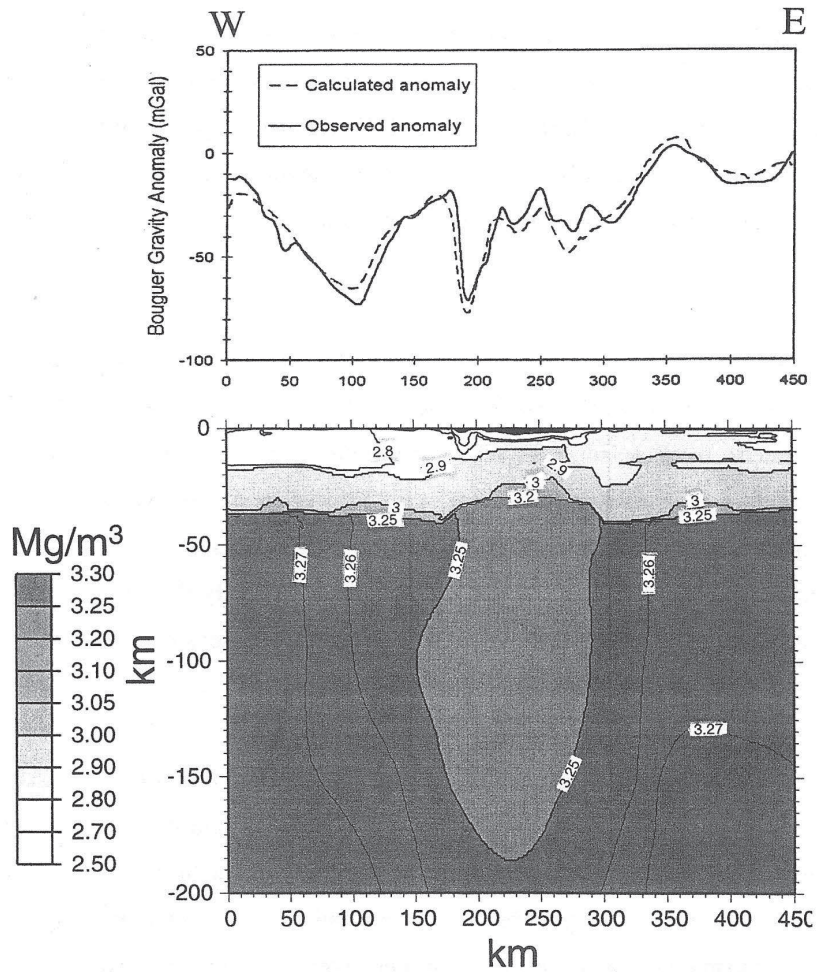


Figure 4.51 Gravity anomaly modeling of the lithosphere to a depth of 200 km beneath the Kenya rift at the equator using pressure-dependent velocity-density relationships and densities within the mantle obtained from seismically measured velocities. Adapted from Ravat et al. (1999).

noted the relationship between gridded patterns in the magnetic anomalies and in the patterns of faulting which he interpreted to indicate the control of pre-existing faults on the rift-bounding faults. Furthermore, Grauch and Hudson (2007) and Grauch et al. (2009) have used detailed magnetic profiling in the basins of the rift to map and characterize structures in the sediments and sedimentary rocks. Finally, Mayhew (1982) has used satellite

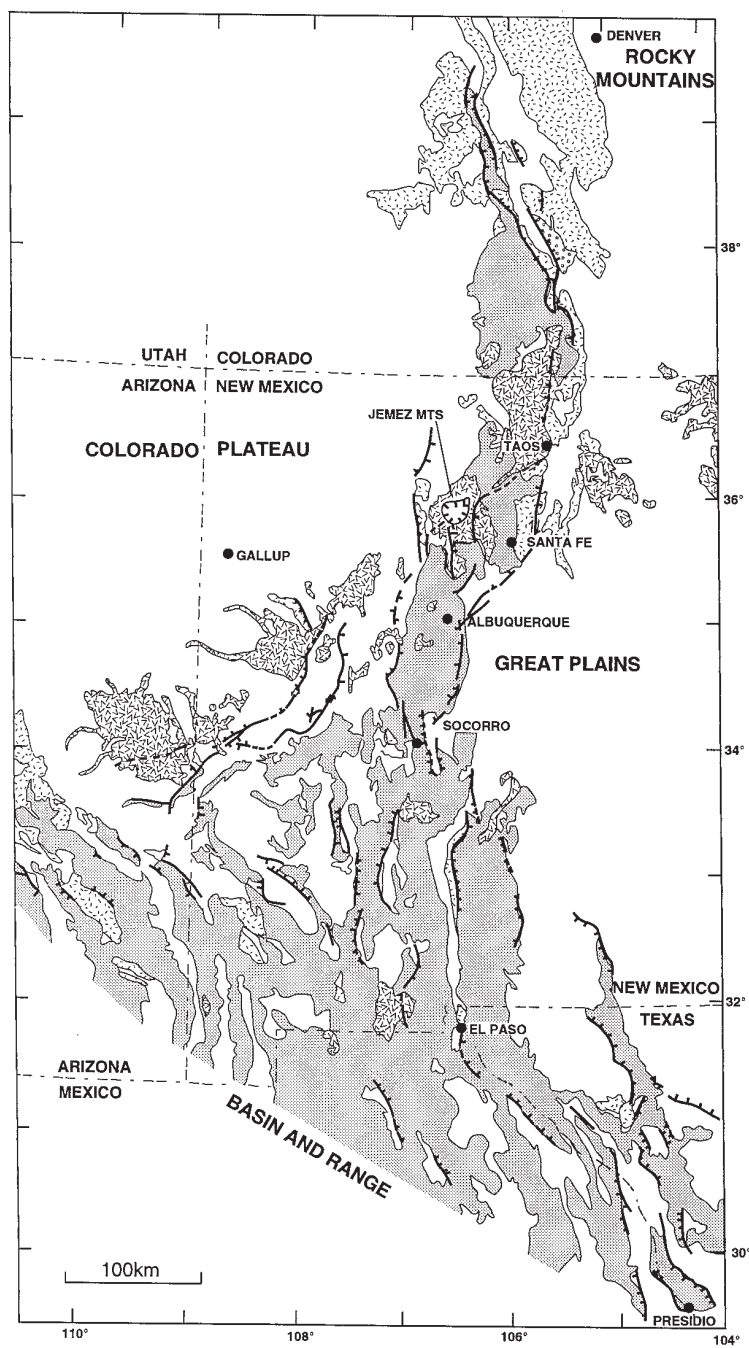


Figure 4.52 Tectonic map of the Rio Grande Rift. Shaded portion is Miocene to Quaternary sediments and sedimentary rocks of middle to late Cenozoic basins. The "V" pattern is volcanic rocks younger than 15 Ma. Dashed pattern is Precambrian rocks of adjoining uplifts. Adapted from Baldrige et al. (1995).

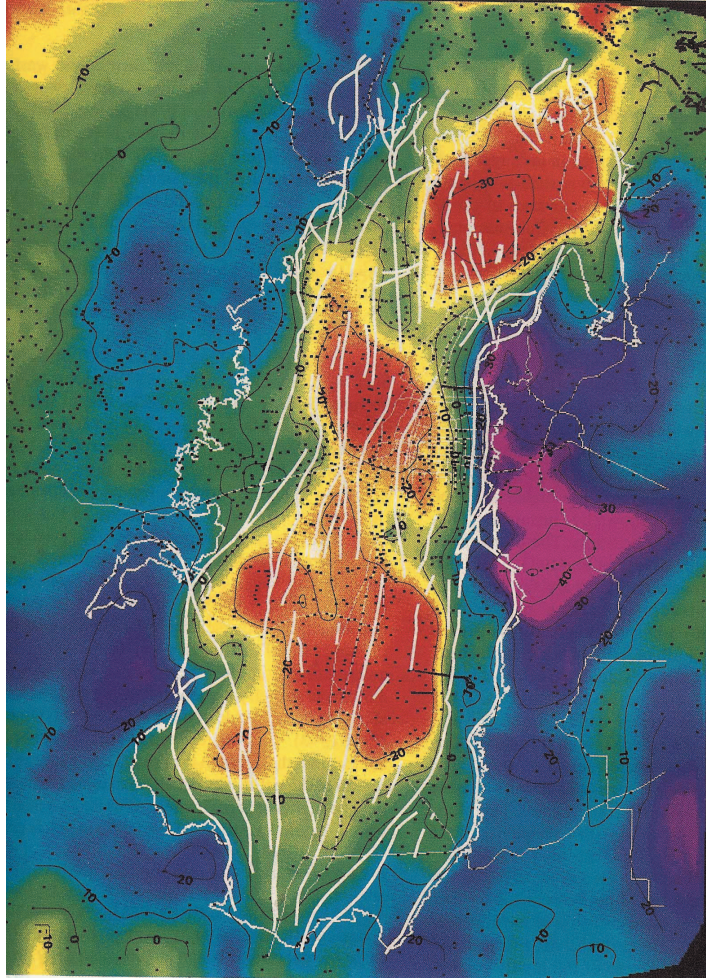


Figure 4.53 Residual isostatic gravity anomaly map of the Albuquerque-Belem basin in the central Rio Grande Rift. Contour interval is 10 mGal. The red colors are gravity anomaly minima and the blue through magenta are high values on the borders of the rift basin. Adapted from Baldrige et al. (1995).

magnetic anomaly data to investigate the isotherms in the Rio Grande Rift region.

4.5.7 d) *Baikal Rift System*

The Baikal Rift System extends for approximately 2,000 km along the southwestern edge of the Siberian platform in south-central Siberia (Figure 4.54).

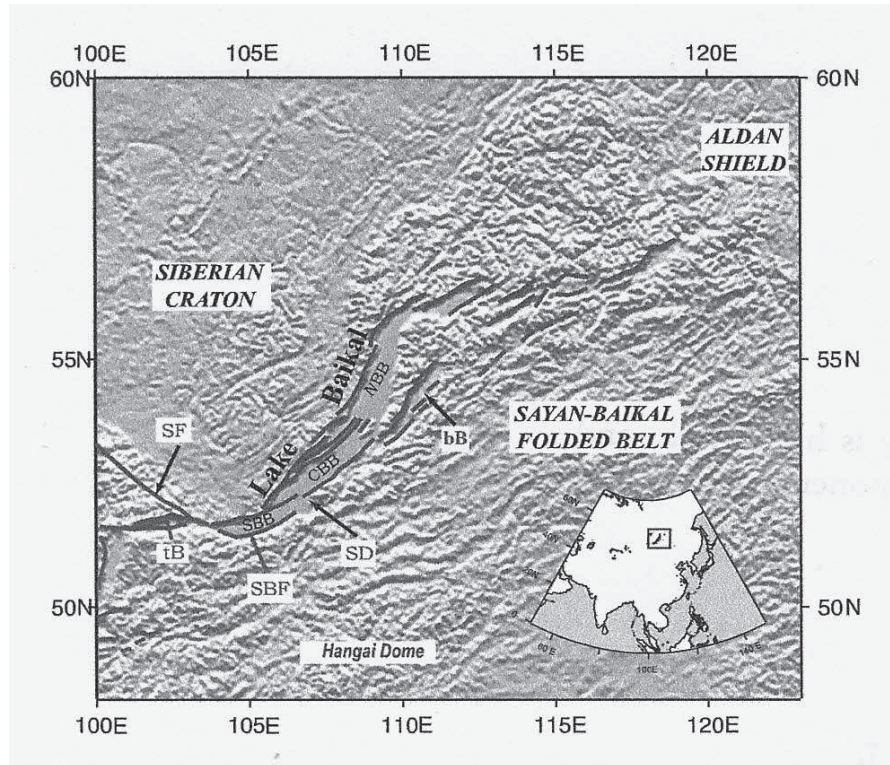


Figure 4.54 Topography and location of the main faults and structural units in the vicinity of the Baikal Rift System. Adapted from Tiberi et al. (2003).

It is most notable for Lake Baikal, the most voluminous and one of the oldest lakes on the Earth, which occupies the central third of the rift. It has been the subject of intensive study both by the Russian and international communities of geoscientists. It occurs on the topographic swell characteristic of modern continental rifts and consists of numerous depressions in much the same way as the East African Rift System. It lies 2,000 km from the nearest plate boundary (Keller et al., 1995) and is the most seismically active continental rift. The rift has been identified by some investigators as a passive rift rather than an active rift as it is currently accepted in the geoscience literature. It has many characteristics in common with the East African Rift System [e.g., Logatchev et al. (1983), but the differences in amount of magmatism and structure suggest that the degree of partial melting is lower in the Baikal Rift System.

Much of the rift is marked by a negative gravity anomaly (Figure 4.55).

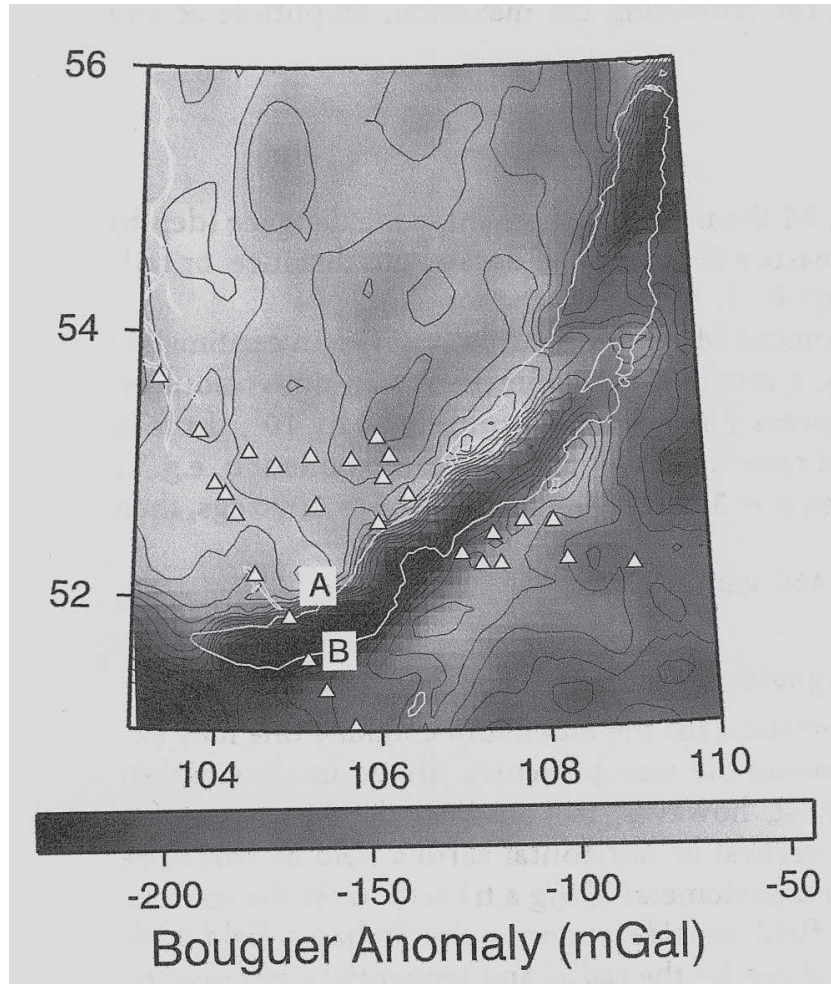


Figure 4.55 Bouguer gravity anomaly map of the Baikal Rift System. White triangles are the seismological stations used by Tiberi et al. (2003) to collect seismic data for joint inversion with the gravity anomaly data. Adapted from Tiberi et al. (2003).

that attains local minima of up to 80 mGal in the southern Lake Baikal region reflecting the sediments in the depression. A regional negative Bouguer gravity anomaly correlates with the uplifted region that is interpreted to be associated with a low-density upper mantle (density contrast of -0.03 gm/cm^3) associated with a rise in the asthenosphere (Logatchev et al., 1983). However, Ruppel et al. (1993) using gravity anomaly data concluded that the lithosphere of the rift may be anomalously cold for an active rift. Tiberi et al. (2003) have studied the deep structure of the rift zone by joint in-

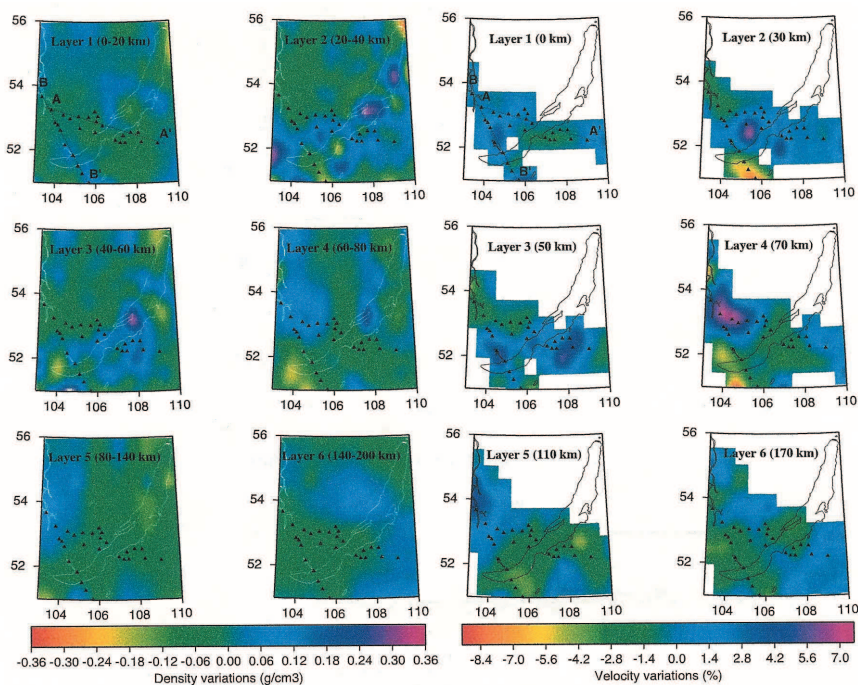


Figure 4.56 Density of layers of the lithosphere at various depths obtained from joint inversion of the gravity anomaly and velocity data obtained from the seismic analysis. Adapted from Tiberi et al. (2003).

version of the gravity anomaly and teleseismic data. Their results that are shown in Figure 4.56, support the effect of lithospheric extension combined with influence from inherited heterogeneities for the origin of the Baikal Rift System. Keller et al. (1995) report on the pattern of aeromagnetic anomalies over the rift system that are subdued over the rift zone and mimic the pattern of the local basement rocks.

4.5.8 Examples of Paleorifts

4.5.9 a) Oslo Rift

The Paleozoic Oslo Rift extends for some 400 km northward within the Precambrian rocks of Norway from its offshore intersection with the Sorgenfrei-Tornquist tectonic zone. It consists of a series of graben segments bounded by roughly N/S trending faults (Figure 4.57). It is noted for its intense and geologically interesting magmatic rocks which are believed to be the combined result of interaction between two lithospheric mantle sources and

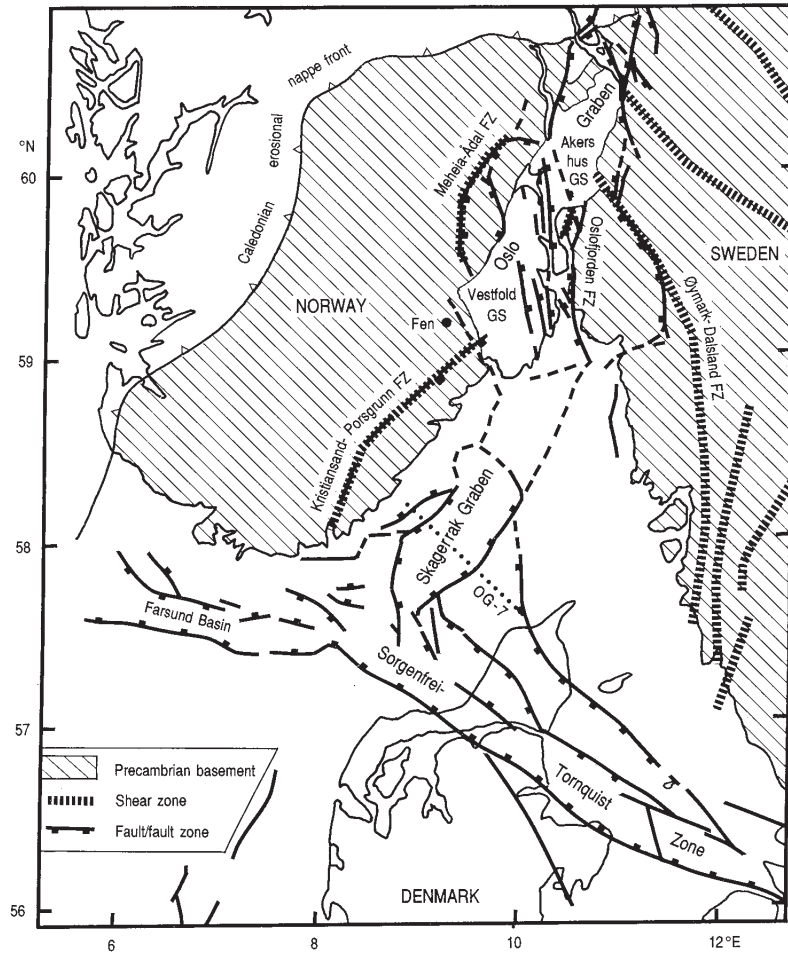


Figure 4.57 Density of layers of the lithosphere at various depths obtained from joint inversion of the gravity anomaly and velocity data obtained from the seismic analysis. Adapted from Tiberi et al. (2003).

contamination from crustal rocks of varying depths Neumann et al. (1992). Magmatic rocks are thought to be a major outcrop component of the rift because of the depth of erosion of the rift that is of the order of 3 km. The structure of the rift has been studied with seismic profiling complemented by gravity data. Figure 4.58, the Bouguer gravity anomaly map of the rift, shows a complex positive anomaly associated with the Permian igneous and sedimentary rocks that fill the graben. Figure 4.59 shows the results of modeling the positive gravity anomaly associated with the Vestfold graben. The gravity interpretation suggests a thinned crust with positive effects from

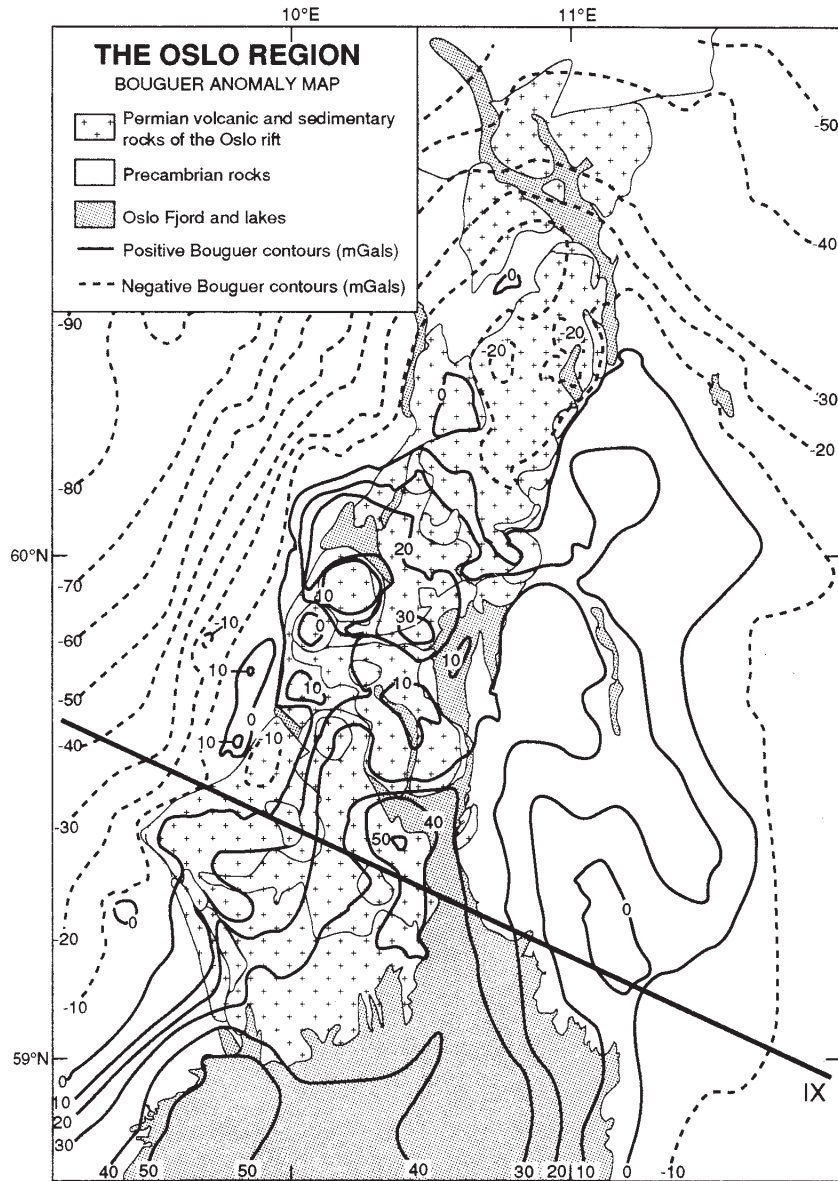


Figure 4.58 Density of layers of the lithosphere at various depths obtained from joint inversion of the gravity anomaly and velocity data obtained from the seismic analysis. Adapted from Tiberi et al. (2003).

lower and upper crustal intrusives of a mafic nature. The magnetic anomalies of the rift reflect the strong magnetization of the Oslo rift igneous rocks

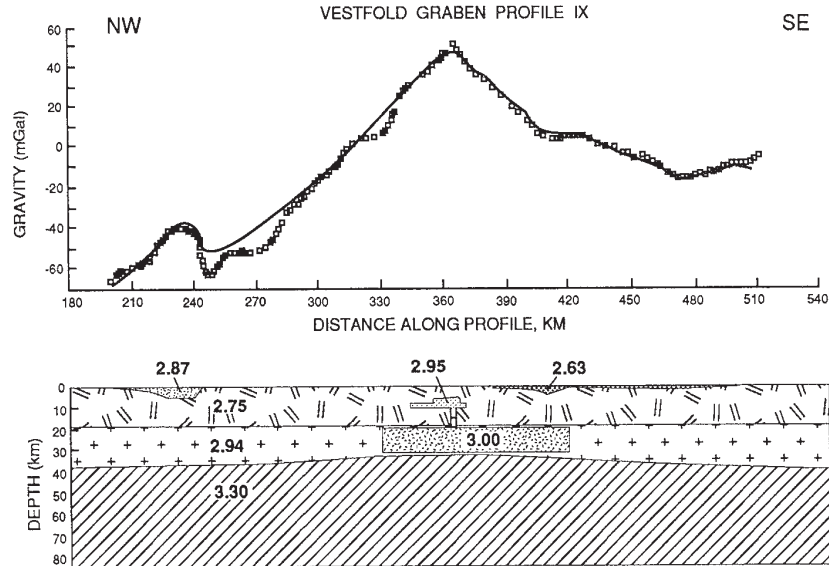


Figure 4.59 Density of layers of the lithosphere at various depths obtained from joint inversion of the gravity anomaly and velocity data obtained from the seismic analysis. Adapted from Tiberi et al. (2003).

in contrast to the generally lower intensities and short-wavelength of the enclosing Precambrian terrane.

4.5.10 b) Midcontinent Rift System

Gravity and magnetic mapping in the central U.S. indicated a major linear basement structural feature that was traced to outcropping mafic volcanic and clastic sedimentary rocks in the Lake Superior region. Subsequently this anomalous feature was mapped extending out of eastern Lake Superior across the Michigan basin as shown on Figure 4.60. These gravity and magnetic anomalies are evident in maps shown in Figures 4.41 and 4.43. Complementary geologic and seismic reflection profiling have shown that this 1,100 Ma Keweenawan rift is composed of linear segmented grabens largely filled with basaltic volcanic rocks and lesser sedimentary rocks which were subsequently thrust upward bringing the basalts into juxtaposition with clastic sedimentary rocks that fill a broad depression over the volcanic-rock-filled grabens at a late stage in the rifting process. The intense density and magnetization contrast between these rocks is a significant source of the gravity and magnetic anomalies, respectively.

The Bouguer gravity anomaly and total magnetic intensity anomaly maps

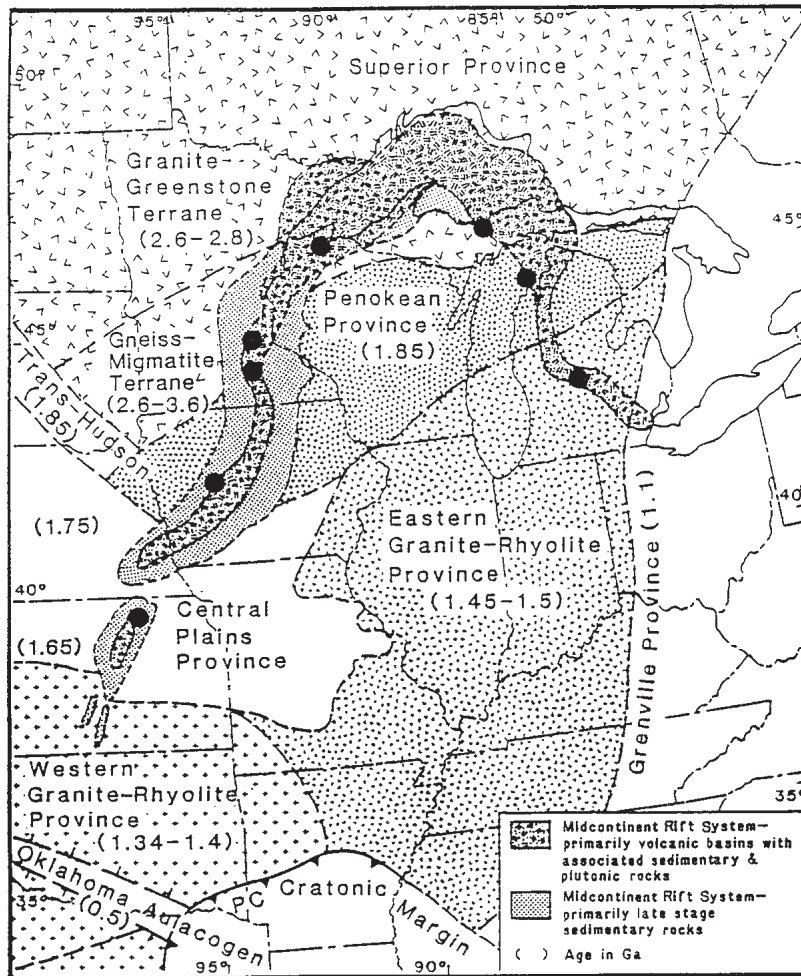


Figure 4.60 The Midcontinent Rift System of the central U.S. as mapped by gravity, magnetic, seismic reflection, and geologic information. Adapted from Allen et al. (1995).

(Figures 4.61 and 4.62, respectively) of the Lake Superior region show the intense anomalies of the rift transecting the basement anomaly patterns and the coinciding major structural components of the rift. The modeled gravity anomalies along a SW/NE seismic reflection profile across eastern Lake Superior (Figure 4.63) illustrate the great thickness of the basalt volcanic rocks in the graben, the lower crust modified by intrusions from the mantle, and the thickening of the crust associated with the rift. The modeled magnetic anomaly profile (Figure 4.64) taking into account the rotation of the intense

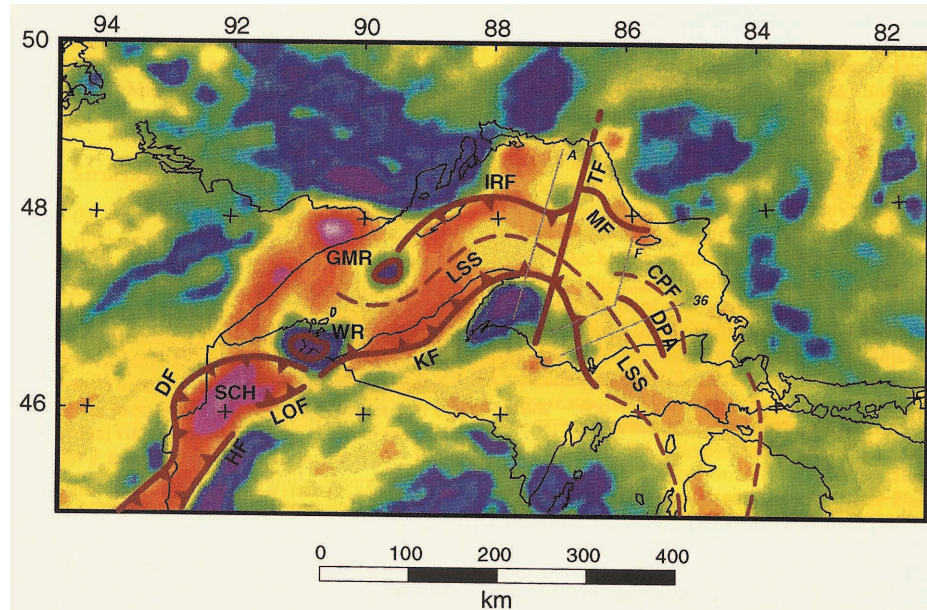


Figure 4.61 Bouguer gravity anomaly map of the Lake Superior region with the major structural elements of the Midcontinent Rift System. The red colors are the anomaly high values and the blue colors are the lows. Adapted from Allen et al. (1995).

remanent magnetization as a result of the structural development of the rift closely duplicates the crustal section modeled in the gravity analysis. The high resolution of magnetic anomalies are particularly useful in mapping the fine-structure of the grabens as shown in Figure 4.65 that compares the magnetic anomaly map along the Minnesota/Wisconsin border with the geologic structure as interpreted from the magnetic anomaly map and related information.

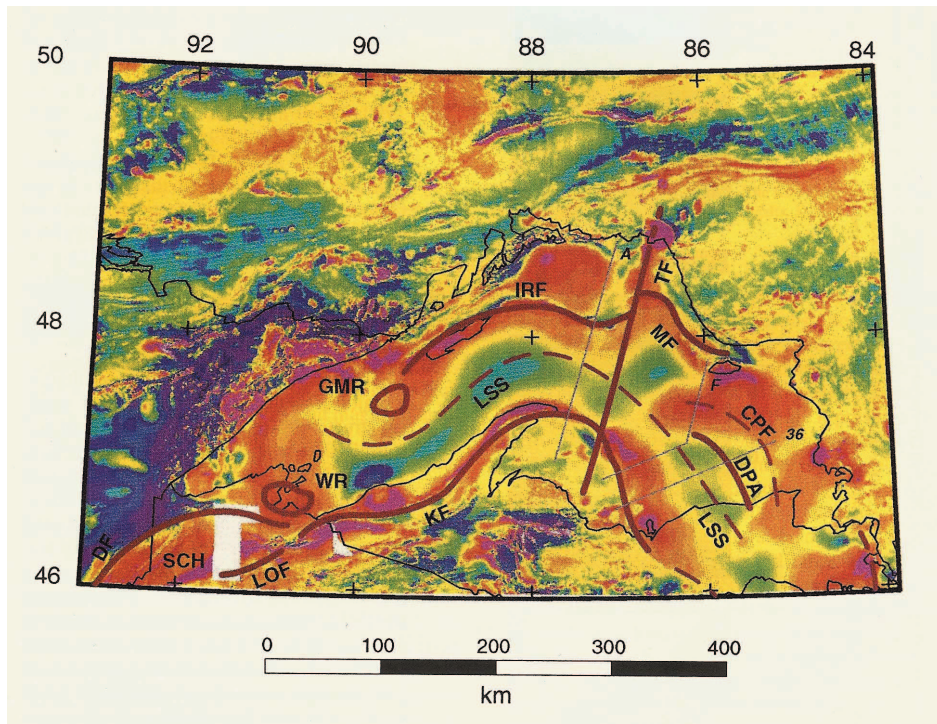


Figure 4.62 Total magnetic intensity anomaly map of the Lake Superior region with the major structural elements related to the Midcontinent Rift System. The red colors are the anomaly high values and the blue colors are the lows. Adapted from Allen et al. (1995).

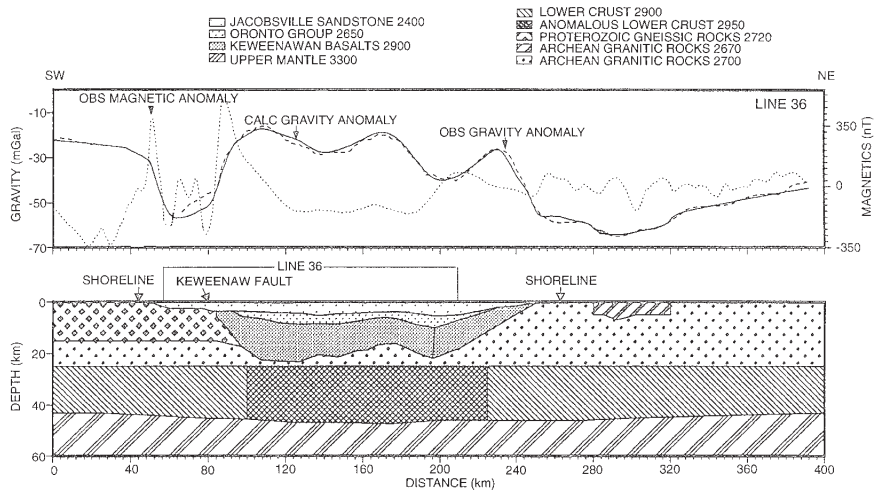


Figure 4.63 Gravity modeling of the Bouguer gravity anomaly over a SW/NE profile across the Midcontinent Rift System in eastern Lake Superior. Densities are indicated in kg/m^3 . Adapted from Mariano and Hinze (1994).

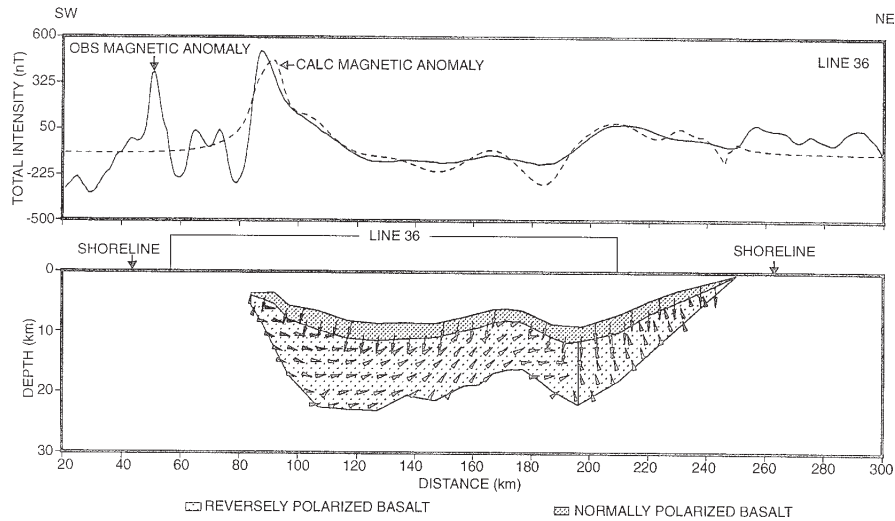


Figure 4.64 Magnetic modeling of the total magnetic intensity anomaly of the same profile shown in the gravity model of Figure 4-56. Arrows indicate the direction of magnetization of the basaltic rocks. The non-magnetic sedimentary strata are not shown. Adapted from Mariano and Hinze (1994).

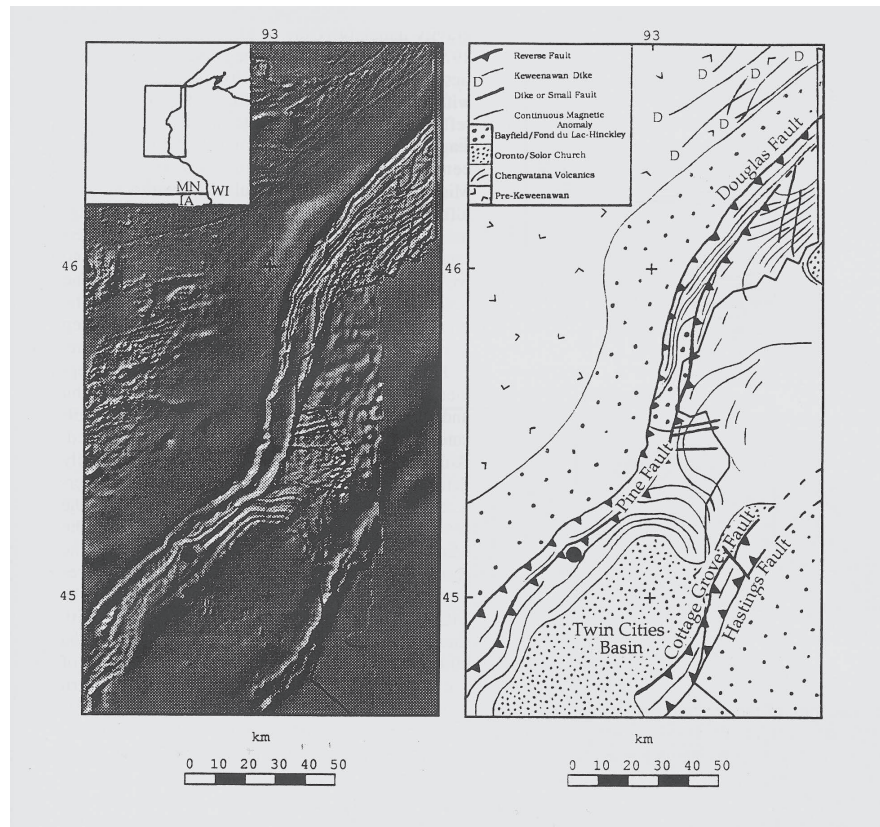


Figure 4.65 Interpretation of the total magnetic intensity map of a portion of the Midcontinent Rift System shown on the left is presented in the geologic map on the right. Adapted from Allen and Chandler (1992).

References

- Abbot, R.E., and Louie, J.N. 2000. *Depth to bedrock using gravimetry in the Reno and Carson City, Nevada area basins*. Geophysics, v. 65.
- Adams, J.M., and Hinze, W.J. 1990. *The gravity-geologic technique of mapping buried bedrock topography, in Ward, S.H. (ed.), Geotechnical and Environmental Geophysics, 3*. Society of Exploration Geophysicists, Tulsa, OK.
- Aitken, O.W., Keller, G.R., and Hinze, W.J. 1983. *Geological significance of surface gravity measurements in the vicinity of the Illinois Deep Drill Holes*. Journal of Geophysical Research, v. 88.
- Al-Rifa'iy, I.A. 1990. *Land subsidence in the Al-Dahr residential area in Kuwait: a case history study*. Quarterly Journal of Engineering Geology, London, v. 23.
- Allen, D. J., and Chandler, V.W. 1992. *The utility of high-resolution aeromagnetic data for investigating the Midcontinent Rift in East-Central Minnesota*. Proceedings and Abstracts, 38th Institute on Lake Superior Geology, Hurley, Wisconsin.
- Allen, D.J., Braile, L.W., Hinze, W.J., and Mariano, J. 1995. *The Midcontinent Rift System, U.S.A.: A major Proterozoic continental rift; in Olsen, K.H. (ed.), Continental Rifts: Evolution, Structure, Tectonics*. Elsevier, NL.
- Allen, D.J., Hinze, W.J., and Dickas, A.B. and Mudrey Jr., M.G. 1997. *Integrated geophysical modeling of the North American mid-continent rift system: new interpretations for western lake superior, northwestern Wisconsin, and eastern Minnesota, in Ojakangas, R.W., Dickas, A.B., Green, J.C., (Eds.), Middle Proterozoic to Cambrian rifting, Central North America*. Geol. Soc. Am. Spec. Paper 312.
- Allis, R.G. 1990. *Geophysical anomalies over epithermal systems; in Hedenquist, J.W., White, N.C., and Siddeley, G. (eds.), Epithermal Gold Mineralization of the Circum-Pacific: Geology, Geochemistry, Origin and Exploration, II*. Journal of Geochemical Exploration, v. 36.
- Allis, R.G., and Hunt, T.M. 1986. *Analysis of exploitation-induced gravity changes at Wairakei geothermal field*. Geophysics, v. 51.
- Alsop, L.E., and Talwani, M. 1984. *The East Coast magnetic anomaly*. Science, v. 226.
- Anderson, N.L., and Cederwell, D.A. 1993. *West Hazel General Petroleum pool: Case history of a salt-dissolution trap in west-central Saskatchewan, Canada*. Geophysics, v. 58.

- Anderson, O.B., and Hinderer, J. 2005. *Global inter-annual gravity changes from GRACE: Early results*. Geophys. Res. Lett., v. 32, doi:10.1029/2004GL020948.
- Arzate, J.A., Flores, L., Chavez, R.E., Barba, L., and Manzanilla, L. 1990. *Magnetic prospecting for tunnels and caves in Teotihuacan, Mexico*, in Ward, S.H. (ed.), *Geotechnical and Environmental Geophysics, 3*. Society of Exploration Geophysicists, Tulsa, OK.
- Astier, J.L., and Paterson, N.R. 1989. *Hydrogeological interest of aeromagnetic maps in crystalline and metamorphic areas*, in Garland, G.D. (ed.), *Proceedings of Exploration 87: Third Decennial International Conference on Geophysical and Geochemical Exploration for Minerals and Groundwater*. Ontario Geological Survey, Special Volume 3.
- Austin, C.T. 1998. *Case history: Reddell oil field, Evangeline Parish, Louisiana; in Gibson, R.I., and Millegan, P.S., (Eds.), Geologic Applications of Gravity and Magnetism: Case Histories*. Society of Exploration Geophysicist, Geophysical References Series, No. 8, American Association of Petroleum Geologists, Studies in Geology, #43.
- Baag, C., and Baag, C-E. 1998. *Aeromagnetic interpretation of southwestern continental shelf of Korea; in Gibson, R.I., and Millegan, P.S., (Eds.), Geologic Applications of Gravity and Magnetism: Case Histories*. Society of Exploration Geophysicist, Geophysical References Series, No. 8, American Association of Petroleum Geologists, Studies in Geology, #43.
- Baldrige, W.S., Keller, G.R., Haak, V., Wendlandt, R.F., Jiracek, G.R., and Olsen, K.H. 1995. *The Rio Grande Rift; in Olsen, K.H. (ed.), Continental Rifts: Evolution, Structure, Tectonics*. Elsevier, NL.
- Barnes, D.F., Mayfield, C.F., Morin, R.L., and Brynm, S. 1982. *Gravity measurements useful in the preliminary evaluation of the Nimiuktuk barite deposit, Alaska*. Economic Geology, v. 77.
- Bascom, W. 1976. *Deep Water, Ancient Ships*. Doubleday and Co., New York.
- Battaglia, M., Gottsmann, J., Carbone, D., and Fernández, J. 2008. *4D Volcano gravimetry*. Geophysics, v. 73.
- Bauer, C., and Fichler, C. 2002. *Quaternary lithology and shallow gas from high resolution gravity and seismic data in the central North Sea*. Petroleum Geoscience, v. 8.
- Beaumont, E.A., and Gay, S.P. Jr. 1999. *Using magnetism in petroleum exploration; in Beaumont, E.A. and Foster, N.H., (Eds.), Exploring for Oil and Gas Traps*. American Association of Petroleum Geologists, Tulsa, OK.
- Becker, G.F. 1909. *Relations between local magnetic disturbances and the genesis of petroleum*. U.S. Geological Survey Bulletin 401.
- Behn, M.D., and Lin, J. 2000. *Segmentation in gravity and magnetic anomalies along the U.S. East Coast passive margin: Implications for incipient structure of the oceanic lithosphere*. J. Geophys. Res., v. 105.
- Behrendt, J.C., and Grim, M.S. 1985. *Structure of the U.S. Atlantic continental margin from derivative and filtered maps of the magnetic field; in Hinze, W.J. (ed.), The Utility of Regional Gravity and Magnetic Anomaly Maps*. Society of Exploration Geophysicists, Tulsa, OK.
- Beres, M., Luetscher, M., and Olivier, R. 2001. *Integration of ground-penetrating radar and microgravimetric methods to map shallow caves*. Journal of Applied Geophysics, v. 46.
- Bertani, R. 2005. *World geothermal power generation in the period 2001-2005*. Geothermics, v. 34.

- Bhattacharyya, B.K., and Leu, L-K. 1975. *An analysis of magnetic anomalies over Yellowstone National Park: Mapping of Curie point isothermal surface for geothermal reconnaissance.* J. Geophys. Res., v. 80.
- Biegert, E., Ferguson, J., and Li, X. 2008. *4-D gravity monitoring introduction.* Geophysics, v. 73.
- Biegert, E.K., and Millegan, P.S. 1998. *Beyond recon: the new world of gravity and magnetics.* The Leading Edge, v. 17.
- Bird, D.E., and Nelson, J.R. 1999. *Aeromagnetic interpretation of basement structure using over 3,000 control wells, Central Alberta: A case history.* Society of Exploration Geophysicists Technical Program and Expanded Abstracts.
- Bird, R.T., Roest, W.R., Pilkington, M., Ernst, R.E., and Buchan, K.L. 1999. *An approach to the reconstruction of deformed continental crust using gridded geophysical data.* Exploration Geophysics, v. 30.
- Bishop, I., Styles, P., Emsley, S.J., and Ferguson, N.S. 1997. *The detection of cavities using the microgravity technique: case histories from mining and karstic environments, in McCann, D.M., Eddleston, M., Fenning, P.J., and Reeves, G.M., (eds.), Modern Geophysics in Engineering Geology.* Geological Society of London, Engineering Geology special Publication No. 12.
- Blackman, D.J. 1973. *Marine Archaeology.* Colstern Research Society, Coulston Papers, v. 23.
- Blaich, O.A., Faleide, J.I., and Tsikalas, F. 2010. *Crustal breakup and continent-ocean transition at South Atlantic conjugate margins.* J. Geophys. Res., v. 116.
- Blakely, R. J., and Connard, G. G. 1989. *Crustal studies using magnetic data; in Pakiser, L.C. and Mooney, W.D. (eds.), Geophysical Framework of the Continental United States.* Geol. Soc. Am. Mem. 172.
- Blakely, R.J. 1988. *Curie temperature isotherm analysis and tectonic implications of aeromagnetic data from Nevada.* J. Geophys. Res., v. 93.
- Blakely, R.J., Langenheim, V.E., Ponce, D.A., and Dixon, G.L. 2000. *Aeromagnetic survey of the Amargosa Desert, Nevada: A tool for understanding near-surface geology and hydrology.* U. S. Geological Survey, Open-file Report 00-188.
- Blakely, R.J., Brocher, T.M., and Wells, R.E. 2006. *Subduction-zone magnetic anomalies and implications for hydrated forearc mantle.* Geology, v. 33.
- Blizkovsky, M. 1979. *Processing and applications in microgravity surveys.* Geophysical Prospecting, v. 27.
- Bott, M.H.P. 1995. *Mechanisms of rifting: Geodynamic modeling of continental rift systems; in Olsen, K.H. (ed.), Continental Rifts: Evolution, Structure, Tectonics.* Elsevier, NL.
- Bott, M.H.P., and Hinze, W.J. 1995. *Potential field methods; in Olsen, K.H. (ed.), Continental Rifts: Evolution, Structure, Tectonics.* Elsevier, NL.
- Bradley, J.W. 1974. *The commercial application and interpretation of the borehole gravimeter, in Contemporary geophysical interpretation, a symposium.* Geophysical Society of Houston, December 4-5.
- Braile, L.W., Keller, G.R., Wendlandt, R.F., Morgan, P., and Khan, M.A. 1995. *The East African rift system; in Olsen, K.H. (ed.), Continental Rifts: Evolution, Structure, Tectonics.* Elsevier, NL.
- Brant, A.A. 1966. *Geophysics in the exploration for Arizona porphyry coppers; in Titley, S.R., and Hicks, C.L. (eds.), Geology of the Porphyry Copper Deposits, Southwestern North America.* University of Arizona Press, Tucson, AZ.

- Breiner, S. 1973. *Applications Manual for Portable Magnetometers*. Geometrics Corporation, Sunnyvale, CA.
- Breivik, A.J., Verhoef, J., and Faleide, J.I. 1999. *Effect of thermal contrasts on gravity modeling at passive margins: Results from the western Barents Sea*. J. Geophys. Res., v. 104.
- Brocher, T.M., Hunter, W.C., and Langenheim, V.E. 1998. *Implications of seismic reflection and potential field geophysical data on the structural framework of the Yucca Mountain-Crater Flat region, Nevada*. Geological Society of America Bulletin, v. 110.
- Brock, J.S. 1973. *Geophysical exploration leading to the discovery of the Faro deposit*. Canadian Mining and Metallurgy Bulletin, v. 66.
- Bullard, E.C. 1936. *Gravity measurements in East Africa*. Phil. Trans. R. Soc. A.
- Butler, D.K. 1984. *Microgravimetric and gravity gradient techniques for detection of subsurface cavities*. Geophysics, v. 49.
- Butler, D.K. 2001. *Potential fields methods for location of unexploded ordnance*. The Leading Edge, v. 20.
- Butler, D.K. 2005. *What is near-surface geophysics?*; in Butler, D.K. (ed.), *Near-Surface Geophysics*. Society of Exploration Geophysicists.
- Butler, D.K., Sjostrom, K.J., and Llopis, J.L. 1997. *Selected short stories on novel applications of near-surface geophysics*. The Leading Edge, v. 16.
- Cannon, W.F., Schulz, K.J., Daniels, D.L., Anderson, R.R., Chandler, V.W., Holm, D.K., Schneider, D.A., and Van Schmus, W.R. 2005. *Geology of Precambrian basement rocks in Iowa and the southern parts of Wisconsin and Minnesota*. 51st Annual Meeting of the Institute on Lake Superior Geology.
- Carlás, D.U., Uteda, L., Li, Y., Barbosa, V.C.F., Braga, M.A., Angeli, G., and Peres, G. 2012. *Iron ore interpretation using gravity gradient inversions in the Carajás, Brazil*. Society of Exploration Geophysicists, Expanded Abstracts.
- Carporzen, L., Glider, S.A., and R.J., Hart. 2005. *Paleomagnetism of the Vredefort meteorite crater and implications for craters on Mars*. Nature, v. 435.
- Cawthorn, R.G., Cooper, G.R.J., and Webb, S.J. 1998. *Connectivity between the western and eastern limbs of the Bushveld Complex*. South African Jour. Geol., v. 101.
- Chai, Y., and Hinze, W.J. 1988. *Gravity inversion of an interface above which the density contrast varies exponentially with depth*. Geophysics, v. 53.
- Chakravarthi, V., Shankar, G.B.K., Muralidharan, D., Harinarayana, T., and Sundararajan, N. 2007. *An integrated geophysical approach for imaging sub basalt sedimentary basins: Case study of Jam River Basin, India*. Geophysics, v. 72.
- Chandler, V.W. 1985. *Interpretation of Precambrian geology in Minnesota using low-altitude, high-resolution aeromagnetic data*, in Hinze, W.J., (ed.), *The Utility of Regional Gravity and Magnetic Anomaly Maps*. Society of Exploration Geophysicists, Tulsa, OK.
- Chandler, V.W. 1996. *Gravity and magnetic studies conducted recently*, in Sims, P.K., (ed.), *Archean and Proterozoic geology of the Lake Superior region U.S.A.* U.S. Geological Survey Prof. Paper 1556.
- Chandler, V.W., Boerboom, T.J., and Jirsa, M.A. 2007. *Penokean tectonics along a promontory-embayment margin in east-central Minnesota*. Precambrian Research, v. 157.
- Chapin, D.A., Yalamanchili, S.V., and Daggett, P.H. 1998. *The St. George Basin, Alaska, COST #1 Well: An example of the need for integrated interpretation*; in Gibson, R.I., and Millegan, P.S., (Eds.), *Geologic Applications of Gravity*

- and Magnetics: Case Histories*. Society of Exploration Geophysicist, Geophysical References Series, No. 8, American Association of Petroleum Geologists, Studies in Geology, #43.
- Chapman, D.S., Sahn, E., and Gettings, P. 2008. *Monitoring aquifer recharge using repeated high-precision gravity measurements: A pilot study in south Weber, Utah*. Geophysics, v. 73.
- Chappell, A.R., and Kuszniir, N.J. 2008. *Three-dimensional gravity inversion for Moho depth at rifted continental margins incorporating a lithosphere thermal gravity anomaly correction*. Geophys. J. Int., v. 174.
- Chen, J.L., Wilson, C.R., and Tapley, B.D. 2010. *The 2009 exceptional Amazon flood and interannual terrestrial water storage change observed by GRACE*. Water Resources Research, v. 46.
- Cisowski, S.M., and Fuller, M. 1987. *The generation of magnetic anomalies by combustion metamorphism of sedimentary rock, and its significance to hydrocarbon exploration*. Geological Society of America Bulletin, v. 99.
- Clark, D.A., French, D.H., Lackie, M.A., and Schmidt, P.W. 1992. *Magnetic petrology: Application of integrated rock magnetic and petrologic techniques to geological interpretation of magnetic surveys*. Exploration Geophysics, v. 23.
- Clark, S.C., Frey, H., and Thomas, H.H. 1985. *Satellite magnetic anomalies over subduction zones: The Aleutian Arc anomaly*. Geophys. Res. Lett., v. 12.
- Cohen, K.K., Mocks, N.N., and Trevits, M.A. 1992. *Magnetometry as a tool to map subsurface conditions in an abandoned iron ore mining district in New Jersey*. SAGEEP Proceedings.
- Cole, J., Webb, S.J., and Finn, C. 2014. *Gravity models of the Bushveld Complex - Have we come full circle?* Jour. African Sci., v. 92.
- Connerney, J.E.P., Acuña, M.H., Ness, N.F., Kletetschka, G., Mitchell, D.L., Lin, R.P., and Reme, H. 2005. *Tectonic implications of Mars crustal magnetism*. Proc. Natl. Acad. Sci. USA, v. 102.
- Cook, A.H., Hospers, J., and Parasnis, D.S. 1951. *The results of a gravity survey in the country between the Clee Hills and Nuneaton*. Quart. J. Geol. Soc. Lond., v. 107.
- Cordell, L. 1973. *Gravity analysis using an exponential density-depth function - San Jacinto graben, California*. Geophysics, v. 38.
- Cordell, L. 1976. *Aeromagnetic and gravity studies of the Rio Grande graben in New Mexico between Belen and Pilar; in Tectonics and Mineral Resources of Southwestern North America: Socorro*. New Mexico Geological Society Special Publication, v. 6.
- Cordell, L. 1982. *Extension in the Rio Grande rift*. J. Geophys. Res., v. 87.
- Corrigan, J., and Sweat, M. 1995. *Heat flow and gravity responses over salt bodies: A comparative model analysis*. Geophysics, v. 60.
- Cosca, M.A., Essene, E.J., Geissman, J.W., Simmons, W.B., and Coates, D.A. 1989. *Pyrometamorphic rocks associated with naturally burned coal beds, Powder River Basin, Wyoming*. American Mineralogist, v. 74.
- Cousins, C.A. 2014. *The structure of the mafic portion of the Bushveld Igneous Complex*. Trans. Geol. Soc. South Africa, v. 62.
- Crane, J.H. 1989. *Late Pleistocene to recent sedimentation and stratigraphy of the Gulf of Mexico outer continental shelf, offshore Louisiana*. M.Sc. thesis, University of Houston, Houston, TX.

- Crider, J. G., Johnson, K.H., and Williams-Jones, G. 2008. *Thirty-year gravity change at Mount Baker volcano, Washington, USA: Extracting the signal from under the ice*. *Geophysical Research Letters*, v. 35.
- Crough, S.T. 1983. *Rifts and swells: geophysical constraints on causality*. *Tectonophysics*, v. 94.
- Currenti, G., Del Negro, C., Johnston, M., and Sasai, Y. 2007. *Close temporal correspondence between geomagnetic anomalies and earthquakes during the 2002 – 2003 eruption of Etna volcano*. *Journal of Geophysical Research*, v. 112.
- Cuss, R.J., and Styles, P. 1999. *The application of microgravity in industrial archaeology: an example from the Williamson tunnels, Edge Hill, Liverpool, in Geoarchaeology: Exploration, Environments, and Resources*. Geological Society of London, Special Publication 165.
- Daniels, J.J. 1988. *Geotechnical applications 2 - Locating caves, tunnels and mines*. The Leading Edge, v. 7.
- de Boer, C.B., Dekkers, M.J., and van Hoof, T.A.M. 2001. *Rock-magnetic properties of TRM carrying baked and molten rocks straddling burnt coal seams*. *Physics of the Earth and Planetary Interiors*, v. 126.
- Dentith, M., and Mudge, S.T. 2014. *Geophysics for the Mineral Exploration Geoscientist*. Cambridge University Press.
- Dentith, M.C., Evans, B.J., Paish, K.F., and Trench, A. 1992. *Mapping the regolith using seismic refraction and magnetic data: Results from the Southern Cross Greenstone Belt, Western Australia*. *Exploration Geophysics*, v. 23.
- Dentith, M.C., Frankcombe, K.F., and Trench, A. 1994. *Geophysical signatures of Western Australian mineral deposits: An overview*. *Exploration Geophysics*, v. 25.
- DeRito, R.F., Cozzarelli, F.A., and Hodge, D.S. 1983. *Mechanism of subsidence of ancient cratonic rift basins*. *Tectonophysics*, v. 94.
- Domzalski, W. 1966. *Importance of aeromagnetism in evaluation of structural control of mineralization*. *Geophysical Prospecting*, v. 14.
- Donovan, T.J., Forgey, R.L., and Roberts, A.A. 1979. *Aeromagnetic detection of diagenetic magnetite over oil fields*. *Am. Assoc. Petr. Geol. Bull.*, v. 63.
- Dragol-Stavar, D., and Hall, S. 2009. *Gravity modeling of the ocean-continent transition along the South Atlantic margins*. *J. Geophys. Res.*, v. 114.
- Drenth, B. 2012. *Airborne gravity gradient expression of a buried niobium and rare earth element deposit: Elk Creek Carbonatite, Nebraska*. Society of Exploration Geophysicists, Expanded Abstracts.
- Droujinine, A., Vasilevsky, A., and Evans, R. 2007. *Feasibility of using full tensor gradient (FTG) data for detection of local lateral density contrasts during reservoir monitoring*. *Geophysical Journal International*, v. 169.
- Eaton, G.P., and Watkins, J.S. 1970. *The use of seismic refraction and gravity methods in hydrogeological investigations, in Morley, L.W. (ed.), Mining and Groundwater Geophysics/1967*. Geological Survey of Canada, Economic Geology Report 26.
- Eiken, O., Zumbege, M., Stenvold, T., Sasagawa, G., and Nooner, S. 2004. *Gravimetric monitoring of gas production from the Troll field*. Society of Exploration Geophysicists Technical Program and Expanded Abstracts.
- Elawadi, E., Mogren, S., Ibrahim, E., Batayneh, A., and Al-Bassam, A. 2012. *Utilizing potential field data to support determination of groundwater aquifers in*

- the southern Red Sea coast, Saudia Arabia.* Journal of Geophysics and Engineering, v. 9.
- Emerson, D.W., Reid, J.E., Clark, D.A., Hallett, M.S.C., and Manning, P.B. 1990. *The geophysical responses of buried drums - Field tests in weathered Hawkesbury sandstone, Sydney Basin, NSW.* Exploration Geophysics, v. 23.
- Ennen, C., and Hall, S. 2011. *Structural mapping of the Vinton salt dome, Louisiana, using gravity gradiometry data.* Society of Exploration Geophysicists, 81st Annual International Meeting Expanded Abstracts, Tulsa, OK.
- Erofeeva, S., and Egbert, G. 2002. *Efficient inverse modelling of barotropic ocean tides.* J. Atmos. Oceanic Technol., v. 19.
- Ervin, C.P., and McGinnis, L.D. 1986. *Temporal variation in the gravitational field of the Mississippi embayment.* Journal of Geophysical Research, v. 91.
- Espersen, J. 1970. *Iron ore prospecting in Scandinavia and Finland; in Morley, L.W. (ed.), Mining and Groundwater Geophysics/1967.* Economic Geology Report No. 26, Geological Survey of Canada, Ottawa.
- Eti, R.P. 2004. *An integrated geophysical study of the Vinton salt dome, Calcasieu Parish, Louisiana.* M.Sc. thesis, University of Houston, Houston, TX.
- Fairhead, J.D., Misener, J.D., Green, C.M., Bainbridge, G., and Reford, S.W. 1997. *Large scale compilations of magnetic, gravity radiometric and electromagnetic data: The new exploration strategy for the 90s; in Gubins, A.G.(ed.), Geophysics and Geochemistry at the Millenium.* Proceedings of Exploration 97, Fourth Decennial International Conference on Mineral Exploration.
- Fajkiewicz, Z. 1976. *Gravity vertical gradient measurements for detection of small geologic and anthropogenic forms.* Geophysics, v. 41.
- Famiglietti, J.S., Lo, M., Ho, S.L., Bethune, J., Anderson, K.J., Syed, T.H., Swenson, S.C., de Linage, C.R., and Rodell, M. 2011. *Satellites measure recent rates of groundwater depletion in Californias Central Valley.* Geophys. Res. Lett., v. 38.
- Farquharson, C., Ash, M., and Miller, H. 2008. *Geologically constrained gravity inversion for the Voisey's Bay ovoid deposit.* Leading Edge, v. 27.
- Fenning, P.J., and Williams, B.S. 1997. *Multicomponent geophysical surveys over completed landfill sites, in McCann, D.M., Eddleston, M., Fenning, P.J., and Reeves, G.M., (eds.), Modern Geophysics in Engineering Geology.* Geological Society of London, Engineering Geology Special Publication No. 12.
- Ferguson, J.F., Chen, T., Aiken, C.L.V., and Seibert, J. 2007. *The 4D microgravity method for waterflood surveillance II gravity measurements for the Prudhoe Bay reservoir, Alaska.* Geophysics, v. 72.
- Ferguson, J.F., Klopping, F.J., Chen, T., Siebert, J.E., Hare, J.L., and Brady, J.L. 2008. *The 4D microgravity method for waterflood surveillance: Part 3 - 4D absolute microgravity surveys at Prudhoe Bay, Alaska.* Geophysics, v. 73.
- Ferré, E.C., Friedman, S.A., Martín-Hernández, F., Feinberg, J.M., Conder, J.A., and Ionov, D.A. 2013. *The magnetism of mantle xenoliths and potential implications for sub-Moho magnetic sources.* Geophys. Res. Lett., v. 40.
- Ferris, C. 1987. *Gravity anomaly resolution at the Garber field.* Geophysics, v. 52.
- Flanagan, G., Davis, S.G., Campbell, C.L., and Doughtie, J.K. 1988. *Integration of high sensitivity aeromagnetics and seismic to define salt and sediment structures in the Gulf of Mexico.* Society of Exploration Geophysicists Technical Program and Expanded Abstracts, 58th Annual Meeting.
- Fowler, C.M.R. 1990. *The Solid Earth.* Cambridge University Press, Cambridge.

- Frischknecht, F.C., and Raab, P.V. 1984. *Location of abandoned wells with geophysical methods*. U.S. Environmental Protection Agency Report 600/4-84-085.
- Frischknecht, F.C., Muth, L., Corette, R., Buckley, T., and Kornegay, B. 1983. *Geophysical methods for locating abandoned wells*. U.S. Geological Survey Open-file Report 83-702.
- Frohlich, R.R. 1989. *Magnetic signatures of zones of fractures in igneous metamorphic rocks with an example from southeastern New England*. Tectonophysics, v. 163.
- Fullagar, P.K., and Fallon, G.N. 1997. *Geophysics in metalliferous mines for ore body delineation and rock mass characterization*, in Gubins, A.G.(ed.), *Geophysics and Geochemistry at the Millenium*. Proceedings of Exploration 97, Fourth Decennial International Conference on Mineral Exploration.
- Garland, G.D. (ed.). 1989. *Proceedings of Exploration 87*. Ontario Geological Survey, Special Volume 3.
- Gasperikova, E., and Hoversten, G.M. 2006. *A feasibility study of nonseismic geophysical methods for monitoring geologic CO₂ sequestration*. The Leading Edge, v. 25.
- Gay, S.P. 1992. *Epigenetic versus syngenetic magnetite as a cause of magnetic anomalies*. Geophysics, v. 57.
- Gay, S.P. 2004. *Glacial till: A troublesome source of near-surface magnetic anomalies*. The Leading Edge, v. 23.
- Gay, S.P., and Hawley, B.W. 1991. *Syngenetic magnetic anomaly sources: three examples*. Geophysics, v. 56.
- Gerryts, E. 1970. *Diamond prospecting by geophysical methods a review of current practice; in Morley, L.W. (ed.), Mining and Groundwater Geophysics/1967*. Geological Survey of Canada, Economic Geology Report No. 26.
- Gibson, R.I. 1998a. *Classic salt dome; in Gibson, R.I. and Millegan, P.S., (Eds.), Geologic Applications of Gravity and Magnetism: Case Histories*. Society of Exploration Geophysicists, Geophysical Reference Series, No. 8, American Association of Petroleum Geologists, Studies in Geology, #43.
- Gibson, R.I. 1998b. *Interpretation of rift-stage faulting in the West Siberian basin from magnetic data; in Gibson, R.I. and Millegan, P.S., (Eds.), Geologic Applications of Gravity and Magnetism: Case Histories*. Society of Exploration Geophysicists, Geophysical Reference Series, No. 8, American Association of Petroleum Geologists, Studies in Geology, #43.
- Gibson, R.I., and Millegan, P.S. (eds.). 1998. *Geologic Applications of Gravity and Magnetism: Case Histories*. Society of Exploration Geophysicists Geophysical Reference Series, No. 8.
- Golynsky, A., Bell, R., Blankenship, D., Damaske, D., Ferraccioli, F., Finn, C., Ivanov, S., Jokat, W., Masolov, V., Riedel, S., von Frese, R., and W.G., ADMAP. 2013. *Air and shipborne magnetic surveys of the Antarctic into the 21st century*. Tectonophysics, v. 585.
- Goussev, S., Shields, G., Rowe, J., and Saad, A. 2008. *Origin and enhancement of gravity and magnetic signatures of the continental-oceanic boundary (COB): examples from West Africa Passive Margin(Slide Presentation)*. Society of Exploration Geophysicists, 78th Annual International Meeting Expanded Abstracts and Multimedia PowerPoint presentation, Tulsa, OK.
- Gow, P.A., Wall, V.J., Oliver, N.H.S., and Valenta, R.K. 1994. *Proterozoic iron oxide (Cu-U-Au-REE) deposits: Further evidence of hydrothermal origins*. Geology, v. 22.

- Grant, F.S. 1984a. *Aeromagnetism, geology, and ore environments; I, Magnetite in igneous, sedimentary and metamorphic rocks An overview*. Geosphere, v. 23.
- Grant, F.S. 1984b. *Aeromagnetism, geology, and ore environments; II, Magnetite and ore environments*. Geosphere, v. 23.
- Grant, F.S., and Elsharty, A.F. 1962. *Bouguer gravity corrections using a variable density*. Geophysics, v. 27.
- Grauch, V.J.S., and Hudson, M.R. 2007. *Guides to understanding the aeromagnetic expression of faults in sedimentary basins: Lessons learned from the central Rio Grande rift, New Mexico*. Geosphere, v. 3.
- Grauch, V.J.S., Phillips, J.D., Koning, D.J., Johnson, P.S., and Bankey, V. 2009. *Geophysical interpretations of the southern Espanola basin, New Mexico, that contribute to understanding its hydrogeologic framework*. U.S. Geological Survey, Professional Paper 1761.
- Grieve, R.A.F. 2005. *Economic mineral resource deposits at terrestrial impact structures; in McDonald, I., Boyce, A.J., Butler, I.B., Herrington, R.J., and Polya, D.A., (eds.), Mineral Deposits and Earth Evolution*. Geological Society, London, Special Publications, 248.
- Grieve, R.A.F. 2006. *Impact Structures in Canada*. Geological Association of Canada.
- Grieve, R.A.F., and Pilkington, M. 1996. *The signature of terrestrial impacts*. AGSO Journal of Australian Geology and Geophysics, v. 16.
- Griffiths, D.H., and King, R.F. 1981. *Applied Geophysics for Geologists and Engineers: The Elements of Geophysical Prospecting*. Pergamon, New York.
- Gubins, A.G. (ed.). 1997. *Geophysics and Geochemistry at the Millennium: Proceedings of Exploration 97*. Fourth Decennial International Conference on Mineral Exploration, Prospectors and Developers Association of Canada.
- Gunn, P.J., and Dentith, M.C. 1997. *Magnetic responses associated with mineral deposits*. Journal of Australian Geology & Geophysics, v. 17.
- Hall, D. J. 1990. *Gulf coast-east coast magnetic anomaly: 1. Root of the main crustal decollement for the Appalachian-Ouachita orogeny*. Geology, v. 18.
- Hall, D.H., and Hajnal, Z. 1962. *The gravimeter in studies of buried valleys*. Geophysics, v. 27.
- Hammer, S., and Anzoleaga, R. 1975. *Exploring for stratigraphic traps with gravity gradients*. Geophysics, v. 40.
- Hammond, S., and Murphy, C. 2003. *Air FTGTM Bell Geospace airborne gravity gradiometer - A description and case study*. Preview, v. 105.
- Hanna, W.F. 1969. *Negative aeromagnetic anomalies over mineralized areas of the Boulder Batholith*. U.S. Geological Survey Professional Paper 650-D.
- Hanna, W.F., R.E., Sweeney, Hildenbrand, T.G., Tanner, J.G., McConnell, R.K., and Godson, R.H. 1989. *The gravity anomaly map of North America; in Balley, A.W., and Palmer, A.R. (eds.), The Geology of North America An overview*. Geological Society of America, The Geology of North America, v. A.
- Hansen, D.A. 1970. *Iron ore exploration in North and South America, in Morley, L.W. (ed.), Mining and Groundwater Geophysics/1967*. Economic Geology Report No. 26, Geological Survey of Canada, Ottawa.
- Hao, T., and Wang, Q. 2000. *Microgravity and vertical gravity prospecting of underground place of Ming tombs, in Choi, S. and Suh, M. (eds.), Proceedings of the New Millennium International Forum on Conservation of Cultural Property*. National Cultural Properties Administration of Korea, Seoul.

- Hare, J.L., Ferguson, J.F., Aiken, C.L.V., and Brady, J.L. 1999. *The 4-D micro-gravity method for waterflood surveillance: A model study for the Prudhoe Bay reservoir, Alaska*. Geophysics, v. 64.
- Harris, K., Samson, C., and van Geel, P. 2013. *Characterization of waste density in a bioreactor landfill via microgravity and settlement analysis*. Jour. of Environmental and Engineering Geophysics, v. 18.
- Harrison, C.G.A. 1989. *The crustal field; in Jacobs, J.A. (ed.), Geomagnetism*. Academic Press, New York.
- Hattula, A., and Rekola, T. 2000. *Exploration geophysics at the Pyhäsalmi mine and grade control work of the Outokumpu Group*. Geophysics, v. 65.
- Hawke, P.J., Buckingham, A.J., and Dentith, M.C. 2006. *Modelling source depth and possible origin of magnetic anomalies associated with the Yallalie impact structure, Perth Basin, Western Australia*. Exploration Geophysics, v. 37.
- Hayes, T.J., Tiampo, K.F. and Rundle, J.B., and Fernández, J. 2006. *Gravity changes from a stress evolution earthquake simulation of California*. Journal of Geophysical Research, v. 111.
- Heincke, B., Jegen, M., and Hobbs, R. 2006. *Joint inversion of MT, gravity, and seismic data applied to sub-basalt imaging*. Society of Exploration Geophysicists, 76th Annual International Meeting Expanded Abstracts, Tulsa, OK.
- Heirtzler, J.R. 1985. *The change in the magnetic anomaly pattern at the ocean-continent boundary; in Hinze, W.J. (ed.), The Utility of Regional Gravity and Magnetic Anomaly Maps*. Society of Exploration Geophysicists, Tulsa, OK.
- Henke, C., Schober, J., Weber, U., Gholami, F., and Tabatabai, H. 2005. *Exploring the High Zagros (Iran): A challenge for geophysical integration*. First Break, v. 23.
- Henkel, H., and Guzman, M. 1977. *Magnetic features of fracture zones*. Geoprospection, v. 15.
- Herwanger, J., Maurer, H., Green, A.G., and Leckebusch, J. 2000. *3-D inversions of magnetic gradiometer data in archeological prospecting: possibilities and limitations*. Geophysics, v. 65.
- Hildebrand, A.R., Pilkington, M., Ortiz-Aleman, C., Chavez, R.E., Urrutia-Fucugauchi, J., Connors, M., Graniel-Castro, E., Camara-Zi, A., Halpenny, J.F., and Niehaus, D. 2005. *Mapping Chicxulub crater structure with gravity and seismic reflection data; in Grady, M.M., Hutchison, R., McCall, G.J.H., and Rothery, D.A. (eds.), Meteorites: Flux with Time and Impact Effects*. Geological Society, London, Special Publications, 140.
- Hildenbrand, T.G., and Ravat, D.N. 1997. *Geophysical setting of the Wabash Valley fault system*. Seismological Research Letters, v. 68.
- Hildenbrand, T.G., Kane, M.F., and Stauder, W. 1977. *Magnetic and gravity anomalies in the northern Mississippi embayment and their spatial relation to seismicity*. U.S. Geological Survey, Map-914.
- Hildenbrand, T.G., Berger, B., Jachens, R.C., and Ludington, S. 2000. *Regional crustal structure and their relationship to the distribution of ore deposits in the Western United States, based on magnetic and gravity data*. Economic Geology, v. 95.
- Hill, I., Grosse, T., and Leech, C. 2004. *High resolution multisensor geophysical surveys for near-surface applications can be rapid and cost-effective*. The Leading Edge, v. 23.
- Hinze, W. J., and Hildenbrand, T.G. 1988. *The utility of geopotential field data*

- in seismotectonic studies in the eastern United States*. Seismological Research Letters, v. 59.
- Hinze, W.J. 1966. *The gravity method in iron ore exploration; in SEG Mining Geophysics Volume Editorial Committee (ed.)*. Mining Geophysics, v. 1.
- Hinze, W.J., and Braile, L.W. 1988. *Geophysical aspects of the craton: in Sloss L.L. (ed.), U.S. Sedimentary Cover - North American Craton*. The Geology of North America Volume D-2, Geological Society of America, Boulder, Colorado.
- Hinze, W.J., and Hood, P.J. 1989. *The magnetic anomaly map of North America: A new tool for regional geologic mapping; in Balley, A.W., and Palmer, A.R. (eds.), The Geology of North America An overview*. Geological Society of America, The Geology of North America, v. A.
- Hinze, W.J., and Kelly, W.C. 1988. *Scientific drilling into the Midcontinent Rift System*. Eos (Transactions, American Geophysical Union), v. 69.
- Hinze, W.J., and Zietz, I. 1985. *The composite magnetic-anomaly map of the conterminous United States; in Hinze, W.J. (ed.), The Utility of Regional Gravity and Magnetic Anomaly Maps*. Society of Exploration Geophysicists, Tulsa, OK.
- Hinze, W.J., Braile, L.W., Keller, G.R., and Lidiak, E.G. 1988. *Models for midcontinent tectonism: an update*. Reviews of Geophysics, v. 26.
- Hinze, W.J. (ed.). 1985. *The Utility of Regional Gravity and Magnetic Anomaly Maps*. Geological Survey of Canada, Economic Geology Report No. 26.
- Holbrook, W. S., Purdy, G.M., Sheridan, R.E., Glover, L., Talwani, M., Ewing, J., and Hutchinson, D. 1994. *Seismic structure of the U.S. Mid-Atlantic continental margin*. J. Geophys. Res., v. 99.
- Hood, L.L. 2010. *Central magnetic anomalies of Nectarian-aged lunar impact basins: Probable evidence for an early dynamo*. Icarus, v. 211.
- Hood, P.J. (ed.). 1979. *Proceedings of Exploration 77: Geophysics and Geochemistry in the Search for Metallic Ores*. Geological Survey of Canada, Economic Geology Report 31.
- Humphreys, G.L., Linford, J.G., and West, S.M. 1990. *Application of geophysics to the reclamation of saline farm land in Western Australia, in Ward, S.H., (ed.), Geotechnical and Environmental Geophysics, 2, Environment and Groundwater*. Society of Exploration Geophysicists, Tulsa, Oklahoma.
- Hunt, T., and Bowyer, D. 2007. *Reinjection and gravity changes at Rotokawa geothermal field, New Zealand*. Geothermics, v. 36.
- Hunt, T., Sugihara, M., Sato, T., and Takemura, T. 2002. *Measurement and use of vertical gravity gradient in correcting repeat microgravity measurements for the effects of ground subsidence in geothermal systems*. Geothermics, v. 31.
- Hunt, T.M., and Tosha, T. 1994. *Precise gravity measurements at Inferno Crater, Waimangu, New Zealand*. Geothermics, v. 23.
- Huston, D.C., Huston, H.H., and Johnson, E. 2004. *Geostatistical integration of velocity cube and log data to constrain 3D modeling, deepwater Gulf of Mexico*. The Leading Edge, v. 23.
- Hutchins, D.G., Milner, S.C., and Korkiakoski, E. 1997. *Regional airborne geophysics and geochemistry: A Namibian perspective; in Gubins, A.G.(ed.), Geophysics and Geochemistry at the Millennium*. Proceedings of Exploration 97, Fourth Decennial International Conference on Mineral Exploration.
- Ibrahim, A., and Hinze, W.J. 1972. *Mapping buried bedrock topography with gravity*. Ground Water, v. 10.

- Innes, M.J.S., and Gibb, R.A. 1970. *A new gravity anomaly map of Canada: an aid to mineral exploration*, in Morley, L.W. (ed.), *Mining and Groundwater Geophysics/1967*. Economic Geology Report No. 26, Geological Survey of Canada, Ottawa.
- Irvine, R.J., and Smith, M.J. 1990. *Geophysical exploration for epithermal gold deposits*; in Hedenquist, J.W., White, N.C., and Siddeley, G. (eds.), *Epithermal Gold Mineralization of the Circum-Pacific: Geology, Geochemistry, Origin and Exploration, II*. J. Geochem. Explor., v. 36.
- Ishihara, S. 1981. *The granitoid series and mineralization*. Economic Geology, v. 75.
- Jackson, M.P.A., and Talbot, C.J. 1986. *External shapes, strain rates, and dynamics of salt structures*. Geological Society of America Bulletin, v. 97.
- Jacob, T., Chery, J., Bayer, R., Le Moigne, N., Boy, J-P., Vernant, P., and Boudin, F. 2009. *Time-lapse surface to depth gravity measurements on a karst system reveal the dominant role of the epikarst as a water storage entity*. Geophysics Journal International, v. 177.
- Jacques, J.M., Price, A.D., and Bain, J.E. 2004. *Digital integration of potential fields and geologic data sets for plate tectonic and basin dynamic modeling the first step toward identifying new play concepts in the Gulf of Mexico Basin*. The Leading Edge, v. 23.
- Jansen, J., and Witherly, K. 2004. *The Tli Kwi Cho kimberlite complex, Northwest Territories, Canada: A geophysical case study*. Society of Exploration Geophysicists Expanded Abstracts.
- Joesting, H.R., and Plouff, D. 1958. *Geophysical studies of the Upheaval Dome area, San Juan County, Utah*. International Association of Petroleum Geologists, Annual Field Conference Guidebook, 9.
- Kane, M.F. 1977. *Correlation of major eastern earthquake centers with mafic/ultramafic basement masses*. U.S. Geological Survey, Professional Paper 1028-D.
- Karner, G.D., and Watts, A.B. 1982. *On isostasy at an Atlantic-type continental margin*. J. Geophys. Res., v. 87.
- Kazama, T., Okubo, S., Sugano, T., Matsumoto, S., Sun, W., Tanaka, Y., and Koyama, E. 2015. *Absolute gravity change associated with magma mass movement in the conduit of Asama Volcano (Central Japan), revealed by physical modeling of hydrological gravity disturbances*. J. Geophys. Res., v. 120.
- Keating, P., and Sailhac, P. 2004. *Use of the analytical signal to identify magnetic anomalies due to kimberlite pipes*. Geophysics, v. 69.
- Keller, F.J., Meuschke, J.L., and Alldredge, L.R. 1954. *Aeromagnetic surveys in the Aleutian, Marshall, and Bermuda islands*. Eos (Transactions, American Geophysical Union), v. 35.
- Keller, G.R., Bott, M.H.P., Wendlandt, R.F., Doser, D.I., and Morgan, P. 1995. *The Baikal Rift System*; in Olsen, K.H. (ed.), *Continental Rifts: Evolution, Structure, Tectonics*. Elsevier, NL.
- Kick, J.F. 1985. *Depth to bedrock using gravimetry*. The Leading Edge, v. 4.
- King, M.A., Bingham, R.J., Moore, P., Whitehouse, P.L., Bentley, M.J., and Milne, G.A. 2012. *Lower satellite-gravimetry estimates of Antarctic sea-level contribution*. Nature, v. 491.
- Klasner, J.S., King, E.R., and Jones, W.J. 1985. *Geologic interpretation of gravity and magnetic data for northern Michigan and Wisconsin*, in Hinze, W.J.,

- (ed.), *The Utility of Regional Gravity and Magnetic Anomaly Maps*. Society of Exploration Geophysicists, Tulsa, OK.
- Klepper, M.R., Robinson, G.D., and Smedes, H.W. 1971. *On the nature of the Boulder Batholith of Montana*. Geological Society of America Bulletin, v. 82.
- Kuo, B.Y., and Forsyth, D.W. 1989. *Gravity anomalies of the ridge-transform system in the South-Atlantic between 31°S and 34.5°S upwelling centres and variations in crustal thickness*. Marine Geophys. Res., v. 10.
- Lambert, A., and Beaumont, C. 1977. *Nano variations in gravity due to seasonal groundwater movements: implications for the gravitational detection of tectonic movements*. Journal of Geophysical Research, v. 82.
- Langenheim, V.E., Kirchoff-Stein, K.S., and Oliver, H.W. 1993. *Geophysical investigations of buried volcanic centers near Yucca Mountain, southwest Nevada*. American Nuclear Society Proceedings of the Fourth Annual International Conference on High Level Waste Management, v. 2.
- Larson, M.S., Stone, W.E., Morris, W.A., and Crocket, J.H. 1998. *Magnetic signature of magnetite-enriched rocks hosting platinum-group element mineralization within the Archean Boston Creek flow, Ontario*. Geophysics, v. 63.
- Lawton, D.C., and Isaac, J.H. 2007. *Case History Integrated gravity and seismic interpretation in the Norman Range, Northwest Territories, Canada*. Geophysics, v. 72.
- Leap, D.I., Fritz, S.J., and Hinze, W.J. 1991. *Non-invasive methods for assessing ground-water pollution from landfills: A comparative study from field experiments*. Environment Protection Engineering, v. 17.
- Leblanc, G.E., and Morris, W.A. 1999. *Aeromagnetism of southern Alberta within areas of hydrocarbon accumulation*. Bulletin of Canadian Petroleum Geology, v. 47.
- Levato, L., Veronese, L., Lozej, A., and Tabacco, E. 1999. *Seismic image of the ice-bedrock contact at the Lobbia Glacier, Adamello Massif, Italy*. Journal of Applied Geophysics, v. 42.
- Li, Y., and Oldenburg, D.W. 1996. *3-D inversions of magnetic data*. Geophysics, v. 61.
- Lodha, G.S., Davison, C.C., and Whitaker, S.H. 1990. *Geophysical techniques for characterizing plutonic rocks for nuclear fuel waste disposal*. Society of Exploration Geophysicists, 60th Annual International Meeting Expanded Abstracts, Tulsa, OK.
- Logatchev, N.A., Zorin, Y.A., and Rogozhina, V.A. 1983. *Baikal rift: Active or passive? - Comparison of the Baikal and Kenya Rift zones*. Tectonophysics, v. 94.
- Lund, J.W., Freeston, D.H., and Boyd, T.L. 2005. *Direct application of geothermal energy: 2005 worldwide review*. Geothermics, v. 34.
- Lyatsky, H.V. 2000. *Cratonic basement structures and their influence on the development of sedimentary basins in western Canada*. The Leading Edge, v. 19.
- Lyness, D. 1985. *The gravimetric detection of mining subsidence*. Geophysical Prospecting, v. 33.
- Mabey, D.R. 1989. *Geophysical lineaments in mineral exploration; in Quershy, M.N. and Hinze, W.J. (eds.), Regional Geophysical Lineaments: Their Tectonic and Economic Significance*. Geological Society of India, Memoir 12, Bangalore.
- Magsino, S.L., Connor, C.B., Hill, B.E., Stamatakos, J.A., La Femina, P.C., Sims, D.A., and Martin, R.H. 1998. *CNWRRA Ground magnetic Surveys in the Yucca*

- Mountain Region, Nevada (1996–1997)*. CNWRA 98–001. Center for Nuclear Waste Regulatory Analyses, San Antonio, TX.
- Mahrer, K.D., Bradley, C., and Newsom, S. 1984. *Magnetic-terrain anomalies from arroyos in an alluvial fan*. Geophysics, v. 49.
- Mandal, A., Mohanty, W.K., and Sharma, S.P. 2013. *3D compact inverse modeling of gravity data for chromite exploration - A case study from Tanagarparha Odisha, India*. Society of Exploration Geophysicists, Expanded Abstracts.
- Mandal, A., Mohanty, W.K., and Sharma, S.P. 2014. *Exploration of a sulfide deposit using joint inversion of magnetic and induced polarization data*. Society of Exploration Geophysicists, Expanded Abstracts.
- Mariano, J., and Hinze, W.J. 1994. *Gravity and magnetic models of the Midcontinent Rift in eastern Lake Superior*. Canadian Journal of Earth Science, v. 31.
- Martinek, B.C. 1988. *Groundbased magnetometer survey of abandoned wells at the Rocky Mountain Arsenal - A case history*. SAGEEP Proceedings.
- Maus, S., and Kuvshinov, A. 2004. *Ocean tidal signals in observatory and satellite magnetic measurements*. Geophys. Res. Lett., v. 31, doi:10.1029/2004GL020090.
- Maus, S., Barckhausen, U., Bournas, N., Brozena, J., Childers, V., Dostaler, F., Fairhead, J.D., Finn, C., von Frese, R.R.B., Gaina, C., Golynsky, S., Kucks, R., Lühr, H., Milligan, P., Mogren, S., Müller, R.D., Olesen, O., Pilkington, M., Saltus, R., Schreckenberger, B., Thébaud, E., and Caratori-Tontini, F. 2009. *EMAG2: A 2-arc min resolution Earth Magnetic Anomaly Grid compiled from satellite, airborne, and marine magnetic measurements*. Geochemistry, Geophysics, Geosystems, Q08005, v. 10, doi: 10.1029/2009GC002471, ISSN: 1525-2027.
- Mayhew, M. A. 1982. *Application of satellite magnetic anomaly data to Curie isotherm mapping*. J. Geophys. Res., v. 87.
- McCall, L.M., Dentith, M.C., Li, Z.X., and Trench, A. 1995. *The magnetic signature of komatiitic peridotite-hosted nickel sulphide deposits in the Widgiemooltha area, Western Australia*. Exploration Geophysics, v. 26.
- McCulloh, T.H. 1980. *Mass properties of sedimentary rocks and gravimetric effects of petroleum and natural-gas reservoirs; in Guion, D. and Prieto, C., (Eds.), Gravity/Magnetic Exploration Applications*. Society of Exploration Geophysicists, Tulsa, OK.
- Melosh, H.J. 1989. *Impact Cratering: A Geologic Process*. Oxford University Press.
- Meshref, W., and Hammauda, X. 1982. *Magnetic and gravity investigation of deep oil prospects in the Gulf of Suez*. Society of Exploration Geophysicists Technical Program and Expanded Abstracts.
- Miller, C.H. 1988. *Geophysical studies to detect the Acme Underground Coal Mine, Wyoming*. U.S. Geological Survey Bulletin 1677.
- Miller, R.H. 1931. *Analysis of some torsion-balance results in California*. American Association of Petroleum Geologists Bulletin, v. 15.
- Moon, C.J., Whateley, M.K.G., and Evans, A.M. 2006. *Introduction to Mineral Exploration*. Blackwell Publishing.
- Morey, G. B., and Sims, P. K. 1996. *Metallogeny*. In: Sims, P.K., (ed.), *Archean and Proterozoic geology of the Lake Superior region U.S.A.* U.S. Geological Survey Prof. Paper 1556.
- Morgan, P. 1995. *Diamond exploration from the bottom up: regional geophysical signatures of lithospheric conditions favorable for diamond exploration*, In:

- Griffin, W.L. (ed.), *Diamond Exploration: Into the 21st Century*. J. Geochem. Explor., v. 53.
- Morgan, P., and Baker, B.H. 1983. *Introduction - Processes of continental rifting*. Tectonophysics, v. 94.
- Morley, L.W. (ed.). 1970. *Mining and Groundwater Geophysics/1967*. Geological Survey of Canada, Economic Geology Report No. 26.
- Muller, P. M., and Sjogren, W.L. 1968. *Mascons: Lunar mass concentrations*. Science, v. 161.
- Mushayandebvu, M.F., and Davies, J. 2006. *Magnetic gradients in sedimentary basins: examples from the western Canada sedimentary basin*. The Leading Edge, v. 25.
- Nelson, T.H. 1991. *Salt tectonics and listric-normal faults; in Salvador, A., (ed.), The Gulf of Mexico basin, The Geology of North America*. Geological Society of America, v. J.
- Nettleton, L.L. 1939. *Determination of density for reduction of gravimeter observations*. Geophysics, v. 4.
- Nettleton, L.L. 1957. *Gravity survey over a Gulf Coast Continental Shelf mound*. Geophysics, v. 22.
- Neumann, E.R., Olsen, K.H., Baldrige, W.S., and Sunvoll, B. 1992. *The Oslo rift: A review*. Tectonophysics, v. 208.
- Neumann, R. 1967. *La gravimetrie de haute precision application aux recherches de cavites*. Geophysical Prospecting, v. 15.
- Norton, M.G., Arthur, J.C.R., and Dyer, K.J. 1997. *Geophysical survey planning for the Dounreay and Sellafield geological investigations, in McCann, D.M., Eddleston, M., Fenning, P.J., and Reeves, G.M. (eds.), Modern Geophysics in Engineering Geology*. Geological Society of London, Engineering Geology Special Publication No. 12.
- O'Donnell, T.M., Miller, K.C., and Witcher, J.C. 2001. *A seismic and gravity study of the McGregor geothermal system, southern New Mexico*. Geothermics, v. 66.
- O'Driscoll, E.S.T. 1990. *Lineament tectonics of Australian ore deposits; in Hughs, F.E. (ed.) Geology of the Mineral Deposits of Australia and Papua New Guinea*. Australasian Institute of Mining and Metallurgy, Monograph 14, Melbourne.
- Okubo, Y., Graf, R.J., Hansen, R.O., Ogawa, K., and Tsu, H. 1985. *Curie point depths of the Island of Kyushu and surrounding areas, Japan*. Geophysics, v. 53.
- Oldenburg, D.W., Li, Y., and Ellis, R.G. 1997. *Inversion of geophysical data over a copper gold porphyry deposit: A case history of Mt. Milligan*. Geophysics, v. 62.
- O'Leary, D.W., Mankinen, E. A., Blakely, R.J., Langenheim, V.E., and Ponce, D.A. 2002. *Aeromagnetic expression of buried basaltic volcanoes near Yucca Mountain, Nevada*. U.S. Geological Survey, Open-file Report 02-020.
- Olsen, K.H., and Morgan, P. 1995. *Introduction: Progress to understanding continental rifts; in Olsen, K.H. (ed.), Continental Rifts: Evolution, Structure, Tectonics*. Elsevier, NL.
- Onesti, L.A., and Hinze, W.J. 1970. *Magnetic observations over eskers in Michigan*. Geological Society of America Bulletin, v. 81.
- Oray, E., and Sanderson, D. 1967. *Application of the gravity method to a study of a collapse feature in Grand Rapids, Michigan*. Compass, v. 45.

- Ormö, J., Sturkell, E., Blomqvist, G., and Törnberg, R. 1999. *Mutually constrained geophysical data for the evaluation of a proposed impact structure: Lake Hummeln, Sweden*. Tectonophysics, v. 311.
- Paillet, F.L. 1993. *Integrating geophysical well logs, surface geophysics, and hydraulic test and geologic data in groundwater studies - theory and case histories*. SAGEEP Proceedings.
- Parasnis, D.S. 1979. *Principles of Applied Geophysics*. Chapman and Hall, London.
- Pawlowski, R. 2008. *The use of gravity anomaly data for offshore continental margin demarcation*. The Leading Edge, v. 27.
- Perry, F.V., Cogbill, A.H., and Kelley, R.E.. 2005. *Uncovering buried volcanoes at Yucca Mountain*. EOS (Trans. Amer. Geophys. Union), v. 86.
- Peters, B., and Buck, P. 2000. *The Maggie Hays and Emily Ann nickel deposits, Western Australia: a geophysical case history*. Exploration Geophysics, v. 31.
- Peters, J.W. 1960. *Geophysical case history of the Horse Creek field, Laramie County, Wyoming*. Geophysics, v. 25.
- Peters, J.W., and Dugan, A.F. 1945. *Gravity and magnetic investigations at the Grand Saline dome, Van Zandt County, Texas*. Geophysics, v. 10.
- Petersen, S.A., and Saxov, S. 1982. *Gravity applied to boundary conditions for nuclear waste and natural gas deposits*. Society of Exploration Geophysicists, 52nd Annual International Meeting Expanded Abstracts, Tulsa, OK.
- Phillips, J.D., Saltus, R.W., and Reynolds, R.L. 1998. *Sources of magnetic anomalies over a sedimentary basin: Preliminary results for the coastal plain of the Arctic National Wildlife Refuge, Alaska; in Gibson, R.I. and Millegan, P.S. (Eds), Geologic Applications of Gravity and Magnetics: Case Histories*. SEG Geophysical Reference Series, No. 8.
- Pierce, J., Ebner, E., and Marchand, N. 1998a. *High resolution aeromagnetic interpretation over Sierra and Yoyo reefs, northeastern British Columbia; in Gibson, R.I. and Millegan, P.S., (Eds.), Geologic Applications of Gravity and Magnetics: Case Histories*. Society of Exploration Geophysicists, Geophysical Reference Series, No. 8, American Association of Petroleum Geologists, Studies in Geology, #43.
- Pierce, J., Goussev, S.A., Charters, R.A., Abercrombie, H.J., and De Paoli, G.R. 1998b. *Intrasedimentary magnetization by vertical fluid flow and exotic geochemistry*. The Leading Edge, v. 17.
- Pilkington, M., and Crossley, D.J. 1986. *Determination of crustal interface topography from potential fields*. Geophysics, v. 51.
- Pilkington, M., and Grieve, R.A.F. 1992. *The geophysical signature of terrestrial impact craters*. Reviews of Geophysics, v. 30.
- Pilkington, M., and Hildebrand, A.R. 2000. *Three-dimensional magnetic imaging of the Chicxulub crater*. Journal of Geophysical Research, v. 105.
- Pilkington, M., Pesonen, L.J., Grieve, R.A.F., and Masaitis, V.L. 2002. *Geophysics and petrophysics of the Popigai Impact Structure, Siberia; in Plado, L. and Pesonen, L.J. (eds.), Impacts in Precambrian Shields*. Springer-Verlag, Heidelberg.
- Piskarev, A.L., and Tchernyshev, M.Y. 1997. *Magnetic and gravity anomaly patterns related to hydrocarbon fields in northern West Siberia*. Geophysics, v. 62.
- Plado, L., and Pesonen, L.J. 2002. *Impacts in Precambrian Shields*. Springer-Verlag, Heidelberg.

- Pohl, J.D., Stoffler, D., Gell, H., and Ernstson, K. 1977. *The Ries impact crater; in Roddy, D.J. (ed.), Impact and Explosion Cratering*. Pergamon Press, New York.
- Pohly, R.A. 1954. *Gravity case history: Dawn no. 156 pool, Ontario*. Geophysics, v. 19.
- Ponce, D.A. 1996. *Interpretive Geophysical Fault Map Across the Central Block of Yucca Mountain, Nevada*. U.S. Geological Survey Open-File Report 96-285.
- Ponce, D.A., and Oliver, H.W. 1998. *Gravity investigations, in Oliver, H.W., Ponce, D.A., and Hunter, W.C. (eds.), Major Results of Geophysical Investigations at Yucca Mountain and Vicinity, Southern Nevada*. U.S. Geological Survey Open-File Report 95-74.
- Pool, D.R. 2008. *The utility of gravity and water-level monitoring of alluvial aquifer wells in southern Arizona*. Geophysics, v. 73.
- Pool, D.R., and Eychaner, J.H. 1995. *Measurement of aquifer storage change and specific yield using gravity surveys*. Ground Water, v. 33.
- Potts, L.V., and von Frese, R.R.B. 2003a. *Comprehensive mass modeling of the Moon from spectrally correlated free-air and terrain gravity data*. J. Geophys. Res., v. 108.
- Potts, L.V., and von Frese, R.R.B. 2003b. *Crustal attributes of lunar basins from terrain-correlated free-air gravity anomalies*. J. Geophys. Res., v. 108.
- Potts, L.V., von Frese, R.R.B., Leftwich, T.E., Taylor, P.T., Shum, C.K., and Li, R. 2004. *Gravity-inferred crustal attributes of visible and buried impact basins on Mars*. J. Geophys. Res., v. 109.
- Power, M., Belcourt, G., and Rockel, E. 2004. *Geophysical methods for kimberlite exploration in northern Canada*. The Leading Edge, v. 23.
- Pratson, L.F., Bell, R.E., Anderson, R.N., Dosch, D., White, J., Affleck, C., Grier-son, A., Korn, B.E., Phair, R.L., Biegert, E.K., and Gale, P.E. 1998. *Results from a high-resolution, 3-D marine gravity gradiometry survey over a buried salt structure, Mississippi Canyon area, Gulf of Mexico; in Gibson, R.I. and Millegan, P.S., (Eds.), Geologic Applications of Gravity and Magnetics: Case Histories*. Society of Exploration Geophysicists, Geophysical Reference Series, No. 8, American Association of Petroleum Geologists, Studies in Geology, #43.
- Pratt, R.M., Rutstein, M.S., Walton, F.W., and Buschur, J.A. 1972. *Extension of Alaskan structural trends beneath Bristol Bay, Bering Shelf, Alaska*. J. Geophys. Res., v. 77.
- Pratt, W.P., and Sims, P.K. 1990. *The Midcontinent of the United States - Permissive Terrane for an Olympic Dam-Type Deposit*. U.S. Geological Survey, Bull. 1932.
- Prieto, C. 1998. *Gravity/magnetic signatures of various geologic models - An exercise in pattern recognition; in Gibson, R.I. and Millegan, P.S., (Eds.), Geologic Applications of Gravity and Magnetics: Case Histories*. Society of Exploration Geophysicists, Geophysical Reference Series, No. 8, American Association of Petroleum Geologists, Studies in Geology, #43.
- Prieto, C., Perkins, C., and Berkman, E. 1985. *Columbia River Basalt Plateau An integrated approach to interpretation of basalt-covered areas*. Geophysics, v. 50.
- Prodehl, C., Mueller, S., and Haak, V. 1995. *The European Cenozoic rift system; in Olsen, K.H. (ed.), Continental Rifts: Evolution, Structure, Tectonics*. Elsevier, NL.

- Rajagopalan, S., Carson, J., and Wituik, D. 2008. *Kimberlite exploration using integrated airborne geophysics*. Preview, v. 132.
- Rampton, V.N., and Walcott, R.I. 1974. *Gravity profiles across ice-covered topography*. Canadian Journal of Earth Sciences, v. 11.
- Ravat, D. 1996. *Magnetic properties of unruled steel drums from laboratory and field-magnetic measurements*. Geophysics, v. 61.
- Ravat, D., Lu, Z., and Braile, L.W. 1999. *Velocity-density relationships and modeling the lithospheric density variations of the Kenya Rift*. Tectonophysics, v. 302.
- Ravat, D., Finn, C., Hill, P., Kucks, R., Phillips, J., Bouligand, C., Sabaka, T., Elshayat, A., Aref, A., and Elawadi, E. 2009. *A preliminary, full spectrum, magnetic anomaly grid of the United States with improved long wavelengths for studying continental dynamics: A website for distribution of data*. U.S. Geological Survey Open-File 2009-1258.
- Ravat, D.N., Braile, L.W., and Hinze, W.J. 1987. *Earthquakes and plutons in the midcontinent - evidence from the Bloomfield pluton*. Seismological Research Letters, v. 58.
- Reddi, A.G.B., and Ramakrishna, T.S. 1989. *Relevance of gravity lineaments to mineral exploration in Rajasthan-Gujarat, India; in Quershy, M.N. and Hinze, W.J. (eds.), Regional Geophysical Lineaments: Their Tectonic and Economic Significance*. Geological Society of India, Memoir 12, Bangalore.
- Reeves, C.V., Reford, S.W., and Millegan, P.R. 1997. *Airborne geophysics: Old methods, new images; in Gubins, A.G.(ed.), Geophysics and Geochemistry at the Millenium*. Proceedings of Exploration 97, Fourth Decennial International Conference on Mineral Exploration.
- Regan, R.D., and Hinze, W.J. 1975. *Gravity and magnetic investigations of Meteor crater, Arizona*. Journal of Geophysical Research, v. 80.
- Rene, R.M. 2000. *Three-dimensional gravity inversion with an application over an abandoned underground limestone mine in Indiana*. Journal of Environmental and Engineering Geophysics, v. 5.
- Reynolds, L.J. 2001. *Geology of the Olympic Dam Cu-U-Ag-REE deposit*. MESA Journal, v. 23.
- Reynolds, R.L., Fishman, N.S., and Hudson, M.R. 1991. *Sources of aeromagnetic anomalies over Cement oil field (Oklahoma), Simpson oil field (Alaska), and the Wyoming-Idaho-Utah thrust belt*. Geophysics, v. 56.
- Reynolds, R.L., Rosenbaum, J.G., Hudson, M.R., and Fishman, N.S. 1990. *Rock magnetism, the distribution of magnetic minerals in the Earth's crust, and aeromagnetic anomalies, in Hanna, W.F. (ed.), Geologic Application of Modern Aeromagnetic Surveys*. U.S. Geological Survey Bulletin 1924.
- Richardson, R.M., and MacInnes, S.C. 1989. *The inversion of gravity data into three-dimensional polyhedral models*. Journal of Geophysical Research, v. 94.
- Riddell, P.A. 1966. *Magnetic observations at the Dayton Iron Deposit, Lyon County, Nevada; in SEG Mining Geophysics Volume Editorial Committee (ed.)*. Mining Geophysics, v. 1.
- Robbins, E.I. 1983a. *Accumulation of fossil fuels and metallic minerals in active and ancient rift lakes*. Tectonophysics, v. 94.
- Robbins, E.I. 1983b. *Mechanisms of active and passive rifting*. Tectonophysics, v. 94.
- Roberts, R.L., Hinze, W.J., and Leap, D.I. 1990a. *Application of the gravity method to investigation of landfill in the glaciated mid-continent, USA, in Ward, S.H.*

- (ed.), *Geotechnical and Environmental Geophysics, 2*. Society of Exploration Geophysicists, Tulsa, OK.
- Roberts, R.L., Hinze, W.J., and Leap, D.I. 1990b. *Data enhancement procedures on magnetic data from landfill investigations*, in Ward, S.H. (ed.), *Geotechnical and Environmental Geophysics, 2*. Society of Exploration Geophysicists, Tulsa, OK.
- Rohrman, M. 2007. *Prospectivity of volcanic basins: Trap delineation and acreage de-risking*. American Association of Petroleum Geologists, DOI:10.1306/12150606017.
- Rose, M., Zeng, Y., and Dransfield, M. 2006. *Applying FALCON gravity gradiometry to hydrocarbon exploration in the Gippsland basin, Victoria*. *Exploration Geophysics*, v. 37.
- Ross, H.E., Blakely, R.J., and Zoback, M.D. 2006. *Testing the use of aeromagnetic data for the determination of Curie depth in California*. *Geophysics*, v. 71.
- Rotstein, Y., Edel, J.B., Gabriel, G., Boulanger, D., Schaming, M., and Munsch, M. 2006. *Insight into the structure of the Upper Rhine Graben and its basement from a new compilation of Bouguer gravity*. *Tectonophysics*, v. 425.
- Rousset, D., Bayer, R., Guillon, D., and Edel, J.B. 1993. *Structure of the southern Rhine Graben from gravity and reflection seismic data (ECORS-DEKORP Program)*. *Tectonophysics*, v. 221.
- Roy, B., and Clowes, R.M. 2000. *Seismic and potential-field imaging of the Guichon Creek batholith, British Columbia, Canada, to delineate structures hosting porphyry copper deposits*. *Geophysics*, v. 65.
- Rummel, R., Horwath, M., Yi, W., Albertella, A., Bosch, W., and R., Haagmans. 2011. *Satellite gravimetry and Antarctic mass transports*. *Surv. Geophys.*, v. 32.
- Ruppel, C., Kogan, M., and McNutt, M. 1993. *Implications of new gravity data for the Baikal rift zone structure*. *Geophys. Res. Lett.*, v. 20.
- Rutter, H., and Esdale, D.J. 1985. *The geophysics of the Olympic Dam discovery*. *Exploration Geophysics*, v. 16.
- Rybakov, M., Rotstein, Y., Shirman, B., and Al-Zoubi, A. 2005. *Cave detection near the Dead Sea - a Micromagnetic feasibility study*. *The Leading Edge*, v. 23.
- Rymer, H., and Brown, G.C. 1987. *Causes of microgravity change at Poás volcano, Costa Rica: an active but non-erupting system*. *Bulletin of Volcanology*, v. 49.
- Saad, A.H. 1986. *High-frequency intrasedimentary magnetic anomalies in the NPR-Alaska*. Chevron InterCompany Geophysics Conference, ICGC paper 34.
- Saad, A.H. 1987. *Detection and mapping of salt and shale structures by aeromagnetism: Garden Banks test profiles*. Chevron InterCompany Geophysics Conference, ICGC paper 23.
- Saad, A.H. 1993. *Interactive integrated interpretation of gravity, magnetic, and seismic data tools and examples*. Offshore Technology Conference, Paper Number OTC# 7079.
- Saad, A.H. 2009a. *Spatial-domain filters for short wavelength sedimentary magnetic anomalies*. Society of Exploration Geophysicists, 79th Annual International Meeting Expanded Abstracts, Tulsa, OK.
- Saad, A.H. 2009b. *Spatial-domain filters for short wavelength sedimentary magnetic anomalies (Slide Presentation)*. Society of Exploration Geophysicists, 79th Annual International Meeting Expanded Abstracts Multimedia (32 slides), Tulsa, OK.

- Saad, A.H., and Sisemore, L.K. 1988. *The use of high resolution aeromagnetics for sand channel exploration in offshore Louisiana*. Chevron InterCompany Geophysics Conference, ICGC paper 35.
- Sánchez, M.G., Allan, M.M., Hart, C.J.R., and Mortensen, J.K. 2014. *Extracting ore-deposit-controlling structures from aeromagnetic, gravimetric, topographic, and regional geologic data in western Yukon and eastern Alaska*. Interpretation, v. 2.
- Sander, B.K., and Cawthorn, R.G. 1996. *2.5 gravity model of the Ni-Cu-PGM mineralized Mount Ayliff Intrusion (Insizwa Complex), South Africa*. Journal of Applied Geophysics, 35.
- Sanderson, T.J.O., Berrino, G., and Corrado, G. 1983. *Ground deformation and gravity changes accompanying the March 1981 eruption of Mount Etna*. Journal of Volcanology, v. 16.
- Sandrin, A., Berggren, R., and Elming, S.A. 2007. *Geophysical targeting of Fe-oxide Cu-(Au) deposits west of Kiruna, Sweden*. J. Appl. Geophys., v. 61.
- Sarma, B.S.P., Verma, B.K., and Satyanarayana, S.V. 1999. *Magnetic mapping of Majhgawan diamond pipe of central India*. Geophysics, v. 64.
- Schenk, R.L., Morris, J.J., and Hall, S.A. 1998. *Integrated gravity modeling of salt features in the Mississippi Salt basin; in Gibson, R.I., and Millegan, P.S., (Eds.), Geologic Applications of Gravity and Magnetics: Case Histories*. Society of Exploration Geophysicist, Geophysical References Series, No. 8, American Association of Petroleum Geologists, Studies in Geology, #43.
- Schilinger, C.M. 1990. *Magnetometer and gradiometer surveys for detection of underground storage tanks*. Bulletin of the Association of Engineering Geologists, v. 27.
- Schmidt, P.W., and Clark, D.A. 2006. *The magnetic gradient tensor: its properties and uses in source characterization*. The Leading Edge, v. 25.
- Schrama, E.J.O., Wouters, B., and Lavallée, D.A. 2007. *Signal and noise in Gravity Recovery and Climate Experiment (GRACE) observed surface mass variations*. J. Geophys. Res., v. 112, doi:10.1029/2006JB004882.
- Schubert, G., Yuen, D.A., and Turcotte, D.L. 1975. *Role of phase transitions in a dynamic mantle*. J. R. Astr. Soc., v. 42.
- Schultz, A.K. 1989. *Monitoring fluid movement with the borehole gravity meter*. Geophysics, v. 54.
- Schultz, R.A., and Frey, H.V. 1990. *A new survey of multiring impact basins on Mars*. J. Geophys. Res., v. 95.
- Scott, R.G., Pilkington, M., and Tanczyk, E.I. 1997. *Magnetic investigations of the West Hawk, Deep Bay and Clearwater impact structures, Canada*. Meteoritics & Planetary Science, v. 32.
- SEG. 1966. *Geophysical signatures of Western Australian mineral deposits: An overview; in Mining Geophysics: Case Histories, v. I*. Society of Exploration Geophysicists Mining Geophysics Volume Editorial Committee.
- Seigel, H.O. 1993. *Designing geophysical instrumentation specifically for environmental applications*. Proceedings of the Symposium on the Application of Geophysics to Engineering and Environmental Problems, Environmental and Engineering Geophysical Society.
- Sherlock, D., Toomey, A., Hoversten, E., and Dodds, K. 2006. *Gravity monitoring of CO₂ storage in a depleted gas field: a sensitivity study*. Exploration Geophysics, v. 37.

- Shevchenko, S.I., and Lasky, R.P. 2004. *Is there room for gravity in petroleum exploration or is the door shut?* Exploration Geophysics, v. 35.
- Silva, J.B.C., Costa, D.C.L., and Barbosa, V.C.F. 2006. *Gravity inversion of basement relief and estimation of density contrast variation with depth.* Geophysics, v. 71.
- Simpson, R.W., and Jachens, R.C. 1989. *Gravity methods in regional studies, in Pakiser, L.C., and Mooney, W.D., (Eds.), Geophysical Framework of the Continental United States.* Geological Society of America memoir 172.
- Simpson, R.W., Jachens, R.C., and Blakely, R.J. and Saltus, R.W. 1986. *A new isostatic residual gravity map of the conterminous United States with a discussion on the significance of isostatic residual anomalies.* J. Geophys. Res., v. 91.
- Singh, B., and Rao, V.B. 1990. *Magnetic signatures of zones of fractures in igneous metamorphic rocks with an example from southeastern New England - Comment.* Tectonophysics, v. 179.
- Sjostrom, K.J., and Berry, T.E. 1996. *Weight determination of stockpiled ferromagnetic rocks using microgravity measurements.* U.S. Army Corps of Engineers, Waterways Experiment Station Miscellaneous Paper GL-96-34, Vicksburg, MS.
- Smith, A.G., Hurley, A.M., and ., J. C. Briden. 1981. *Phanerozoic Paleogeographic World Maps.* Cambridge Univ. Press, London.
- Smith, R.J. 1985. *Geophysics in Australian mineral exploration.* Geophysics, v. 50.
- Soengkono, S. 2001. *Interpretation of magnetic anomalies over the Waimangu geothermal area, Taupo volcanic zone, New Zealand.* Geothermics, v. 30.
- Spudis, P.D. 2005. *The Geology of Multi-Ring Impact Basins.* Cambridge Univ. Press, New York.
- Stanley, J.M., and Cattach, M.K. 1990. *The use of high-definition magnetics in engineering site investigation.* Exploration Geophysics, v. 21.
- Stauder, W., Kramer, M., Fischer, G., Schaefer, S., and Morrissey, S. 1977. *Seismic characteristics of southeast Missouri as indicated by a regional-telemetered microearthquake array.* Bull. Seismol. Soc. Am., v. 66.
- Steenland, N.C. 1965. *Oil fields and aeromagnetic anomalies.* Geophysics, v. 30.
- Stewart, M., and Wood, J. 1990. *Geologic and geophysical character of fracture zones in a Tertiary carbonate aquifer, Florida, in Ward, S.H., (ed.), Geotechnical and Environmental Geophysics, 2, Environmental and Groundwater.* Society of Exploration Geophysicists, Tulsa, OK.
- Street, G.J., and Engel, R. 1990. *Geophysical surveys of dryland salinity, in Ward, S.H., (ed.), Geotechnical and Environmental Geophysics, 2, Environmental and Groundwater.* Society of Exploration Geophysicists, Tulsa, Oklahoma.
- Tanner, J.G., and Gibb, R.A. 1979. *Gravity method applied to base metal exploration, in Hood, P.J. (ed.), Economic Geology Report 31.* Geological Survey of Canada, Ottawa.
- Tapley, B.D., Bettadpur, S., J.C., Ries, Thompson, P.F., and Watkins, M.M. 2004. *GRACE measurements of mass variability in the Earth system.* Science, v. 305.
- Taylor, P.T., Zietz, I., and Dennis, L.S. 1968. *Geologic implications of aeromagnetic data for the eastern continental margin of the United States.* Geophysics, v. 33.

- ten Brink, U.S., Rybakov, M., Al-Zoubi, A.S., and Rotstein, Y. 2007. *Magnetic character of a large continental transform: An aeromagnetic survey of the Deadm Sea Fault*. *Geochem., Geophys., and Geosyst.*, v. 8.
- Tessara, A., Götze, H., Schmidt, S., and Hackney, R. 2006. *Three dimensional model of the Nasca plate and the Andean continental margin*. *J. Geophys. Res.*, v. 111.
- Thomas, M.D. 1997. *Gravity prospecting for massive sulphide deposits I the Bathurst Mining Camp, New Brunswick, Canada*, in Gubins, A.G. (ed.), *Proceedings of Exploration97*. Fourth Decennial International Conference on Mineral Exploration, Prospectors and Developers Association of Canada.
- Tiberi, C., Diament, M., Déverchère, J., Petit-Mariani, C., Mikhailov, V., Tikhotsky, S., and Achauer, U. 2003. *Deep structure of the Baikal rift zone revealed by joint inversion of gravity and seismology*. *J. Geophys. Res.*, v. 108.
- Torge, W. 1989. *Gravimetry*. Walter de Gruyter, Amsterdam.
- Tsikalas, F., Gudlaugsson, S.T., Eldholm, O., and Faleide, J.I. 1998. *Integrated geophysical analysis supporting the impact origin of the Mjölknir structure, Barents Sea*. *Tectonophysics*, v. 289.
- Tudor, D.S. 1971. *A geophysical study of the Kentland disturbed area*. Ph.D. thesis, University of Indiana, Bloomington, IN.
- Tyagi, S., Lord, A.E. Jr., and Koermer, R.M. 1983. *Use of proton precession magnetometer to detect buried drums in sandy soil*. *Journal of Hazardous Materials*, v. 8.
- Tyler, R.H., Maus, S., and Lühr, H. 2003. *Satellite observations of magnetic fields due to ocean tidal flow*. *Science*, v. 299.
- Ugalda, H.A., Artemieva, N., and Milkereit, B. 2005. *Magnetization on impact structures - constraints from numerical modeling and petrophysics; in Kenkmann, T. and Hörz, F. (eds.), Large Meteorite Impacts III*. GSA Special Paper 384.
- Uhley, R.P., and Scharon, L. 1954. *Gravity surveys for residual barite deposits in Missouri*. *Mining Engineering*, v. 6.
- Vallée, M.A., Smith, R.S., and Keating, P. 2011. *Metalliferous mining geophysics - State of the art after a decade in the new millennium*. *Geophysics*, v. 76.
- Vella, L. 1997. *Interpretation and modeling, based on petrophysical measurements, of the Wirrda Well potential field anomaly, South Australia*. *Exploration Geophysics*, v. 28.
- Vella, L., and Cawood, M. 2006. *Carrapateena: discovery of an Olympic Dam-style deposit*. *Preview*, v. 122.
- Vening Meinesz, F.A. 1948. *Gravity expeditions at sea*. *Neth. Geod. Comm.*, Waltman, Delft.
- von Frese, R.R.B., and Noble, V.E. 1984. *Magnetometry for archaeological exploration of historical sites*. *Historical Archaeology*, v. 18.
- von Frese, R.R.B., Hinze, W.J., Olivier, R., and Bentley, C.R. 1986. *Regional magnetic anomaly constraints on continental breakup*. *Geology*, v. 14.
- von Frese, R.R.B., Jones, M.B., Kim, J.W., and Kim, J.H. 1997. *Analysis of anomaly correlations*. *Geophysics*, v. 62.
- von Frese, R.R.B., Potts, L.V., Wells, S.B., Leftwich, T.E., Kim, H.R., Kim, J.W., Hernandez, O., Golynsky, A.V., and Gaya-Piqué, L.R. 2009. *GRACE gravity evidence for an impact basin in Wilkes Land, Antarctica*. *Geochemistry, Geophysics, Geosystems*, v. 10.

- von Frese, R.R.B., Kim, H.R., Leftwich, T.E., Kim, J.W., and Golynsky, A.V. 2013. *Satellite magnetic anomalies of the Antarctic Wilkes Land impact basin inferred from regional gravity and terrain data*. *Tectonophysics*, v. 585.
- Wahr, J., Swenson, S., Zlotnicki, V., and Velicogna, I. 2004. *Time-variable gravity from GRACE: First results*. *Geophys. Res. Lett.*, v. 31, doi:10.1029/2004GL019779.
- Wasilewski, P.J., Thomas, H.H., and Mayhew, M.A. 1979. *The Moho as a magnetic boundary*. *Geophys. Res. Lett.*, v. 6.
- Watts, A.B., and Talwani, M. 1974. *Gravity anomalies seaward of deep-sea trenches and their tectonic implications*. *Geophys. J. R. Astr. Soc.*, v. 36.
- Watts, A.B., and Talwani, M. 1975. *Gravity effect of downgoing lithospheric slabs beneath island arcs*. *Geol. Soc. Am. Bull.*, v. 86.
- Webb, S.J., Cawthorn, R.G., Nguuri, T., and James, D. 2004. *Gravity modeling of Bushveld Complex connectivity supported by Southern Africa Seismic Experiment results*. *South African J. Geol.*, v. 107.
- Weber, M.E., Lyman, G., and Anderson, B.S. 2000. *Enhancing seismic depth migration with simultaneous gravity*. *Offshore*, v. 60.
- West, R.E., and Sumner, J.S. 1972. *Groundwater volumes from anomalous mass determinations for alluvial basins*. *Ground Water*, v. 10.
- Wijns, C., Perez, C., and Kowalczyk, P. 2005. *Theta map: Edge detection in magnetic data*. *Geophysics*, v. 70.
- Williams, P.K. 1997. *Towards a multidisciplinary integrated exploration process for gold discovery; in Gubins, A.G., Proceedings of Exploration 97: Fourth Decennial International Conference on Mineral Exploration*. Fourth Decennial International Conference on Mineral Exploration.
- Wise, D.U., and Yates, M.T. 1970. *Mascons as structural relief on a lunar Moho*. *J. Geophys. Res.*, v. 75.
- Witherly, K., and Diorio, F. 2012. *Assessment of Falcon Airborne gravity gradiometer data from the Athabasca Basin, Saskatchewan, Canada*. Society of Exploration Geophysicists, Expanded Abstracts.
- Withers, R., Eggers, D., Fox, T., and Crebs, T. 1994. *A case study of integrated hydrocarbon exploration through basalt*. *Geophysics*, v. 59.
- Wolfe, P.J., and Richard, B.H. 1990. *Geophysical studies of Cedar Bog, in Ward, S.H. (ed.), Geotechnical and Environmental Geophysics 2*. Society of Exploration Geophysicists, Tulsa, OK.
- Won, I.J., Murphy, V., Hubbard, P., Oren, A., and Davis, K. 2004. *Geophysics and weapons inspection*. *The Leading Edge*, v. 23.
- Wood, G., and Thomas, M.D. 2002. *Modeling of high-resolution gravity data near the McArthur River uranium deposit, Athabasca Basin; in Summary of Investigations 2002, Volume 2, Saskatchewan Geological Survey*. Sask. Industry Resources, Misc. Rep. 2002-4.2, CD-ROM, Paper D-16.
- Wright, P.M. 1981. *Gravity and magnetic methods in mineral exploration*. *Economic Geology*, v. 75.
- Wright, P.M., Ward, S.H., Ross, H.P., and West, R.C. 1985. *State-of-the-art geophysical exploration for geothermal resources*. *Geophysics*, v. 50.
- Wynn, J.C. 1986. *Archaeological prospection: an introduction to the Special Issue*. *Geophysics*, v. 51.
- Wynn, J.C. 1990. *Applications of high-resolution geophysical methods to archaeology, in Lasca, N.P., and Donahue, J. (eds.), Archaeological geology of North America*. Geological Society of America, Centennial Special Volume 4.

- Wynn, J.C., and Roseboom, E.H. 1987. *Role of geophysics in identifying and characterizing sites for high-level nuclear waste repositories*. Journal of Geophysical Research, v. 92.
- Yuhr, L., Benson, R., and Butler, D. 1993. *Characterization of karst features using electromagnetics and microgravity: a strategic approach*. SAGEEP Proceedings.
- Yule, D.E., Sharp, M.K., and Butler, D.K. 1998. *Microgravity investigations of foundation conditions*. Geophysics, v. 63.
- Yungul, S.H. 1961. *Gravity prospecting for reefs: Effects of sedimentation and differential compaction*. Geophysics, v. 26.
- Zeil, P., Volk, P., and Saradeth, S. 1991. *Geophysical methods for lineament studies in groundwater exploration. A case history from SE Botswana*. Geoexploration, v. 27.
- Zeng, H., Meng, X., Yao, C., Li, X., Lou, H., Guang, Z., and Li, Z. 2002. *Detection of reservoirs from normalized full gradient of gravity anomalies and its application to Shengli oil field, east China*. Geophysics, v. 67.
- Ziegler, P.A. 1992. *European Cenozoic Rift System; in Ziegler, P.A. (ed.), Geodynamics of Rifting, v. I, Case history studies on rifts: Europe and Asia*. Tectonophysics, v. 208.
- Zumberge, M., Alnes, H., Eiken, O., Sasagawa, G., and Stenvold, T. 2008. *Precision of seafloor gravity and pressure measurements for reservoir monitoring*. Geophysics, v. 73.